

# **For Reference**


---

**NOT TO BE TAKEN FROM THIS ROOM**

Ex LIBRIS  
UNIVERSITATIS  
ALBERTAENSIS







Digitized by the Internet Archive  
in 2023 with funding from  
University of Alberta Library

<https://archive.org/details/Roodselaar1976>





THE UNIVERSITY OF ALBERTA

RELEASE FORM

NAME OF AUTHOR ..... Albert van Roodselaar .....  
TITLE OF THESIS ..... Rate Constants for the Reactions of  
..... S(<sup>3</sup>P) Atoms .....  
.....  
DEGREE FOR WHICH THESIS WAS PRESENTED ..... Ph.D. ....  
YEAR THIS DEGREE GRANTED ..... 1976 .....

Permission is hereby granted to THE UNIVERSITY OF ALBERTA LIBRARY to reproduce single copies of this thesis and to lend or sell such copies for private, scholarly or scientific research purposes only.

The author reserves other publication rights, and neither the thesis nor extensive extracts from it may be printed or otherwise reproduced without the author's written permission.



THE UNIVERSITY OF ALBERTA

RATE CONSTANTS FOR THE REACTIONS  
OF S(<sup>3</sup>P) ATOMS



by

ALBERT VAN ROODSELAAR

A THESIS

SUBMITTED TO THE FACULTY OF GRADUATE STUDIES AND RESEARCH  
IN PARTIAL FULFILMENT OF THE REQUIREMENTS FOR THE DEGREE  
OF DOCTOR OF PHILOSOPHY

DEPARTMENT OF CHEMISTRY  
UNIVERSITY OF ALBERTA  
EDMONTON, CANADA

FALL, 1976



THE UNIVERSITY OF ALBERTA  
FACULTY OF GRADUATE STUDIES AND RESEARCH

The undersigned certify that they have read, and recommend  
to the Faculty of Graduate Studies and Research, for acceptance, a  
thesis entitled

RATE CONSTANTS FOR THE REACTIONS  
OF S(<sup>3</sup>P) ATOMS

submitted by

ALBERT VAN ROODSELAAR

in partial fulfilment of the requirements for the degree of Doctor  
of Philosophy.



## ABSTRACT

The technique of flash photolysis-vacuum ultraviolet kinetic absorption spectroscopy has been used to determine the absolute rate constants for the reactions of  $S(^3P)$  atoms with a variety of substrates. In addition, the temperature dependence of a number of these reactions was examined.

Ground state  $S(^3P)$  atoms were produced by flash photolyzing COS in an excess of diluent, generally  $CO_2$ . It has been shown that under the conditions employed  $S(^3P)$  atoms are generated in a thermalized distribution and decay via first order kinetics.

The determination of the rate constant for the reaction with oxygen was necessary to resolve the discrepancy in the literature. Our value is in agreement with one of the previous determinations, suggesting that the other is low by three orders of magnitude.

Since NO is an effective scavenger in many reaction systems, a knowledge of its rate of reaction with  $S(^3P)$  atoms would prove advantageous. From the observed pressure dependence and reaction order studies it is shown that nitric oxide undergoes reaction with  $S(^3P)$  atoms via a termolecular energy transfer mechanism. The extremely high efficiency of the reaction is in keeping with the rates reported for other reactions of atomic and radical species with NO.



Rate constants and Arrhenius parameters for the reactions of S(<sup>3</sup>P) atoms with a number of olefins were determined. Activation energies decrease with increasing substitution demonstrating the electrophilic nature of sulfur atoms and  $E_a$  for the reaction with tetramethylethylene is  $-1.3 \text{ kcal mole}^{-1}$ .

The rate constant for abstraction from ethylene episulfide was determined in order to assess its importance in the S + olefin system. From the results, together with a computer simulation of the S + olefin system it is concluded that under the conditions employed in this study at least 95% of the observed decay is due to reaction with olefin. Rate constants were also determined for abstraction from propylene and *trans*-2-butene episulfide.

Rate constants were determined for the reactions of S(<sup>3</sup>P) atoms with a number of alkynes and Arrhenius parameters measured for the reactions with acetylene and propyne. The experimentally determined secondary H/D kinetic isotope effect for C<sub>2</sub>H<sub>2</sub> and C<sub>2</sub>D<sub>2</sub> of  $k_H/k_D = 1.0$  could be reproduced by detailed calculations if a biradical model for the activated complex is assumed.



## ACKNOWLEDGMENTS

The author wishes to express his sincere gratitude to Dr. O.P. Strausz for his guidance and support throughout the course of this investigation.

Thanks go to all the members of the photochemistry group, particularly Drs. I. Safarik, R.W. Fair, R. Gosavi, M. Torres and F.C. James for helpful discussions.

The author would like to extend a special thanks to Dr. E.M. Lown for her assistance with the manuscript.

The contribution of Mrs. K. James in typing this thesis is greatly appreciated.

The author would like to express his deepest gratitude to his wife, Christine, whose co-operation and encouragement made this work possible.

The financial assistance provided by the University of Alberta is gratefully acknowledged.



## TABLE OF CONTENTS

	<u>Page</u>
ABSTRACT.....	iv
ACKNOWLEDGEMENTS.....	vii
LIST OF TABLES.....	xv
LIST OF FIGURES.....	xxi
 CHAPTER I      INTRODUCTION	 1
A.   The Sulfur Atom	2
B.   Sulfur Atom Sources	2
C.   The Reactivity of Sulfur Atoms	10
1. $S(^3P_{2,1,0})$ Atoms.....	12
2. $S(^1D_2)$ Atoms.....	15
3. $S(^1S_0)$ Atoms.....	20
D.   Reactivity of Other Ground State Group VI A Atoms	22
1. $O(^3P)$ Atoms.....	22
2. $Se(^3P)$ Atoms.....	27
3. $Te(^3P)$ Atoms.....	28
E.   Flash Photolysis	31
1.   Development.....	31
2.   Types of Flash Photolysis Apparatus	32
3.   Light Sources.....	33



## TABLE OF CONTENTS (cont'd)

	<u>Page</u>
4. Electronics.....	36
i. Triggering.....	36
ii. Delays.....	36
iii. Detection.....	37
5. Measurement of Absorption Densities.	37
6. Determination of Absolute Concentration.....	38
7. Complications of Detection in the Vacuum Ultraviolet.....	39
F. Aim of the Present Investigation	39
 CHAPTER II   EXPERIMENTAL	 43
1. Vacuum Systems.....	43
2. Materials.....	44
3. Flash Photolysis Apparatus.....	44
a) Optical System.....	48
b) Housing.....	56
c) Electrical.....	56
4. Operating Procedure.....	58
 CHAPTER III   THE FLASH PHOTOLYSIS OF CARBONYL SULFIDE	 60
A. Results	60



## TABLE OF CONTENTS (cont'd)

	<u>Page</u>
1. Experimental Beer-Lambert	
Coefficient.....	60
a) Cell Length Variation.....	62
b) Flash Energy Variation.....	62
2. Population of the $^3P_{2,1,0}$ States..	65
3. Estimation of Absolute $S(^3P_{2,1,0})$	
Concentrations.....	70
a) Variation of the Extent of	
Decomposition of COS.....	70
b) Measurement of CO.....	74
4. Decay of $S(^3P)$ .....	74
 B. Discussion	 77
 <u>CHAPTER IV</u>	
THE REACTION OF $S(^3P)$ ATOMS WITH	
MOLECULAR OXYGEN	84
 A. Results	 84
1. Kinetics of Decay of $S(^3P)$ Atoms	
with Molecular Oxygen.....	84
2. $O_2$ Pressure Study.....	86
3. Effect of Total Pressure.....	90
4. Effect of Flash Energy.....	92
5. Observation of the SO Spectrum....	94
 B. Discussion	 99



## TABLE OF CONTENTS (cont'd)

		<u>Page</u>
CHAPTER V	THE REACTION OF S( <sup>3</sup> P) ATOMS WITH NITRIC OXIDE	107
	A. Results	107
	1. Kinetics of S( <sup>3</sup> P) Atom Decay.....	107
	2. Effect of NO Pressure.....	107
	3. Effect of Total Pressure.....	110
	B. Discussion	115
CHAPTER VI	THE REACTIONS OF S( <sup>3</sup> P) ATOMS WITH EPISULFIDES	122
	A. Results	122
	1. S( <sup>3</sup> P) Atom Decay as a Function of Ethylene Episulfide Pressure.....	122
	2. S( <sup>3</sup> P) Atom Decay as a Function of Total Pressure.....	125
	3. The Bimolecular Rate Constant for the Reaction of S( <sup>3</sup> P) Atoms with Propylene Episulfide.....	125
	4. The Bimolecular Rate Constant for the Reaction of S( <sup>3</sup> P) Atoms with <i>trans</i> -2-Butene Episulfide.....	125
	B. Discussion	133



## TABLE OF CONTENTS (cont'd)

		<u>Page</u>
CHAPTER VII	THE REACTIONS OF S( <sup>3</sup> P) ATOMS WITH OLEFINS	143
	A. Results - Part I	143
	1. The Reaction of S( <sup>3</sup> P) Atoms with Ethylene.....	143
	i) S( <sup>3</sup> P) Atom Decay.....	143
	ii) Effect of Ethylene Pressure.	146
	iii) Effect of Total Pressure and Nature of the Diluents.....	146
	iv) Effect of Flash Energy.....	146
	2. The Reaction of S( <sup>3</sup> P) Atoms with Propylene.....	146
	3. The Reaction of S( <sup>3</sup> P) Atoms with 1-Butene.....	150
	4. The Reaction of S( <sup>3</sup> P) Atoms with <i>trans</i> -2-Butene.....	150
	5. The Reaction of S( <sup>3</sup> P) Atoms with Isobutene.....	150
	6. The Reaction of S( <sup>3</sup> P) Atoms with Tetramethylethylene.....	157
	7. The Reaction of S( <sup>3</sup> P) Atoms with Vinyl Fluoride.....	157
	B. Results - Part II	164



## TABLE OF CONTENTS (cont'd)

	<u>Page</u>
1. Temperature Dependence of the $S(^3P)$ plus Ethylene System.....	164
2. Temperature Dependence of the $S(^3P)$ plus Propylene System.....	164
3. Temperature Dependence of the $S(^3P)$ plus 1-Butene System.....	164
4. Temperature Dependence of the $S(^3P)$ plus Tetramethylethylene System...	169
C. Discussion	171
CHAPTER VIII THE REACTIONS OF $S(^3P)$ ATOM WITH ACETYLENES	187
A. Results - Part I	187
1. The Bimolecular Rate Constant for the Reaction of $S(^3P)$ Atoms with Acetylene.....	187
2. The Bimolecular Rate Constant for the Reaction of $S(^3P)$ Atoms with Acetylene- $d_2$ .....	187
3. The Bimolecular Rate Constant for the Reaction of $S(^3P)$ Atoms with Propyne.....	190
4. The Bimolecular Rate Constant	



## TABLE OF CONTENTS (cont'd)

	<u>Page</u>
for the Reaction of S( <sup>3</sup> P) Atoms with 1-Butyne.....	190
5. The Bimolecular Rate Constant for the Reaction of S( <sup>3</sup> P) Atoms with 2-Butyne.....	190
6. The Bimolecular Rate Constant for the Reaction of S( <sup>3</sup> P) Atoms with 2-Pentyne.....	197
7. The Bimolecular Rate Constant for the Reaction of S( <sup>3</sup> P) Atoms with 2-Perfluorobutyne.....	197
B. Results - Part II	205
1. The Temperature Dependence of the S( <sup>3</sup> P) Atom plus Acetylene Reaction.....	205
2. The Temperature Dependence of the S( <sup>3</sup> P) Atom plus Propyne Reaction.....	205
C. Discussion	209



# TABLE OF CONTENTS (cont'd)

	<u>Page</u>
CHAPTER IX      SUMMARY AND CONCLUSIONS	222
BIBLIOGRAPHY	225
APPENDIX I      DERIVATION OF THE RELATIONSHIP BETWEEN THERMAL POPULATION DISTRIBUTION AND THE MAGNITUDE OF THE OBSERVED ABSORPTIONS	235
APPENDIX II     DERIVATION OF THE RATE EXPRESSION DESCRIBING THE ENERGY-TRANSFER MECHANISM	238
APPENDIX III    ANALOG COMPUTER SIMULATION OF THE S( <sup>3</sup> P) PLUS ETHYLENE REACTIONS	239



## LIST OF TABLES

<u>Number</u>		<u>Page</u>
I-1	Energy Levels of the Atoms of the Group VI A Elements.....	3
I-2	Sources of Atomic Sulfur.....	11
I-3	Relative Rates and Arrhenius Parameters for S( <sup>3</sup> P) Additions.....	13
I-4	Product Distribution from the Reaction of S( <sup>1</sup> D <sub>2</sub> ) Atom with Olefins Relative to Episulfide.....	16
I-5	Half Lives of the Transients Formed in the Reactions of S( <sup>1</sup> D <sub>2</sub> ) with Acetylenes.....	18
I-6	Relative Rate Data for S( <sup>1</sup> D <sub>2</sub> ) Atoms.....	21
I-7	Absolute Rate Data for S( <sup>1</sup> S <sub>0</sub> ) Atoms.....	23
I-8	Relative Rate Data for the Reactions of O( <sup>3</sup> P) Atoms with Olefins.....	26
I-9	Rate Parameters for the Addition of Se( <sup>3</sup> P) Atoms with Olefins.....	29
I-10	Rate Parameters for Addition of Te( <sup>3</sup> P <sub>2</sub> ) Atoms to Olefins.....	30
II-1	Materials Used.....	45
II-2	Window Materials.....	50
II-3	Lamp Data.....	54
III-1	Determination of the Beer-Lambert Coefficient by Variation of the Flash Energy.....	66



# LIST OF TABLES (cont'd)

<u>Number</u>		<u>Page</u>
III-2	Determination of the $S(^3P_2)$ to $S(^3P_1)$ Peak Height Ratios at 55 kV.....	67
III-3	Determination of the $S(^3P_2)$ to $S(^3P_1)$ Peak Height Ratios at 9 kV.....	68
III-4	Determination of the $S(^3P_1)$ to $S(^3P_0)$ Peak Height Ratios.....	69
IV-1	Effect of Oxygen Pressure on the Rate of Decay of $S(^3P)$ Atoms.....	87
IV-2	Band Head Assignments for the $B^3\Sigma^- \leftarrow X^3\Sigma^-$ Transition in SO.....	95
IV-3	Band Head Assignments for the $D^3\Pi \leftarrow X^3\Sigma$ Transition in SO.....	98
IV-4	Absolute Rate Constants for the Reaction of $S(^3P_1)$ Atoms with Molecular Oxygen.....	104
IV-5	Absolute Rate Constants for the Reaction of Radicals and Atomic Species with Molecular Oxygen.....	105
V-1	Effect of NO Pressure on the Rate of Decay of $S(^3P_2)$ Atoms.....	112
V-2	Effect of Total Pressure on the Bimolecular Rate Constant.....	113



## LIST OF TABLES (cont'd)

<u>Number</u>		<u>Page</u>
V-3	Rate Constants for Bimolecular Recombination of Atomic Species.....	118
V-4	Rate Constants for Atomic and Radical Addition to NO.....	121
VI-1	First Order Rate of Decay as a Function of Ethylene Episulfide Concentration.....	123
VI-2	First Order Decay Rate of S( <sup>3</sup> P) Atoms in the Presence of Propylene Episulfide.....	127
VI-3	First Order Decay Rate of S( <sup>3</sup> P) Atoms in the Presence of <i>trans</i> -2-Butene Episulfide.....	130
VI-4	Rates Constants for Reaction of S( <sup>3</sup> P) Atoms with Episulfide at 25°C.....	132
VII-1	First Order Decay Rate of S( <sup>3</sup> P) Atoms in the Presence of Ethylene.....	145
VII-2	First Order Decay Rate of S( <sup>3</sup> P) Atoms in the Presence of Propylene.....	149
VII-3	First Order Decay Rate of S( <sup>3</sup> P) Atoms in the Presence of 1-Butene.....	152
VII-4	First Order Decay Rate of S( <sup>3</sup> P) Atoms in the Presence of <i>trans</i> -2-Butene.....	154



## LIST OF TABLES (cont'd)

<u>Number</u>		<u>Page</u>
VII-5	First Order Decay Rate of $S(^3P)$ Atoms in the Presence of Isobutene.....	156
VII-6	Effect of Tetramethylethylene Pressure on the Rate of Constant for Decay of $S(^3P)$ Atoms.....	159
VII-7	Absolute Rate Constants for the Reaction of $S(^3P)$ Atoms with Olefins at 298°K.....	163
VII-8	Temperature Dependence of the Bimolecular Rate Constant for the Reaction of $S(^3P)$ Atoms with Ethylene.....	166
VII-9	Temperature Dependence of the Bimolecular Rate Constant for the Reaction of $S(^3P)$ Atoms with Propylene.....	167
VII-10	Temperature Dependence of the Bimolecular Rate Constant for the Reaction of $S(^3P)$ Atoms with 1-Butene.....	168
VII-11	Temperature Dependence of the Bimolecular Rate Constant for the Reaction of $S(^3P)$ Atoms with Tetramethylethylene.....	170
VII-12	Absolute Rate Data for the Reactions of $S(^3P)$ Atoms with Olefins.....	173
VII-13	Arrhenius Parameters for the Reactions of Group VIA Atoms with Olefins.....	178



# LIST OF TABLES (cont'd)

<u>Number</u>		<u>Page</u>
VIII-1	First Order Decay Rate of $S(^3P_2)$ Atoms in the Presence of Acetylene.....	188
VIII-2	First Order Decay Rate of $S(^3P_2)$ Atoms in the Presence of Acetylene- $d_2$ .....	191
VIII-3	First Order Decay Rate of $S(^3P_2)$ Atoms in the Presence of Propyne.....	193
VIII-4	First Order Decay Rate of $S(^3P_2)$ Atoms in the Presence of 1-Butyne.....	195
VIII-5	First Order Decay Rate of $S(^3P_2)$ Atoms in the Presence of 2-Butyne.....	198
VIII-6	First Order Decay Rate of $S(^3P_2)$ Atoms in the Presence of 2-Pentyne.....	200
VIII-7	First Order Decay Rate of $S(^3P_2)$ Atoms in the Presence of 2-Perfluorobutyne.....	202
VIII-8	Room Temperature Rate Constants for the Reactions of $S(^3P)$ Atoms with Alkynes.....	204
VIII-9	Temperature Dependence of the Reaction of $S(^3P)$ Atoms with Acetylene.....	206
VIII-10	Temperature Dependence of the Reaction of $S(^3P)$ Atoms with Propyne.....	208
VIII-11	Absolute Rate Data for the Reaction of $S(^3P)$ Atoms with Propyne.....	210



LIST OF TABLES (cont'd)

<u>Number</u>		<u>Page</u>
VIII-12	Summary of Data for Isotope Effect Calculation.....	217



## LIST OF FIGURES

<u>Number</u>		<u>Page</u>
I-1	Grotrian Diagram for Sulfur.....	4
I-2	Absorption Spectrum of COS.....	7
I-3	Lamp Energy Output versus Width at Half-Peak Height	35
II-1	Reactor Components.....	47
II-2	Structural Details of Intersystem Connectors.....	49
II-3	Lamp-Cell Symmetry.....	51
II-4	Dependence of Flash Profile on Capacitance.....	52
II-5	Reciprocal of Object Distance versus Reciprocal of Image Distance from the Lens.,.....	55
II-6	Oven Temperature versus Operating Voltage.....	57
II-7	Electronic Schematic of Flash Apparatus.....	59
III-1	Optical Density from a Fully Exposed Cell, O.D., for $S(^3P_2)$ [180.7 nm].....	63
III-2	Optical Density from a Fully Exposed Cell, O.D. <sup>o</sup> , versus Optical Density from a Half Exposed Cell, O.D., for $S(^3P_1)$ [182.0 nm].....	64
III-3	Microdensitometered Peak Heights of $S(^3P) \rightarrow$ $S(^3S_1)$ Absorptions.....	71
III-4	Depletion of COS by Photolysis Flashes.....	73
III-5	First of Decay Plots of $S(^3P_2)$ in $CO_2$ and Argon....	75



## LIST OF FIGURES (cont'd)

<u>Number</u>		<u>Page</u>
IV-1	First Order Plot of Sulfur ( $^3\text{P}$ ) Atom Decay in the Presence of $\text{O}_2$ .....	85
IV-2	First Order Plots of $\text{S}(^3\text{P}_2)$ Decay.....	88
IV-3	Plot of the Observed First Order Rate Constant versus Molecular Oxygen Concentration.....	89
IV-4	Plot of Bimolecular Rate Constant versus Total Pressure for ( $^3\text{P}_2$ ) and ( $^3\text{P}_1$ ) Atoms.....	91
IV-5	Plot of Bimolecular Rate Constant versus Flash Energy.....	93
V-1	First Order Decay Plot of $\ln \text{S}(^3\text{P}_2)$ versus time	108
V-2	Second Order Decay Plot of $1/\text{S}(^3\text{P}_2)$ versus time	109
V-3	First Order Rate Constant as a Function of NO Pressure.....	111
V-4	Bimolecular Rate Constant as a Function of Total Pressure.....	114
V-5	Inverse of Bimolecular Rate Constant versus Inverse of Total Pressure.....	119
VI-1	First Order Decay Plot of $\text{S}(^3\text{P}_2)$ in the Presence of Ethylene Episulfide.....	124
VI-2	First Order Rate Constants of $\text{S}(^3\text{P})$ Atoms versus Ethylene Episulfide Concentration.....	126



## LIST OF FIGURES (cont'd)

<u>Number</u>		<u>Page</u>
VI-3	First Order Decay Plot of $S(^3P_2)$ Atoms in the Presence of Propylene Episulfide.....	128
VI-4	First Order Decay Plot of $S(^3P_2)$ Atoms in the Presence of <i>Trans</i> -2-Butene Episulfide.....	131
VI-5	The Absorption Spectrum of Ethylene Episulfide	135
VI-6	Empirical Correlation of the Bimolecular Rate Constant of Abstraction with the Number of Methyl Substituents on the Episulfide.....	139
VI-7	EHMO Potential Energy Curves for the Reaction of Sulfur Atom with Ethylene Episulfide.....	140
VII-1	First Order Decay Plot of $S(^3P_2)$ Atoms in the Presence of Ethylene.....	144
VII-2	First Order Rate Constants for Decay of $S(^3P)$ Atoms versus Ethylene Concentration.....	147
VII-3	Plot of the Bimolecular Rate Constant versus Total Pressure.....	148
VII-4	First Order Decay Plot of $S(^3P_2)$ Atoms in the Presence of Propylene.....	151
VII-5	First Order Decay Plot of $S(^3P_2)$ Atoms in the Presence of 1-Butyne.....	153
VII-6	First Order Decay Plot of $S(^3P_2)$ Atoms in the Presence of <i>trans</i> -2-Butene.....	155



## LIST OF FIGURES (cont'd)

<u>Number</u>		<u>Page</u>
VII-7	First Order Decay Plot of $S(^3P_2)$ Atoms in the Presence of Isobutene.....	158
VII-8	First Order Decay Plot of $S(^3P_2)$ Atoms in the Presence of Tetramethylethylene.....	160
VII-9	First Order Rate Constant for Decay of $S(^3P)$ Atoms versus Tetramethylethylene Concentration	161
VII-10	First Order Decay Plot of $S(^3P_2)$ Atoms in the Presence of Vinyl Fluoride.....	162
VII-11	Arrhenius Plot showing Temperature Dependence of the Reaction of $S(^3P)$ with Ethylene, Propylene, 1-Butene and Tetramethylethylene..	165
VII-12	Plot showing Correlation of $E_a$ for the Reaction with Olefin as a Function of the Ionization Potential of the Olefin.....	177
VII-13	Qualitative Depiction of Curve Crossing for Positive and Negative Temperature Dependence.	181
VII-14	Energy of Electronic Configurations as a Function of S-Ethylene Separation.....	183
VII-15	Energy of Electronic States as a Function of CCS Angle.....	184
VIII-1	First Order Decay Plot of $S(^3P_2)$ Atoms in the Presence of Acetylene.....	189



## LIST OF FIGURES (cont'd)

<u>Number</u>		<u>Page</u>
VIII-2	First Order Decay Plot of $S(^3P_2)$ Atoms in the Presence of Acetylene- $d_2$ .....	192
VIII-3	First Order Decay Plot of $S(^3P_2)$ Atoms in the Presence of Propyne.....	194
VIII-4	First Order Decay Plot of $S(^3P_2)$ Atoms in the Presence of 1-Butyne.....	196
VIII-5	First Order Decay Plot of $S(^3P_2)$ Atoms in the Presence of 2-Butyne.....	199
VIII-6	First Order Decay Plot of $S(^3P_2)$ Atoms in the Presence of 2-Pentyne.....	201
VIII-7	First Order Decay Plot of $S(^3P_2)$ Atoms in the Presence of 2-Butyne- $F_6$ .....	203
VIII-8	Arrhenius Plot showing Temperature Dependence of the Reaction of $S(^3P)$ with Acetylene and Propyne.....	207
VIII-9	Empirical Plot of Ionization Potential versus Arrhenius Activation Energy.....	212
VIII-10	State Correlation Diagram for the lowest Singlet and Triplet States of Thiirene.....	219
AIII-1	Schematic of Analogue Computer Program.....	240
AIII-2	Illustration of Match between Simple and Complex Reaction Schemes.....	242



## LIST OF FIGURES (cont'd)

<u>Number</u>		<u>Page</u>
AIII-3	Concentration Profiles as a Function of Time for the S( <sup>3</sup> P) Plus Ethylene Reaction.....	243



## CHAPTER I

### INTRODUCTION

The structure and reactivity of divalent atoms and radicals have been the subject of numerous investigations over the past two decades, the foremost examples being methylene<sup>1-4</sup> and ground state oxygen atoms<sup>5</sup>. Although a large quantity of mechanistic and kinetic data is currently available and several theoretical studies on the detailed reaction surfaces have been published, certain controversial aspects concerning the chemistry of these species remain.

Mechanistic studies of sulfur, the second row element in the Group VI A series, were initiated in these laboratories<sup>6</sup> in 1962. During subsequent years, the reactions of sulfur atoms with a wide variety of substrates were explored in conventional photolysis systems and a large number of relative rate data became available. It then became necessary to obtain absolute rate constants for these reactions in order that they may be properly evaluated. The technique of flash photolysis - kinetic absorption spectroscopy was utilized in the present investigation for this purpose.

To place the present investigation in proper perspective, a brief review will follow of the general chemistry and currently available sources of sulfur atoms; the chemistry of the other groups VI A elements, oxygen, selenium, and tellurium, and the technique of flash photolysis.



## A. The Sulfur Atom

The sulfur atom has sixteen electrons. In the  $s^2 p^4$  ground electron configuration the outer four electrons are distributed over three p-orbitals and give rise to five spectroscopic states designated as  $^3P_{2,1,0}$ ,  $^1D_2$  and  $^1S_0$ . The energy separation of the states<sup>7</sup> is tabulated in Table I-1, along with those of the other group VI A atoms. The spin orbital components of the  $^3P$  ground state are  $^3P_2$ ,  $^3P_1$  and  $^3P_0$  in increasing energy respectively. Radiative transitions from the  $^1D_2$  and  $^1S_0$  states to the  $^3P$  ground states are forbidden by rigid spin selection rules. Consequently, these excited atoms have long lifetimes and can undergo chemical reactions in addition to deactivation to the ground state. The wavelengths for various optical transitions in sulfur are depicted in Figure I-1.

## B. Sulfur Atom Sources

A good source compound for the production of sulfur atoms must absorb in a convenient region of the spectrum, be readily available, and produce sulfur atoms in clearly defined spectroscopic states. The remaining photofragments should be either neutral molecules or stable radicals which disappear solely by recombination or diffusion. The ultraviolet photolysis of  $SPF_3$ ,  $CS_2$ ,  $C_2H_4S$  and  $COS$  have been examined in this context.



TABLE I-1

Energy Levels of the Atoms of the  
Group VI A Elements<sup>a</sup>

Term	Energy, kcal/mole			
	O	S	Se	Te
$^3P_2$	0	0	0	0
$^3P_1$	0.45	1.14	5.69	13.5
$^3P_0$	0.65	1.64	7.25	13.6
$^1D_2$	45.4	26.4	27.4	30.2
$^1S_0$	96.6	63.4	64.2	66.3

a. from reference 7



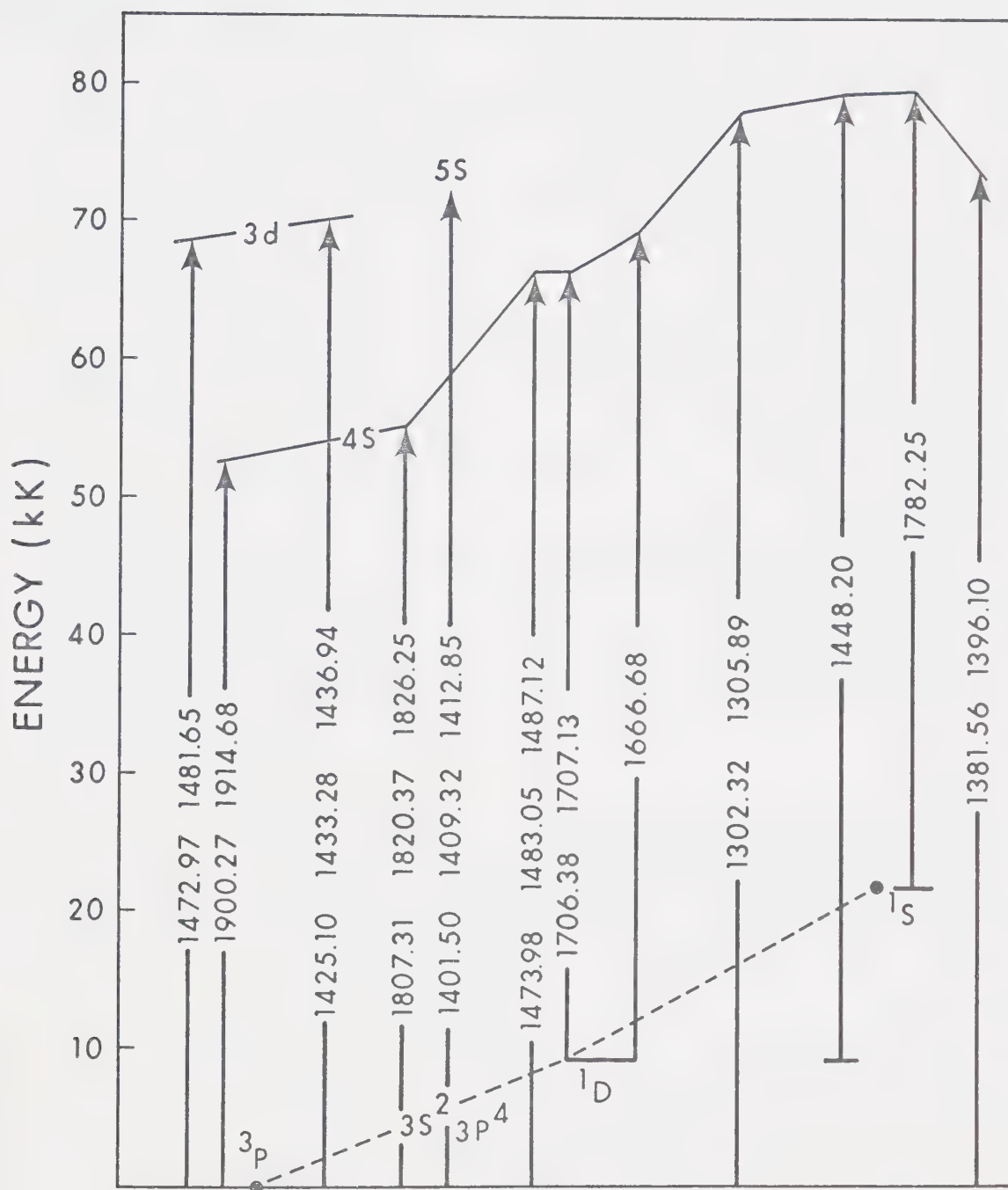
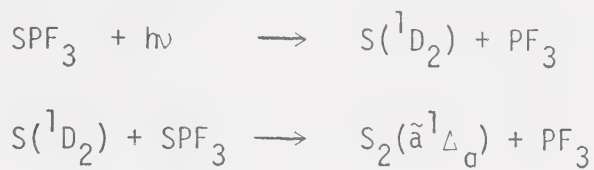


FIGURE I-1: Grotrian Diagram for Sulfur<sup>7</sup>.



1) The presence of sulfur atoms in the photolysis of  $\text{SPF}_3$  was proposed<sup>8</sup> on the basis of the observed spectrum of  $\text{S}_2(\tilde{\text{a}}^1\Delta_g)$ , via the reactions,

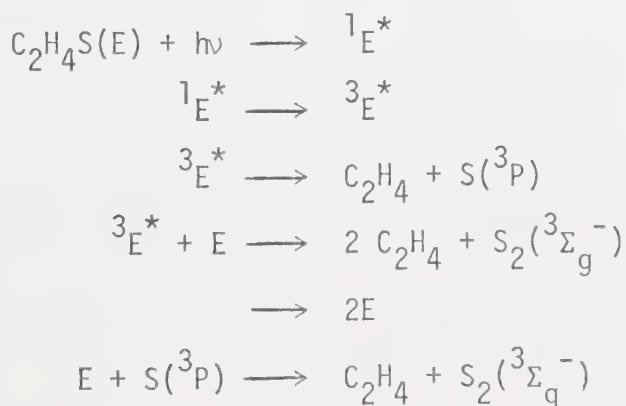


2) It has been demonstrated<sup>9</sup> that photolysis of  $\text{CS}_2$  in the 210-190 nm region produces ground state sulfur atoms,



and  $\text{CS}_2$  was later used<sup>10</sup> in quantitative rate determinations. In static photolysis<sup>11</sup>, however, the low yield of sulfur atoms and extensive copolymerization of CS radicals make  $\text{CS}_2$  an unattractive choice.

3) The appearance of the  $\text{S}_2(^3\Sigma_g^-)$  spectrum in the flash photolysis of ethylene episulfide<sup>12</sup> was interpreted in terms of the following reactions:



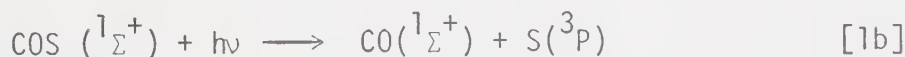


where the superscript on E denotes the multiplicity of the electronically excited states. However, recent work<sup>13</sup> has shown that decomposition to  $C_2H_4 + S(^3P)$  is completely quenched above about 75 torr total pressure. This, as well as other observations, militate against its use as a source in conventional photolysis.

4) The photolysis of COS has been extensively employed<sup>14</sup> as a sulfur atom source under a great variety of conditions. The first u.v. absorption band<sup>15</sup> extends from 260.0 nm to the vacuum region (Figure I-2). The mean radiative lifetime of the excited state is  $\sim 3 \times 10^{-7}$  sec. Although several transitions are buried in this broad absorption band, the long wavelength portion probably arises from a  $\Pi - \Pi^*$  excitation<sup>15,16</sup>. The primary photolytic dissociation into CO and  $S(^1D_2)$  atoms which is both spin and symmetry allowed, becomes energetically feasible at  $\lambda < 289.5$  nm (98.8 kcal/mole)



Although dissociation into ground state atoms is formally spin forbidden,



there is indirect evidence<sup>14</sup> that as much as 30% of the primary process proceeds via [1b].

The quantum yield of CO formation in the gas phase is



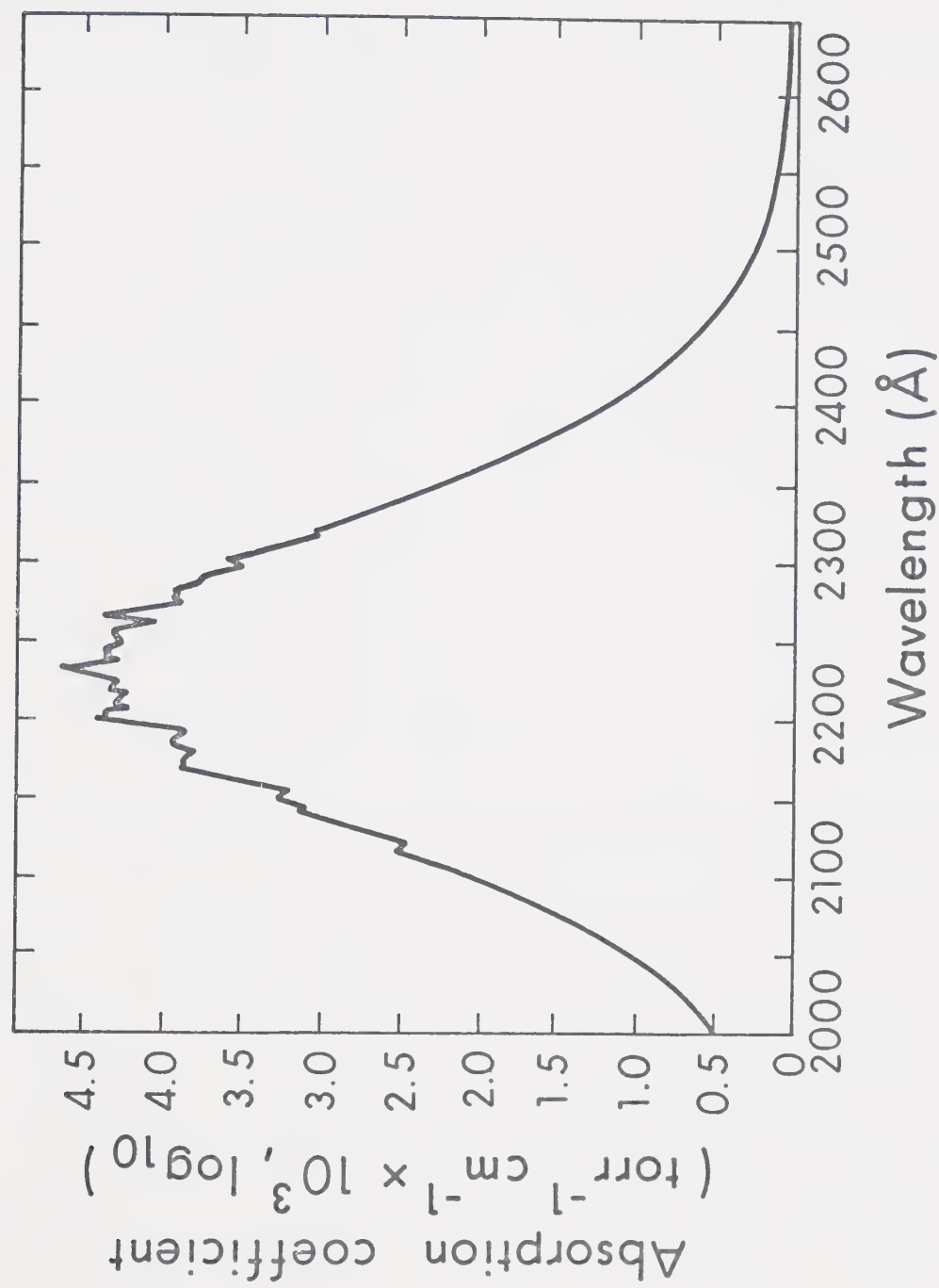


FIGURE I-2: Absorption Spectrum of  $\text{COS}^{15}$ .

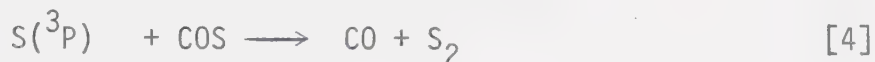


1.8 at  $\lambda = 249.0$  and  $228.8 \text{ nm}$ <sup>16</sup>, indicating that step [1] is followed by



Since step [2] should proceed with unit efficiency it is not known why  $\phi(\text{CO})$  is less than the expected value of 2.0. It may be related to an inherent inefficiency in the primary dissociation or the measurements themselves may be in error.

The  $\text{S}_2(\tilde{\text{a}}^1\Delta_g)$  state has been detected by flash spectroscopy<sup>18,17</sup>. Additional steps to be considered are

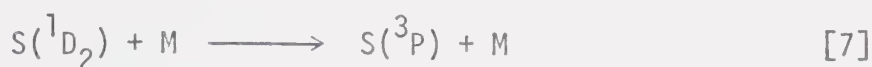


The possibility of collisional deactivation, step [3], has made it difficult to evaluate the extent of primary formation of  $\text{S}(^3\text{P}_{2,1,0})$  atoms via step [1b]. However, it would now appear that as much as thirty percent of the sulfur atoms are formed in the  $\text{S}(^3\text{P}_{2,1,0})$  state. At the outset of this investigation, only relative rates were available for  $k_4$ . Gunning and Strausz<sup>14</sup> obtained a value of 25 while Jakubowski, et al<sup>19</sup> reported a value of 83 for the ratio of  $\text{S}(^3\text{P})$  addition to ethylene relative to step [4]. Step [5] was postulated from observation of the formation of the  $\text{S}_2$  species<sup>12,20</sup>. The  $\text{S}_2$  species decays fairly rapidly via [6] to



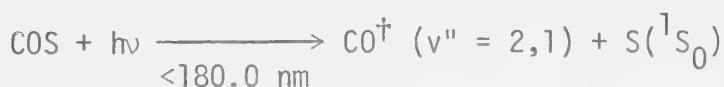
higher polymeric forms of sulfur. The rate of recombination<sup>12</sup> is pressure dependent, with values ranging from  $0.41 \times 10^9$  at 17 torr COS pressure to  $4.3 \times 10^9$  l mole<sup>-1</sup> sec<sup>-1</sup> at 410 torr.

Carbon dioxide, xenon, and argon have been demonstrated to be efficient quenchers of S(<sup>1</sup>D<sub>2</sub>) atoms<sup>14,21</sup>,



The values of  $k_7$  are  $>1 \times 10^{10}$ ,  $4 \times 10^9$  and  $1.1 \times 10^8$  l mole<sup>-1</sup> sec<sup>-1</sup> for CO<sub>2</sub>, Xe, and Ar respectively<sup>21-23</sup>. Since the rate of quenching by CO<sub>2</sub> is comparable to the rate of reaction of S(<sup>1</sup>D<sub>2</sub>) atoms with hydrocarbons, the introduction of a large excess of CO<sub>2</sub> will result in virtually complete deactivation of S(<sup>1</sup>D<sub>2</sub>) atoms to the ground state and thus the CO<sub>2</sub> + COS system is a "clean" source of S(<sup>3</sup>P) atoms.

Photolysis of COS in the vacuum ultraviolet produces a <sup>1</sup>S<sub>0</sub> sulfur atom and a vibrationally excited CO molecule<sup>24</sup>:



The COS spectrum in this region consists of two intense diffuse bands centered at 166.7 nm and 152.7 nm<sup>25</sup>. Due to restrictions imposed by symmetry, the transitions from S(<sup>1</sup>S<sub>0</sub>) to S(<sup>1</sup>D<sub>2</sub>) and S(<sup>3</sup>P<sub>2,1,0</sub>) have a combined rate<sup>24</sup> of  $6 \times 10^9$  l mole<sup>-1</sup> sec<sup>-1</sup>. Therefore, it has been possible to obtain rate data for reactions involving this species<sup>23,24,26</sup>.

Sulfur <sup>3</sup>P atoms can also be produced by the triplet



mercury photosensitization of COS<sup>16</sup>:



As in the case of direct u.v. photolysis, the primary quantum yield is 0.9.

In addition, COS has proven to be a good source of sulfur atoms in the liquid phase<sup>27</sup> due to its high solubility in organic solvent. The primary quantum yield is the same as in the gas phase, 0.9, but the relative yields of singlet to triplet atom formation are solvent-dependent and in general lower than in the gas phase. In inert solvents, essentially complete deactivation of the  $\text{S}(^1\text{D}_2)$  atoms to the ground state occurs.

From the preceeding discussion, it is obvious that COS fulfills all the prerequisites of a desirable photochemical source of sulfur atoms. In addition, the CO produced in the reaction can serve as a useful internal actinometer for the amounts of sulfur atoms produced and scavenged when other substrates are present. Table I-2 summarizes all the sulfur atom sources investigated to date.

### C. The Reactivity of Sulfur Atoms

It has been demonstrated<sup>14</sup> that both the nature and the rates of the chemical reactions of sulfur atoms are dependent on the spectroscopic state of the sulfur atom. The ground ( $^3\text{P}$ ) and metastable ( $^1\text{D}_2$ ) states have been extensively studied and some data



TABLE I-2

## Sources of Atomic Sulfur

Process	Quantum yield	Phase	Wavelength of photolysis, nm.	References
$\text{COS} \xrightarrow{h\nu} \text{CO} + \text{S}(^1\text{D}_2)$	0.9	Gas	260.0 - 210.0	16
$\text{COS} \xrightarrow{h\nu} \text{CO} + \text{S}(^1\text{D}_2)$	0.9	Liquid	300.0 - 210.0	27
$\text{COS} \xrightarrow{h\nu} \text{CO} + \text{S}(^1\text{S}_0), \text{S}(^1\text{D}_2)$	-	Gas	< 200.0	12, 26
$\text{COS} \xrightarrow{h\nu/\text{CO}_2} \text{CO} + \text{S}(^3\text{P})$	0.9	Gas	260.0 - 210.0	16
$\text{COS} \xrightarrow{\text{Hg}(^3\text{P}_1)} \text{CO} + \text{S}(^3\text{P})$	0.9	Gas	253.7	16
$\text{CS}_2 \xrightarrow{h\nu} \text{CS} + \text{S}(^3\text{P})$	-	Gas	< 210.0	9, 10
$\text{CH}_2=\text{CH}_2-\text{S} \xrightarrow{h\nu} \text{C}_2\text{H}_4 + \text{S}(^3\text{P})$	-	Gas	< 270.0	12
$\text{PF}_3\text{S} \xrightarrow{h\nu} \text{PF}_3 + \text{S}(^1\text{D}_2)$	-	Gas	< 230.0	8



are available for the reactivity of the ( $^1S_0$ ) state.

### 1. $S(^3P_{2,1,0})$ Atoms

Detailed studies have shown that  $S(^3P)$  atoms react readily with olefins and acetylenes. The reaction with simple olefins is uncomplicated in that it yields only the cyclic adduct, episulfide, in nearly quantitative yields. Table I-3 lists relative rate data for a variety of olefins. The increase in the rate of addition with increasing alkyl substitution on the double bond clearly manifests the electrophilic nature of ground state sulfur atoms. The reaction with *cis*-2-butene or *cis*-1,2-difluoroethylene is of particular interest because it is highly stereoselective, in contrast with the comparable reactions of  $O(^3P)$  atoms<sup>5</sup>.

To gain information about the nature and structure of the transition state involved in the addition of  $S(^3P)$  atoms to ethylene, the secondary kinetic isotope effects were measured for addition to ethylene-1,1- $d_2$ , *cis*-ethylene- $d_2$ , *trans*-ethylene- $d_2$ , and ethylene- $d_4$ <sup>28</sup>. A complete study of the effect of isotopic substitution in this reaction has recently been published<sup>29</sup>. Extensive theoretical calculations<sup>30-35</sup> are now available on the sulfur plus ethylene reaction path and the ground and excited states of ethylene episulfide. The calculations predict that in the reaction with sulfur  $^3P$  atoms, the product episulfide is formed in a distorted triplet state with the sulfur closer to one methylene



TABLE I-3

Relative Rates and Arrhenius Parameters  
For S(<sup>3</sup>P) Additions <sup>c</sup>

	$k/k_{\text{Eth}}^a$	$k/k_{\text{Eth}}^b$	$E_{\text{Eth}} - E$	$A/A_{\text{Eth}}$
$\text{CH}_2=\text{CH}_2$	1.0	1.0	0.0	1.0
$\text{CH}_3-\text{CH}=\text{CH}_2$	6.8	6.7	1.14	1.0
<i>cis</i> $\text{CH}_3-\text{CH}=\text{CH}-\text{CH}_3$	18	17	2.09	0.53
<i>trans</i> $\text{CH}_3-\text{CH}=\text{CH}-\text{CH}_3$	23	18	2.01	0.65
$\text{CH}_3\cdot\text{CH}_2-\text{CH}=\text{CH}_2$	11	-	-	-
$(\text{CH}_3)_2\text{C}=\text{CH}_2$	54	50	2.36	0.97
$(\text{CH}_3)_2\text{C}=\text{CH}(\text{CH}_3)$	88	77	3.01	0.51
$(\text{CH}_3)_2\text{C}=\text{C}(\text{CH}_3)_2$	131	135	3.36	0.50
$\text{CH}_2=\text{CH}-\text{CH}=\text{CH}_2$	77	72	2.04	2.4
$\text{CH}_3\text{CH}_2\text{C}(\text{CH}_3)=\text{CH}_2$	63	87	2.83	0.78
$\text{CH}_3\text{CH}_2\text{CH}_2=\text{CH}_2$	11	13	1.72	0.75
$\text{C}-\text{C}_5\text{H}_8$	21	24	2.15	0.67
$\text{CH}_2=\text{CHF}$	-	0.42	-0.73	1.40
<i>cis</i> $\text{CHF}=\text{CHF}$	-	0.018	-2.71	1.66
<i>trans</i> $\text{CHF}=\text{CHF}$	-	0.043	-2.62	3.36
$\text{CF}_2=\text{CH}_2$	-	0.10	-1.7	1.9
$\text{CF}_2=\text{CFH}$	-	0.07	-2.0	2.1
$\text{CF}_2=\text{CF}_2$	-	0.14	-1.38	1.35
$\text{CH}_3\text{CF}=\text{CH}_2$	2.6	-	-	-



TABLE I-3 (continued)

	$k/k_{\text{Eth}}^{\text{a}}$	$k/k_{\text{Eth}}^{\text{b}}$	$E_{\text{Eth}} - E$	$A/A_{\text{Eth}}$
$\text{CF}_3\text{CH}=\text{CH}_2$	-	0.104	-1.46	1.18
$\text{CF}_3(\text{CH}_3)\text{C}=\text{CH}_2$	1.2	-	-	-
$\text{CF}_3\text{CF}_2-\text{CH}=\text{CH}_2$	0.094	-	-	-
$\text{SiF}_3-\text{CH}=\text{CH}_2$	0.4	-	-	-
$\text{CH}_2=\text{CHCl}$	1.4	1.4	-0.52	3.4
<i>trans</i> $\text{CHCl}=\text{CHCl}$	>4.6	-	-	-
<i>cis</i> $\text{CDH}=\text{CDH}$	-	1.04	-	-
<i>trans</i> $\text{CDH}=\text{CDH}$	-	1.12	-	-
$\text{CD}_2=\text{CH}_2$	-	1.07	-	-
$\text{CD}_2=\text{CD}_2$	-	1.144	-	-
$\text{CH}\equiv\text{CH}$	0.35	-	-2.03	6.2
$\text{CD}_3-\text{C}\equiv\text{CH}$	2.3	-	-0.89	6.2
$\text{CH}_3-\text{C}\equiv\text{C}-\text{CH}_3$	29	24	1.32	2.7

a. Measured at 27°C

b. Calculated from Arrhenius parameters

c. Reference 28



group than the other. The barrier to rotation of the distant methylene group is some 3 kcal higher than the total energy content of the molecule.

The primary adduct of the reaction of  $S(^3P)$  atoms with acetylenes could be thiirene,  $\text{H}_2\text{C}=\text{CH}_2\text{S}$ , or an unsaturated biradical  $\text{H}_2\text{C}=\text{CH}_2\text{S}^\cdot$ . It has been shown<sup>11</sup> that the addition of a limited quantity of  $\text{CO}_2$  to a reaction system containing  $S(^1D_2)$  atoms causes a reduction in thiophene yield. Thus, it can be concluded that the triplet adduct undergoes more extensive polymerization relative to the product of  $S(^1D_2)$  plus acetylene reaction.

Unlike  $O(^3P)$  atoms<sup>5</sup>,  $S(^3P)$  atoms do not abstract hydrogen from paraffinic C-H bonds. This can be attributed to the lower bond strength of the S-H bond. Both  $\text{Se}(^3P)$  and  $\text{Te}(^3P)$ , like  $S(^3P)$ , are unreactive towards paraffins.  $O(^3P)$  is unique among the group VI A atoms in this respect.

## 2. $S(^1D_2)$ Atoms

Since  $S(^1D_2)$  atoms are metastable, their chemical reactivity can be deduced from product and kinetic analysis<sup>34</sup>.  $S(^1D_2)$  atoms react with olefins to yield episulfides, vinylic and alkenyl mercaptans. The mercaptan product yields are nearly statistical. Product distributions obtained for various olefins in the gas, liquid, and solid phases are given in Table I-4. At present it is not known how much of the episulfide is produced via a state and symmetry allowed addition of  $S(^1D_2)$  atoms to the double bond,



TABLE I-4

Product Distribution from the Reaction of  $S(^1D_2)$  Atom  
with Olefins Relative to Episulfide. <sup>35</sup>

Gas Phase	Vinylic	Alkenyl
	Mercaptan	
$C_2H_4$	1.0	-
$C_3H_6$	0.31	0.31
<i>i</i> - $C_4H_8$	0.21	0.57
2- $C_4H_8$	nil	0.47
1- $C_4H_8$	0.20	0.51
$(CH_3)_2CCHCH_3$	nil	0.72
<u>Liquid Phase</u>		
$C_2H_4$	0.44	-
$C_3H_6$	0.15	0.18
<u>Solid at -196°</u>		
$C_2H_4$	0.2	-
$C_3H_6$	0.1	0.03





and what fraction arises from addition of  $S(^3P)$  atoms via,



Relative rate data<sup>35</sup> derived from the  $S(^1D_2) + \text{olefin}$  system yielded episulfide ratios quite different from the  $S(^3P)$  plus olefin systems, and the sensitivities of these ratios to the relative concentrations of the two olefins demonstrated the occurrence of the deactivation reaction.

The primary addition products for the reaction of  $S(^1D_2)$  atoms with acetylenes are unstable entities. In the reaction with acetylene, the retrievable products are  $CS_2$ , benzene and thiophene in low, pressure dependent yields. Flash photolysis-mass spectrometric studies have shown the presence of one or more species with a mass corresponding to an acetylene-sulfur adduct<sup>36</sup>. The lifetime of these species varied with the alkyne used, but was of the order of  $\sim 1$  sec (see Table I-5).

A reasonable structure would be either thiirene or thioketene, since the long lifetimes are not consistent with excited or free radical intermediates as carriers.

The intermediacy of thiirene in this system is substantiated by the photolysis of 1,2,3-thiadiazole and its 4-



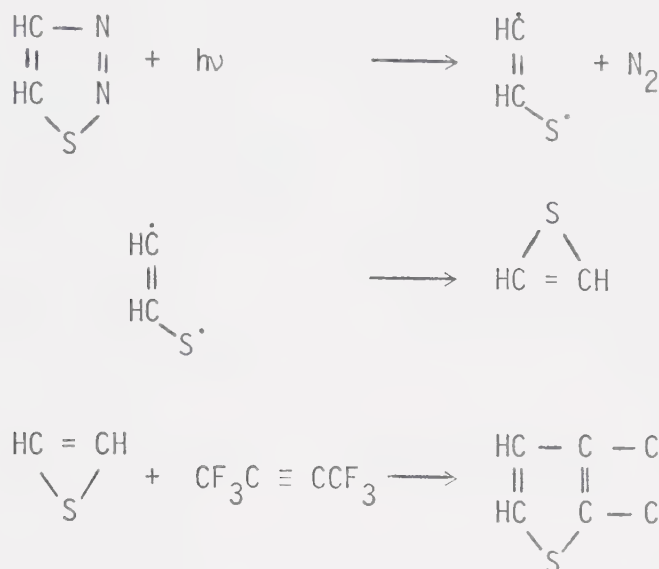
TABLE I-5

Half Lives of the Transients Formed in  
the Reactions of  $S(^1D_2)$  with Acetylenes<sup>36</sup>

Alkyne	Decay Half Life (sec)
Acetylene	2
Propyne	5
Butyne-2	7
Hexafluorobutyne-2	0.1



methyl and 5-methyl derivatives<sup>37</sup> in the presence of hexafluoro-butene-2:



If thiirene is the intermediate, then the two hydrogen positions should be equivalent. Substitution of a methyl group in either the 5- or 4- positions of the thiadiazole leads to the same compound, 2,3 *bis* (trifluoromethyl) -5- methylthiophene as the sole thiophene product. This would be inconsistent with a thioketene intermediate.

Reactions with paraffins yield mercaptans which are probably formed by an insertive attack on the C-H bond. In the gas phase, the insertion is indiscriminate but some selectivity has been observed in the liquid phase. The rate of insertion increases with increasing kinetic energy of the sulfur atom, e.g. by photolyzing COS at shorter wavelengths, and therefore the process appears to require an activation energy. Parallel to



insertion, the  $S(^1D_2)$  atoms can be deactivated to the ground state.



Absolute rate determinations for reactions involving  $S(^1D_2)$  have been complicated by the inability to directly monitor this species. However, a lower limit of  $4 \times 10^{10} \text{ l mole}^{-1} \text{ sec}^{-1}$  has been determined<sup>21</sup> for the rate of abstraction from COS



by monitoring the  $S_2(g^1\Delta_u \longleftarrow a^1\Delta_g)$  absorption spectrum. This corresponds to a collision efficiency of one in four. From this, lower limits can be set for a number of other reactions and these are listed in Table I-6. The extreme efficiency of these reactions is evident.

### 3. $S(^1S_0)$ Atoms

The only information on the reactivity of this species are the recent studies<sup>23,24,26</sup> on the absolute rates of quenching and/or reaction with various substrates. Product analysis has not been attempted. It was found that the  $S(^1S_0)$  state is relatively long-lived (it decays over  $\sim 100 \mu\text{sec}$ ) due to the forbidden nature of the transition to the ground state. The species was monitored either by its absorption at 178.2 nm ( $^1P_1 \longleftarrow ^1S_0$ )



TABLE I-6

Relative Rate Data for S( $^1D_2$ ) Atoms <sup>a</sup>

Reactant	$k_n/k_{C_2H_4}$
$C_2H_6$	$1.7 \times 10^{-1}$
$C_2H_4$	1.0
$CH_4$	$7.6 \times 10^{-2}$
$CO_2$	$2.4 \times 10^{-1}$
NO	$6.8 \times 10^{-1}$
CO	$1.9 \times 10^{-1}$
$N_2$	$6.2 \times 10^{-2}$
$H_2$	$2.2 \times 10^{-1}$
Ar	$9.7 \times 10^{-3}$
Kr	$2.8 \times 10^{-2}$
Xe	$1.6 \times 10^{-1}$
$C_2H_2$ <sup>b</sup>	$6.0 \times 10^{-1}$

a. reference 38

b. reference 39



or by emission at 772.5 ( $^1S_0 \rightarrow ^1D_2$ ) and at 458.9 nm ( $^1S_0 \rightarrow ^3P_1$ ). A summary of the absolute rate data derived from these experiments is given in Table I-7. Considerably more work with this species is warranted.

#### D. Reactivity of Other Ground State, Group VI A Atoms

##### 1. $O(^3P)$ Atoms

Of all the Group VI A atoms, oxygen has the longest history of investigation. The reactions it undergoes are thoroughly documented<sup>5</sup> and the products well established. However, even for this species, measurements of absolute rate data<sup>40-59</sup> are of more recent origin.

The products of the  $O(^3P)$  plus olefin reaction are epoxides, aldehydes and ketones in varying proportions depending on the nature of the olefin. The original mechanism proposed by Cvetanovic<sup>5</sup> featured a triplet biradical intermediate which could either cyclize to epoxide or undergo an intramolecular H-atom or  $CH_3$  radical shift to a carbonyl compound.

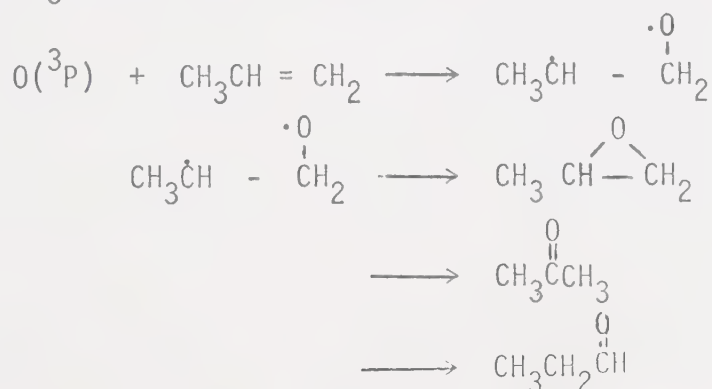




TABLE I-7

Absolute Rate Data for  $S(^1S_0)$  Atoms

Molecule	$k$ ( $l \text{ mole}^{-1} \text{ sec}^{-1}$ )
Ar	$< 2.1 \times 10^4$ a $< 3.0 \times 10^6$ c
$H_2$	$4.6 \times 10^5$ a $2.4 \times 10^6$ b
$O_2$	$3.7 \times 10^8$ a
CO	$< 2.1 \times 10^5$ a
NO	$1.9 \times 10^{11}$ a
$NO_2$	$3.7 \times 10^{11}$ a
$N_2O$	$< 1.8 \times 10^6$ a
$CO_2$	$< 3.6 \times 10^4$ a
COS	$2.4 \times 10^8$ a $6.0 \times 10^9$ b
$CS_2$	$4.9 \times 10^{11}$ a
$SO_2$	$6.0 \times 10^{10}$ a
$H_2S$	$3.0 \times 10^{11}$ a
$CH_4$	$9.0 \times 10^5$ a
$C_2H_6$	$2.6 \times 10^7$ a
$C_2H_4$	$7.8 \times 10^7$ a

/continued...



TABLE I-7 (continued)

Molecule	$k$ (1 mole <sup>-1</sup> sec <sup>-1</sup> )
$C_2H_2$	$9.6 \times 10^7$ a
Xe	$< 3.0 \times 10^6$ c
He	$< 7.8 \times 10^5$ c

a. from reference 26

b. from reference 24

c. from reference 23



The driving force behind carbonyl formation is presumably the high strength of the C = O bond. Relative rate data<sup>5,60,61</sup>, Table I-8, obtained from conventional studies are remarkably similar to those obtained for S(<sup>3</sup>P) atom reactions except that the latter appear to be somewhat more sensitive to molecular structure.

The room temperature reaction with *cis*-2-butene affords *cis*- and *trans*- epoxides in nearly equivalent yields.

However, it has been demonstrated that the relative isomer yields are temperature dependent<sup>62-65</sup> and a hydrogen bridged intermediate was proposed in which hydrogen bonding restricts rotation about the C-C bond. For example,



Neither of these two alternatives is entirely satisfactory and in fact recent *ab initio* calculations<sup>66</sup> on the O(<sup>3</sup>P) plus C<sub>2</sub>H<sub>4</sub> reaction path and the ground and excited states of ethylene epoxide indicate that in the first excited triplet state of the epoxide the rotational barrier is prohibitively high and rapid intersystem crossing to a ground state surface takes place from where the isomerization occurs. The nature of the ground state surface is not known but is probably ionic in character.

The addition of O(<sup>3</sup>P) atoms to acetylenes is characterized by extensive cracking of the primary adduct. The non-intervention of oxirene has been shown in recent comparative studies of



TABLE I-8

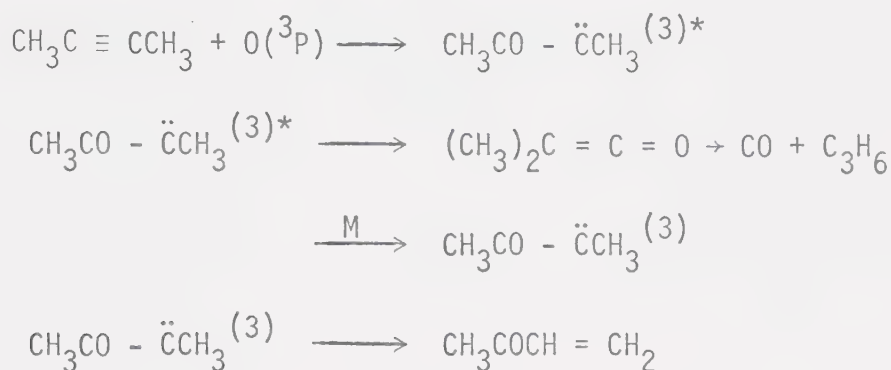
Relative Rate Data for the Reactions  
of  $O(^3P)$  Atoms with Olefins <sup>a</sup>

Olefin	$k/k_{\text{eth}}$	$E_a(\text{eth}) - E_a$ (kcal, mole <sup>-1</sup> )	$A/A_{\text{eth}}$
Ethylene	1.0	0	1.0
Propylene	5.8	-	-
1-Butene	5.8	1.2	0.73
<i>trans</i> -2-butene	28	-	-
<i>cis</i> -2-butene	24	-	-
Isobutene	25	2.13	0.66
Cyclopentene	30	2.0	1.0
Trimethylethylene	79	2.5	1.1
Tetramethylethylene	109	2.6	1.2
1-3 Butadiene	24	1.8	1.1

a. Reference 5



the O plus dimethyl acetylene system<sup>67</sup>. The principal products of the reaction are CO and C<sub>3</sub>H<sub>6</sub> in nearly equal yields along with methyl vinyl ketone. CO production is suppressed and methyl vinyl ketone production enhanced by pressure, but the sum is pressure independent. Therefore, the reaction sequence would appear to be:



Thus, at very high pressures, the only major product should be methyl vinyl ketone. Methyl acetylene follows a similar reaction path<sup>67</sup>, giving as principal products CO and ethylene from the decomposition of the methyl ketene intermediate, acrolein, and several hydrocarbons derivable from free radical precursors. The reaction of O(<sup>3</sup>P) atoms with acetylene<sup>68-70</sup> yields CO, C<sub>3</sub>H<sub>4</sub>, H<sub>2</sub> and solid polymer as final products with ketene as a definite intermediate in a complex overall reaction scheme.

## 2. Se(<sup>3</sup>P) Atoms

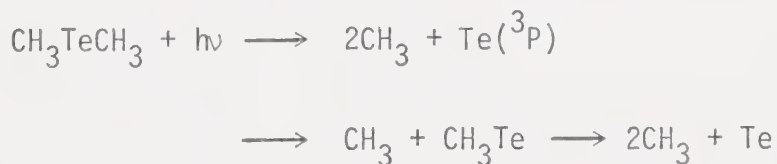
Although more limited in scope, the data available<sup>71-74</sup> on the reactions of Se(<sup>3</sup>P) atoms with olefins are useful in that they complement the trends already established for oxygen and



sulfur. Absolute rates and Arrhenius parameters with a number of olefins have been determined<sup>71,72</sup> via the technique of flash photolysis and employing the photolysis of  $\text{CSe}_2$  as a source of  $\text{Se}(^3\text{P})$  atoms. Identification of the primary adduct was established by spectroscopic observation of the episelenide. Episelenides are very unstable and decompose readily to  $\text{Se}_2$  plus two olefins, and therefore the system is not very suitable for conventional photolysis experiments. Table I-9 summarizes the kinetic data presently available. The selectivity parallels quite closely that obtained for  $\text{S}(^3\text{P})$  atoms and the trends in  $E_a$  are directly comparable to those observed in  $\text{S}(^3\text{P})$  and  $\text{O}(^3\text{P})$  systems.

### 3. $\text{Te}(^3\text{P})$ Atoms

The reactions of  $\text{Te}(^3\text{P})$  atoms have been investigated by the technique of flash photolysis<sup>75,76</sup>.  $\text{Te}(^3\text{P})$  atoms were produced by flashing dimethyltelluride, and the unstable epitelluride adduct which formed in the presence of olefins was detected by kinetic absorption spectroscopy and kinetic mass spectrometry.



The rate constants and Arrhenius parameters available are summarized in Table I-10. The selectivity of  $\text{Te}(^3\text{P})$  atoms is somewhat enhanced relative to the other Group IV A atoms. However, the relative trend in  $E_a$  established for  $\text{O}(^3\text{P})$ ,  $\text{S}(^3\text{P})$  and  $\text{Se}(^3\text{P})$



TABLE I-9

Rate Parameters for the Addition  
of  $\text{Se}(^3\text{P})$  Atoms to Olefins <sup>a</sup>

Olefin	$k/k_{\text{eth}}$	$E_A$ (kcal mole <sup>-1</sup> )	$A \times 10^{-10}$ (l mole <sup>-1</sup> sec <sup>-1</sup> )
ethylene	1	2.8	1.1
propylene	3.5	2.4	1.3
1-butene	7.1	2.3	3.1
<i>cis</i> -2-butene	24	1.2	2.0
<i>trans</i> -2-butene	56	0.6	1.7
isobutene	45	1.0	2.4
1,3-butadiene	98	0.9	5.3

a. references 71 and 72



TABLE I-10

Rate Parameters for Addition of  $\text{Te}(^3\text{P}_2)$ Atoms to Olefins <sup>a</sup>

Olefin	$k/k_{\text{eth}}$ <sup>b</sup>	$E_A$ (kcal mole <sup>-1</sup> )	$\log A$ (l mole <sup>-1</sup> sec <sup>-1</sup> )
ethylene	1	2.5	8.9
propylene	9.4	0.6	8.5
1-butene	12	-	-
<i>cis</i> -2-butene	50	-	-
tetramethyl- ethylene	308	-1.6	8.4

a. reference 76

b.  $T = 25^\circ\text{C}$



is maintained for  $\text{Te}(^3\text{P})$ . The slow decrease in the A-factor may be attributed to the greater importance of steric considerations in the case of tellurium relative to the other Group VI A atoms.

## E. Flash Photolysis

### 1. Development

The technique of flash photolysis was developed by Norrish and Porter<sup>77</sup> in 1949. The equipment was further described by Porter in a 1950 publication<sup>78</sup>. Components of such a system had previously been described, for example, White's spectroscopic flash lamp (1  $\mu\text{F}$  at 15 kV) in 1940<sup>79</sup>. However, the apparatus used by Norrish and Porter was the first complete assembly to fit the required specifications. The flash lamp was filled with 50 torr Krypton and was fired at 500  $\mu\text{F}$  and 4 kV (4000 joules), and had a lifetime of 1.5 milliseconds. The spectroscopic lamp was filled with 100 torr Krypton and was fired at 70  $\mu\text{F}$  and 4.5 kV. It had a lifetime of 50  $\mu\text{seconds}$  and was thus capable of monitoring transients having lifetimes in the millisecond region. The basic design was adopted in 1950 by Herzberg and Ramsay<sup>80</sup> who developed equipment with extremely long path lengths, allowing the detection of very small concentrations of absorbents. A photomultiplier was used in 1951 for direct kinetic measurements of the rate of recombination of I atoms<sup>81</sup>.

The originators of this equipment followed two diverging paths of research. Porter applied the technique largely to the



study of liquid phase systems and Norrish, largely to the study of gas phase systems. The method has since been applied to studies at low temperatures<sup>82</sup> and to temperatures as high as 1273°K<sup>83</sup>. It has also been expanded to include the generation and monitoring of transients in the vacuum ultra-violet<sup>84,85</sup>. At present laser technology is providing continuing improvements in the apparatus, allowing studies to be carried out at shorter time scales (nanoseconds and picoseconds)<sup>86</sup>. It is interesting that even now, commercial apparatus is not readily available and this may have accelerated the development of modifications in the basic design first described by Norrish and Porter<sup>77</sup>.

## 2. Types of Flash Photolysis Apparatus

Flash apparatus can be separated into two classes, depending on the method of detection: those employing flash spectroscopy and those employing kinetic spectrophotometry. In the first technique, the spectrum is recorded photographically at a given delay; by repeating this procedure at various delays a time profile may be obtained for the transients observable in that spectral region. Where kinetic spectrophotometry is used, the spectrograph and photographic plate are replaced by a monochromator (or a filter system) and a photoelectric detection system. This then allows the continuous monitoring of a given wavelength as a function of time.



The two techniques are complementary. For the initial study of a system, flash spectroscopy is preferred since it allows identification of spectra and clarification of the various processes in the system; in other words, it provides a more comprehensive look at the system. However, once the overall features of a system have been established, it then may be desirable to monitor preselected wavelengths in order to follow the kinetics of the system. This has the advantage of greater time economy since a total decay curve is obtained at each flash. Kinetic spectrophotometry should therefore not be utilized to study a system which has not been previously examined in a more detailed manner by flash spectroscopy, since the fate of the decaying species would be uncertain.

### 3. Light Sources

An area critical to the success of a flash photolysis apparatus is the type of lamp used. The flash lamp is required to produce a sufficient concentration of intermediates in order to allow monitoring by a given detection technique, but the efficiency required of the lamp must be compatible with the lifetime of the observed transient. This is an important consideration in the investigation of very short-lived species, since the greater the energy outlay, the longer the time profile of the light output. The design of any given apparatus must therefore be a compromise between energy output and time profile for decay.



The extension of investigations to increasingly shorter decay times<sup>86</sup> has required the development of consistently better detection systems. Figure I-3 illustrates a rough correlation between energy output and flash duration (width at half peak height)<sup>87</sup>. Some improvement in the total energy output can be obtained to a limited degree without sacrificing delay times by decreasing capacitance and increasing voltage. An alternative method is to arrange a number of lamps with individual capacitors around the cell, and firing these lamps from a common trigger.

A typical flash lamp is filled with krypton and provides a continuum extending into the vacuum ultraviolet. For a given flash lamp, it has been demonstrated that ~15% of the available energy is dissipated within the reaction cell in the 200-400 nm region<sup>88</sup>. To maximize this incident radiation reflectors consisting of surfaces coated with magnesium oxide are frequently placed around the lamp-cell assembly.

The characteristics of the lamp undergo little change with temperature<sup>88</sup>. A common design for temperature-controlled systems encloses the entire cell-lamp assembly inside a thermostated oven. Another design is a jacketed cell in which a temperature-controlled liquid with the required transparency is circulated. Two examples of this liquid are silicon oil, which transmits above 350 nm and can be heated to 250°C, and ethylene glycol, which can be used below 240 nm but can only be heated to 140°C<sup>88</sup>. An additional advantage of this technique is the



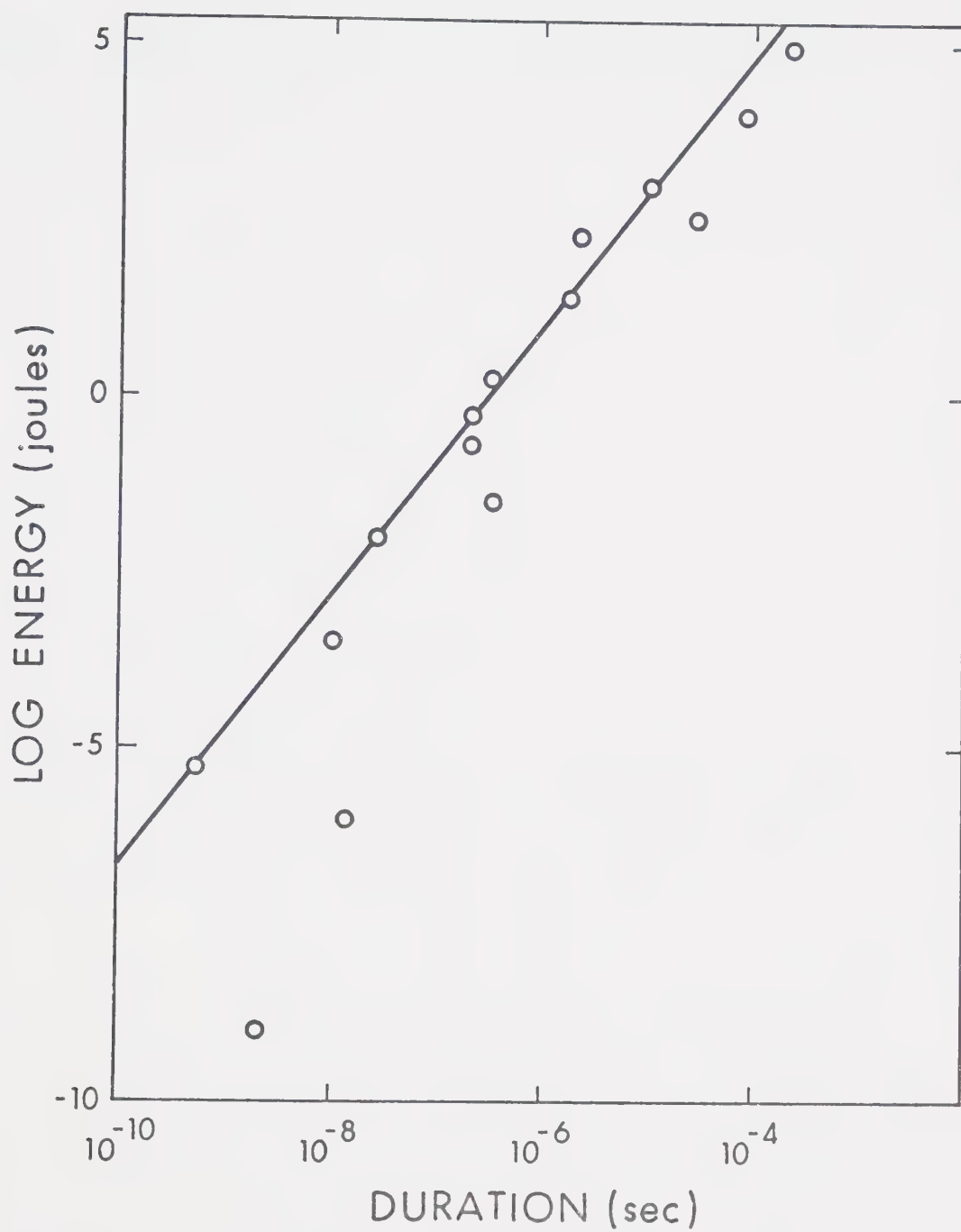


FIGURE I-3: Lamp Energy Output versus Width at Half Peak Height<sup>52</sup>.



ability to dissolve filtering dyes into the heating solvent.

To ensure that reproducible flash profiles can be obtained, an essential requirement of an apparatus used for kinetic measurements is that a mercury-free system be used to fill the lamp<sup>86</sup>.

#### 4. Electronics

##### i, Triggering

In the first stages of development a spark gap was used to trigger the spectroscopic lamp. A trigger circuit initiated by the delay apparatus discharges a high voltage from a side electrode across the gap. This causes electrical breakdown between the two primary electrodes and the capacitor discharges across the spectroscopic lamp. Thyretrons and ignitrons have since replaced this device. Advantages of the ignitron are economy and simplicity coupled with low-radiation characteristics<sup>89</sup>.

##### ii. Delays

Pre-set delays can be achieved by mechanical devices for delay times in the millisecond range. For microsecond delays, electronic circuitry must be used. A novel delay technique has been described by Porter<sup>90</sup> for a nanosecond laser-photolysis apparatus. Variations in the path length travelled by a u.v. pulse used to trigger a spark gap were utilized as a means of controlling delay times. Since light travels 30 cm per nano-



second, the delays could be easily and accurately determined by the use of an optical system of mirrors.

### iii. Detection

Although photographic recording has many inherent advantages, the necessity of detecting short, low-energy pulses has accelerated the development of extremely sensitive photoelectric detection devices. Coupling these devices with repetitive techniques, extremely small signals may be successfully monitored. As a result, optical states having rates of decay as short as  $10^{12} \text{ sec}^{-1}$  have been successfully detected<sup>91</sup>.

## 5. Measurement of Absorption Densities

Spectroscopic investigations of transient substances are frequently complicated because neither the concentration nor the absolute extinction coefficients are known. Relative magnitudes obtained from plate photometry allow the determination of first order rates of the transient. General behaviour can also be studied from this data. If the reaction in the transient is higher than first order, then the concentration under a given set of conditions must be determined. Comparison with all other data can then be made using one of two techniques.

The density of the photographic image is dependent on the intensity and duration of the incident light and on the  $\gamma$  value



of the plate.  $\gamma$  is designated as the slope of the straight-line portion of the film response curve (plot of density versus exposure) and is dependent on emulsion characteristics and the degree of development. If, for any given emulsion, the plates are processed under controlled conditions,  $\gamma$  is constant and the plates can be interpreted by direct comparison. Alternatively, each individual plate can be calibrated with the use of a set of standard density wedges. This method is more reliable since one has a constant check of the value of  $\gamma$ , but it is not necessarily more accurate than the first method performed with due care since in this case  $\gamma$  must be invariant. Also, the calibration of each separate plate is time consuming, and therefore this method is generally used as a check on the other.

## 6. Determination of Absolute Concentration

The absolute concentration of a short-lived species may be obtained by one of two methods, both of which require that the kinetics of the system be known. If this is so, then it may be possible to determine the rate of depletion of the starting material or the rate of formation of the final product by conventional analytical techniques. The concentration of the intermediate can then be calculated. Alternatively the per cent depletion of the starting material can be measured by spectroscopic means. The conversion of these types of measurements to absolute concentration data is not necessarily a simple task since they may be



associated with relatively large errors arising from the small quantities and low conversions often employed in flash photolytic studies.

## 7. Complications of Detection in the Vacuum Ultraviolet

Additional problems exist for operation in the vacuum ultraviolet. The exclusion of all air from the optical path is the primary concern, since oxygen absorbs strongly below 190 nm. Furthermore, considerable expense is involved in the acquisition of a grating instrument with an efficient pumping system. Special window and lens materials must be used since quartz only transmits above ~185.0 nm. Materials commonly used are suprasil, sapphire and lithium fluoride (see Table II-2 for the transmission characteristics of window materials). Normal film is unsuitable due to the absorption in this region by the binding medium. To overcome this problem, the light-sensitive grains actually protrude from the surface of the film; hence it is extremely prone to abrasion damage.

## F. Aim of the Present Investigation

At the time this project was initiated, a great deal of information was available on the chemistry of sulfur atoms. The gross features of the reactions of ( $^1D_2$ ) and ( $^3P$ ) states with COS, paraffins, olefins and acetylenes had been delineated and a substantial amount of relative rate data had been reported.



At that point it was obvious that absolute rate constants, activation energies and Arrhenius parameters for these reactions would have to be determined in order to correctly evaluate the reactivity of sulfur atoms. The main purpose of this investigation was therefore to measure the absolute rate parameters for the reactions of ( $^3\text{P}$ ) sulfur atoms with a variety of olefins and alkynes. The absolute rate studies with alkynes were of particular importance since the relative rate data could not be obtained from direct product yields in competitive experiments but had to be evaluated on the basis of the rate of disappearance of an episulfide using an olefin as the competitive reagent. The errors in these determinations were therefore quite large. The secondary kinetic isotope effects in the  $\text{S} + \text{C}_2\text{H}_4$  reaction had been established in relative rate studies and it was therefore decided that a similar study on the  $\text{S} + \text{C}_2\text{H}_2$  reaction would provide some information regarding the structure of the primary adduct.

In addition to providing kinetic data, it was hoped that these studies might provide added insight into the reaction surfaces followed by these systems. Cvetanovic suggested that the rate of addition of  $\text{O}(^3\text{P})$  atoms to tetramethyl ethylene, which was the most rapid reaction investigated, was near the collision frequency and that the activation energy was close to or equal to zero. If so, then  $E_a$  for the  $\text{O}(^3\text{P}) + \text{ethylene}$  reaction, would be 2.6 kcal/mole. Inspection of the rate data for  $\text{S}(^3\text{P}_2)$ , Table I-3



shows that if this is the case for sulfur as well, then  $E_a$  for the  $S(^3P) + \text{ethylene}$  reaction would be 3.36 kcal/mole. This value appears to be too high and the only reasonable alternative which would agree with the observed trends is if the reaction with tetramethyl ethylene featured a negative activation energy. The necessity of determining absolute rate parameters for this particular reaction is therefore obvious.

The photochemical decomposition of COS in the presence of  $CO_2$  had been shown to be an excellent source of ground state triplet atoms in conventional photolysis and this system was chosen for the present study. Rate constants would be determined by monitoring the  $(^3P_2) \longrightarrow (^3S_1)$  absorption intensity at 180.7 nm. For the decay of  $S(^3P_2)$  atoms to be representative of the total decay of the three metastable states, they must be in thermal equilibrium. Therefore auxiliary experiments were undertaken in order to measure the population ratios of the  $^3P_2$ ,  $^3P_1$  and  $^3P_0$  states. The absolute rate of decay of ground state sulfur atoms in  $COS - CO_2$  had never been measured. In order to apply corrections to the rates of decay observed in the presence of substrate, this aspect of the overall study had to be investigated.

In the  $S(^3P) + \text{olefin}$  system rate determinations, it would be necessary to evaluate the extent of the secondary reactions, the most important of which would be abstraction from the product episulfide, for example,  $S(^3P) + C_2H_4S \longrightarrow S_2(^3\Sigma) + C_2H_4$ . Although there was some evidence from relative rate studies



that this reaction was extremely fast, the rate parameters had to be determined on an absolute basis.

The reaction of sulfur atoms with oxygen was investigated because of its importance in the oxidation of sulfur compounds at higher temperatures. Another purpose of this investigation was to evaluate the importance of oxygen contaminants in other reaction systems studied. At the outset of this investigation, two conflicting rates<sup>92,93</sup> for this reaction existed in the literature and an additional investigation was therefore essential.

Since nitric oxide is used as a radical scavenger, a study of the kinetics of the reaction of sulfur atoms with nitric oxide would be of great interest. The extreme efficiency of the reaction of nitric oxide with various other atomic species had already been established, and the extension of these studies to sulfur atoms was considered to be a worthwhile endeavour.



## CHAPTER II

### EXPERIMENTAL

#### 1. Vacuum Systems

A conventional high-vacuum system, constructed of Pyrex and evacuated to  $10^{-6}$  torr by a two-stage mercury diffusion pump backed by a Welch duoseal model 1402 mechanical pump was used for the preparation and handling of gas mixtures. Parts of the system were connected by glass high-vacuum stopcocks, and Hoke helium-tested, teflon seated valves were connected to the mixture chamber, where long duration exposure to the mixture occurs and greater control of gas passage is required. This assembly was linked to the reaction cell via a helium leak-tested Nupro valve, facilitating removal of the cell. Pressures in the system were monitored with a Pirani vacuum gauge, type G.P. 140, and a McLeod gauge. Absolute measurements were performed with mercury manometer, a type 77, M.K.S. Baratron pressure meter and a gas burette, which also served to check the reliability of the Baratron.

For the evacuation and filling of the lamp system, a mercury-free line was employed, consisting of a three-stage oil diffusion pump backed by a Welch duoseal, model 1402, mechanical pump and operating at less than  $10^{-6}$  torr. Gas pressures were monitored with a Pirani vacuum gauge. Pressures within the lamps were measured by a Wallace and Tiernan absolute pressure gauge.



## 2. Materials

The materials used, their sources and modes of purification are listed in Table II-1. The Phillips reagents are supplied at purities exceeding 99.9% (research grade). All condensable gases were subjected to repeated freeze-pump-thaw cycles at liquid nitrogen temperatures. The purity of the deuterated acetylene was checked by mass spectral analysis.

*Trans*-2-butene episulfide was prepared<sup>94,95,96</sup> by heating the carbonate ester with an equimolar amount of potassium thiocyanate and recovered by distillation. The *trans* and *cis* isomers were separated by g.c. on a ten foot tricresyl phosphate column.

## 3. Flash Photolysis Apparatus

The apparatus (Figure II-1) consisted of a quartz reaction cell, 17.6 cm long and 1.9 cm in diameter, positioned parallel to the limbs of a U-shaped flash lamp inside a thermostated, aluminum lined, oven housing. An aperture at each end of the housing allowed passage of light from the flash spectroscopic lamp (spec lamp) at one end to the vacuum ultra-violet spectrograph at the other, via the necessary optical components. The apparatus was connected to a charging and firing circuit, a delay system, and a monitoring system.



TABLE II-1

Materials Used

Material	Source	Purification
Ethylene	Phillips	Degassed at -196°C
Propylene	Phillips	Degassed at -196°C
1-Butene	Phillips	Degassed at -196°C
<i>Trans</i> -2-Butene	Phillips	Degassed at -196°C
Isobutylene	Phillips	Degassed at -196°C
Tetramethyl ethylene	A.P.I.	Distilled at -63.5      Degassed at -107
Acetylene	Matheson	Distilled at -139°C
Acetylene-d <sub>2</sub>	Merck, Sharp and Dohme	Distilled at -139°C
Propyne	Matheson	Distilled at -130°C
1-Butyne	Matheson	Distilled at -98°C
2-Butyne	Farchan Research Laboratories	Distilled at -78°C
2-Butyne-F <sub>6</sub>	Columbia Organic Chemicals Co.	Distilled at -112°C



# Materials Used (continued)

Material	Source	Purification
2-Pentyne	C.P.L.	Degassed at -98°C, Distilled at -64°C
Ethylene Episulphide	Aldrich	Degassed at -107°C, Distilled at -78°C
Propylene Episulphide	Aldrich	Degassed at -130°C, Distilled at -78°C
<i>trans</i> -Butene "-Episulphide	Prepared (94,95,96)	Degassed at -107°C, Distilled at -78°C
Argon	Linde	Assayed Reagent
Carbon Dioxide	Airco Matheson	Assayed Reagent Dried over P <sub>2</sub> O <sub>5</sub> or Distilled at -98°C
Oxygen	Airco	Assayed Reagent
Nitric Oxide	Matheson	Degassed at -196°C, Distilled at -186°C
Carbonyl Sulfide	Matheson	Bubbled through sat. solutions of NaOH and Pb(OAc) <sub>2</sub> , dried, distilled at -130°C
Krypton	Linde	Assayed Reagent
Vinyl Fluoride	Matheson	Distilled at -160°C



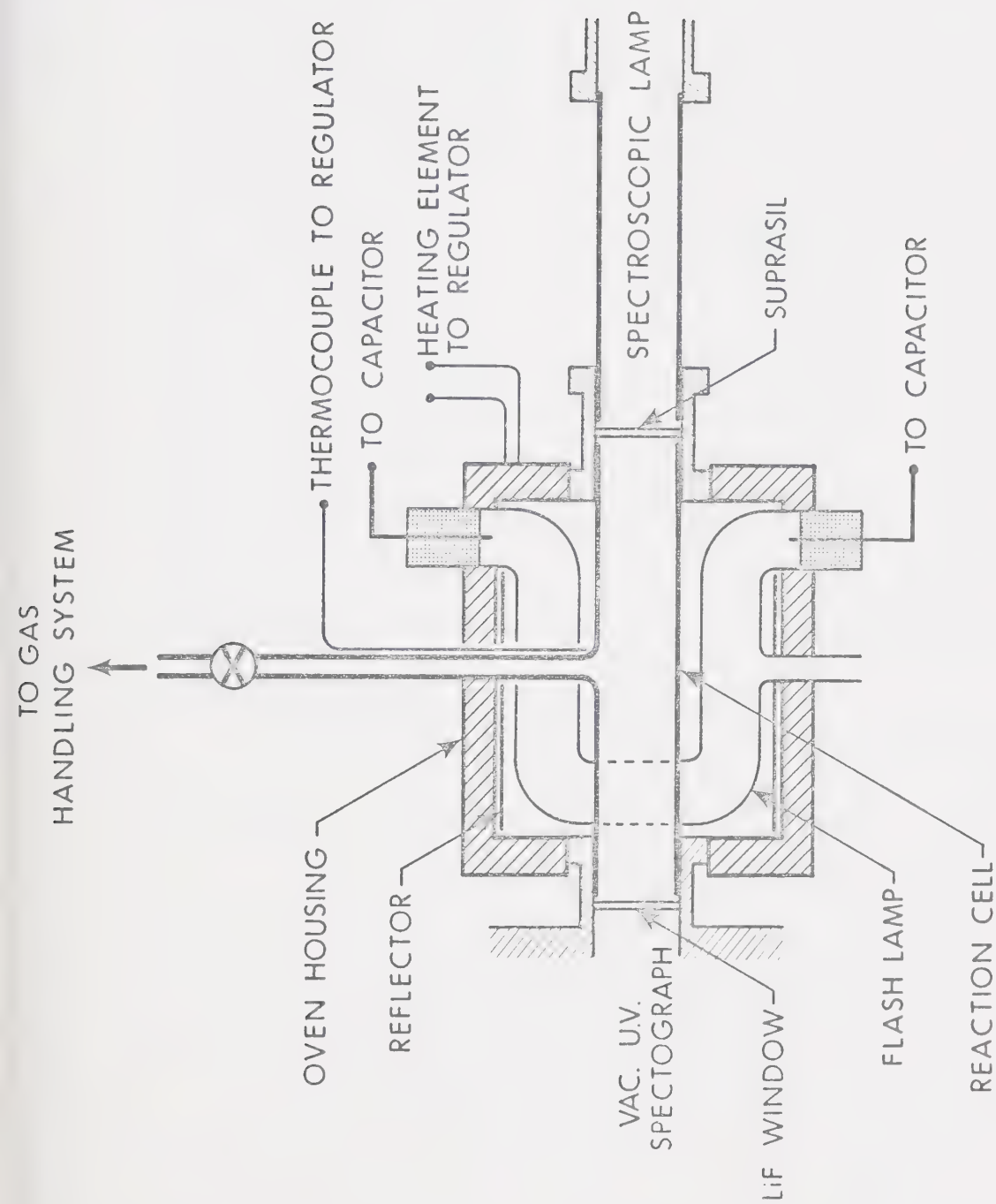


FIGURE II-1: Reactor Components



### a) Optical System

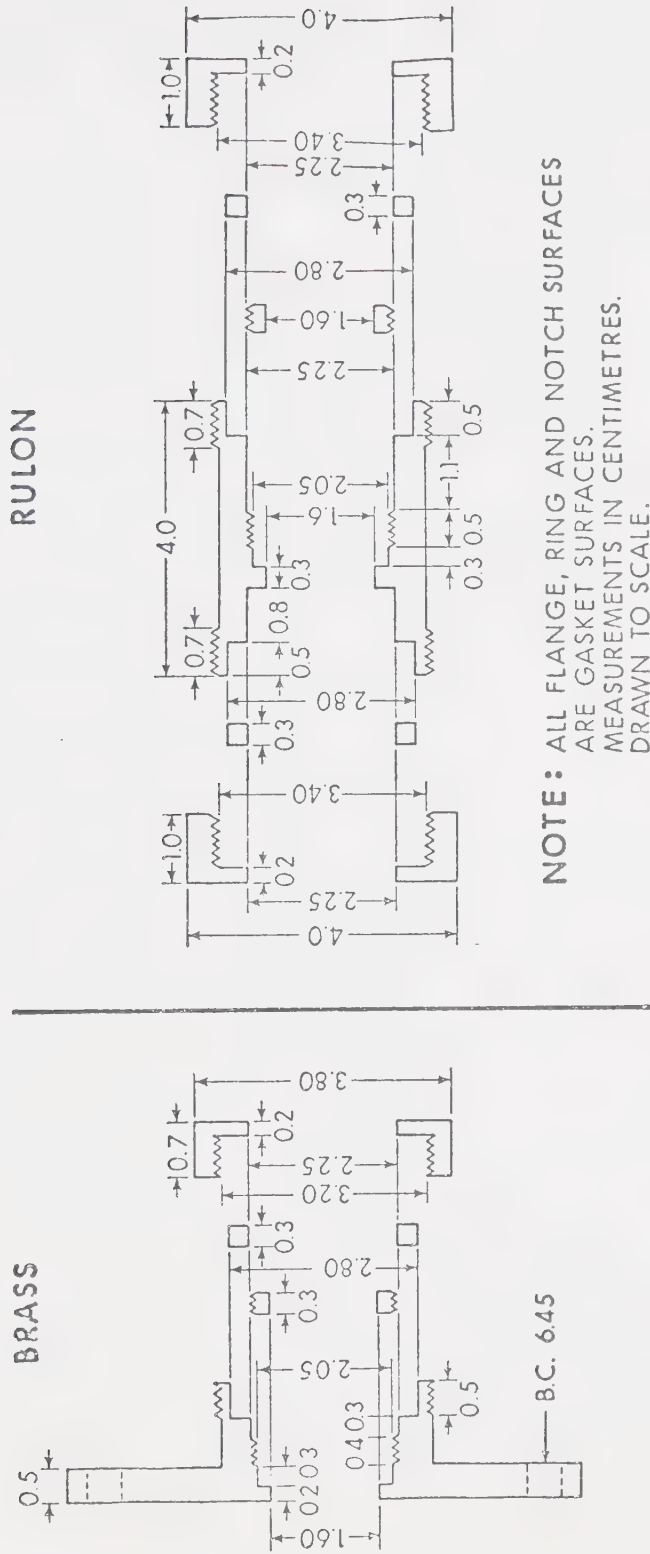
Since the experiments require monitoring of the spectrum in the vacuum ultraviolet, the complete optical path from the spec lamp to the spectrograph had to be sealed and evacuated. The connection from the spec lamp to the cell was machined from rulon (maximum operating temperature  $\sim 250^{\circ}\text{C}$ ), fitted with viton-A O-rings (maximum temperature  $\sim 370^{\circ}\text{C}$ ), to prevent electrical discharge of the spec lamp through the cell assembly. The connection from the cell to the spectrograph was of brass with viton-A O-rings (Figure II-2). The end windows of the cell were fitted inside these components, permitting complete removal of the windows for cleaning purposes. LiF and suprasil were employed as window materials. Suprasil is far less prone to stress damage, however it can only be employed down to  $\sim 160\text{ nm}$ , whereas the transmittance of LiF extends far into the vacuum ultraviolet (Table II-2).

The optics were of a single lens design with the lens (LiF) located between the cell and the spectrograph.

Two types of spec lamps were employed, a conventional capillary discharge lamp or alternately a Garton type lamp. Both lamps gave sufficient intensity, under proper conditions, to permit a spectrum to be obtained from a single flash.

The flash photolysis lamp (photo lamp) used was of a novel U-shaped design, as shown in Figure II-3, and was operated under two sets of conditions, Photo 1 and Photo 2, the resultant profiles of which are shown in Figure II-4. The shortest delay times used were  $40\text{ }\mu\text{sec}$





**NOTE:** ALL FLANGE, RING AND NOTCH SURFACES ARE GASKET SURFACES. MEASUREMENTS IN CENTIMETRES. DRAWN TO SCALE.

FIGURE II-2: Structural Details of Intersystem Connectors



TABLE II-2

Window Materials<sup>a</sup>

Material	Thickness (mm)	Wavelength (nm) for 10% Transmission
LiF	1	105
CaF <sub>2</sub> (synthetic)	3	122
Sapphire (synthetic)	0.5	142
Suprasil	1	155
Quartz, clear fused	10	172
Quartz, crystal	10	186
Vycor 791	1	212
Vycor 790	2	254
Corex D	1	250
Pyrex (Corning 774)	1	280
Window Glass (standard)	1	307

<sup>a</sup> J.G. Calvert and J.N. Pitts, Jr., Photochemistry, John Wiley and Sons, Inc., New York, 1966, p. 748.



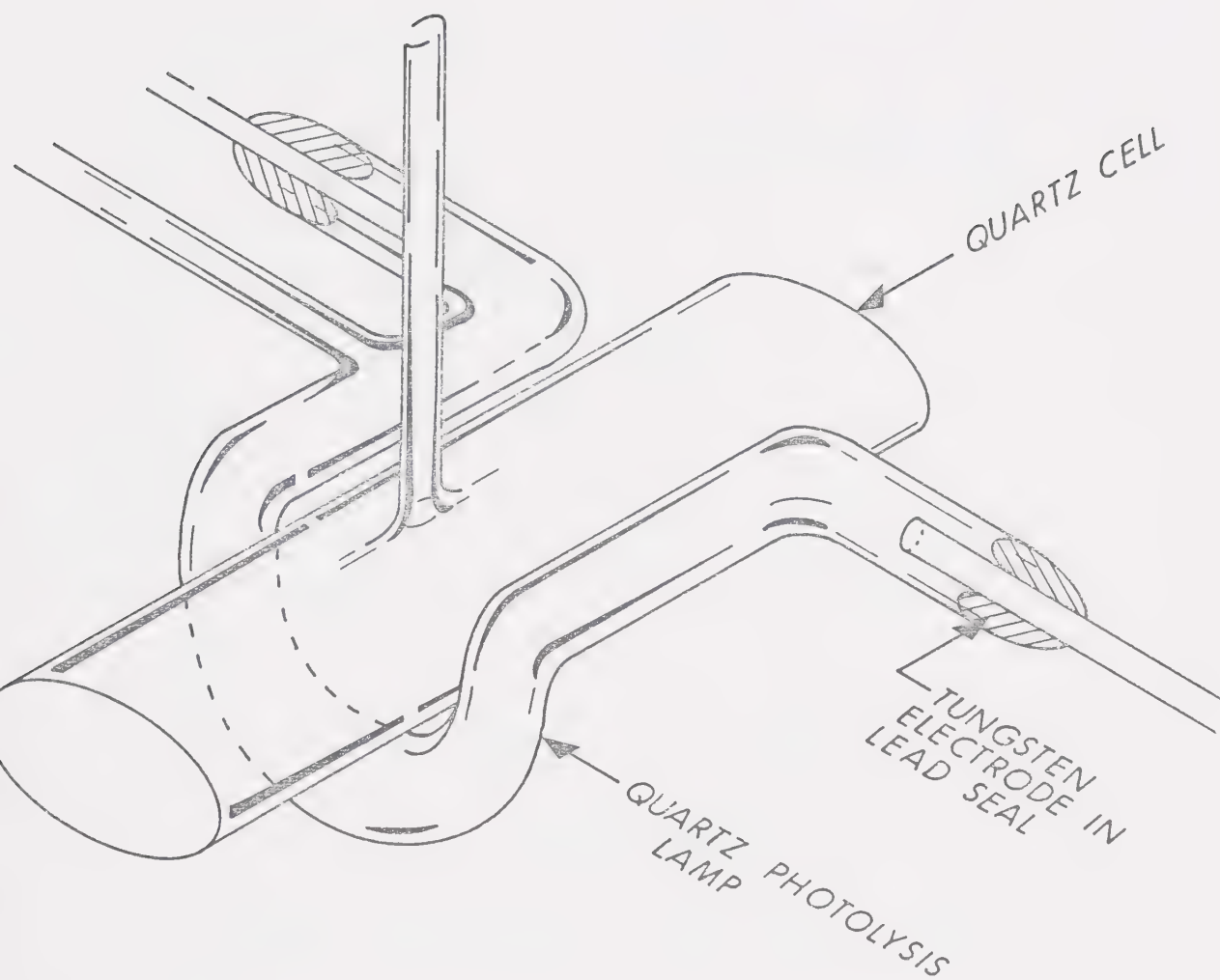


FIGURE II-3: Lamp-cell symmetry



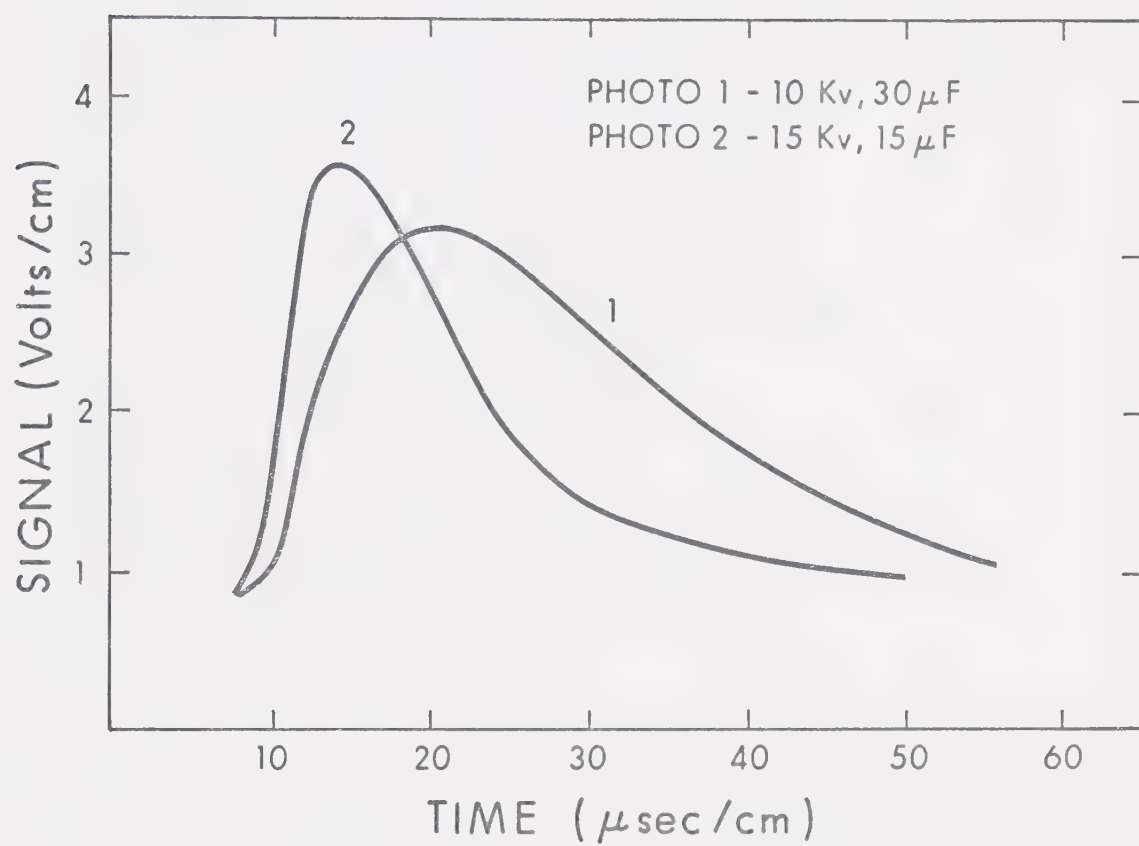


FIGURE II-4: Dependence of Flash Profile on Capacitance



for Photo 1 and 25  $\mu$ sec for Photo 2. The data pertaining to the various lamps are tabulated in Table II-3.

Spectra were recorded over a 40 nm range from 160.0 - 200.0 nm, using a 1M, McPherson 225, normal incidence, vacuum instrument fitted with a 30,000 grooves/inch grating, providing a dispersion of 0.83 nm/mm. Spectra were recorded on Kodak S.W.R. film or Kodak special type 101-01 film, which was developed for four minutes in Kodak D-19 developer at half strength. Subsequently, graphs were produced by a Joyce-Loebl double beam recording microdensitometer.

The light from the spec lamp was focussed on the entrance slit of the spectrograph by a LiF lens. The focal length of the lens was experimentally determined. The position of the image of a pin used as object was located, varying the lens to object distance. Using the formula

$$\frac{1}{U} + \frac{1}{V} = \frac{1}{f}$$

where U is the distance of the object from the lens, V is the distance of the image from the lens, and f is the focal length of the lens, one can easily find the focal length from the plot of  $\frac{1}{U}$  versus  $\frac{1}{V}$  (Figure II-5) since the intercepts correspond to  $U = f$  = V. The average f value found from the intercepts was 9.5 cm. However, this is the focal length of the lens as determined in the visible region. Since  $\mu$  (LiF)  $\sim$  1.45 at 200 nm and only  $\sim$  1.40 at 600 nm<sup>97</sup> and



TABLE II-3

Lamp Data

Lamp	Firing Voltage (KV)	Capacitance ( $\mu$ F)	Kr Gas Filling (torr)	Time of Max. Flash Intensity ( $\mu$ sec)	Width at Half Peak ( $\mu$ sec)
Photo 1	3-9	30	50	14	20
Photo 2	6-14	10	20	55	12
Capillary Spec.	12-16	2.5	10	4	10
Garton Spec.	10.5	9.8	0.3	3	10



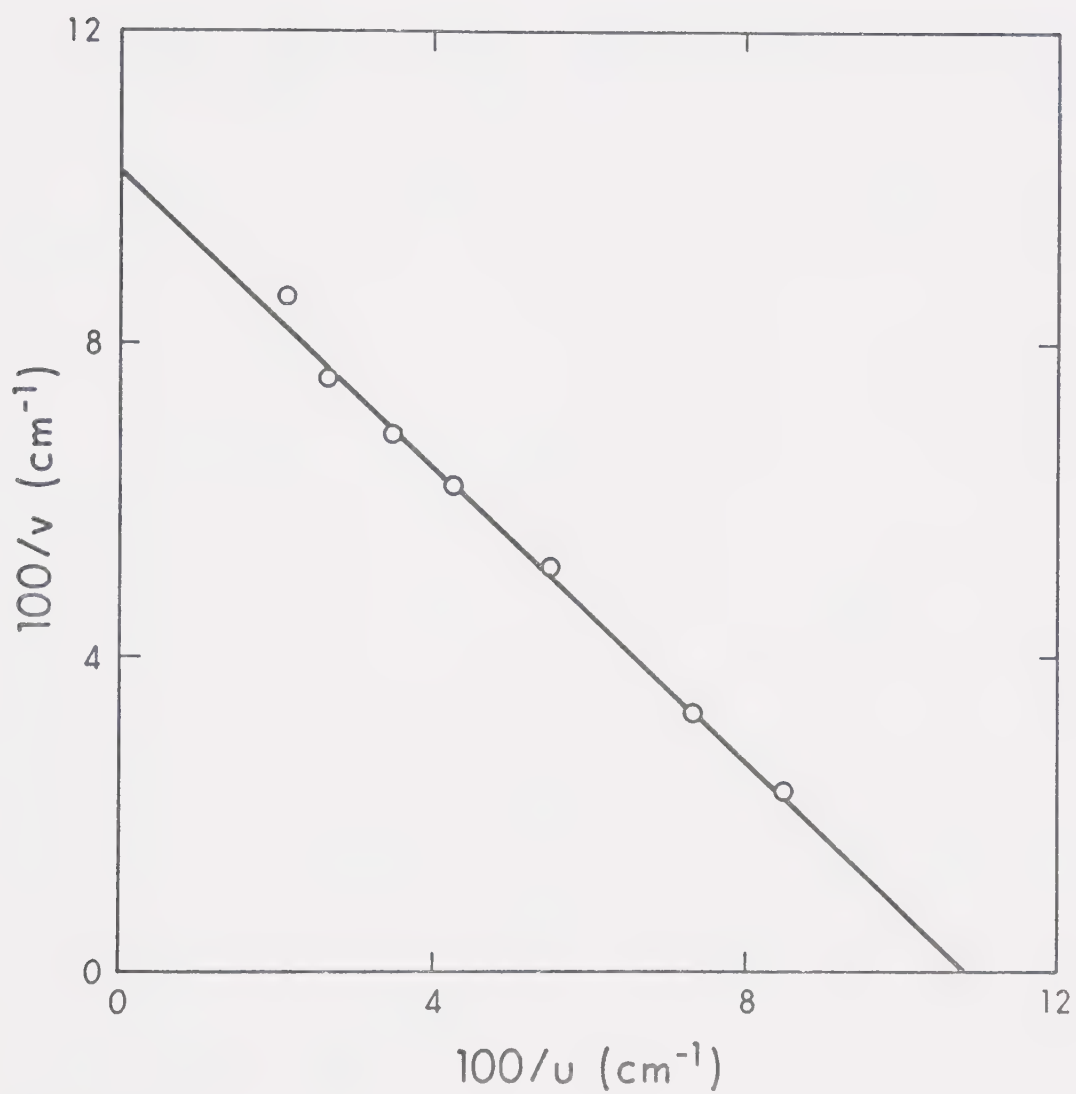


FIGURE II-5: Reciprocal of Object Distance versus  
Reciprocal of Image Distance from the  
Lens.



$$f \propto \frac{1}{\mu - 1}$$

then

$$\frac{f_{200}}{f_{600}} = \frac{\mu_{600} - 1}{\mu_{200} - 1} = \frac{0.40}{0.45} \quad \text{and} \quad f_{200} = 8.5 \text{ cm}$$

Since the distance from the lens to the entrance slit was 10.4 cm, the spec lamp was placed 47.3 cm from the lens.

#### b) Housing

The insulating housing was constructed of transite, lined on the inside with a layer of aluminum to ensure uniform heat distribution. The heating elements ran the length of the housing, co-axial with and surrounding the cell-lamp assembly and were connected to either an Ohmite variable transformer (Figure II-6) or an A.P.I. model 226, 2-mode solid state temperature controller. The temperatures were monitored via iron-constantan thermocouples connected to a Leeds and Northrop potentiometer. After each photo flash, temperature restabilization was allowed to occur and was checked, before proceeding with the following photo flash.

#### c) Electrical

A typical flash photolysis circuit was employed. The capacitors were charged to selected voltages. The



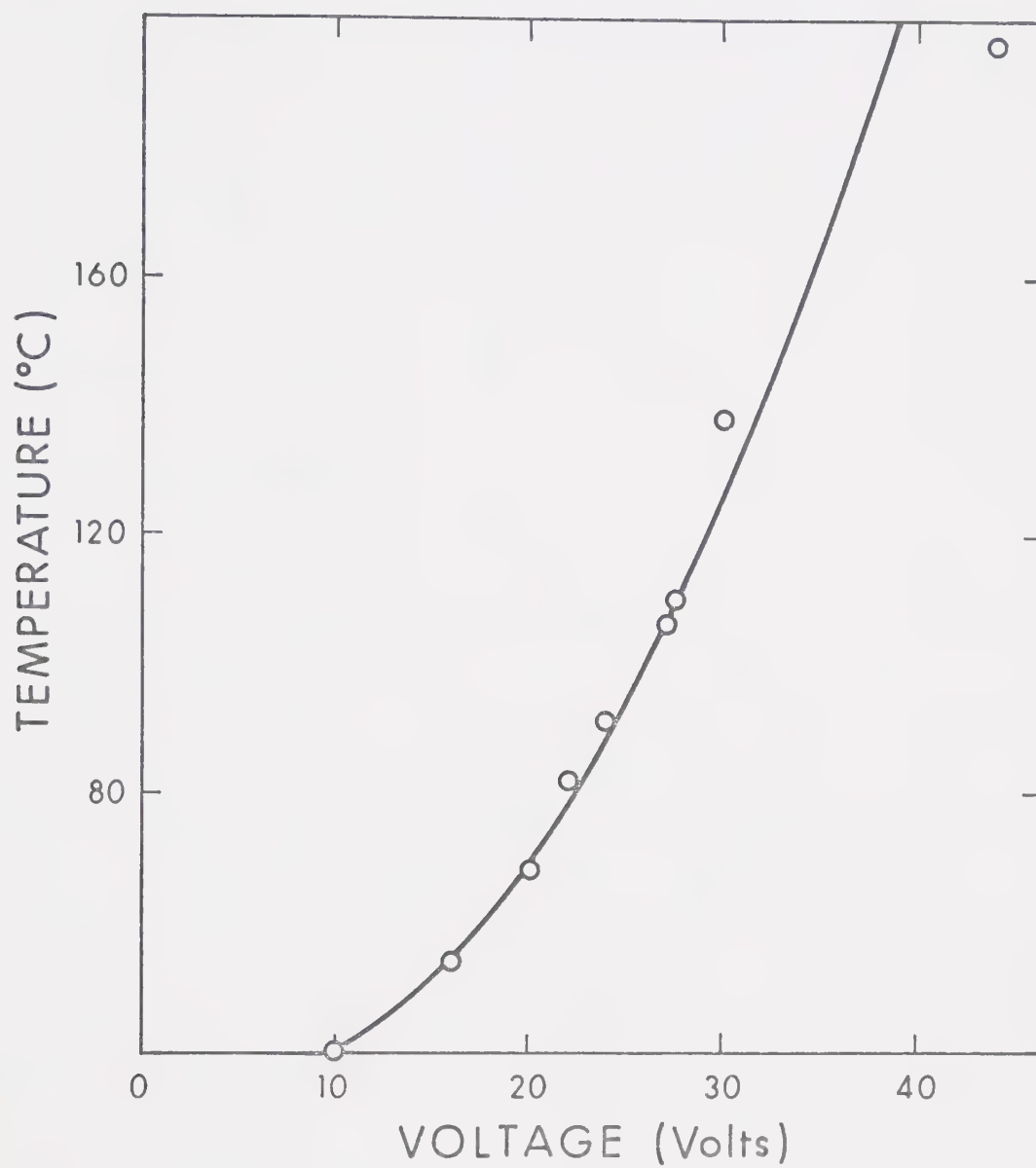


FIGURE II-6: Oven Temperature versus Operating Voltage



closing of a microswitch fired an ignitron, whose breakdown causes the capacitor to discharge through the photolysis lamp. A coil in this circuit caused the firing pulse to activate the delay generator which fired the ignitron of the spectroscopic lamp circuit after a preset delay. The firing of the first lamp also triggered the oscilloscope, initiating a horizontal sweep which recorded photo and spec lamp discharges as sensed by a photocell to check the set delays. A simple schematic representation of this system is shown in Figure II-7.

#### 4. Operating Procedure

The mixtures were prepared in a three litre vessel using a mercury manometer for the measurement of large pressures, > 10 torr, (diluent gas) and a Baratron gauge (or alternately, a gas burette) for small pressures. The mixture was then allowed to stand overnight to ensure homogeneity. Aliquots were then taken directly into the reaction cell, using a mercury manometer to check the total pressure. In a typical run, the 3 litre bulb contained 600 torr of gas and the reactor cell contained 200 torr. After each photolysis flash, the cell was immediately evacuated and a fresh mixture was introduced for a subsequent flash. Employing this technique extended the life of the cell between cleanings and kept the change in optical transmission of the cell during a run to a negligible level.



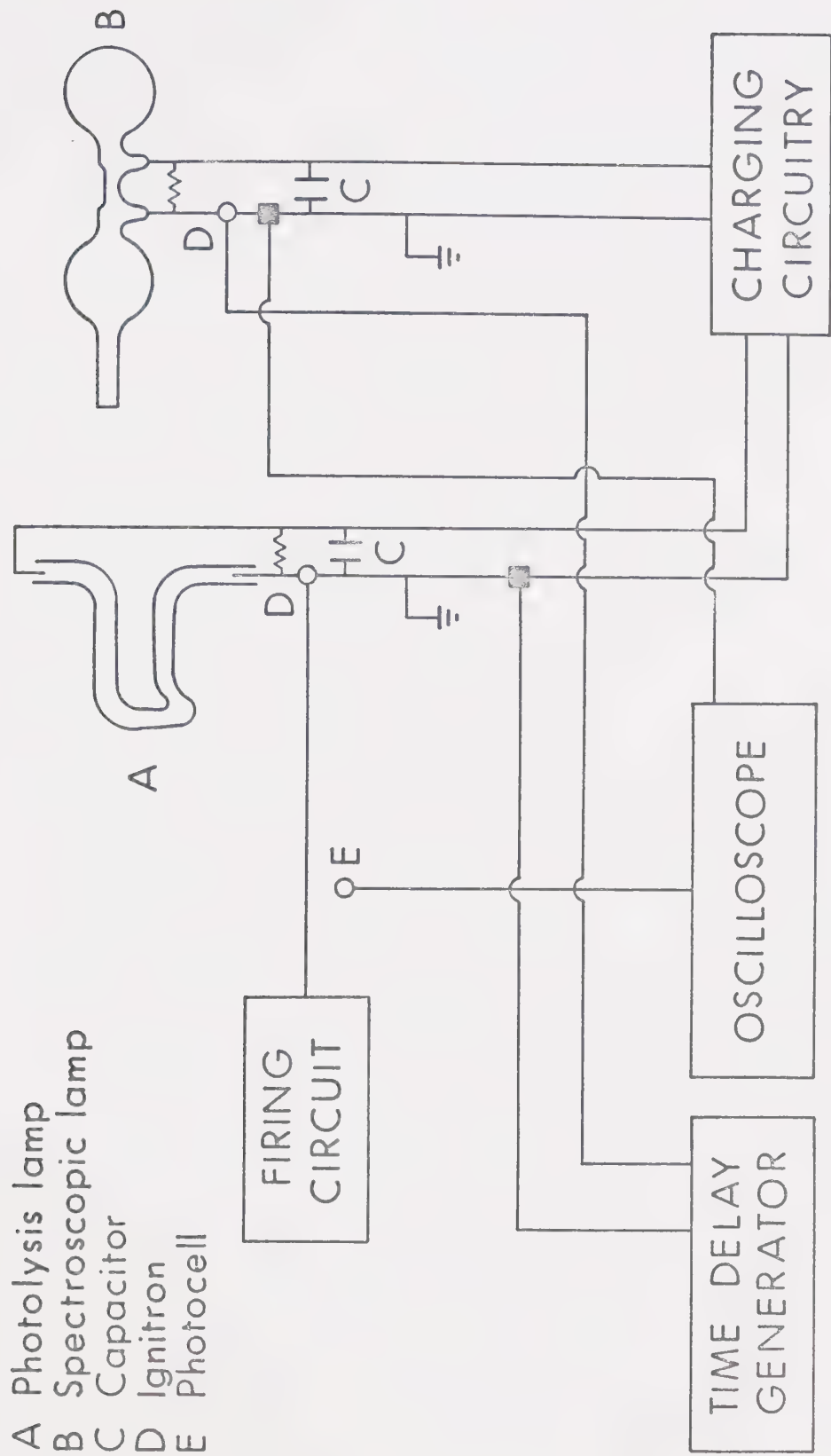


FIGURE II-7: Electronic Schematic of Flash Apparatus



# CHAPTER III

## THE FLASH PHOTOLYSIS OF CARBONYL SULFIDE

### A. Results

To study the reactions of  $S(^3P_{2,1,0})$  atoms, a suitable source of atomic sulfur must first be developed. It has been shown<sup>14</sup> that photolysis of carbonyl sulfide within its first long-wave absorption region produces CO,  $S(^1D)$  and possibly  $S(^3P)$  atoms in the primary dissociative step. Since  $S(^1D)$  atoms can be readily deactivated to the ground  $S(^3P_{2,1,0})$  state in the presence of inert gases, it appeared that COS would be an excellent source compound for the investigation of the reactivity of sulfur atoms and a study was therefore undertaken to establish whether it fulfills the various requirements of the technique presently employed. Areas examined were the relationships between experimental observables and the sulfur atom concentration, the distribution of the concentration over the  $S(^3P_{2,1,0})$  levels, and the mode and kinetics of the disappearance of the atoms in a system free of reactants other than those required for initial  $S(^3P_{2,1,0})$  production.

#### 1. Experimental Beer-Lambert Coefficient

If one is to monitor  $S(^3P_{2,1,0})$  atom concentrations, the correlation between concentration and microdensitometered peak



heights must first be established. Therefore, the experimental Beer-Lambert Coefficient was determined for this system. This variable is part of the empirical relationship between optical density, O.D., measured on a photographic film, and the experimental parameters which are the concentration of the absorber,  $c$ , and the path length,  $l$ , giving the equation<sup>71</sup>,

$$\text{O.D.} = k(cl)^\gamma$$

where  $\gamma$  is the Beer-Lambert Coefficient, and  $k$  is an empirical constant which includes  $e^\gamma$  and plate contrast. For broad molecular absorption bands in solution, the Beer-Lambert Coefficient is unity, and the equation can be simplified to

$$\text{O.D} = kcl$$

However, for atomic lines and sharp molecular bands in the gas phase, the value of  $\gamma$  is often less than unity, and for an atomic line, one would expect a value of 0.5, due to the inability of the spectrograph to resolve a sharp atomic spectral line. If fully resolved,  $\gamma$  for a spectrum is unity; if fully unresolved,  $\gamma$  equals 0.5<sup>71</sup>.

The Beer-Lambert Coefficient for a particular absorbing system can be determined by several independent methods, two of which will now be described.



### a) Cell Length Variation

In this method, a mixture is flashed in a fully exposed cell and then in a cell which is partly covered to produce a lower absorbing path length. In replicate experiments, the covered portion should be varied over the length of the cell to eliminate possible systematic errors. For fully exposed and half covered cells, the expressions for absorbance are

$$O.D.^0 = k(cl)^\gamma$$

$$O.D. = k(c\frac{1}{2}l)^\gamma$$

respectively. Thus,

$$\frac{O.D.^0}{O.D.} = \frac{1}{.5^\gamma} = 2^\gamma$$

for a particular concentration,  $c$ . If these measurements are performed at different concentrations, then the slope of a plot of  $O.D.^0$  vs  $O.D.$ , will be  $2^\gamma$ . Typical results are shown in Figures III-1,2, from which  $\gamma = 0.5 \pm 0.1$  for both the  $^3P_1$  and  $^3P_2$  absorptions. The concentration of sulfur atoms was varied by changing the delay times at which the sulfur atom was monitored. A typical mixture of 0.1 torr COS in 200 torr of  $CO_2$  was used.

### b) Flash Energy Variation

The value of  $\gamma$  can also be determined by the correlation of peak height, P.H., with flash energy. It is assumed that the sulfur



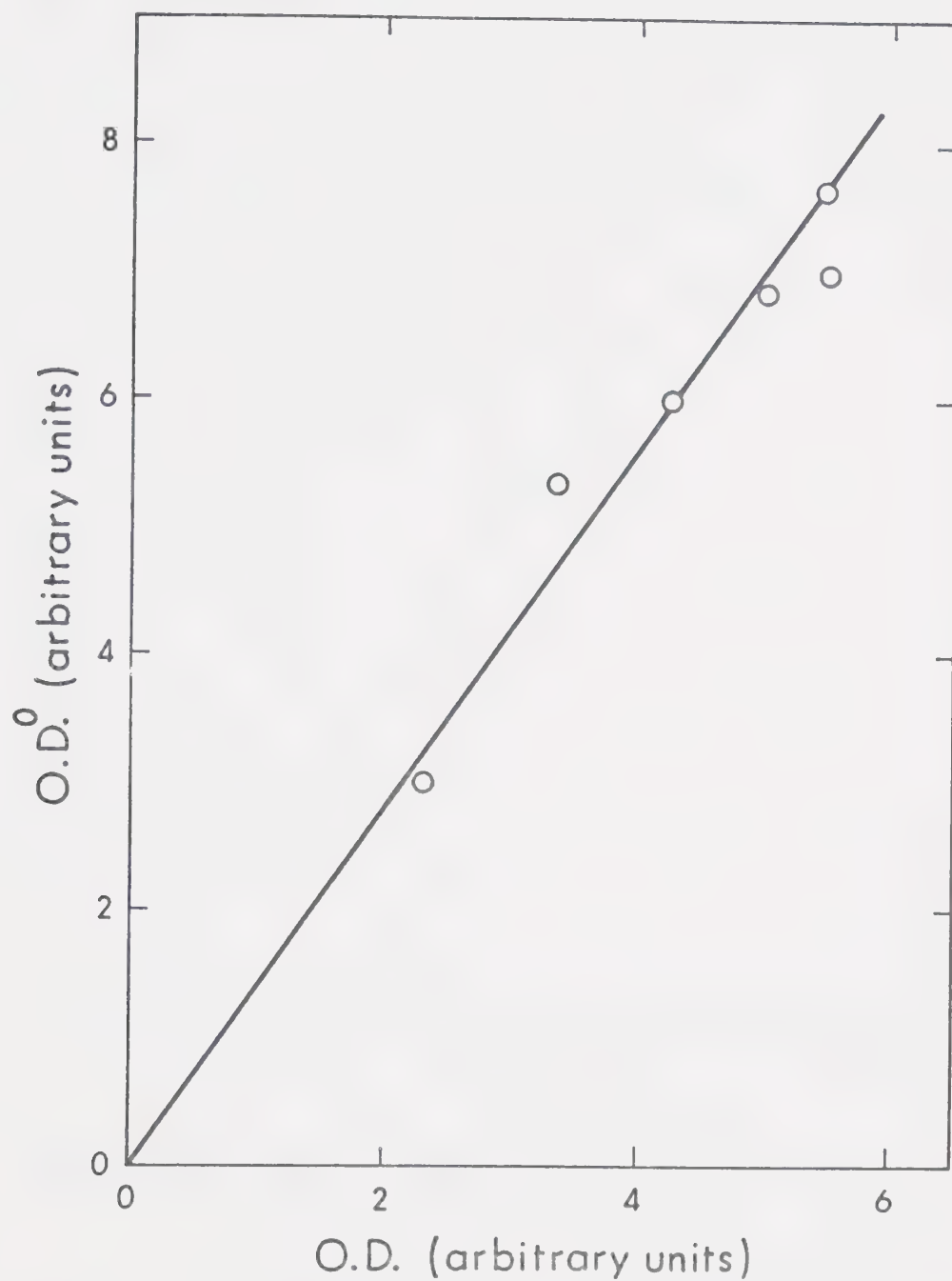


FIGURE III-1: Optical Density from a fully exposed cell,  $O.D.^0$ , versus Optical Density from a half exposed cell,  $O.D.$ , for  $S(^3P_2)$  [180.7 nm].



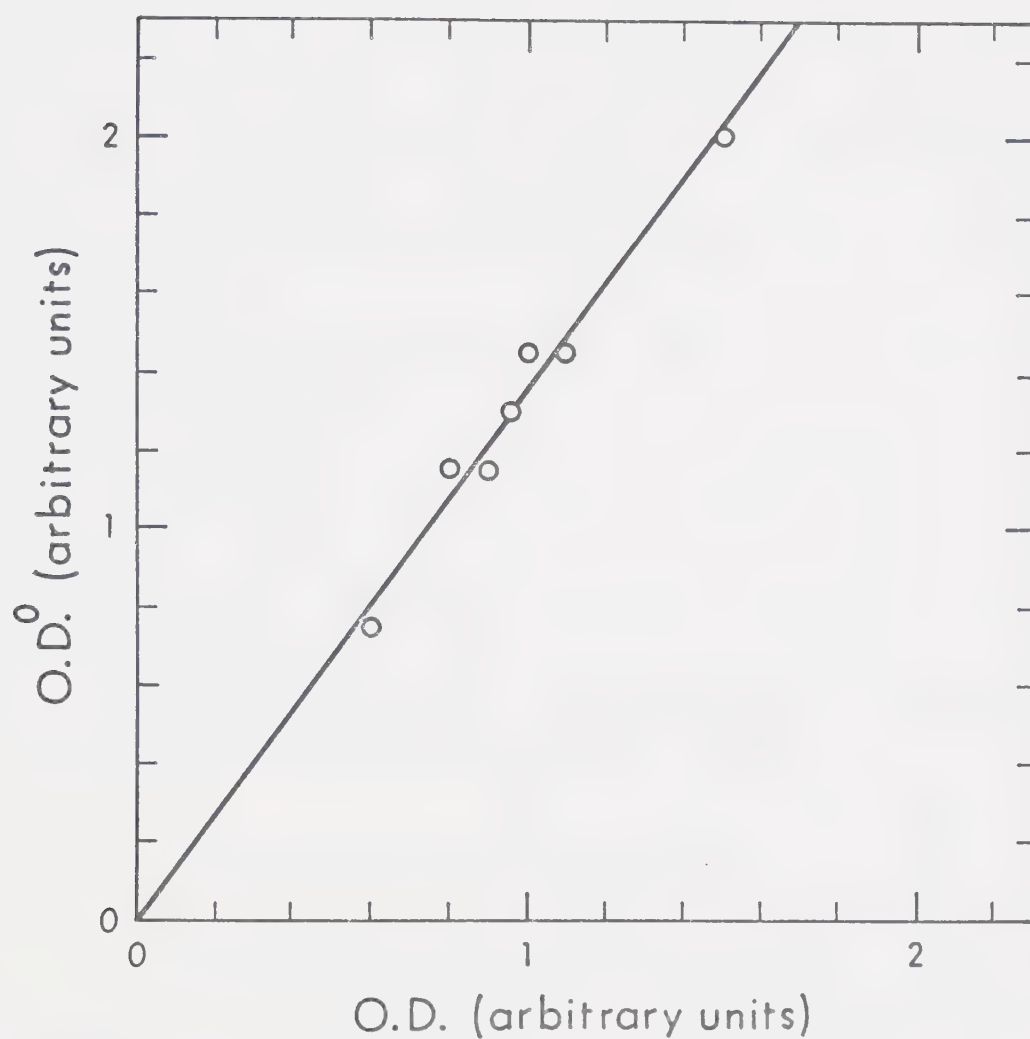


FIGURE III-2: Optical Density from a fully exposed cell,  $O.D.^0$ , versus Optical Density from a half covered cell, O.D., for  $S(^3P_1)$  [182.0].



atom concentration changes linearly with flash energy which is varied by changing the charging voltage of the capacitor. The sulfur atom concentration should therefore vary as the square of the voltage, since

$$E = \frac{1}{2} cV^2$$

where  $E$  is the dissipated energy,  $c$  is the capacitance of the capacitor, and  $V$  is the charging voltage used. Thus

$$\text{P.H.}^{\frac{1}{\gamma}} \propto [S(^3P_2)] \propto E \propto V^2$$

or

$$\left( \frac{\text{P.H.}_1}{\text{P.H.}_2} \right)^{\frac{1}{\gamma}} = \left( \frac{V_1}{V_2} \right)^2$$

where P.H. is the experimentally determined peak height.

As shown in Table III-1, this method gives a value for  $\gamma$  which is in agreement with the previous technique.

## 2. Population of the $^3P_{2,1,0}$ States

The monitored absorptions occur at 180.7( $^3P_2 \rightarrow ^3S_1$ ), 182.0( $^3P_1 \rightarrow ^3S_1$ ), and 182.6( $^3P_0 \rightarrow ^3S_1$ ) nm. The ratios of the absorption intensities for the three states were determined by measuring the peak height ratios at various delay times and flash energies. The results are tabulated in Tables III-2, III-3 and III-4, from which the following absorption intensity ratios were determined:



TABLE III-1

Determination of the Beer-Lambert Coefficient  
by Variation of the Flash Energy

$\frac{V_1}{V_2}$	$\frac{E_1}{E_2}$	Substrate	O.D. ( $S^3P_2$ ) Ratio	$\gamma$
1.38	1.92	Ethylene	1.56	0.68
1.38	1.92	1-Butene-1	1.31	0.41
1.50	2.25	Trans-2-Butene	1.46	0.47
1.36	1.86	Isobutene	1.31	0.44
ave.				$0.50 \pm 0.12$



TABLE III-2

Determination of the  $S(^3P_2)$  to  $S(^3P_1)$   
Peak Height Ratios at 5.5 kV <sup>a</sup>

$h^b_{S(^3P_2)}, \text{ cm}$	$h^b_{S(^3P_1)}, \text{ cm}$	$h_{S(^3P_2)}/h_{S(^3P_1)}$
9.75	2.55	3.82
5.55	1.60	3.47
5.70	1.30	4.38
4.95	1.30	3.81
4.65	0.95	4.90
3.80	1.15	3.31
3.05	0.65	4.69
3.15	0.65	4.85
3.55	0.65	5.47
4.55	1.00	4.55
ave.		$4.33 \pm 0.70$

<sup>a</sup>  $P(\text{COS}) = 0.11 \text{ torr}$ ;  $P(\text{CO}_2) = 200 \text{ torr}$ ;

Photoflash voltage = 5.5 kV

<sup>b</sup>  $h$  = height of microdensitometer trace



TABLE III-3

Determination of the  $S(^3P_2)$  to  $S(^3P_1)$ Peak Height Ratios at 9 kV <sup>a</sup>

Delay time, $\mu\text{sec}$	$h^b_{S(^3P_2)}$ , cm	$h^b_{S(^3P_1)}$ , cm	$h_{S(^3P_2)}/h_{S(^3P_1)}$
47	10.35	2.50	4.14
71	9.55	2.00	4.78
88	9.30	1.60	5.81
110	7.45	1.95	3.82
132	6.65	1.50	4.43
153	4.75	1.10	4.32
172	4.60	1.00	4.60
197	4.45	1.20	3.71
214	3.70	0.85	4.35
			ave $4.44 \pm 0.62$

<sup>a</sup>  $P(\text{COS}) = 0.1$  torr;  $P(\text{C}_2\text{H}_4) = 0.254$  torr; $P(\text{CO}_2) = 57$  torr;  $P(\text{Ar}) = 143$  torr;

Photoflash voltage = 9 kV

<sup>b</sup>  $h$  = height of microdensitometer trace



TABLE III-4

Determination of the  $S(^3P_1)$  to  $S(^3P_0)$   
Peak Height Ratios <sup>a</sup>

$h_{S(^3P_1)}^b$ , cm	$h_{S(^3P_0)}^b$ , cm	$h_{S(^3P_1)}/h_{S(^3P_0)}$
3.20	1.05	3.05
3.10	1.00	3.10
2.75	0.75	3.66
2.80	1.00	2.80
2.90	0.90	3.22
3.10	0.95	3.26
3.00	0.80	3.65
2.80	1.05	2.67
3.00	0.90	3.33
2.75	0.90	3.05
2.70	0.60	4.50
2.65	0.90	2.95
2.35	0.60	3.92
2.25	0.8-	2.65
2.10	0.70	3.00
2.40	0.80	3.00
2.30	0.70	3.28
2.60	0.95	2.74
		ave 3.21 ± 0.47

<sup>a</sup>  $P(\text{COS}) = 0.11$  torr;  $P(\text{CO}_2) = 200$  torr;

Photoflash voltage = 9 kV

<sup>b</sup>  $h$  = height of microdensitometer trace



$$S(^3P_2) : S(^3P_1) : S(^3P_0) = 14.1 : 3.2 : 1$$

under the experimental conditions employed. Since the  $S(^3P_2)$  absorption is dominant, as shown in the microdensitometer trace of the three absorptions, Figure III-3, most of the quantitative data were obtained by monitoring the 180.7 nm line. However, some quantitative data were also obtained from the  $S(^3P_1)$  absorption line and were found to be in good agreement with the data derived from the  $S(^3P_2)$  absorption measurements.

### 3. Estimation of Absolute $S(^3P_{2,1,0})$ Concentrations

Two techniques were used to obtain an estimate of the absolute sulfur atom concentrations initially formed by photolysis:

#### a) Variation of the Extent of Decomposition of COS

The intensity of the COS absorption spectrum was monitored in the wavelength region 173.0-178.5 nm<sup>25</sup> in COS + Ar mixtures after subjecting the mixtures to a number of photolysis flashes ranging from 0 to 10. The Beer-Lambert Coefficient for all the wavelength regions analyzed was assumed to be unity. This approximation is probably valid since the absorption is almost continuous. The results are given in Table III-5 and Figure III-4 and yield an efficiency of decomposition of ~3% per flash. For 0.1 torr of COS, the initial S atom concentration was therefore  $\sim 3.0 \times 10^{-3}$  torr.



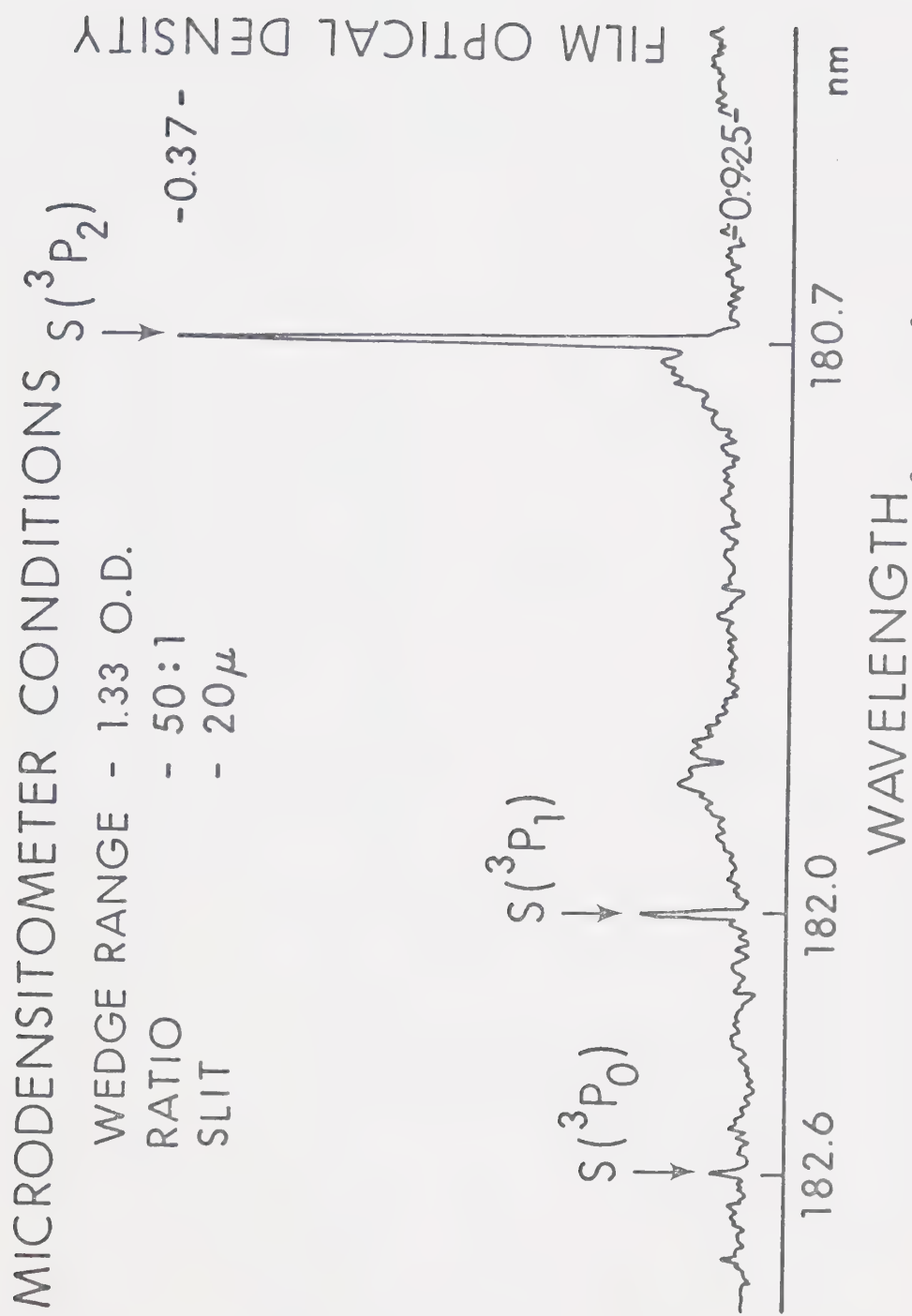


FIGURE III-3: Microdensitometered Peak Heights of  $S(^3P) \rightarrow S(^3S_1)$  Absorptions

$P(CO_2) = 0.1$  torr  $P(CO_2) = 57$  torr  $P(Ar) = 143$  torr.



TABLE III-5  
Effect of Repeated Flashes on the COS  
Absorption Band Intensities

Band Wave-lengths (nm):	178.37	177.58	176.71	175.96	175.11	173.57	172.90	$\Sigma h$
	h, Height (cm) of Vibrational Bands							
No. of Flashes								
0	0.80	0.75	1.80	1.55	5.05	8.30	5.55	23.8
1	0.90	0.65	1.85	1.30	4.45	7.55	5.75	22.45
3	0.90	0.80	1.65	1.35	4.25	7.15	5.65	21.75
5	0.80	0.60	1.55	1.45	4.30	6.60	5.30	20.60
10	0.50	0.70	1.20	1.30	2.90	4.90	4.50	16.0
0	0.95	0.80	1.80	1.70	4.85	7.45	5.45	23.0



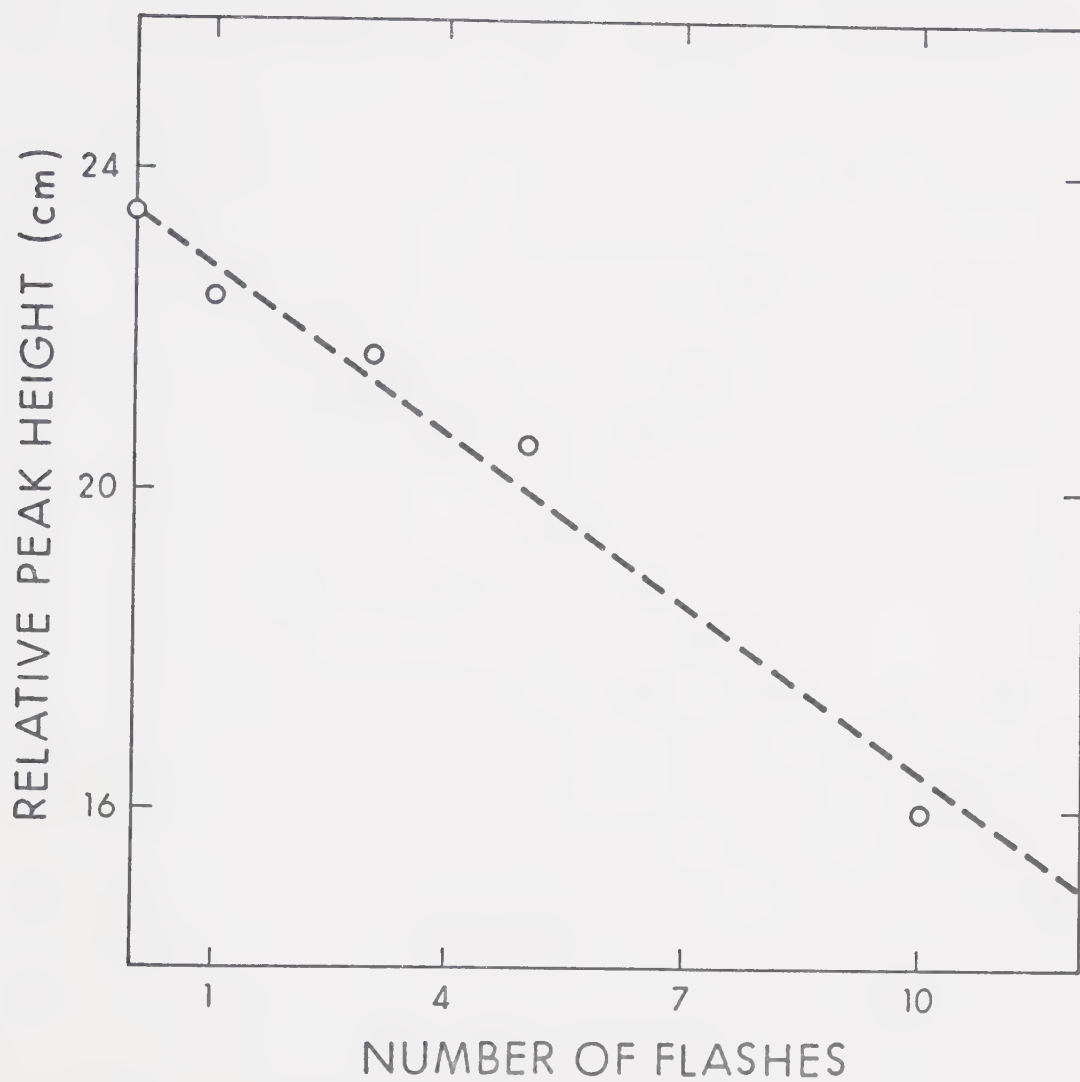


FIGURE III-4: Depletion of COS by Photolysis Flashes

$P(\text{COS}) = 0.1 \text{ torr}$   $P(\text{Ar}) = 200 \text{ torr.}$



#### b) Measurement of CO

Alternatively, the CO produced after flashing 0.1 torr COS in 200 torr CO<sub>2</sub> was measured quantitatively. All condensibles from a mixture flashed 6 times were removed by a solid nitrogen trap and the remaining gas was measured in a gas burette. For an average experiment, the pressure of CO in the cell was found to be  $2.5 \times 10^{-2}$  torr or  $\sim 4.1 \times 10^{-3}$  torr per flash.

Since the results of the two different methods are compatible, it can be concluded that the concentration of sulfur atoms initially produced in the flash photolysis of 0.1 torr COS is  $\sim 2 \times 10^{-7}$  mole/litre.

#### 4. Decay of S(<sup>3</sup>P)

In order to use COS as a sulfur atom source for rate determinations with other substrates, a knowledge of the rate of decay of S(<sup>3</sup>P) atoms in COS alone was necessary. It was found that in either COS + CO<sub>2</sub> or COS + Ar systems, the sulfur atoms disappeared over a millisecond time scale. Plots of [S(<sup>3</sup>P<sub>2</sub>)] versus time were linear, as illustrated in Figure III-5, indicating a first order mode of decay. First order decay rate constants of  $1.1 \times 10^3$  and  $0.7 \times 10^3 \text{ sec}^{-1}$  were obtained in the presence of CO<sub>2</sub> and Ar respectively. To minimize the relative importance of this decay in rate determinations with other substrates, the total first-order decays were thereafter usually adjusted to a rate of  $1 \text{ to } 2 \times 10^4 \text{ sec}^{-1}$ , relegating this portion



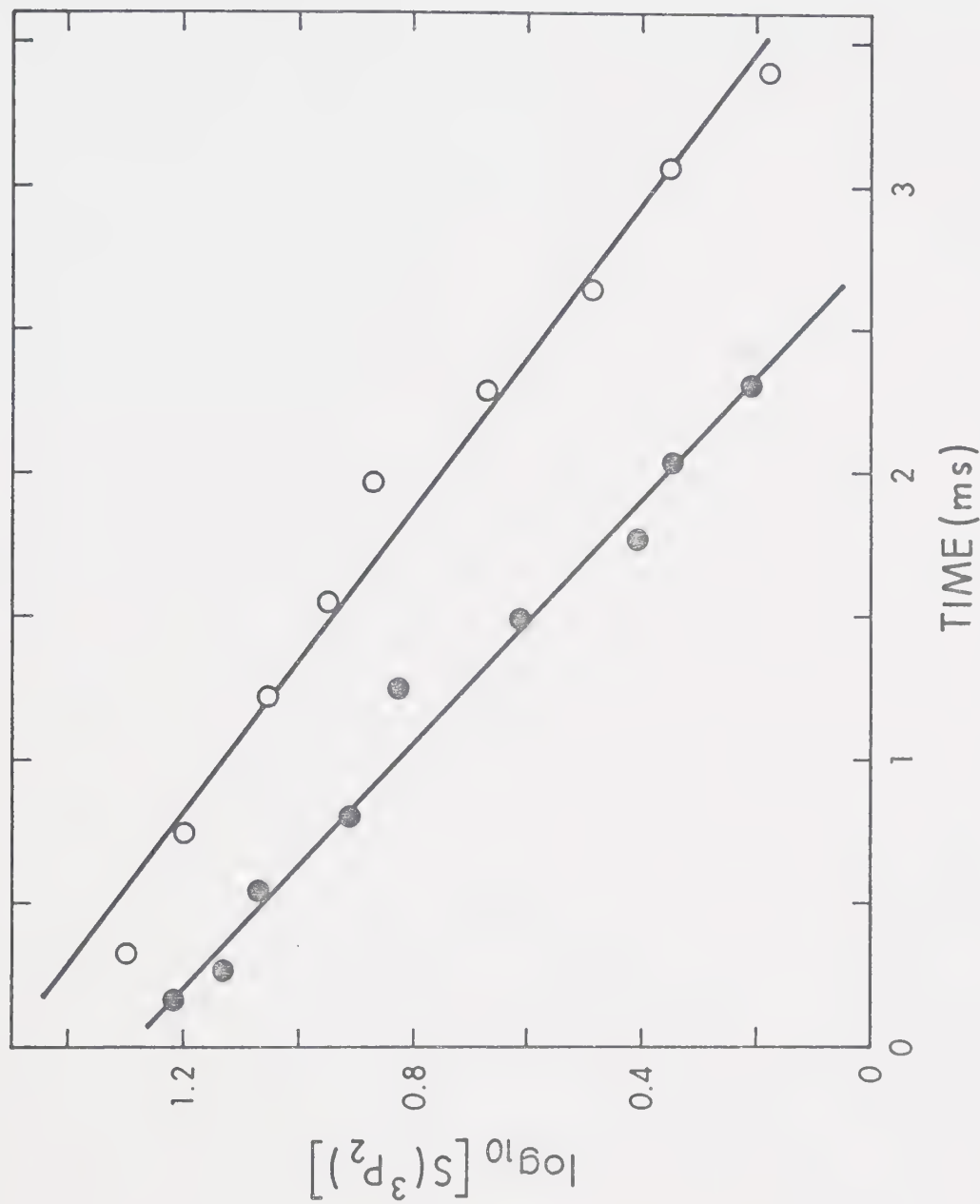


FIGURE III-5: First Order Decay Plots of  $S(^3P_2)$ , ○ in 200 torr  $CO_2$  and ● in 200 torr Ar,  $CO_2 = 0.1$  torr.

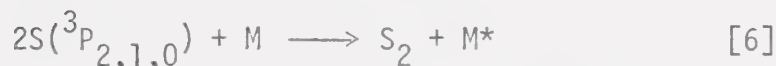
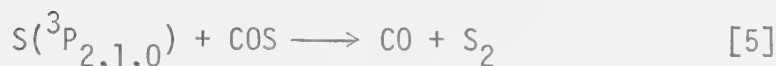
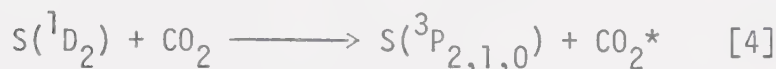
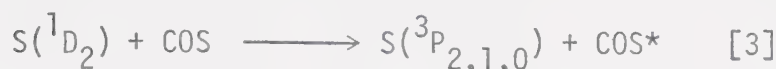
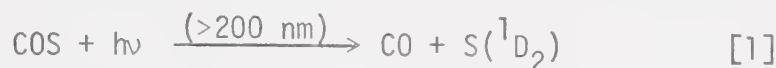


of the decay to ~5-10% of the total. Appropriate corrections were then applied to the observed rates of decay in the presence of other substrates.



## DISCUSSION

In order to evaluate the results, it would be useful at this point to recall the known sequence of elementary steps occurring in the photolysis of COS:



The photolysis of COS produces predominantly  $\text{S}(^1\text{D}_2)$  species. In the absence of an efficient quencher,  $\text{S}(^1\text{D}_2)$  reacts rapidly with COS to form  $\text{S}_2$  with a rate  $k_2 > 4 \times 10^{10} \text{ l/mole sec}^{21}$ . However, it has been demonstrated that  $\text{CO}_2$  is an extremely efficient quencher of  $\text{S}(^1\text{D}_2)$  and that  $\text{S}(^1\text{D}_2)$  atoms would have a half-life of approximately  $0.01 \mu\text{sec}$  in 60 torr of  $\text{CO}_2$ , since Weibe et al<sup>98</sup> have shown that  $k_4 \approx k_2$ . The half-life of  $\text{S}(^1\text{D}_2)$  in the presence of 200 torr of argon would be  $\sim 0.1 \mu\text{sec}^{23}$ . Hence, at the pressures used in this work, the  $\text{S}(^1\text{D}_2)$  atoms are almost entirely quenched to the ground state, at a rate considerably faster than would be experimentally observable. Another reactant,



present in concentrations much smaller than that of  $\text{CO}_2$ , would remove only negligible quantities of  $\text{S}(^1\text{D}_2)$  atoms, even if the reaction proceeded with unit collision frequency. Thus, the photolysis of COS in a  $10^3$ -fold excess of  $\text{CO}_2$  (or Ar) provided a "clean" source of  $\text{S}(^3\text{P}_{2,1,0})$  atoms on the time scale used in this study.

In view of the fact that the total rate of decay of  $\text{S}(^3\text{P}_{2,1,0})$  atoms was assumed to be equal to that of either the  $\text{S}(^3\text{P}_2)$  or the  $\text{S}(^3\text{P}_1)$  atoms, it is important that the three  $\text{S}(^3\text{P})$  states be in thermal equilibrium during the course of the measurement. Donovan and co-workers<sup>23</sup> have noted that this is not the case during the formation stage. However, under our conditions, the  $\text{S}(^3\text{P}_2): \text{S}(^3\text{P}_1): \text{S}(^3\text{P}_0)$  peak heights ratios were found to be 14.1:3.2:1, independent of reaction time. The following equation (see appendix 1 for derivation)

$$\frac{e^{-E_n/kT}}{e^{-E_m/kT}} = \frac{A_{sm}^{\text{sm}}}{A} \left( \frac{\text{P.H.}_{sn}}{\text{P.H.}_{sm}} \right)^{\frac{1}{\gamma}}$$

where  $E$  is the energy of the state  $n$  above the ground state  $m$ ,  $A$  is the transition probability for emission, P.H. is the microdensitometered peak height and  $\gamma$  is the experimental Beer-Lambert coefficient, gives the relationship between the thermalized population distribution and the experimental observables. The energy levels for the  $^3\text{P}_2$ ,  $^3\text{P}_1$  and  $^3\text{P}_0$  states of sulfur are 0, 1.14 and 1.64 kcal mole<sup>-1</sup> respectively. Furthermore, the emission transition



probabilities<sup>99-101</sup> for these three absorptions are  $4.0 \times 10^8$  ( $^3P_2 \rightarrow ^3S_1$ ),  $2.3 \times 10^8$  ( $^3P_1 \rightarrow ^3S_1$ ) and  $7.2 \times 10^7$  ( $^3P_0 \rightarrow ^3S_1$ )  $\text{sec}^{-1}$ . Solving the above equation for  $^3P_1/^3P_2$  and  $^3P_0/^3P_2$ , the value of  $\gamma$  is calculated to be 0.6 for both cases. Since this is in agreement with the experimental value of  $0.5 \pm 0.1$ , it is concluded that the sulfur atoms exist in a thermalized distribution which is not disturbed during the progress of the reaction. The designation  $S(^3P)$  will henceforth refer to thermally equilibrated metastable states.

The relative efficiencies of reactions [5] and [6] will depend on the conditions used, namely the relative concentrations of  $S(^3P)$  and COS. Previous studies<sup>12,20</sup> at high flash intensities and high COS pressures have indicated that the  $S(^3P)$  atoms generated in these systems probably decayed by a recombination process rather than by the abstraction reaction [5]. However, under conditions of low light intensity<sup>98</sup> in conventional photolysis, it has been shown that the dominant mode of decay of  $S(^3P)$  atoms was via the abstraction reaction [5]. Unfortunately, absolute sulfur atom concentrations were not monitored and therefore the order of the sulfur atom decay reaction could not be determined.

In the present system, the decay of  $S(^3P)$  atoms followed first order kinetics and reproducible rate constants were obtained. At a sulfur atom concentration of  $\sim 10^{-7}$  moles litre<sup>-1</sup>, an improbably high rate for reaction [6] of  $\sim 2 \times 10^{11}$  l<sup>2</sup> mole<sup>-2</sup> sec<sup>-1</sup> would be necessary in order for the recombination step [6] to contribute



significantly to the observed decay rate and therefore the importance of this step can be discounted on kinetic grounds as well.

Step [5], abstraction from COS, is a pseudo-first order reaction provided the concentration of S atoms is small relative to that of COS. If this reaction constitutes the major mode of sulfur atom decay then the experimentally measured decay rate  $k = 1.1 \times 10^3 \text{ sec}^{-1}$ , is related to  $k_5$  by

$$k = k_5[\text{COS}]$$

At 100 torr COS,  $k_5 = 1 \times 10^8 \text{ l mole}^{-1} \text{ sec}^{-1}$ . However, the experimentally measured value of  $k_5$  is  $2.1 \times 10^6 \text{ l mole}^{-1} \text{ sec}^{-1}$ <sup>102</sup> in the presence of argon and this is two orders of magnitude smaller than the value derived above. It must be concluded then that abstraction from COS is not important in the present system.

Reaction [7], diffusion from the reaction zone, would be difficult to evaluate directly unless a complete investigation were undertaken of the total reaction mechanism. However, an approximate formula has been developed for molecular diffusion in a cylindrical reaction vessel<sup>103</sup>:

$$k_{\text{diff}} = \frac{23.2 D_A}{d^2}$$

where  $D_A$  is the diffusion coefficient,  $d$  is the reactor diameter and  $k_{\text{diff}}$  is the diffusion rate. The diffusion coefficient,  $D_A$ , can be expressed<sup>104</sup> as



$$D_A = \frac{\lambda C}{3}$$

where  $C$ , the velocity of the particle, is given by

$$C = \frac{3RT}{M}$$

and  $\lambda$ , the mean free path, can be calculated from

$$\lambda = \frac{1}{2\pi\delta^2 r}$$

In this expression,  $\delta$  is the collision diameter,  $r$  is the concentration, in molecules  $\text{cc}^{-1}$  and  $M$  is the molecular weight. Using the values  $\delta = 3.75 \text{ \AA}$ ,  $r = 6.4 \times 10^{18} \text{ molecules cc}^{-1}$ ,  $M = 32.066 \text{ g/atom}$  and  $T = 298^\circ\text{K}$ ,

$$k_{\text{diff}} = 10 \text{ sec}^{-1}.$$

Although the expression for  $k_{\text{diff}}$  is based on several approximations and assumptions, it is probably correct within an order of magnitude and it seems likely therefore that diffusion does not play an important role in the overall decay process. In any case, diffusion always follows first order kinetics and it would be an additive component of the overall decay. Under conditions of much lower lamp intensities<sup>102</sup>,  $k_{\text{diff}}$  was obtained by extrapolation of a decay rate versus COS concentration plot and the value obtained,  $\sim 25 \text{ sec}^{-1}$  at  $298^\circ\text{K}$ , is in satisfactory agreement with the above estimate.



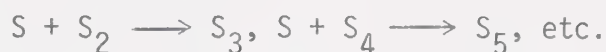
Two other possibilities for sulfur atom decay exist which would formally follow first order kinetics:

1. Catalyzed recombination of sulfur atoms,



where  $k_a \gg k_b$ . However, the overall decay rate should be pressure dependent and there are indications<sup>102</sup> that this is not so.

2. Reaction with  $S_x$  intermediates



Although  $S_2 - S_7$  intermediates are present in photolyzed COS, it is impossible to assess their concentrations or reactivities. What is known with certainty is that they are totally unreactive towards ground state molecules and decay solely by cross-combination and/or reactions with radicals. Provided the rates of addition of S-atoms to all these species are comparable and the relative total concentration of  $S_2 - S_7$  species is unchanged during the course of the reaction, then this mode of decay would follow first order kinetics.

For rate measurements with other substrates, it is important that the first order rate of decay of sulfur atoms be small relative to the rate of reaction with the substrate. In



order to achieve this, the concentrations of added substrate were kept as large as possible, within the limitations imposed by other experimental considerations. Thus, the first order rate constants usually obtained were in the range  $1-2 \times 10^4 \text{ sec}^{-1}$ . Since the sulfur atom concentration is  $\sim 10^{-7} \text{ mole litre}^{-1}$ , a reactant concentration of  $\sim 2 \times 10^{-6} \text{ mole litre}^{-1}$  (.04 torr) would result in a depletion of  $\sim 5\%$  of the initial reactant concentration, allowing the assumption of constant reactant concentration to be applied when calculating rate constants. If this were not the case, curvature of the first order decay curves would be expected. In those cases where the bimolecular reaction with a substrate proceeded at a rate approaching the collisional efficiency, requiring the use of smaller quantities of reactant, the concentration of  $\text{S}(^3\text{P})$  was kept as low as possible within the region of measurable intensities. Curvature of the first order decay plots was never observed in any system reported in this study, thus implying that simple second order kinetic treatments could be applied to the experimental data.



## CHAPTER IV

### THE REACTION OF $S(^3P)$ ATOMS WITH MOLECULAR OXYGEN

#### A. Results

The rate of reaction of  $S(^3P)$  atoms with molecular oxygen was investigated as a function of  $S(^3P)$  concentration, oxygen pressure, total pressure, and flash energy. Since  $SO$  is a plausible intermediate in this system, auxiliary experiments were undertaken in order to identify and monitor the kinetics of formation of this species.

#### 1. Kinetics of Decay of $S(^3P)$ Atoms

Initially, the rates of decay of both the  $S(^3P_1)$  and  $S(^3P_2)$  atoms were monitored at various partial pressures of oxygen, maintaining a constant  $CO_2$  pressure of 0.1 torr and a total pressure of 200 torr. In all cases, the rates of decay followed first order kinetics. A typical decay plot of  $\log [S(^3P)]$  versus time is illustrated in Figure IV-1. Furthermore, the decay rates for the  $S(^3P_2)$  and  $S(^3P_1)$  states were identical, within experimental error, indicating that the three metastable ground states maintain a Boltzmann distribution. Both the  $S(^3P_2)$  and  $S(^3P_1)$  absorption intensities were used to calculate decay kinetics.



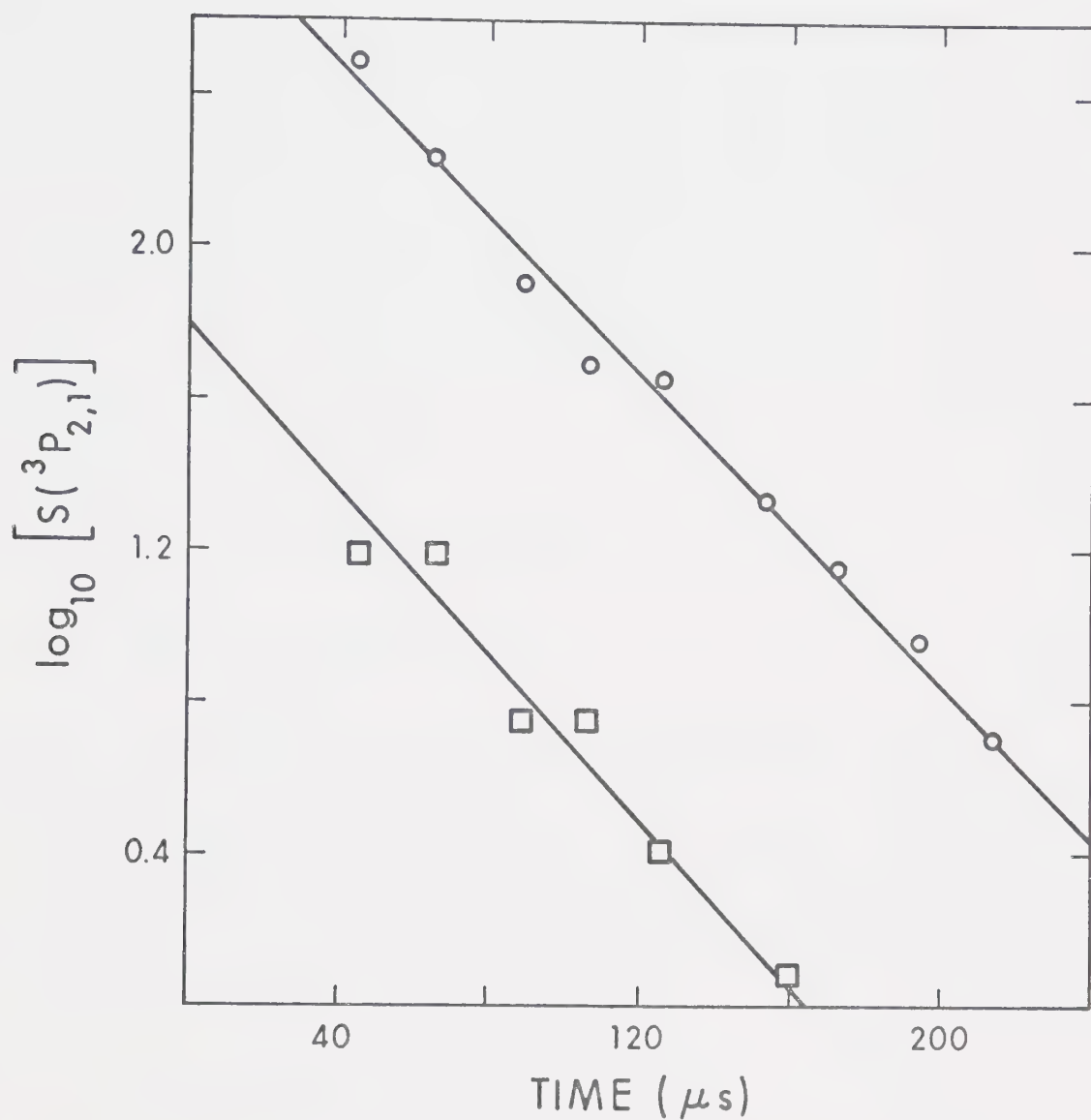


FIGURE IV-1: First Order Plot of Sulfur ( $^3P$ ) Atom Decay in the Presence of  $O_2$ ;  $\circ$ ,  $^3P_2$ ;  $\square$ ,  $^3P_1$ .  $P(COS) = 0.1$  torr,  $P(O_2) = 0.257$  torr; total pressure = 200 torr.



## 2. O<sub>2</sub> Pressure Study

The effect of a five-fold variation in O<sub>2</sub> pressure on the first order decay rate was examined. Increasing the oxygen pressure from 0.06 to 0.29 torr (Table IV-1) caused a considerable enhancement in the rate of removal of atomic sulfur as illustrated in Figure IV-2. Since it was demonstrated in Chapter III that the decay of S(<sup>3</sup>P) atoms is first order in the absence of substrate, the observed first order decay in the presence of O<sub>2</sub> must consist of two contributions: one corresponding to the observed rate of decay in pure COS/diluent, the rate constant of which is  $1.1 \times 10^3 \text{ sec}^{-1}$  and one corresponding to reaction with O<sub>2</sub>:

$$-\frac{dS}{dt} = k_1[O_2][S] + k_2[S]$$

where  $k_1$  is the bimolecular rate constant for reaction with molecular oxygen and  $k_2$  is the decay rate constant in the absence of substrate. Therefore, the net experimentally observed first order rate constant,  $k_{\text{exptl}}$ , for the decay of S(<sup>3</sup>P) atoms obtained at a given concentration of O<sub>2</sub> would be

$$k_{\text{exptl}} = k_1[O_2] + k_2$$

The slope and intercept of a plot of  $k_{\text{exptl}}$  versus molecular oxygen concentration, Figure IV-3, should yield  $k_1$  and  $k_2$ , respectively. The intercept  $1.0 \pm 0.3 \times 10^3 \text{ sec}^{-1}$ , is in good agreement with the value  $k_2 = 1.1 \times 10^3 \text{ sec}^{-1}$  obtained by direct



TABLE IV-1

Effect of Oxygen Pressure on the Rate of Decay  
of S(<sup>3</sup>P) Atoms

$10^5[\text{O}_2]$ (mole/liter)	S( <sup>3</sup> P) species monitored	No. of runs	$10^{-4} k_{\text{exptl}}$ (sec <sup>-1</sup> )
0.33	<sup>3</sup> P <sub>2</sub>	4	0.66 <sup>a</sup>
0.33	<sup>3</sup> P <sub>1</sub>	2	0.60 <sup>a</sup>
0.67	<sup>3</sup> P <sub>2</sub>	2	1.31 <sup>a</sup>
0.69	<sup>3</sup> P <sub>2</sub>	1	1.20 <sup>b</sup>
0.99	<sup>3</sup> P <sub>2</sub>	4	1.80 <sup>a</sup>
0.99	<sup>3</sup> P <sub>1</sub>	1	1.84 <sup>a</sup>
1.11	<sup>3</sup> P <sub>2</sub>	4	2.02 <sup>c</sup>
1.38	<sup>3</sup> P <sub>2</sub>	4	2.24 <sup>d</sup>
1.38	<sup>3</sup> P <sub>1</sub>	4	2.40 <sup>d</sup>
1.55	<sup>3</sup> P <sub>2</sub>	3	2.66 <sup>a</sup>

<sup>a</sup> P(COS) = 0.1 torr; P(CO<sub>2</sub>) = 200 torr.

<sup>b</sup> P(COS) = 0.05 torr; P(CO<sub>2</sub>) = 30 torr; P(Ar) = 70 torr.

<sup>c</sup> P(COS) = 0.1 torr; P(CO<sub>2</sub>) = 60 torr.

<sup>d</sup> P(COS) = 0.1 torr; P(CO<sub>2</sub>) = 60 torr; P(Ar) = 140 torr.



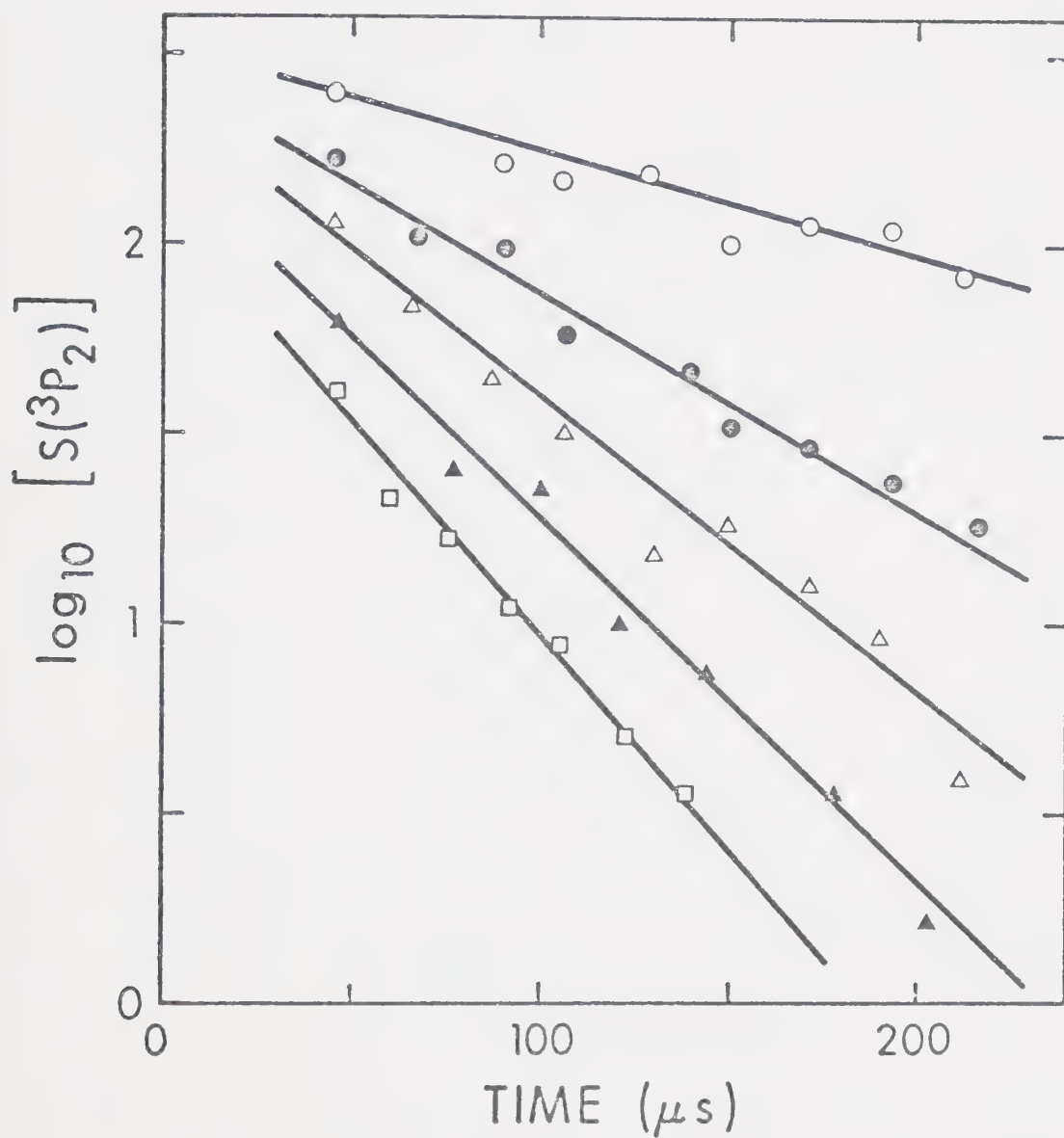


FIGURE IV-2: First Order Plots of  $S(^3P_2)$  decay.  $10^6[O_2]$  (mole liter<sup>-1</sup>): ○, 3.3; ●, 6.7; △, 9.9; ▲, 13.8, □, 15.5. Total pressure = 200 torr.



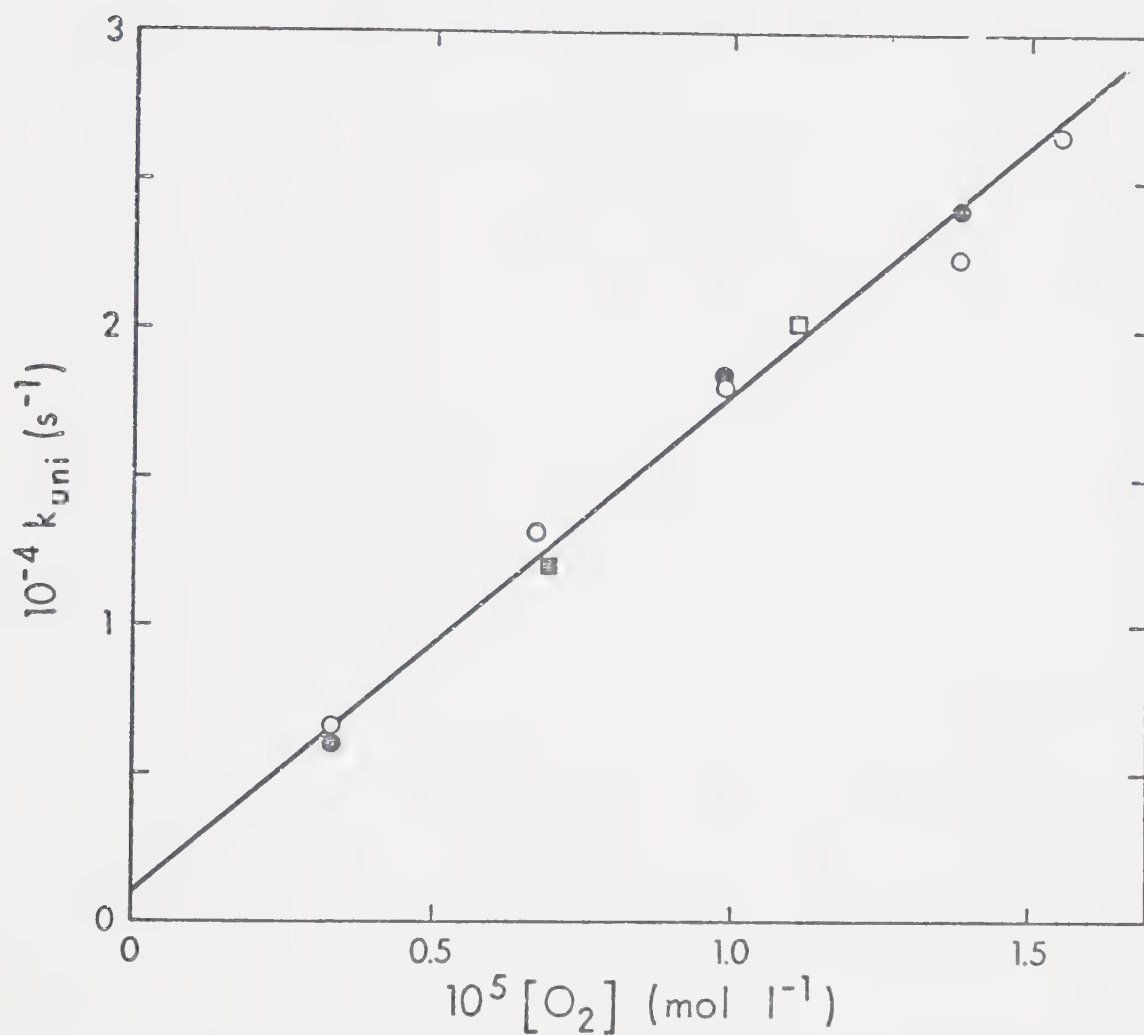


FIGURE IV-3: Plots of the Observed First Order Rate Constant versus molecular oxygen concentration; ○,  $S(^3P_2)$  decay at 200 torr total pressure, ●,  $S(^3P_1)$  decay at 200 torr; ■,  $S(^3P_2)$  decay at 100 torr; □,  $S(^3P_2)$  decay at 60 torr.



measurements (cf. Chapter III). From the slope,  $k_1 = 1.7 \pm 0.2 \times 10^9 \text{ l mole}^{-1} \text{ sec}^{-1}$ . The good linearity obtained in this plot and the nearly identical values of  $k_2$  derived from the intercept and from direct measurements support the assumption of an additive relationship between the two contributions to the rate of decay.

The range of molecular oxygen concentrations which can be used in this study is limited by instrumental design. The minimum useable delay time of the apparatus was 40  $\mu\text{sec}$ , and the decay rate must be sufficiently slow so that the bulk of  $\text{S}(^3\text{P})$  atoms were still present in the system in order that absorption spectra of sufficient intensity for quantitative measurement could be obtained. The maximum first order rate constant for this requirement was  $\leq 2.7 \times 10^4 \text{ sec}^{-1}$ , corresponding to a maximum partial oxygen pressure of 0.29 torr. On the other hand, the minimum  $\text{O}_2$  concentration which can be used is limited by the fact that the total observed decay rate must correspond to a predominant ( $\geq 80\%$ ) contribution from  $k_1$ , i.e. reaction with  $\text{O}_2$ . Therefore, oxygen pressures were kept in the range 0.06 to 0.29 torr, giving first order rate constants of  $0.66 - 2.66 \times 10^4 \text{ sec}^{-1}$ .

### 3. Effect of Total Pressure

The effect of total pressure on the bimolecular rate constant was examined over the pressure range 60 - 200 torr. From the data given in Table IV-1 and Figure IV-4, it is seen that the



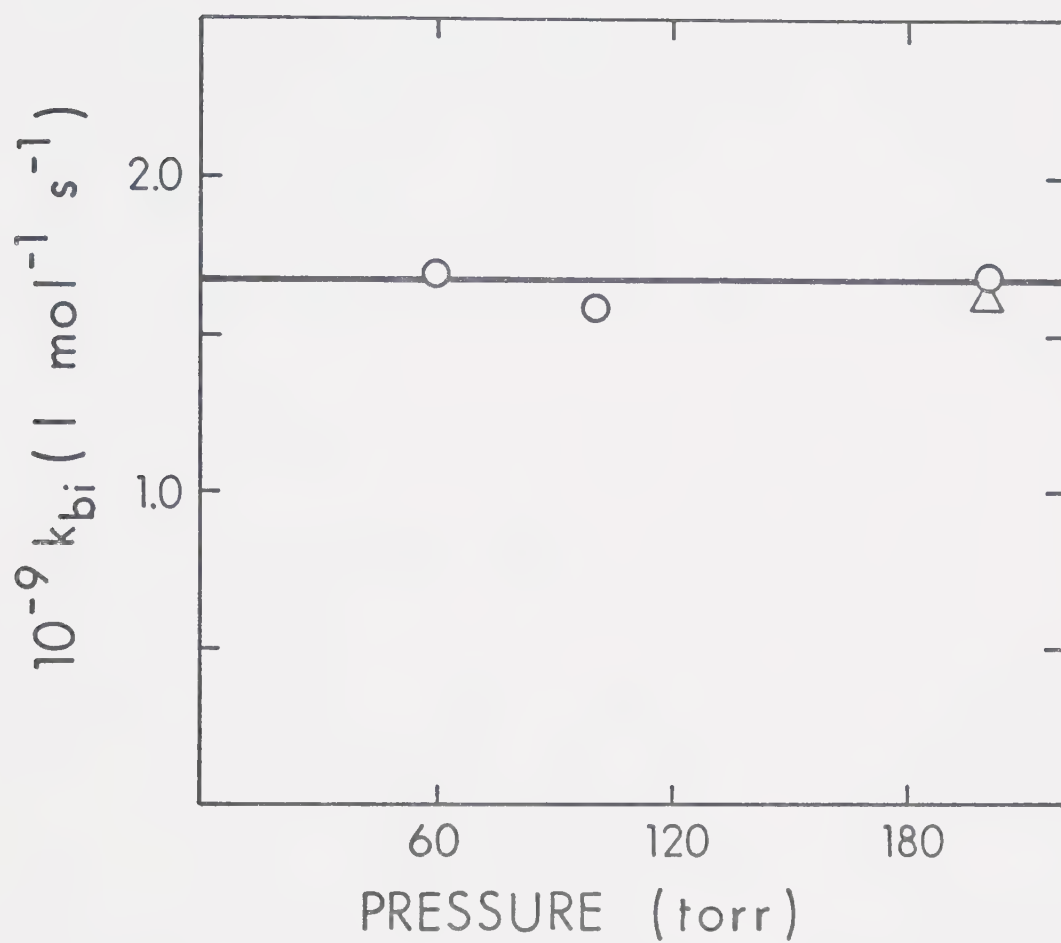


FIGURE IV-4: Bimolecular Rate Constant versus Total Pressure for  $^3\text{P}_2(\circ)$  and  $^3\text{P}_1(\Delta)$  atoms.



rate constant is unaffected by total pressure. It should be noted that below ca. 50 torr pressure, the extent of pressure broadening of an atomic line is not very large. Under these conditions the atomic absorption line is relatively narrow and since the resolving power of the microdensitometer is a direct function of the width of the line, the instrumental response is insufficient for quantitative determinations. This limitation only applies to the case where atomic lines are monitored. In the present system, it was found experimentally that ca. 50 torr CO<sub>2</sub> is the lowest practical limit.

#### 4. Effect of Flash Energy

The effect of flash energy on the second order rate constant was examined in the range 3 - 9 kV. The results are illustrated in Figure IV-5. No significant variation in the rate constant with flash energy was observed. This result is important for several reasons. Firstly, it indicates that the results obtained are independent of the sulfur atom concentration used, since the flash energy,  $E$ , and the concentration of sulfur atoms produced are related in a linear manner over a limited energy range:

$$S(^3P) \propto E = \frac{1}{2}CV^2,$$

where  $C$  is the capacitance of the capacitor and  $V$  is the charging voltage at which the unit is operated. Secondly, the lack of a



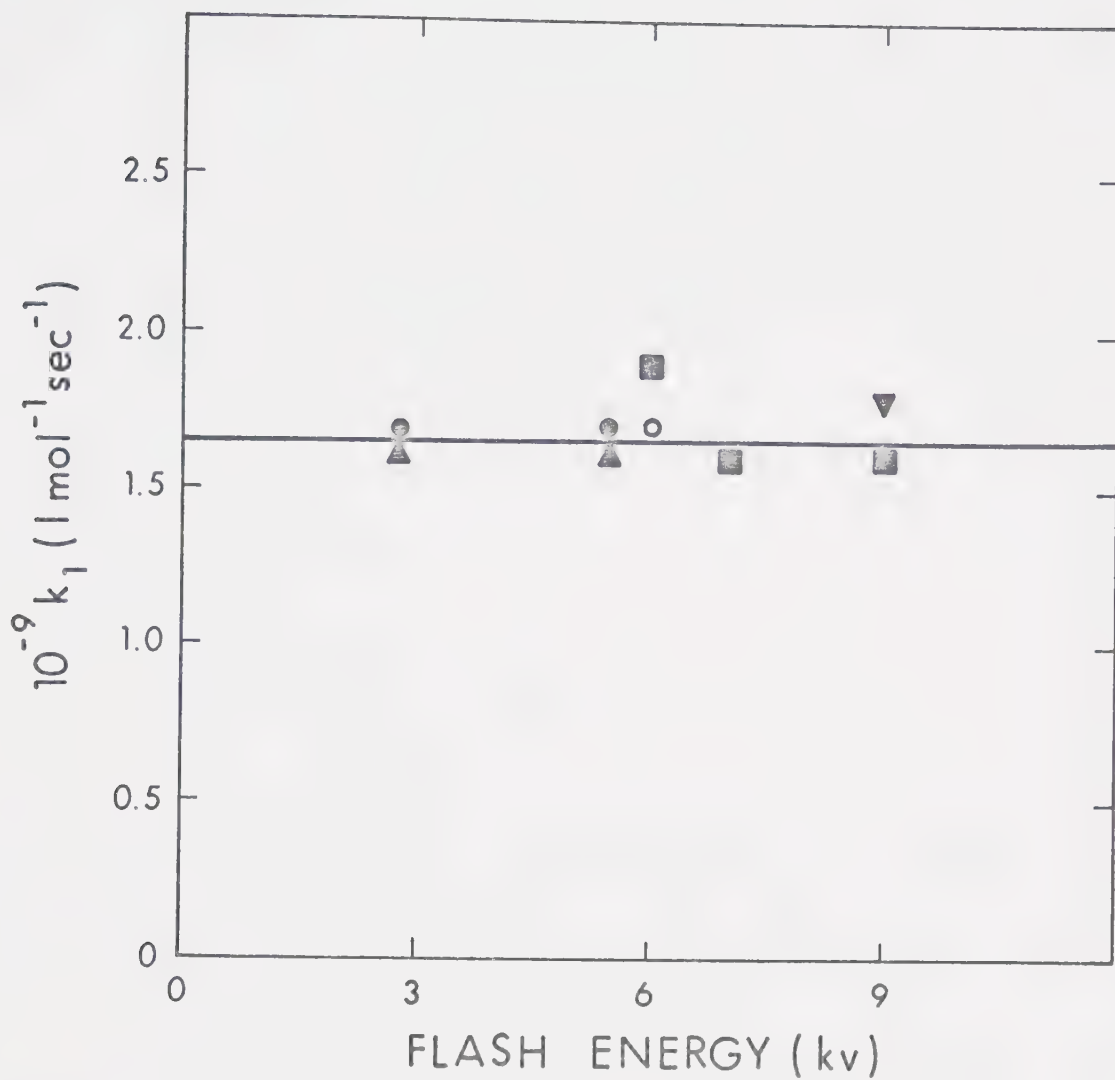


FIGURE IV-5: Bimolecular Rate Constant versus Flash Energy.

$P(\text{COS}) = 0.10 \text{ torr}$ ; total pressure = 200 torr.

$\Delta$ ,  $\text{O}_2 = 0.06 \text{ torr}$ ;  $\bullet$ ,  $\text{O}_2 = 0.18 \text{ torr}$ ;  $\circ$ ,  $\text{O}_2 =$

$0.29 \text{ torr}$ ;  $\blacksquare$ ,  $\text{O}_2 = 0.21 \text{ torr}$ ;  $\blacktriangledown$ ,  $\text{O}_2 = 0.12 \text{ torr}$ .



flash energy dependence indicates that the photolysis of substrate can be neglected as a complicating factor in the reaction mechanism. This is important since molecular oxygen absorbs weakly above the quartz cut-off of the cell. Thirdly, and most importantly, if secondary reactions contribute to the overall rate of decay then some variation should be observed at high flash energies where larger concentrations of transients are produced. The lack of such an effect indicates that the measured rate constant of decay can be identified with the primary reaction of  $S(^3P)$  atoms with  $O_2$ .

## 5. Observation of the SO Spectrum

At the usual concentration of COS employed in the kinetic studies, ca 0.1 torr, SO could not be detected. However, when the COS pressure was increased to 0.3 torr, the (14,0), (15,0), (16,0), (17,0), (18,0), (19,0) and (21,0) bands of the  $B^3\Sigma^- \leftarrow X^3\Sigma^-$  system<sup>105</sup> of SO could be observed weakly in the region 195.0 - 204.0 nm (see Table IV-2). Quantitative measurement of the kinetics of SO formation was not possible due to the low intensity of the bands, but qualitatively at least, the rise in the SO concentration appeared to correspond to the decay of atomic sulfur.

A very weak, diffuse band centered at 183.15 nm was observed in flashed COS(0.1 torr) +  $O_2$  +  $CO_2$  mixtures. Its intensity increased during the period of the sulfur atom decay.



TABLE IV-2

Band Head Assignments for the  
 $B^3\Sigma^- \leftarrow X^3\Sigma^-$  Transition in  $SO$  <sup>a</sup>

$v', v''$	Band Head $\lambda_{VAC}$ (nm)	Relative Intensity
0,0	-	-
1,0	-	-
2,0	-	-
3,0	231.46	3
4,0	228.34	3
5,0	225.32	5
6,0	222.47	5
7,0	219.76	6
8,0	216.93	6
9,0	214.43	7
10,0	212.02	7
11,0	209.75	8
12,0	207.48	9
13,0	205.34	9
14,0 <sup>b</sup>	203.34	9
15,0 <sup>b</sup>	201.36	10
16,0 <sup>b</sup>	199.70	8
17,0 <sup>b</sup>	198.37	5
18,0 <sup>b</sup>	197.55	4
19,0 <sup>b</sup>	196.72	3
20,0	195.97	4
21,0 <sup>b</sup>	195.22	2
22,0	194.48	3

/continued..



TABLE IV-2 (continued)

$\nu', \nu''$	Band Head $\lambda_{\text{VAC}} (\text{nm})$	Relative Intensity
23,0	193.81	3
24,0	193.24	3
25,0	192.74	3
26,0	192.16	1
27,0	191.67	1
28,0	191.33	1
29,0	190.92	1

<sup>a</sup> from reference 105

<sup>b</sup> monitored in this work



With 0.3 torr COS, additional bands centered at 183.8 and 184.4 nm were observed. These are the most intense bands of a set of six which McGarvey and McGrath<sup>105</sup> attributed to an isomeric form of SO<sub>2</sub>. However, this assignment has been questioned by two independent groups of workers<sup>106,107</sup>, who concordantly suggest that the band system in fact is due to the  $D^3\Pi \leftarrow X^3\Sigma^-$  transition of the SO molecule. The band head assignments are tabulated in Table IV-3.



TABLE IV-3

Band Head Assignments for the  
 $D^3_{\Pi} \leftarrow X^3_{\Sigma^-}$  Transition in SO <sup>a</sup>

$\nu', \nu''$	Band Head $\lambda_{\text{vac}}$ (nm)
	184.30 <sup>b</sup>
0,0	183.84 <sup>b</sup>
	183.20 <sup>b</sup>
	180.14
1,0	179.63
	178.94

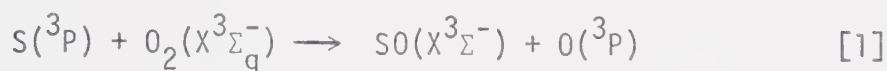
<sup>a</sup> from reference 106

<sup>b</sup> monitored in this work



## B. DISCUSSION

The spin and symmetry allowed reaction of ground state  $^3P_{2,1,0}$  sulfur atoms with molecular oxygen



has often been postulated<sup>105,108-112</sup> as an elementary process occurring in the oxidation of simple sulfur compounds. At the time this study was initiated, two conflicting rate constants had been reported for this reaction. Homann et al.<sup>93</sup>, using an isothermal flow system under reduced pressure and high dilution with inert gas to investigate the elementary reactions in the oxidation of  $CS_2$  at temperatures up to 1450°K, obtained the relationship

$$k_1 = 1 \times 10^{10} \exp (-5600)/RT \text{ l mole}^{-1} \text{ sec}^{-1}$$

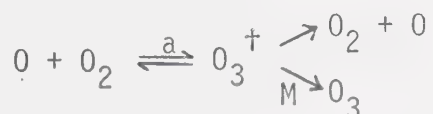
in the temperature range 675 - 1090°K. But extrapolation of this expression to 298°K yields  $k_1 = 8.3 \times 10^5 \text{ l mole}^{-1} \text{ sec}^{-1}$  which is three orders of magnitude lower than that obtained by Fair and Thrush<sup>92</sup>, using a discharge flow system to study the reactions of the system,  $H + H_2S + O_2$  in argon, who reported a rate constant value of  $1.2 \pm 0.3 \times 10^9 \text{ l mole}^{-1} \text{ sec}^{-1}$  at 298°K.

We determined a rate constant value for  $k_1$  of  $1.7 \pm 0.2 \times 10^9 \text{ l mole}^{-1} \text{ sec}^{-1}$ . This value is in reasonable agreement with that obtained by Fair and Thrush<sup>92</sup> and therefore the results



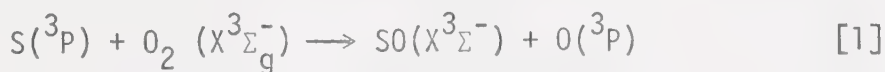
of Homann et al<sup>93</sup> appear to be in error. This has been corroborated by the result of Klemm and Davis<sup>113</sup>, who recently reported a value of  $1.35 \pm 0.14 \times 10^9 \text{ l mole}^{-1} \text{ sec}^{-1}$ , using the technique of flash photolysis-resonance fluorescence to study the reaction in a  $\text{COS} + \text{O}_2 + \text{Ar}$  system. In addition, a value of  $1.0 \pm 0.2 \times 10^9 \text{ l mole}^{-1} \text{ sec}^{-1}$  has been reported by Donovan and Little<sup>114</sup> using flash photolysis with kinetic absorption spectrophotometry in the investigation of a  $\text{COS} + \text{O}_2 + \text{Ar}$  system.

Considering the analogous sequence for the reaction of  $\text{O}(^3\text{P})$  atoms with  $\text{O}_2$ <sup>115</sup>,

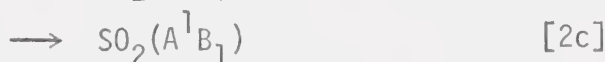
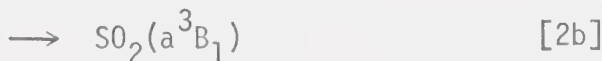


the calculated value of  $k_a = 0.9 \times 10^9 \text{ l mole}^{-1} \text{ sec}^{-1}$  corresponds closely with our data on the  $\text{S}(^3\text{P}) + \text{O}_2$  system.

With regard to the primary step, the following reactions are energetically feasible and spin allowed:



$$\Delta H = -5.6 \text{ kcal mole}^{-1}$$

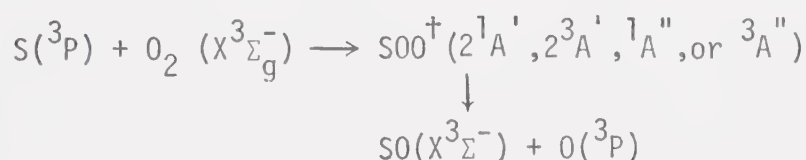


To date, no evidence has been found for the formation of  $\text{SO}_2$ , and it is doubtful whether reactions[2] occur at all. On the other



hand, the observation of the SO absorption spectrum and its parallel formation with  $S(^3P)$  decay point to the occurrence of step [1] as the major primary process. This is substantiated by the recent study employing resonance fluorescence<sup>113</sup>, where it was possible to monitor the formation of  $O(^3P)$  atoms. It was shown that the decay rate of  $S(^3P)$  atoms agreed with the rate of formation of  $O(^3P)$ . Thus since both primary products have been observed in this system, there is little doubt that [1] is the reaction path followed.

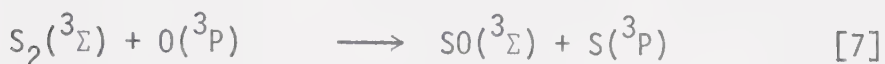
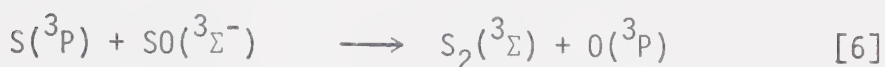
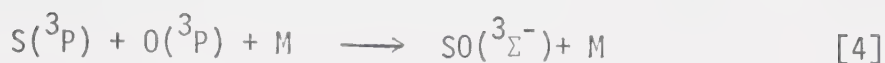
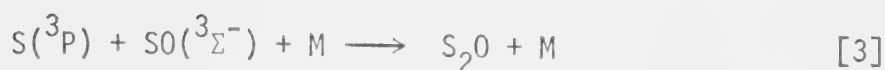
The most likely structure for the reaction complex is  $SOO$  and the absence of a pressure effect indicates that it rapidly falls apart to give  $SO$  and  $O(^3P)$ . Correlation rules predict nine states for this complex: three singlets, three triplets and three quintets. The latter would probably lie too high to be energetically attainable. The overall decomposition should follow the sequence,



where the dagger signifies vibrational excitation.

To evaluate the possible complications introduced by secondary reaction processes in the determination of the first order rate constant, the following reactions must be considered:





If reactions [3] and [4] were important in the overall kinetics, then the overall decay rate constant should be pressure dependent. Since this was not the case, these reactions are unimportant. Reactions [6] and [7] can be eliminated for two reasons: at the low sulfur atom concentration present in this system, the rates would have to be unreasonably large and secondly, reaction [6] is endothermic by 25 kcal mole<sup>-1</sup>. The rate of reaction [5] is reported<sup>113</sup> to be  $1 \times 10^7$  l mole<sup>-1</sup> sec<sup>-1</sup> and therefore, this process would be negligibly slow at the concentrations of SO present in our system. From these considerations and from experimental evidence it can therefore be concluded that secondary radical reactions are unimportant in the S(<sup>3</sup>P) + O<sub>2</sub> system.

The reported<sup>93</sup> activation energy of 5.6 kcal mole<sup>-1</sup> is too large to be reconcilable with the present value for the room temperature rate constant. The maximum value of the activation energy consistent with this is ~ 2.8 kcal mole<sup>-1</sup> if the A factor is equal to the gas kinetic collision frequency. In addition, the overall reaction, step 1, is exothermic by ~ 5.6 kcal mole<sup>-1</sup>, and



therefore would not be expected to have an activation energy larger than the thermoneutral isotopic exchange reaction<sup>116-118</sup>



which is reported to have an  $E_a$  of 1.1 kcal.

Very recently, it has been shown by resonance fluorescence experiments<sup>113</sup> that temperature has no effect on  $k_1$  and therefore that Homann et al.'s results<sup>93</sup> are completely erroneous. This can possibly be attributed to the complexity of the reaction system from which the rate data was extracted. Intermediates in the reaction sequence which were monitored included O, S, CS, SO, COS, S<sub>2</sub>O, S<sub>2</sub>O<sub>2</sub> as well as sulfur polymers S<sub>2</sub>, S<sub>3</sub>, S<sub>4</sub>, S<sub>5</sub> and S<sub>8</sub>. Since  $E_a = 0$ , the resulting low A factor can be explained via the formation of SOO in an end-on collision.

The presently available absolute rate constants for the S(<sup>3</sup>P) + O<sub>2</sub> reaction are tabulated in Table IV-4. With the exception of Homann et al.<sup>93</sup>, they are in reasonable agreement, with only the value of Donovan and Little<sup>114</sup> lying slightly outside the range of our assigned error limits.

Table IV-5 lists the absolute room temperature rate constants for the reaction of a number of biradical species with oxygen. It can be seen that the rates for ground state sulfur, oxygen<sup>115-118</sup> and methylene<sup>1</sup> are very similar but the rate of reaction with C(<sup>3</sup>P) atoms<sup>119</sup> is enhanced tenfold. It would appear that the steric limitation in the case of C(<sup>3</sup>P) is less



TABLE IV-4

Absolute Rate Constants for the Reaction of  $S(^3P_J)$   
Atoms with Molecular Oxygen

$k \times 10^{-9}$ , $l \text{ mole}^{-1} \text{ sec}^{-1}$ <sup>a</sup>	Technique	Reference
$1.7 \pm 0.2$	Flash Photolysis - Kinetic Absorption Spectroscopy	Present Work
$1.2 \pm 0.3$	Flow Tube	R.W. Fair & B.A. Thrush <sup>92</sup>
$1.35 \pm 0.14$	Flash Photolysis - Resonance Fluorescence	D.D. Davis, R.B. Klemm & M. Pilling <sup>113</sup>
$1.0 \pm 0.2$	Flash Photolysis - Kinetic Absorption Spectrophotometry	R.J. Donovan & D.J. Little <sup>114</sup>
0.00083	Flow System	K.H. Homann, G. Krome & H.Gg. Wagner <sup>93</sup>

<sup>a</sup> at 25°C



TABLE IV-5

Absolute Rate Constants for the Reaction of Radicals  
and Atomic Species with Molecular Oxygen

Reaction	$k \times 10^{-9}$ , 1 mole <sup>-1</sup> sec <sup>-1</sup>
$S(^3P_J) + O_2(^3\Sigma_g^-) \longrightarrow SO(^3\Sigma^-) + O(^3P)$	1.7 <sup>a</sup>
$^{18}O(^3P_J) + ^{16}O_2(^3\Sigma_g^-) \longrightarrow ^{18}O^{16}O + ^{16}O(^3P)$	0.9 <sup>b</sup>
$CH_2(^3\Sigma) + O_2(^3\Sigma_g^-) \longrightarrow \text{products. (CO, CO}_2, H_2)$	0.9 <sup>c</sup>
$C(^3P_J) + O_2(^3\Sigma_g^-) \longrightarrow CO + O$	20.0 <sup>d</sup>

<sup>a</sup> This work

<sup>b</sup> References 115-118

<sup>c</sup> Reference 1

<sup>d</sup> Reference 119



severe than that of the attack of  $S(^3P)$  on molecular oxygen. There is also a large difference in exothermicity, this reaction being exothermic by  $148 \text{ kcal mole}^{-1}$ .



## CHAPTER V

### THE REACTION OF $S(^3P)$ ATOMS WITH NITRIC OXIDE

#### A. Results

The reaction of  $S(^3P)$  atoms with nitric oxide was investigated as a function of total pressure and partial nitric oxide pressure. The order, with respect to  $S(^3P)$  atoms, was also determined.

##### 1. Kinetics of $S(^3P)$ Atom Decay

The  $S(^3P_2)$  atom concentration was monitored in the time range 25-250  $\mu\text{sec}$ . The method of integration<sup>120</sup> was used to determine the order of the reaction with respect to  $S(^3P)$  atoms. The first order plot of  $\ln [S(^3P)]$  versus time, Figure V-1, is linear whereas if the data are plotted in the second order form, Figure V-2, definite curvature is evident. The reaction is therefore first order with respect to  $S(^3P)$ .

##### 2. Effect of NO Pressure

The first order decay was determined over a range of NO pressures from 0.025 to 0.30 torr. Assuming that the first order decay in the absence of NO and the decay due to reaction with NO were additive, as shown in the previous chapter for the  $S + O_2$  system, then a correction can be applied for the decay



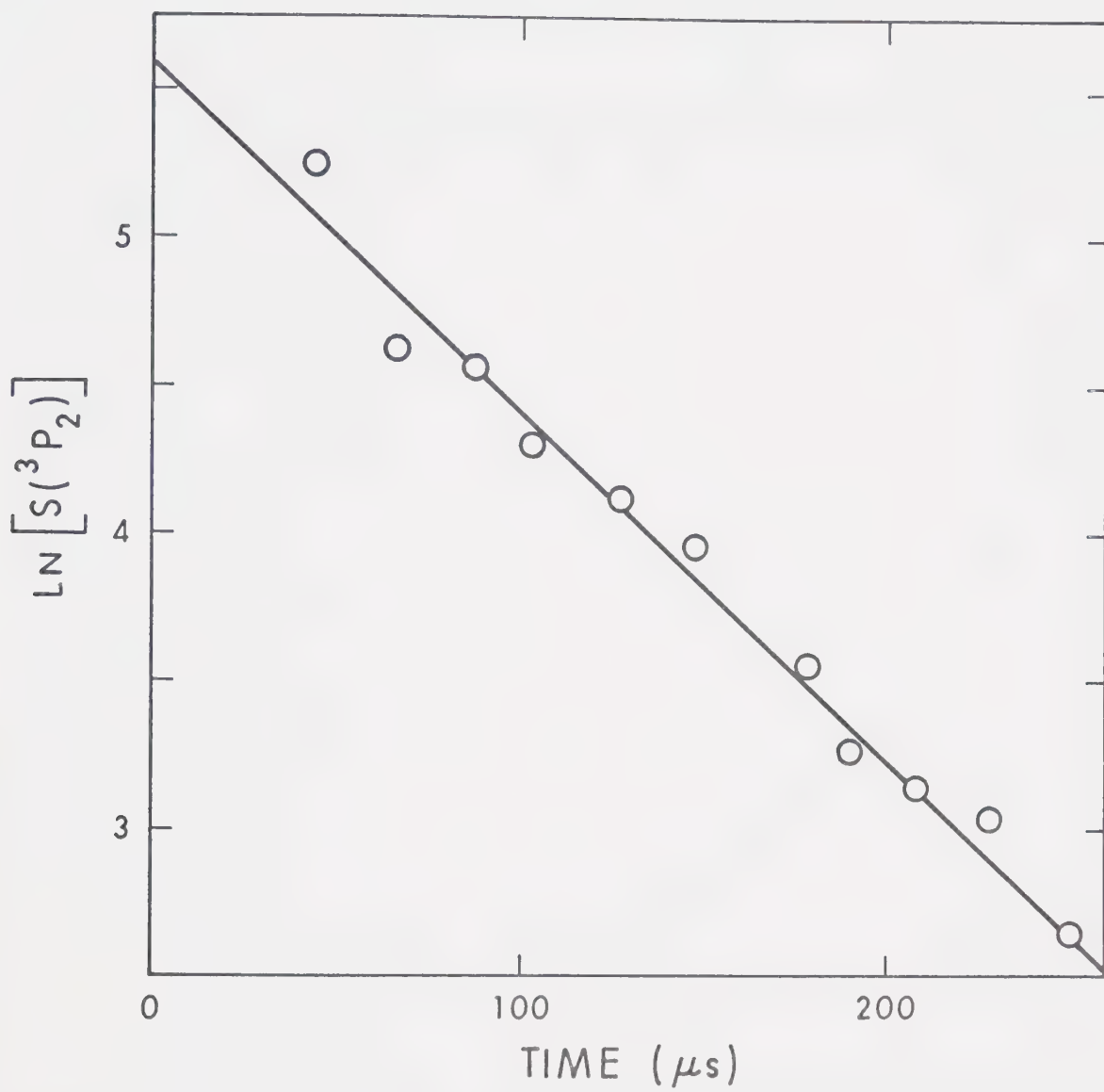


FIGURE V-1: First Order Decay Plot of  $\ln [S(^3P_2)]$  versus time.

$P(\text{COS}) = 0.12$  torr,  $P(\text{NO}) = 0.10$  torr, Total Pressure  
= 200 torr.



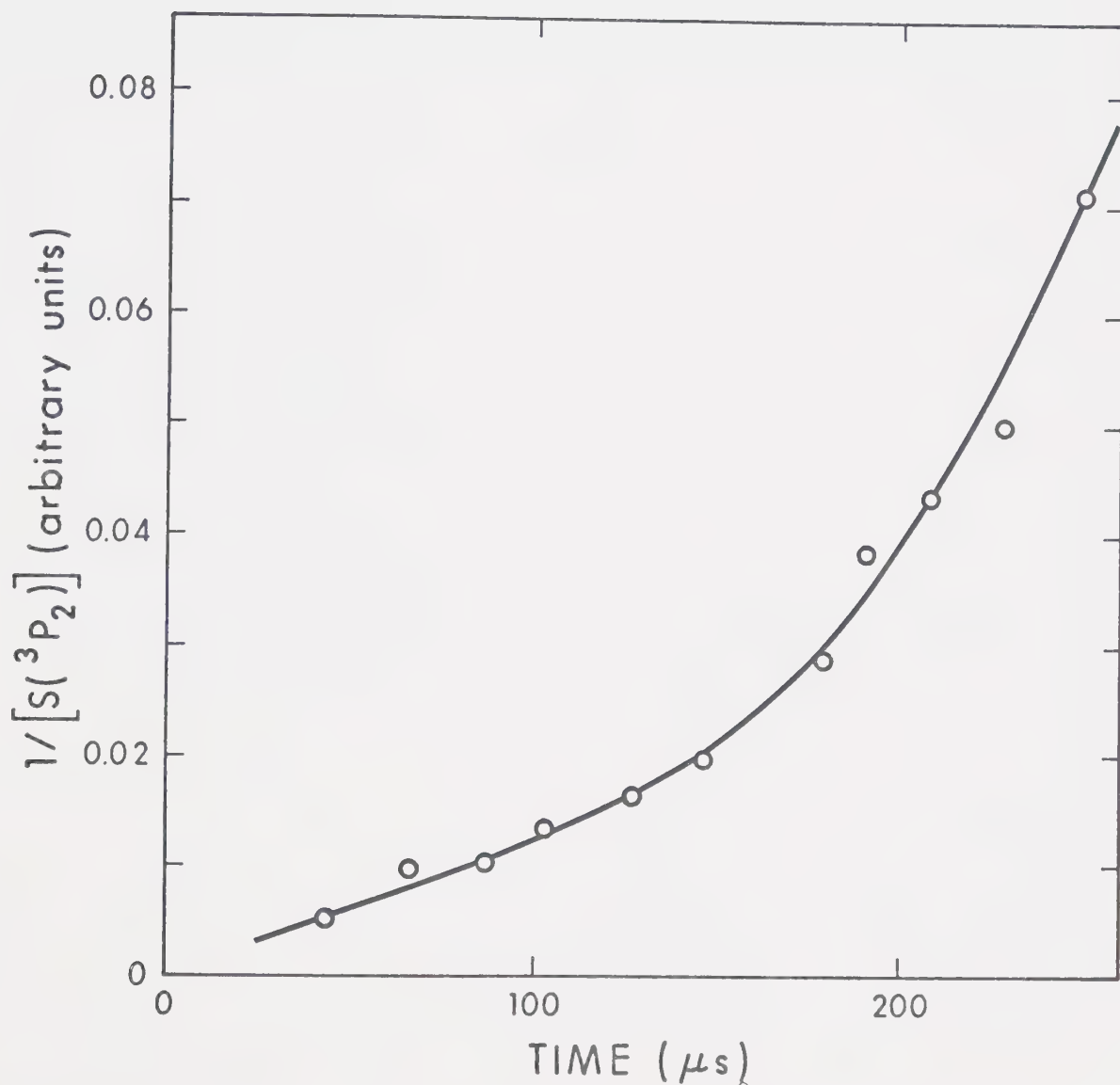


FIGURE V-2: Second Order Decay Plot of  $1/[S(^3P_2)]$  versus time,  
 $P(COS) = 0.12$  torr,  $P(NO) = 0.10$  torr, Total  
 Pressure = 200 torr.



rate in the absence of NO, which has been determined experimentally (Chapter III). Thus, as the NO pressure approaches zero, the corrected first order rate constant should approach zero and this is indeed the case as illustrated in Figure V-3. The corresponding data are given in Table V-1. The bimolecular rate constant derived from the slope of the plot is  $1.6 \pm 0.2 \times 10^9 \text{ l mol}^{-1} \text{ sec}^{-1}$ .

### 3. Effect of Total Pressure

The value of the bimolecular rate constant was determined over a wide range of total pressures from 50 - 600 torr using  $\text{CO}_2$  as a diluent. The results are tabulated in Table V-2. The plot of the bimolecular rate constant as a function of total pressure, Figure V-4, shows a very definite curvature. However, a linear relationship appears to hold below 100 torr and determination of the slope over this limited range yields a value of  $1.8 \times 10^{11} \text{ l}^2 \text{ mole}^{-2} \text{ sec}^{-1}$  for the termolecular rate constant.



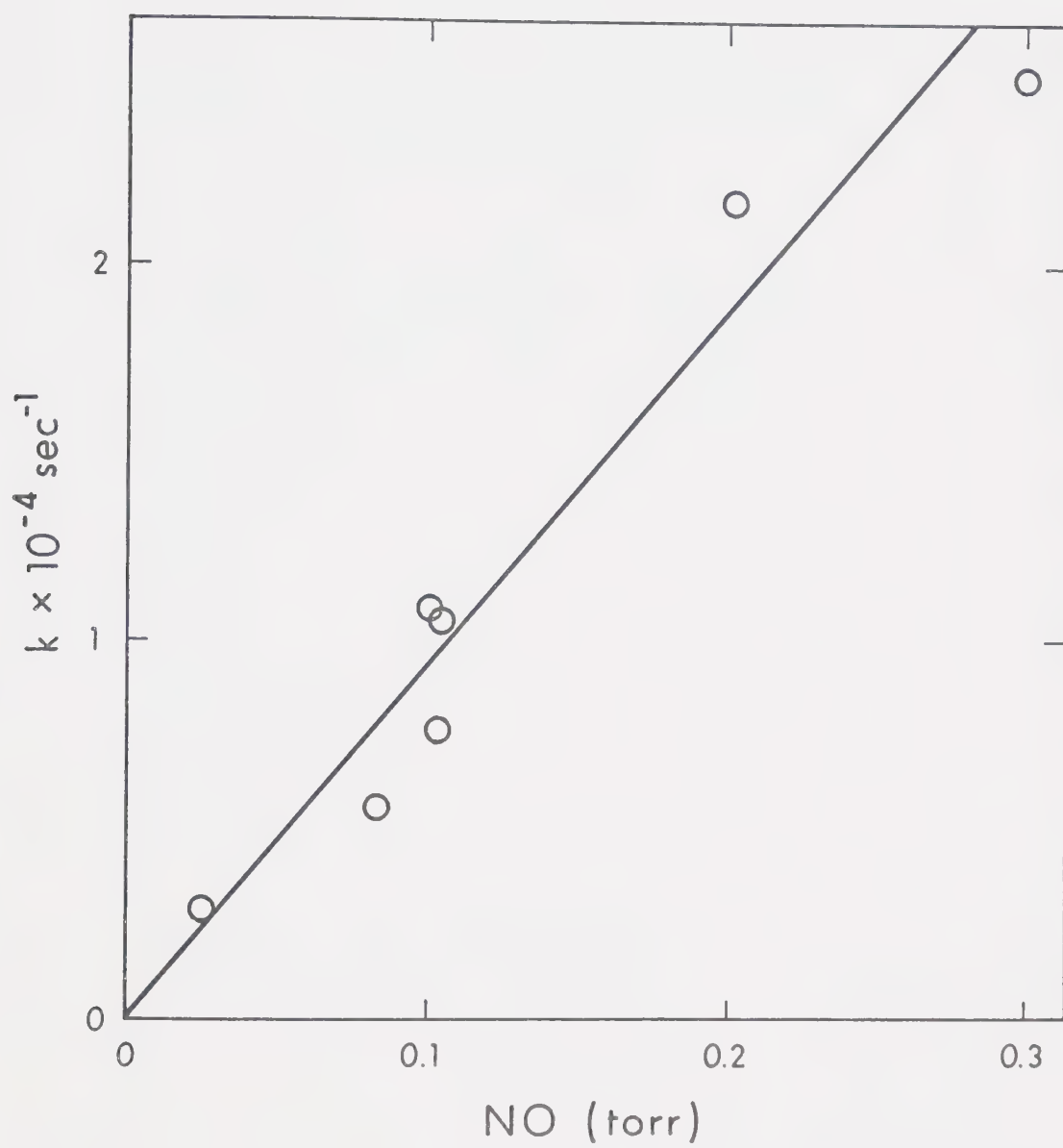


FIGURE V-3: Corrected First Order Rate Constant as a Function of NO Pressure.



TABLE V-1

Effect of NO Pressure on the Rate of Decay  
of S( $^3P_2$ ) Atoms <sup>a</sup>

NO (torr)	No. of runs	$10^{-4} k, \text{sec}^{-1}$
0.0256	1	0.39
0.0832	2	0.56
0.101	2	1.09
0.103	1	0.77
0.104	3	1.06
0.202	2	2.16
0.299	2	2.50

<sup>a</sup> COS = 0.12 torr, CO<sub>2</sub> = 200 torr



TABLE V-2

Effect of Total Pressure on the  
Bimolecular Rate Constant <sup>a</sup>

CO <sub>2</sub> (torr)	No. of runs	10 <sup>-9</sup> x k (l mol <sup>-1</sup> sec <sup>-1</sup> )
50	2	0.48
100	4	0.97
200	10	1.60
400	4	2.76
600	3	3.75

<sup>a</sup> COS = 0.12 torr, NO = 0.10 torr



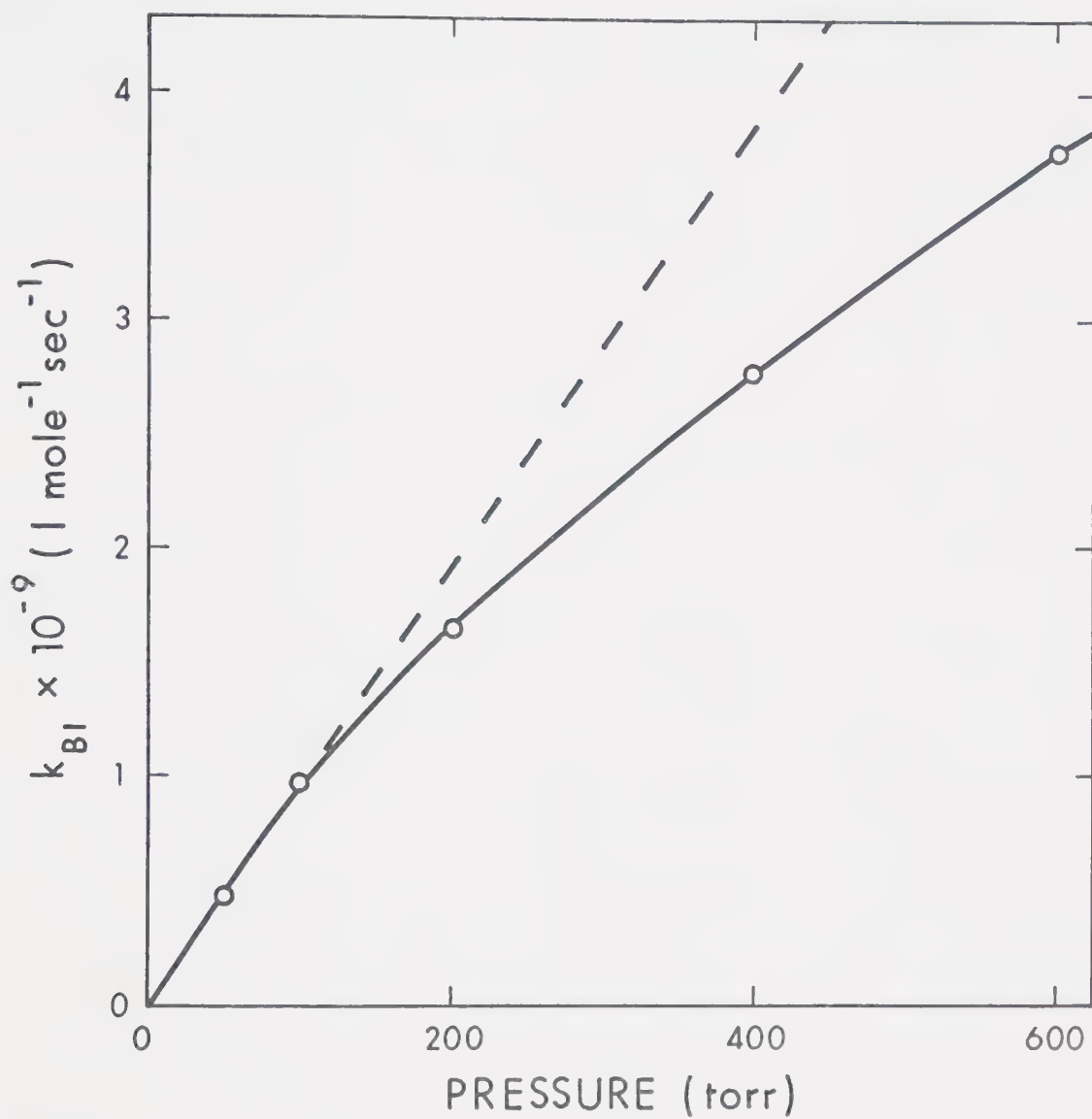
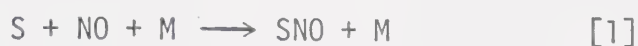


FIGURE V-4: Bimolecular Rate Constant as Function of Total Pressure.



## B. Discussion

Basco and Pearson<sup>20</sup> have reported that the rate of formation of  $S_2$  in  $CS_2 + Ar$  or  $COS + Ar$  systems is greatly enhanced in the presence of small amounts of NO and suggested a catalytic recombination sequence,



where  $k_1 \ll k_2$  at low total pressures.

In the present study, the disappearance of  $S(^3P)$  atoms was found to be dependent on total pressure, Figure V-4. Up to 100 torr, the rate was linear with pressure but above this region a fall-off from the third order dependence was observed.

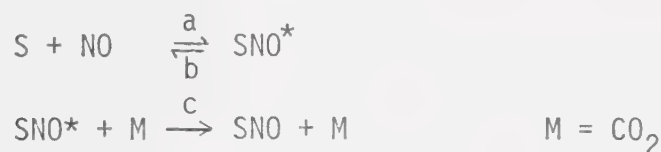
The relative importance of steps [1] and [2] in our system can be assessed in the following manner. If it is assumed that step [2] contributes significantly to the overall process, then its rate constant should be of the same order of magnitude as the observed first order rate constant, i.e.  $k_2[SNO] \sim 10^4 \text{ sec}^{-1}$ . Since the concentration of S atoms is  $\sim 10^{-7} \text{ mole l}^{-1}$  then  $k_2 = -dS/dt/[S][SNO] = 10^{11} \text{ l mole}^{-1} \text{ sec}^{-1}$ . Thus, to compete successfully with step [1], step [2] would have to proceed at a rate very close to the collision frequency. This appears to be unlikely since the rate constant for the comparable reaction with iodine atoms,



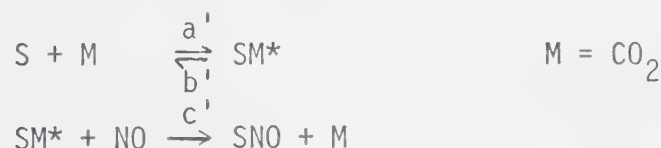


has been reported<sup>121</sup> to be  $4 \times 10^9 \text{ l mole}^{-1} \text{ sec}^{-1}$ . However, at sufficiently low pressures of NO, step [2] would be important and the observed rate constant would be simply  $2k_1$ .

Assuming that the observed rates pertain to reaction [1], the results can be interpreted in two ways<sup>122</sup>, in terms of an energy-transfer (ET) mechanism:



or a radical-molecular complex (RMC) mechanism:



The ET mechanism yields the expression (see Appendix II):

$$-\frac{dS}{dt} = \frac{dSNO}{dt} = \frac{k_a k_c [S][NO][M]}{k_b + k_c [M]} \quad I$$

which is third order when  $k_b \gg k_c M$ . From the RMC mechanism,

$$-\frac{dS}{dt} = \frac{dSNO}{dt} = \frac{k_a k_c' [S][NO][M]}{k_{b'} + k_{c'} [NO]} \quad II$$

which is third order when  $k_{b'} \gg k_{c'} [NO]$ .



Equation I predicts third order kinetics at low pressures and then complex behaviour at  $k_b \sim k_c[M]$ , which was actually observed in the present system. Equation II, on the other hand, does not account for the pressure dependence of the rate constant. It can therefore be concluded that the ET mechanism is operative in the  $S + NO + CO_2$  system. This is in keeping with the well documented role of  $CO_2$  as an inert third body in other radical recombination reactions, some rate constants of which are listed in Table V-3.

At any given pressure  $M$ , the bimolecular rate constant is given by

$$k_{bi \text{ observed}} = \frac{k_a k_c}{k_b + k_c M} M$$

and a plot of  $1/k_{bi \text{ observed}}$  versus  $1/M$  should yield a straight line having a slope of  $k_b/k_a k_c$  and an intercept of  $1/k_a$ . From Figure V-5,  $k_a = 9.3 \pm 2.1 \times 10^9 \text{ l mole}^{-1} \text{ sec}^{-1}$  and  $k_c/k_b = 20.7 \pm 4.4$ . Thus the limiting high pressure rate constant for the  $S + NO$  association will be  $9.3 \times 10^9 \text{ l mole}^{-1} \text{ sec}^{-1}$  and, at low pressures, the rate can be expressed as  $1.9 \pm 0.1 \times 10^{11} \text{ l}^2 \text{ mole}^{-2} \text{ sec}^{-1}$ .

Since  $k_b = k_c M$  when the total pressure is  $\sim 900$  torr, the lifetime of  $SNO^*$  can be calculated if we assume unit collisional efficiency for  $k_c$ :

$$k_c = \pi d_{AB}^2 \left( \frac{8kt}{\pi\mu} \right)^{1/2} = 2 \times 10^{11} \text{ l mole}^{-1} \text{ sec}^{-1}$$

where  $d_{AB}$  is the collision diameter taken as  $4.6 \times 10^{-8} \text{ cm}$  and  $\mu$



TABLE V-3

Rate Constants for Bimolecular Recombination of Atomic Species <sup>a</sup>

Third Body	$k_{TRI} \text{ (1}^2\text{mole}^{-2}\text{sec}^{-1}\text{)}$			
	I	O	H	N
He	1.2 - 3.3 x 10 <sup>9</sup>	3 x 10 <sup>8</sup>	-	4.0 - 8.2 x 10 <sup>8</sup>
Ar	2.9 - 6.9 x 10 <sup>9</sup>	3 x 10 <sup>8</sup>	5.6 x 10 <sup>9</sup>	1.6 - 6.2 x 10 <sup>9</sup>
N <sub>2</sub>	4.5 - 12 x 10 <sup>9</sup>	1 x 10 <sup>8</sup>	-	2.8 - 6.2 x 10 <sup>9</sup>
CO <sub>2</sub>	13.4 - 33. x 10 <sup>9</sup>	3 x 10 <sup>8</sup>	-	-
NO	3.1 - >48 x 10 <sup>13</sup>	1.9 x 10 <sup>10</sup>	1.1 x 10 <sup>10</sup>	-

<sup>a</sup> reference 122



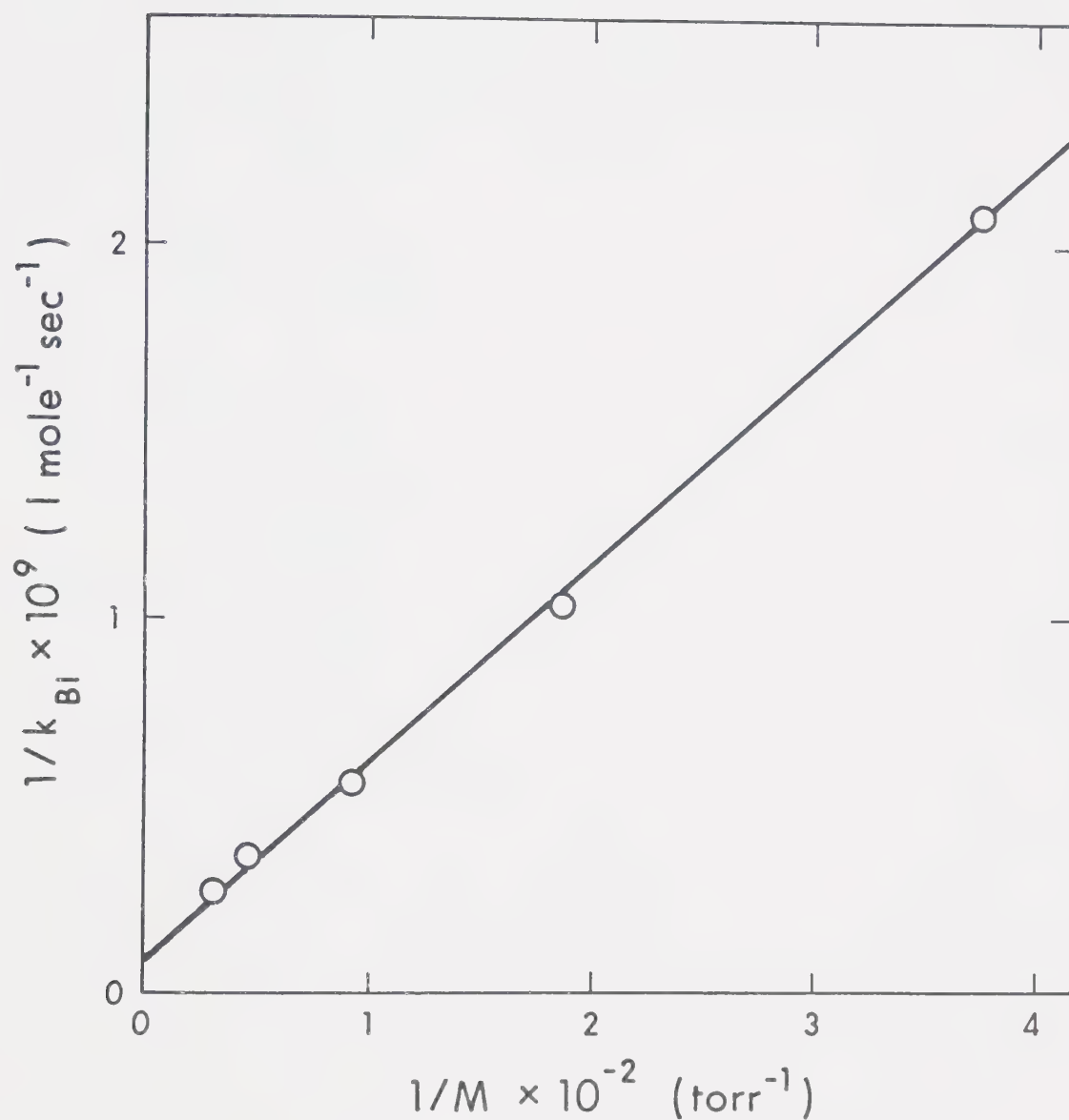


FIGURE V-5: Inverse of Bimolecular Rate Constant versus  
Inverse of Total Pressure.

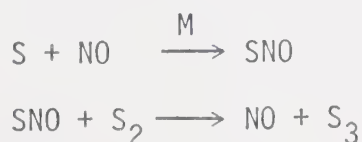


is the reduced mass. At 900 torr of  $\text{CO}_2$ ,  $k_b = k_c M$ , and thus  $k_b \approx 1 \times 10^{10} \text{ sec}^{-1}$  and  $\tau$ , the lifetime of  $\text{SNO}^*$  is  $\tau = \frac{1}{k_b} \approx 1 \times 10^{-10} \text{ sec}$ , which corresponds to  $\sim 1,000$  vibrations ( $\sim 10^{-13} \text{ sec/vibration}$ ). This is not an unreasonable estimate when compared with the lifetime of  $\text{N}_2\text{O}$  with respect to unimolecular decomposition which is  $5 \times 10^{-11} \text{ sec}$  at  $888^\circ\text{K}$ <sup>123</sup>.

$$\frac{\text{SNO}^*}{\text{S}} = \frac{k_a (\text{NO})}{k_b + k_c M} = \sim 4 \times 10^{-6}$$

at 200 torr total pressure. Thus, very small concentrations of  $\text{SNO}^*$  are present in the reaction mixture at any given time.

The product of the primary step,  $\text{SNO}$ , could not be detected in this study but has been identified in other systems. Thus, in the low temperature matrix photolysis<sup>124</sup> of *cis*- $\text{HNSO}$  two new absorptions at  $1523.0$  and  $789.7 \text{ cm}^{-1}$  were assigned as  $\text{NO}$  stretching and  $\text{SNO}$  bending frequencies respectively. Also, in flash photolysis-kinetic mass spectroscopy studies<sup>125</sup> of  $\text{COS-NO}$  mixtures, a mass corresponding to the  $\text{SNO}$  adduct was detected. A transient spectrum observed in the flash photolysis of  $\text{CS}_2$  or  $\text{COS}$  in the presence of  $\text{NO}$  has subsequently been assigned to  $\text{S}_3$  which is presumably formed in a catalyzed process<sup>8</sup>:



This is in keeping with the proven efficiency of  $\text{NO}$  as a chaperon



in atomic recombination processes, as illustrated in Table V-3. With NO as a third body, the recombinations of I, O and H atoms take place via a radical-molecule mechanism and the efficiencies are greatly enhanced.

At this point, it would be of interest to compare the rate constant for the S + NO reaction with those for other radical and atomic additions to NO, Table V-4. In the case of atom addition, eg. O(<sup>3</sup>P), H(<sup>2</sup>P) and Cl(<sup>2</sup>P) atoms, the third order rate constants are comparable and of the same order of magnitude to that determined for S + NO. In the case of radical addition to NO the intermediate adduct might be expected to have a longer lifetime owing to a greater number of vibrational modes and the observed rates should approach second order kinetics at lower pressures than would be the case for atom + NO systems. However, it can be seen that the values of these rate constants are comparable to the high pressure limiting rate constant for S + NO + M.

Because of its unpaired electron, NO has been demonstrated to be a remarkably efficient radical scavenger in a variety of systems. In many cases where monoradicals are present, stable isolable products can be formed. The NO-catalyzed recombination of atoms is equally efficient and, not surprisingly, is initiated by rapid addition of the atom to NO to form an intermediate adduct having a finite lifetime. The rate of addition is nearly equal to the collision frequency and thus NO is by far the most efficient chaperon in atomic recombination reactions.



TABLE V-4  
Rate Constants for Atomic and Radical Addition to NO

Third Body	$10^{-10}k_{\text{TRI}} \text{ (1}^2\text{mole}^{-2}\text{sec}^{-1}\text{)}$				$10^{-9}k_{\text{BI}} \text{ (1 mole}^{-1}\text{sec}^{-1}\text{)}$	
	$\text{S(}^3\text{P)}^{\text{a}}$	$\text{O(}^3\text{P)}^{\text{b}}$	$\text{H(}^2\text{P)}^{\text{c}}$	$\text{Cl(}^2\text{P)}^{\text{d}}$	$\text{CH}_3(^2\text{A)}^{\text{e}}$	$\text{S(}^3\text{P)}^{\text{a}}$ $\text{}^3\text{CH}_2^{\text{b}}$ $\text{CH}_3(^2\text{A)}^{\text{c}}$
He	-	-	.66	3.5	-	-   9.6   -
Ar	-	2 - 2.7	.87	2.9	-	-   -   -
N <sub>2</sub>	-	2 - 2.5	-	3.5	22 - 28	-   -   2.4 - 10
CO <sub>2</sub>	19	4 - 5	-	-	-	9.3   -   -

a this work                      d reference 127  
b reference 122                    e reference 128, 129  
c reference 126                    f reference 1



## CHAPTER VI

### THE REACTIONS OF $S(^3P)$ ATOMS WITH EPISULFIDES

#### A. Results

The reaction of  $S(^3P)$  atoms with ethylene episulfide was investigated as a function of ethylene episulfide pressure and total pressure. Rate constants were also determined for the reactions of  $S(^3P)$  atoms with propylene episulfide and *trans*-2-butene episulfide.

#### 1. $S(^3P)$ Atom Decay as a Function of Ethylene Episulfide Pressure

First order rate constants were determined over a range of ethylene episulfide pressures of 0.009 to 0.030 torr. The data are tabulated in Table VI-1. By comparison of the microdensitometered peak heights, it was estimated that the  $S(^3P) : C_2H_4S$  ratio varied between 1 : 20 and 1 : 70 in the pressure range 0.009 - 0.030 torr  $C_2H_4S$ . In this range of concentrations, linear first order decay plots were obtained, as illustrated in Figure VI-1. Furthermore, in a comparable study<sup>128</sup>, reliable first order rate constants were obtained for methyl radical : reactant ratios of 1 : 22 and therefore the concentration ratios used in the present study are sufficiently large so that accurate kinetic data can be derived.



TABLE VI-1

First Order Rate Constants as a Function of  
Ethylene Episulfide Concentration <sup>a</sup>

Ethylene Episulfide		$K_{\text{UNI}}$ sec <sup>-1</sup>	CO <sub>2</sub> , torr
mole l <sup>-1</sup>	torr		
0	0	$1.1 \times 10^3$	200
$0.48 \times 10^{-6}$	$0.897 \times 10^{-2}$	$7.6 \times 10^3$	200
$0.52 \times 10^{-6}$	$0.972 \times 10^{-2}$	$9.8 \times 10^3$	100
$1.04 \times 10^{-6}$	$1.94 \times 10^{-2}$	$15.8 \times 10^3$	200
$1.62 \times 10^{-6}$	$3.03 \times 10^{-2}$	$22.0 \times 10^3$	200

<sup>a</sup> P(COS) = 0.10 torr



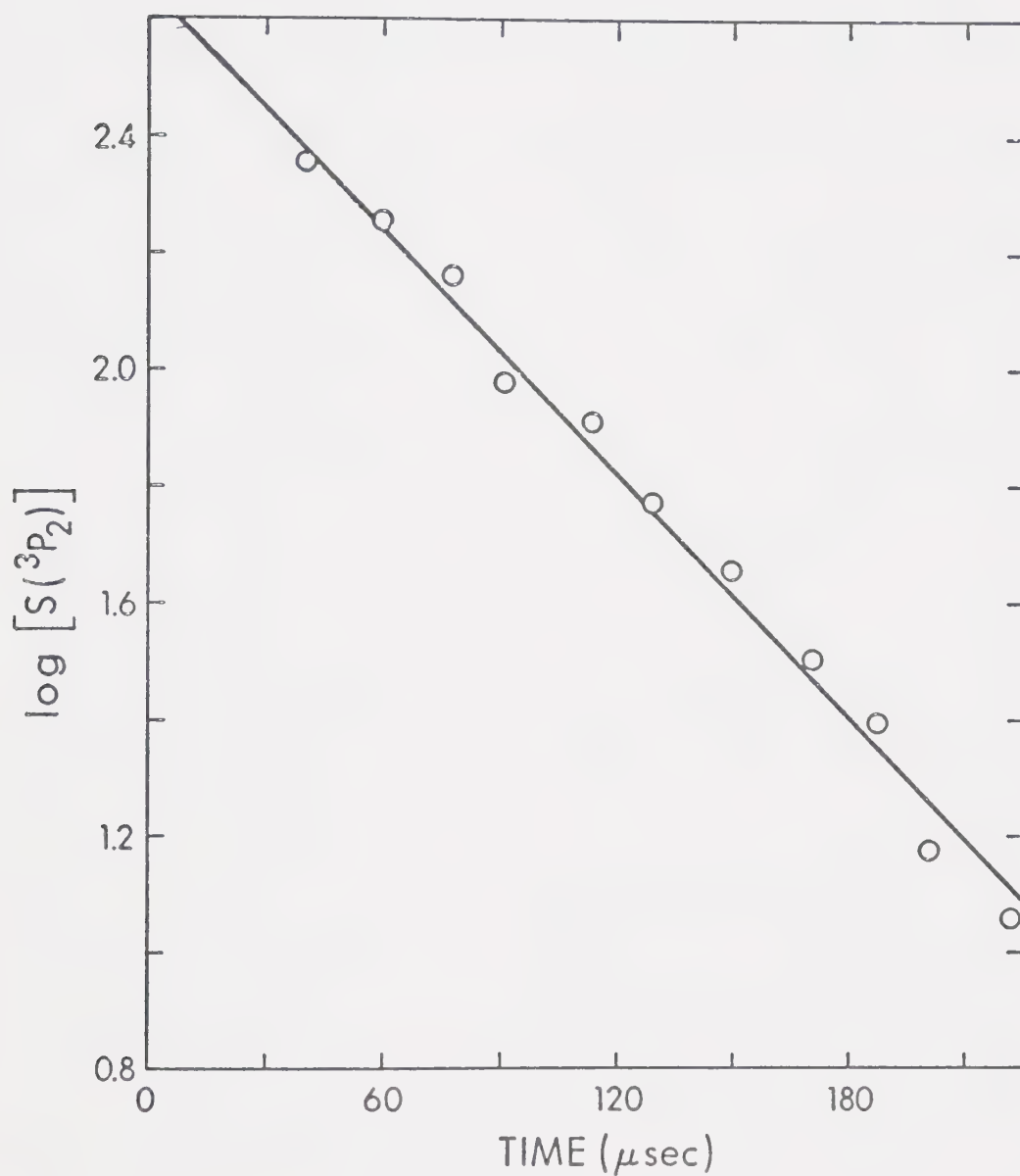


FIGURE VI-1: First Order Decay Plot of  $[S(^3P_2)]$  in the Presence of Ethylene Episulfide.  $P(\text{COS}) = 0.1$  torr,  $P(\text{C}_2\text{H}_4\text{S}) = 0.0194$  torr,  $P(\text{CO}_2) = 200$  torr.



A plot of  $S(^3P_2)$  first order rate constants versus ethylene episulfide concentration (Figure VI-2) shows no evidence of a significant deviation from a linear relationship. The bimolecular rate constant was determined to be  $1.4 \pm 0.2 \times 10^{10} \text{ l mole}^{-1} \text{ sec}^{-1}$ .

## 2. $S(^3P)$ Atom Decay as a Function of Total Pressure

The decay of  $S(^3P)$  atoms was determined at 100 and 200 torr total pressure. As illustrated in Figure VI-2, no significant difference could be observed in the rates constants.

## 3. The Bimolecular Rate Constant for the Reaction of $S(^3P)$ Atoms with Propylene Episulfide

The reaction of  $S(^3P)$  atoms with propylene episulfide was monitored at a total pressure of 200 torr of  $\text{CO}_2$  and a COS pressure of 0.1 torr. The average observed first order rate constant was  $1.07 \pm 0.11 \times 10^4 \text{ sec}^{-1}$ . Applying the correction for the rate constant in the absence of reactant yields a first order rate constant due to reaction with propylene episulfide of  $0.96 \times 10^4 \text{ sec}^{-1}$  and the bimolecular rate constant was determined to be  $2.7 \pm 0.3 \times 10^{10} \text{ l mole}^{-1} \text{ sec}^{-1}$ . The data are summarized in Table VI-2 and illustrated in Figure VI-3.

## 4. The Bimolecular Rate Constant for the Reaction of $S(^3P)$ Atoms with *Trans*-2-Butene Episulfide

The reaction of  $S(^3P)$  atoms with *trans*-2- $\text{C}_4\text{H}_8\text{S}$  was



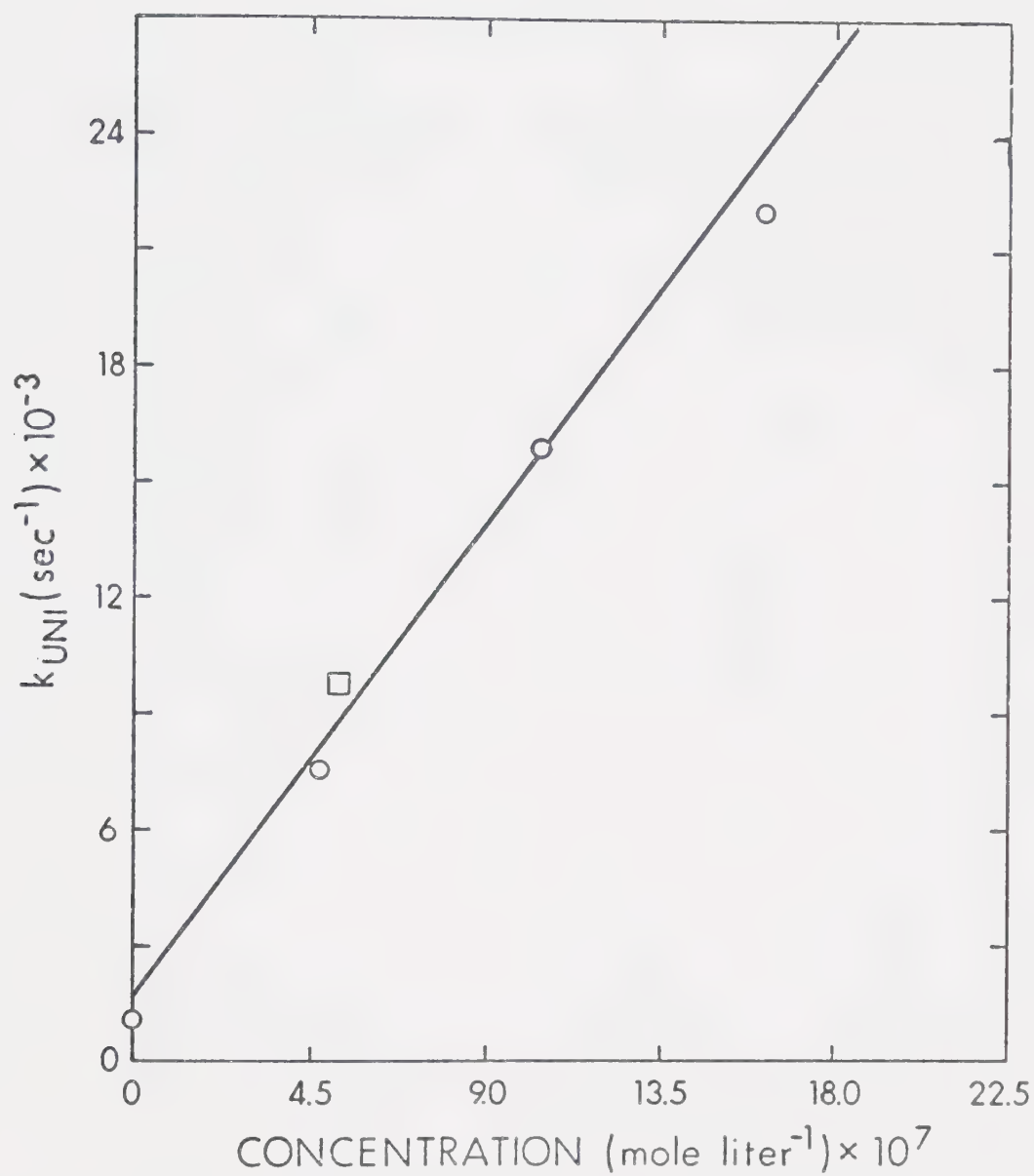


FIGURE VI-2: First Order Rate Constants of  $\text{S}(^3\text{P})$  Atoms versus Ethylene Episulfide Concentration,  $\circ$  in 200 torr  $\text{CO}_2$ ,  $\square$  in 100 torr  $\text{CO}_2$ .



TABLE VI-2

First Order Decay Rate of  $S(^3P)$  Atoms  
in the Presence of Propylene Episulfide

$C_3H_6S$ (torr)	$CO_2$ (torr)	$COS$ (torr)	$10^{-4}k,_{sec^{-1}}$
0.00673	200	0.10	0.97
0.00673	200	0.10	1.19
0.00673	200	0.10	<u>1.06</u>
		average	$1.07 \pm 0.11$



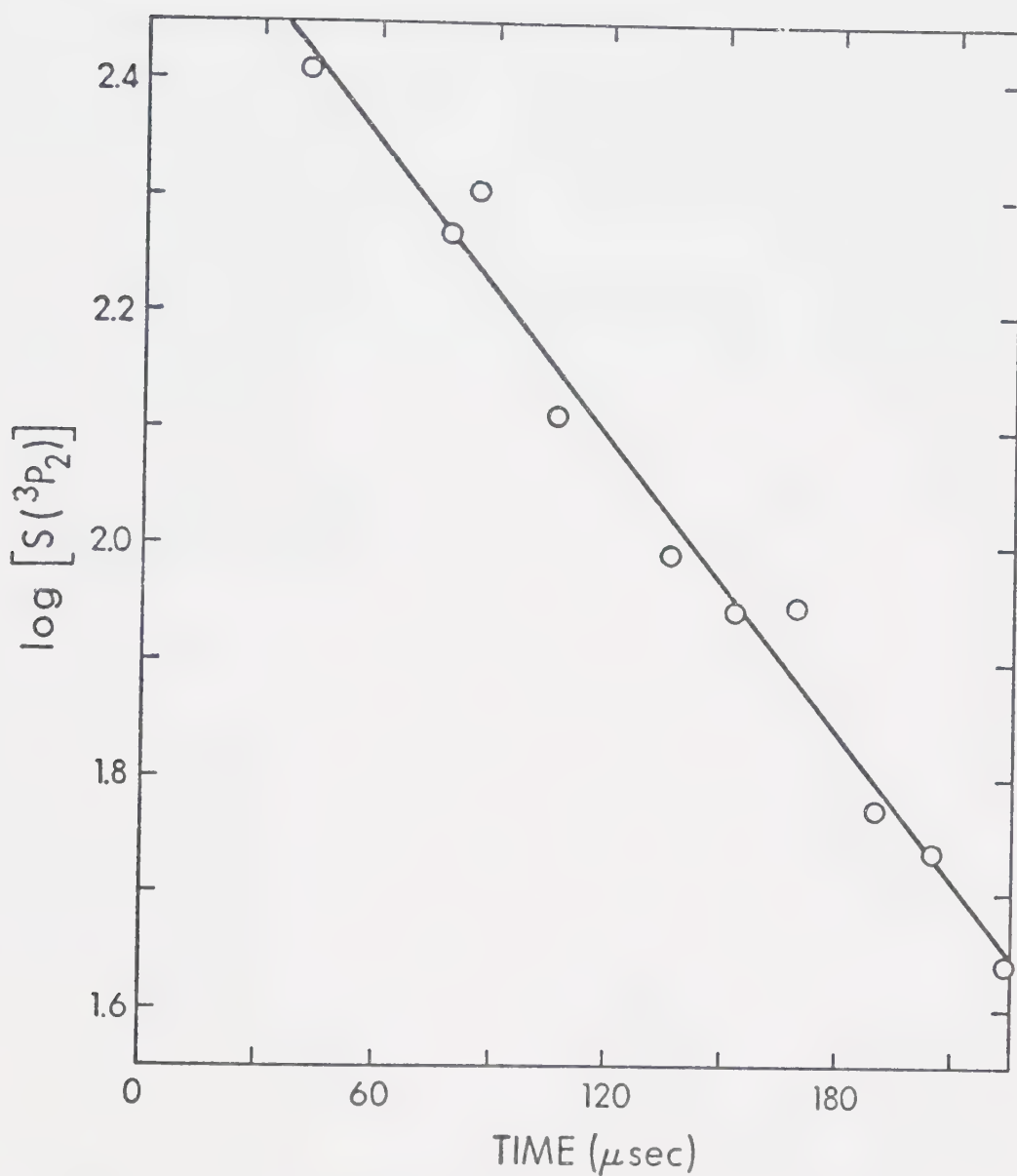


FIGURE VI-3: First Order Decay Plot of  $S(^3P_2)$  Atoms in the Presence of Propylene Episulfide,  $P(\text{COS}) = 0.1$  torr,  $P(\text{C}_3\text{H}_4\text{S}) = 0.0057$  torr,  $P(\text{CO}_2) = 200$  torr.



monitored at a total pressure of 200 torr of  $\text{CO}_2$  and a COS pressure of 0.10 torr. The average observed first order rate constant was  $1.26 \pm 0.02 \times 10^4 \text{ sec}^{-1}$  and the first order rate constant due to reaction with *trans*-2- $\text{C}_4\text{H}_6\text{S}$  is  $1.15 \times 10^4 \text{ sec}^{-1}$ . The bimolecular rate constant was determined to be  $4.0 \pm 0.2 \times 10^{10} \text{ l mole}^{-1} \text{ sec}^{-1}$ . The data are summarized in Table VI-3 and a typical decay plot for this reaction is illustrated in Figure VI-4.

At 150 torr total pressure, the bimolecular rate constant was  $4.1 \times 10^{10} \text{ l mole}^{-1} \text{ sec}^{-1}$ , in good agreement with the previous value, indicating the absence of a pressure effect.

The bimolecular rate constants determined for the S + episulfide reactions are summarized in Table VI-4.



TABLE VI-3

First Order Decay Rate of  $S(^3P)$  Atoms in the  
Presence of *Trans*-2-Butene Episulfide

$C_4H_8S$ (torr)	$CO_2$ (torr)	$COS$ (torr)	$10^{-4}k, \text{ sec}^{-1}$
0.00540	200	0.10	1.24
0.00540	200	0.10	1.28
0.00540	200	0.10	1.25
		average	$1.26 \pm .02$
0.00405	150	0.075	1.01



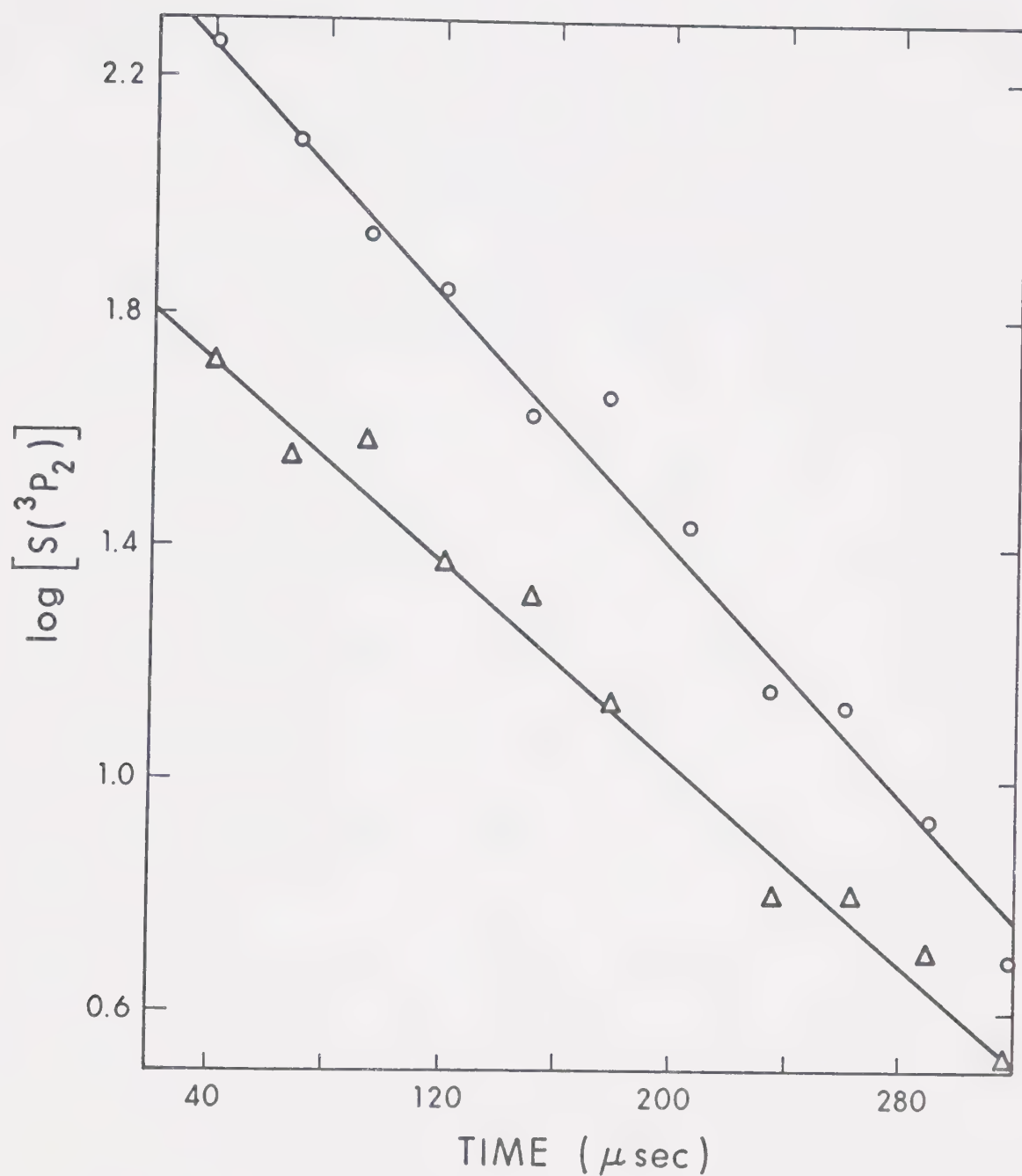


FIGURE VI-4: First Order Decay Plot of  $S(^3P_2)$  Atoms in the Presence of *Trans*-2-butene episulfide: ○;  $P(COS) = 0.1$  torr,  $P(trans-2-C_4H_8S) = 0.0054$  torr,  $P(CO_2) = 200$  torr: Δ;  $P(COS) = 0.075$  torr,  $P(trans-2-C_4H_8S) = 0.0041$  torr,  $P(CO_2) = 150$  torr.



TABLE VI-4

Rate Constants for Reaction of  $S(^3P)$  Atoms  
with Episulfides at 25°C

Substrate	Rate ( $l \text{ mole}^{-1} \text{ sec}^{-1}$ )
Ethylene Episulfide	$1.4 \pm 0.2 \times 10^{10}$
Propylene Episulfide	$2.7 \pm 0.3 \times 10^{10}$
<i>Trans</i> -2-Butene Episulfide	$4.0 \pm 0.2 \times 10^{10}$

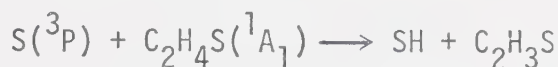


## B. Discussion

Sulfur atoms react with episulfide in a spin and probably orbital symmetry allowed process,

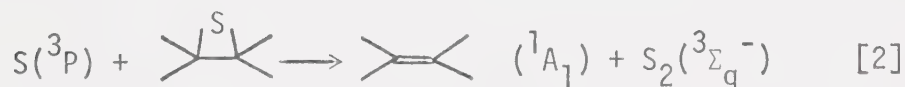


The room temperature rate constant is very close to the collision frequency. The possible competing process, hydrogen abstraction



can be ruled out since ground state sulfur atoms have been shown<sup>35</sup> to be completely inert towards paraffinic C-H bonds.

The reactions of  $S(^3P)$  atoms with episulfides are of importance for a number of reasons. In conventional photolysis studies<sup>28</sup> of the reaction of  $S(^3P)$  atoms with olefins, it was observed that significant deviations from the expected product yields and relative rates took place with increasing conversions. This effect was attributed to the occurrence of secondary reactions of  $S(^3P)$  atoms with the product episulfide:



Consequently, quantitative studies were undertaken at relatively low olefin pressures so that step [2] could compete favourably with step [1]. It was found that with increasing conversion the



episulfide yields increased initially, then levelled off to a constant value. In this linear region

$$k_1[S] [\text{Olefin}] = k_2[S] [\text{Episulfide}]$$

$$\text{and} \quad \frac{k_2}{k_1} = \frac{[\text{Olefin}]}{[\text{Episulfide}]}$$

It was found that  $k_2/k_1 = 81$  in the case of ethylene and 40 in the case of propylene<sup>28</sup>. This treatment, however, is oversimplified since it is certain that the episulfide products must undergo secondary photolysis, the extent of which cannot be assessed. These rate ratios are upper limits only, and it was necessary to determine the absolute value for  $k_2$  so that the absolute rate data for the  $S(^3P) + \text{olefins}$  systems (Chapter VII) could be properly evaluated.

Before the present results can be discussed, it is necessary to examine the possible effects of photochemical decomposition of  $C_2H_4S$  in the primary flash. The onset of absorption, Figure VI-5<sup>130</sup>, is at 370 nm and there are two distinct absorptions, a weak one centered at ca 250 nm and a more intense one below 220 nm. The long wavelength absorption, which probably corresponds to an  $n, \sigma^*$  transition, leads to the formation of  $S_2$  and  $C_2H_4$  primarily, along with minor amounts of  $C_2H_2$ ,  $H_2S$ ,  $H_2$  and  $CH_4$  via molecular mechanisms<sup>12,131</sup>. Extensive photolysis would deplete the episulfide concentration and a corrected average value would have to be used when calculating the bimolec-



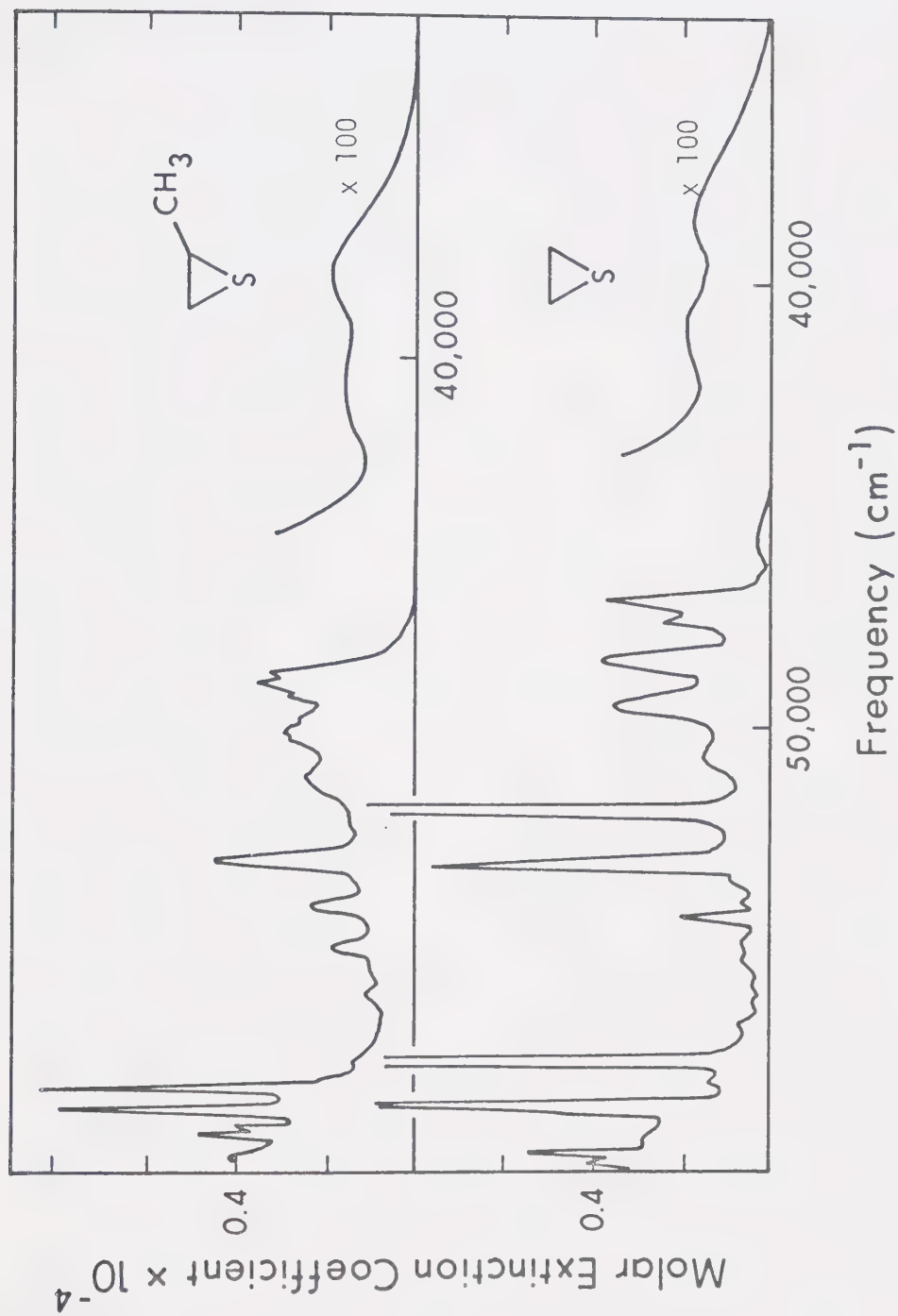


FIGURE VI-5: The Absorption Spectrum of Ethylene Episulfide<sup>130</sup>.



ular rate constants. Furthermore, if sulfur atoms reacted with the photolysis products, then the rate of abstraction would be smaller than the observed rate of decay.

It is highly unlikely that these processes are of any importance in the present system since in a previous study<sup>12</sup> of the flash photolysis of  $C_2H_4S$  where flash energies larger by 2.5 and concentrations larger by a factor of  $10^3$  were employed, it was found that only 2% of the substrate was decomposed by the flash. Moreover, the invariance of the bimolecular rate constant with  $C_2H_4S$  concentration, Figure VI-2, illustrates that the concentration of  $C_2H_4S$  is unchanged during the course of the reaction.

The absolute rate constant for the  $S + C_2H_4S \longrightarrow S_2 + C_2H_4$  reaction has also been determined by Donovan et al<sup>10</sup> using a similar apparatus and by Klemm and Davis<sup>132</sup> using resonance fluorescence to monitor the S atom concentration. The latter study also reported  $E_a = 0$ . The data are summarized in Table VI-5. The agreement between our value and that reported by Donovan et al<sup>10</sup> is excellent but the rate constant determined by Klemm and Davis<sup>132</sup> is higher by a factor of 2 and there is no obvious explanation for the discrepancy. The relative values obtained here do not agree with those derived from conventional studies<sup>28</sup> but, as was stated previously the rate ratios are only upper limits and it would be unreasonable to attribute a high degree of accuracy to them.

It appears that the rate of abstraction increases slightly with increasing alkyl substitution. From an empirical plot of the bimolecular rate constants versus number of methyl



TABLE VI-5

Rate Data for the Reaction of Group VIA Atoms with Episulfides

Reactant	$10^{-10}k, \text{ 1 mole}^{-1} \text{ sec}^{-1}$		Rel. Rates ( $S^3P$ )	
	$S(^3P)^a$	$O(^3P)^d$	This Work	O'Callaghan <sup>f</sup>
Ethylene Episulfide	$1.4 \pm 0.2$	$0.8 \pm 0.1$ (~1 for reaction with episelenide)	1	1
	$1.8 \pm 0.4^b$			
	$2.7 \pm 0.2^c$			
Propylene Episulfide	$2.7 \pm 0.3$		1.93	3.35
<i>Trans</i> -2-Butene Episulfide	$4.0 \pm 0.2$		2.85	
a. This work	c. reference 132	e. reference 71		
b. reference 10	d. reference 133	f. reference 28		



substituents, Figure VI-6, the rate constant for reaction of  $S(^3P)$  atoms with tetramethylethylene episulfide should be  $6.6 \times 10^{10} \text{ l mole}^{-1} \text{ sec}^{-1}$ . This is comparable to the rate constant for addition of  $S(^3P)$  atoms to tetramethylethylene (of Chapter VII) and therefore in this system a correction for the abstraction reaction is unnecessary.

The collisional frequency for the  $S + C_2H_4S$  reaction is  $\sim 2.6 \times 10^{10} \text{ l mole}^{-1} \text{ sec}^{-1}$  if  $d_{AB} \approx 5 \text{ \AA}$ . Therefore the reaction is occurring at a rate of once in  $\sim 18$  collisions. The maximum  $E_a$  which would correspond with this rate is  $\sim 1.7 \text{ kcal mole}^{-1}$  whereas an experimental value of 0 has been reported. Semi-empirical EHMO calculations have been carried out<sup>19</sup> on the reaction path of  $S(^3P)$  plus ethylene episulfide and the lowest energy path for the reaction which corresponds to attack from above the ring plane (path Z in Figure VI-7), has a calculated activation energy of  $\sim 1 \text{ kcal mole}^{-1}$ . The computed value of the enthalpy change,  $-44.5 \text{ kcal mole}^{-1}$  is in good agreement with the thermochemical value of  $-43.4 \text{ kcal mole}^{-1}$ . Thus, the experimental value of  $E_a = 0$  may be due to a small negative temperature dependence of the A factor coupled with a small positive activation energy, of the order of a few tenths of a  $\text{kcal mole}^{-1}$ .

Desulfurization of episulfides can be accomplished by a variety of reagents. In the case of organic nucleophiles such as triethyl phosphite<sup>134-136</sup>, organolithium compounds<sup>134,137</sup>, triphenyl<sup>135,138</sup> or tributylphosphine<sup>138</sup> the product olefin retains the configuration of the substrate episulfide, indicating that the



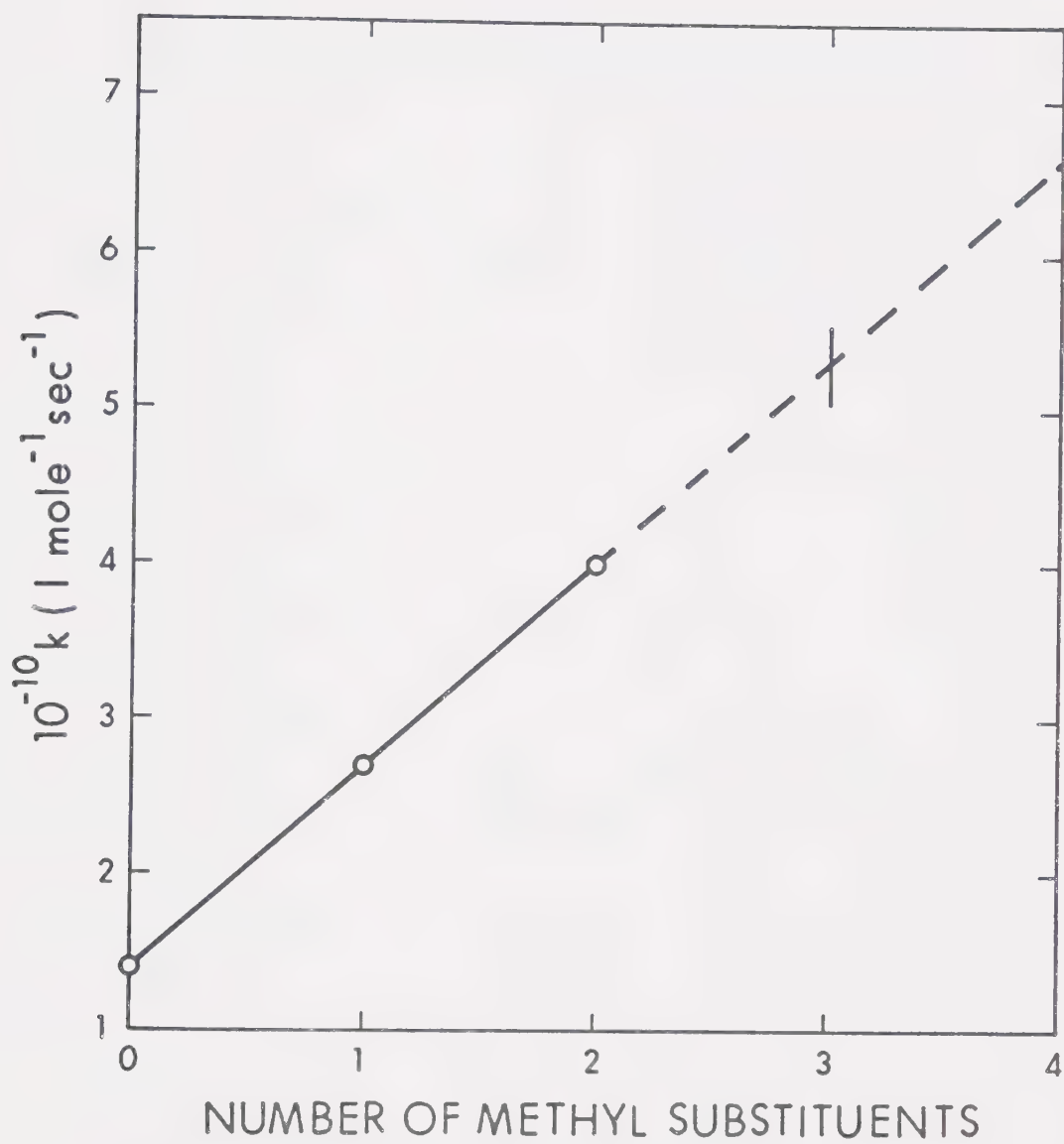


FIGURE VI-6: Empirical Correlation of the Bimolecular Rate Constant of Abstraction with the Number of Methyl Substituents on the Episulfide.



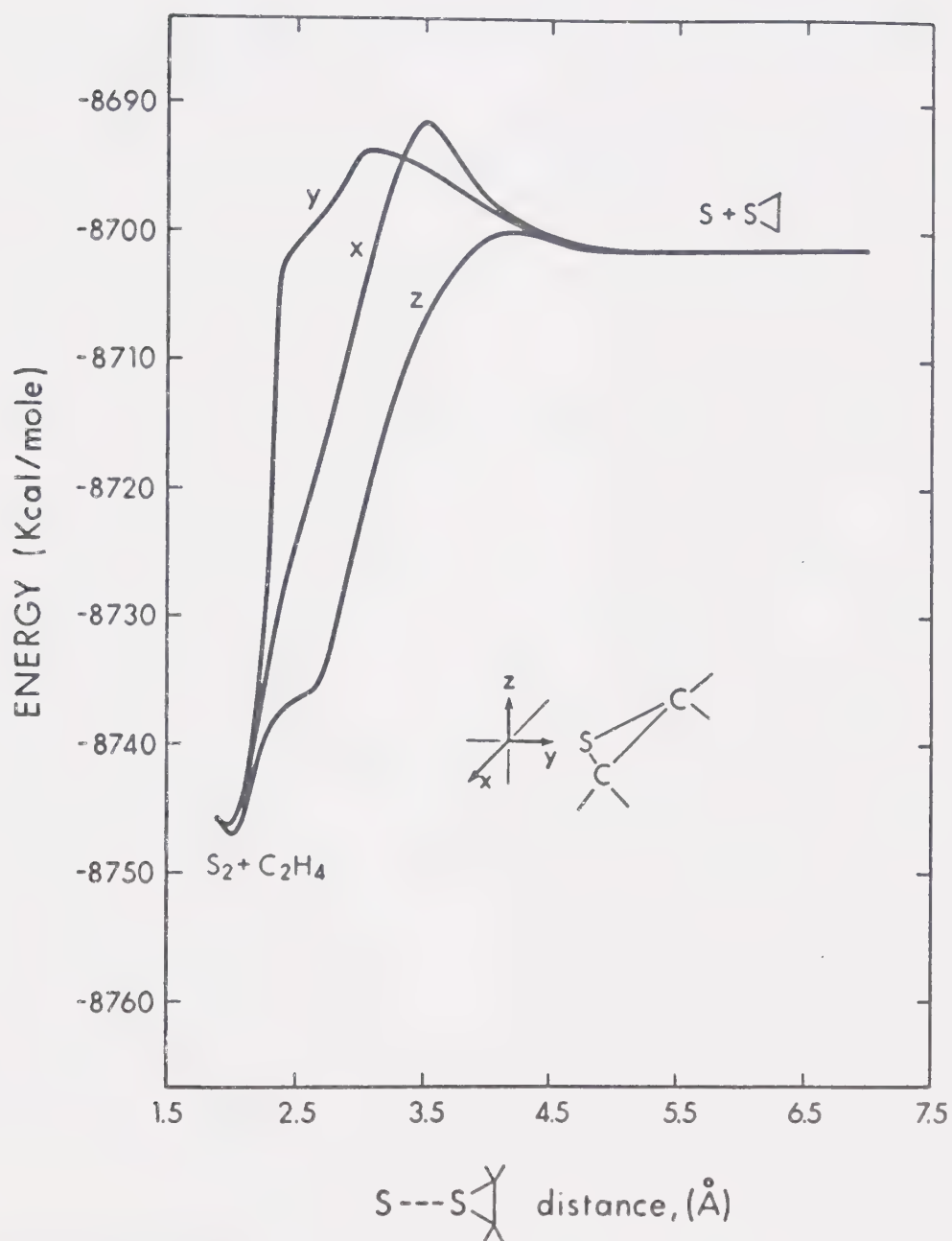
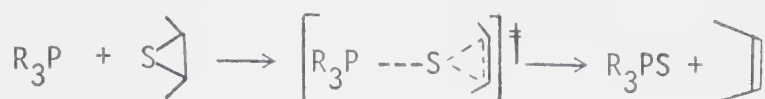


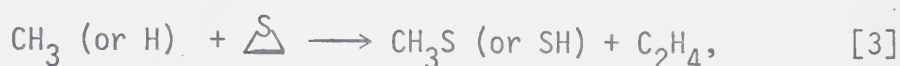
FIGURE VI-7: EHMO Potential Energy Curves for the Reaction of Sulfur Atom with Ethylene Episulfide<sup>19</sup>.



reaction is a concerted molecular process:



Methyl radicals<sup>19</sup> and hydrogen atoms<sup>139</sup> also abstract sulfur from episulfides

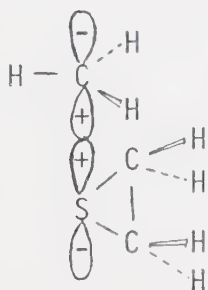


in parallel and in competition with hydrogen abstraction. The rate parameters are

$$\log k = 7.9 - (6700/RT) \text{ l mole}^{-1} \text{ sec}^{-1} \text{ for } CH_3 \text{ and}$$

$$\log k = 10.8 - (1944/RT) \text{ l mole}^{-1} \text{ sec}^{-1} \text{ for H.}$$

The reaction of methyl radicals with *cis*-2-butene episulfide is stereoselective, yielding > 80% *cis*-2-butene. This, together with kinetic observations indicates that the reaction is a single step concerted process and that the thioalkyl radical is not an intermediate. The initial interaction was postulated to involve the  $\pi$  orbital of the  $CH_3$  radical with the nonbonding 3p orbital of the S-atom::



The intermediate in the  $H + C_2H_4S$  system was believed to be similar.

The absolute rate constants for desulfurization of ethylene



episulfide have been reported for several of the Group VI A elements. The data are summarized in Table VI-5. The reactions are all spin and orbital symmetry allowed, to yield a ground state olefin molecule and a ground state triplet  $S_2$ , SO or  $Se_2$  species and proceed at rates near the collision frequency with little or no activation energy. The  $O(^3P)$  atom +  $C_2H_4S$  system<sup>133</sup> is interesting since ground state  $O(^3P)$  atoms are known to abstract from paraffinic C-H bonds but the activation energies are of the order of several kcal. The near-zero temperature dependence observed experimentally would imply that desulfurization is the only measurable process. In fact, SO was detected by kinetic mass spectroscopy<sup>133</sup>.

Finally, it is of interest to note that atomic or radical attack on epoxides proceeds exclusively via hydrogen abstraction and deoxygenation has never been observed although the process is thermodynamically favourable. A Bond Energy-Bond Order calculation reported in the literature on this reaction predicted a prohibitively high activation energy<sup>19</sup>.



## CHAPTER VII

### THE REACTIONS OF $S(^3P)$ ATOMS WITH OLEFINS

#### A. Results - Part I

The room temperature reactions of  $S(^3P)$  atoms with olefins were investigated using 200 torr  $CO_2$  diluent and 0.1 torr of COS by monitoring the decay of  $S(^3P_2)$  and  $S(^3P_1)$  atoms. The reactions of  $S(^3P)$  atoms with ethylene were examined extensively in order to define the experimental parameters for this series of studies; in this system the effects of ethylene pressure, total pressure, nature of the diluent and flash energy were investigated.

#### 1. The Reaction of $S(^3P)$ Atoms with Ethylene

##### i) $S(^3P)$ Atom Decay

The time dependence of the  $S(^3P_2)$  and  $S(^3P_1)$  atom concentrations were examined as a function of a number of experimental variables such as partial ethylene concentrations, total pressures and flash energies, and the method of integration was used to check the order of the reaction with respect to  $S(^3P_2)$  atoms. Under the experimental conditions employed, the decay rates followed first order kinetics. A typical first order plot of  $\log [S(^3P_2)]$  versus time is shown in Figure VII-1 and the data are summarized in Table VII-1.



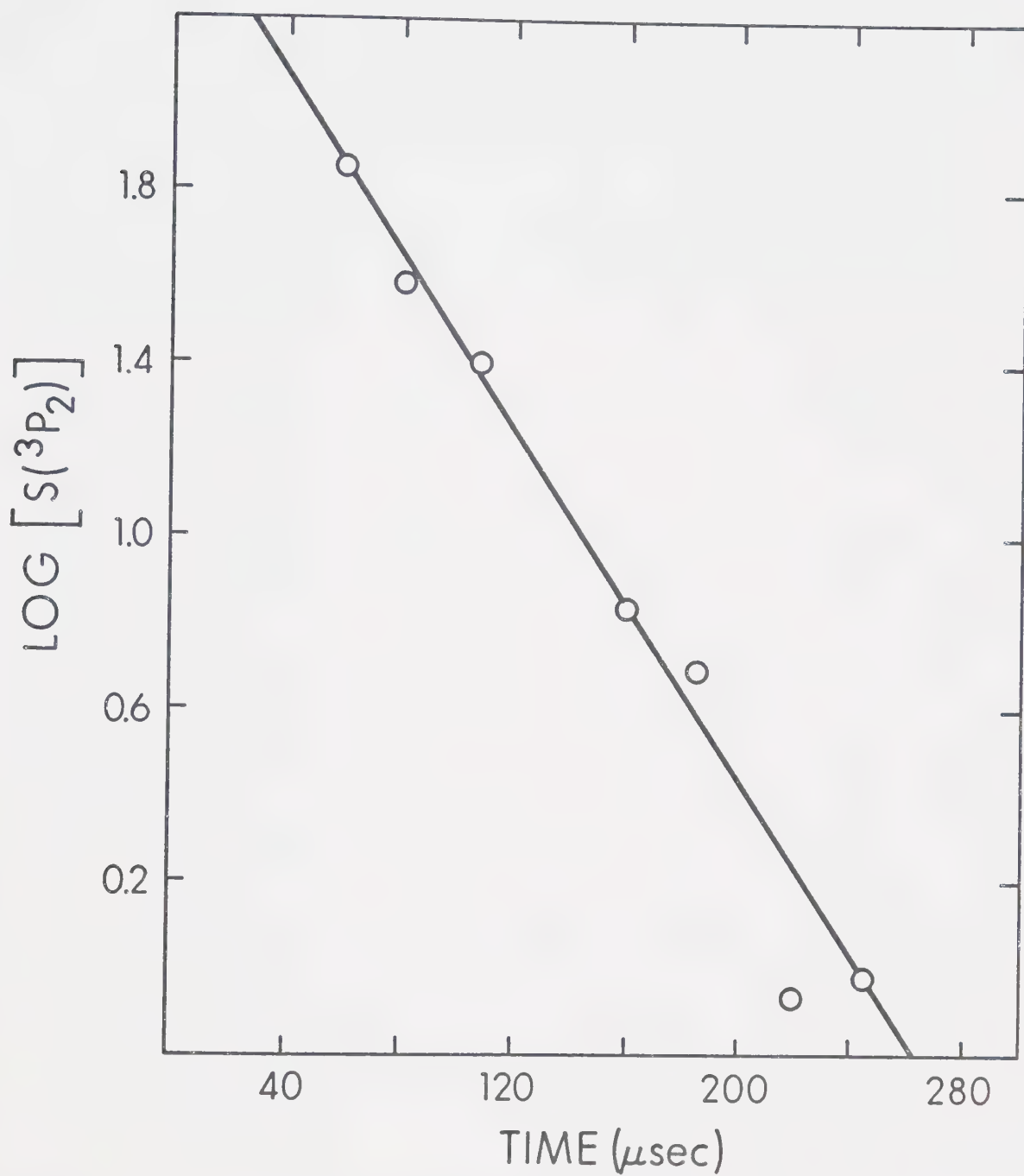


FIGURE VII-1: First Order Decay Plot of  $S(^3P_2)$  Atoms in the Presence of Ethylene,  $P(\text{COS}) = 0.1$  torr,  $P(\text{C}_2\text{H}_4) = 0.437$  torr,  $P(\text{CO}_2) = 500$  torr.



TABLE VII-1

First Order Decay Rate of S(<sup>3</sup>P) Atoms  
in the Presence of Ethylene

S species	C <sub>2</sub> H <sub>4</sub> (torr)	CO <sub>2</sub> (torr)	Flash Energy (kV)	10 <sup>-4</sup> k, sec <sup>-1</sup>
<sup>3</sup> P <sub>2</sub>	0.408	50	9	2.16
<sup>3</sup> P <sub>2</sub>	0.254	200	9	1.38
<sup>3</sup> P <sub>1</sub>	0.254	200	9	1.43
<sup>3</sup> P <sub>2</sub>	0.254	200	9	1.22
<sup>3</sup> P <sub>2</sub>	0.254	200	9	1.21
<sup>3</sup> P <sub>1</sub>	0.254	200	9	1.31
<sup>3</sup> P <sub>2</sub>	0.200	0 <sup>b</sup>	9	1.06
<sup>3</sup> P <sub>2</sub>	0.254	200	6.5	1.22
<sup>3</sup> P <sub>2</sub>	0.437	500	9	2.43
<sup>3</sup> P <sub>2</sub>	0	200	9	0.11

<sup>a</sup> P(COS) = 0.1 torr

<sup>b</sup> P(Ar) = 200 torr



## ii) Effect of Ethylene Pressure

The first order rate constants obtained in the pressure range 0.20 - 0.44 torr ethylene, Table VII-1, were plotted versus ethylene concentration, Figure VII-2. A good linear relationship was obtained, yielding a bimolecular rate constant of  $9.0 \pm 0.5 \times 10^8 \text{ l mole}^{-1} \text{ sec}^{-1}$ .

## iii) Effect of Total Pressure and Nature of the Diluent

The value of the bimolecular rate constant was determined over a range of total pressures from 50 to 500 torr using  $\text{CO}_2$ , and then with 200 torr argon as diluent. As illustrated in Figure VII-3, the bimolecular rate constant is virtually independent of the total pressure.

## iv) Effect of Flash Energy

The first order rate constant was determined at 9 and 6.5 kV using a mixture of 200 torr  $\text{CO}_2$ , 0.1 torr COS and 0.256 torr ethylene. The values obtained (Table VII-1) are in agreement, indicating no dependence of the rate constant on flash energy.

## 2. The Reaction of $\text{S}(^3\text{P})$ Atoms with Propylene

The first order rate constants determined for this reaction are tabulated in Table VII-2, and give an average first order



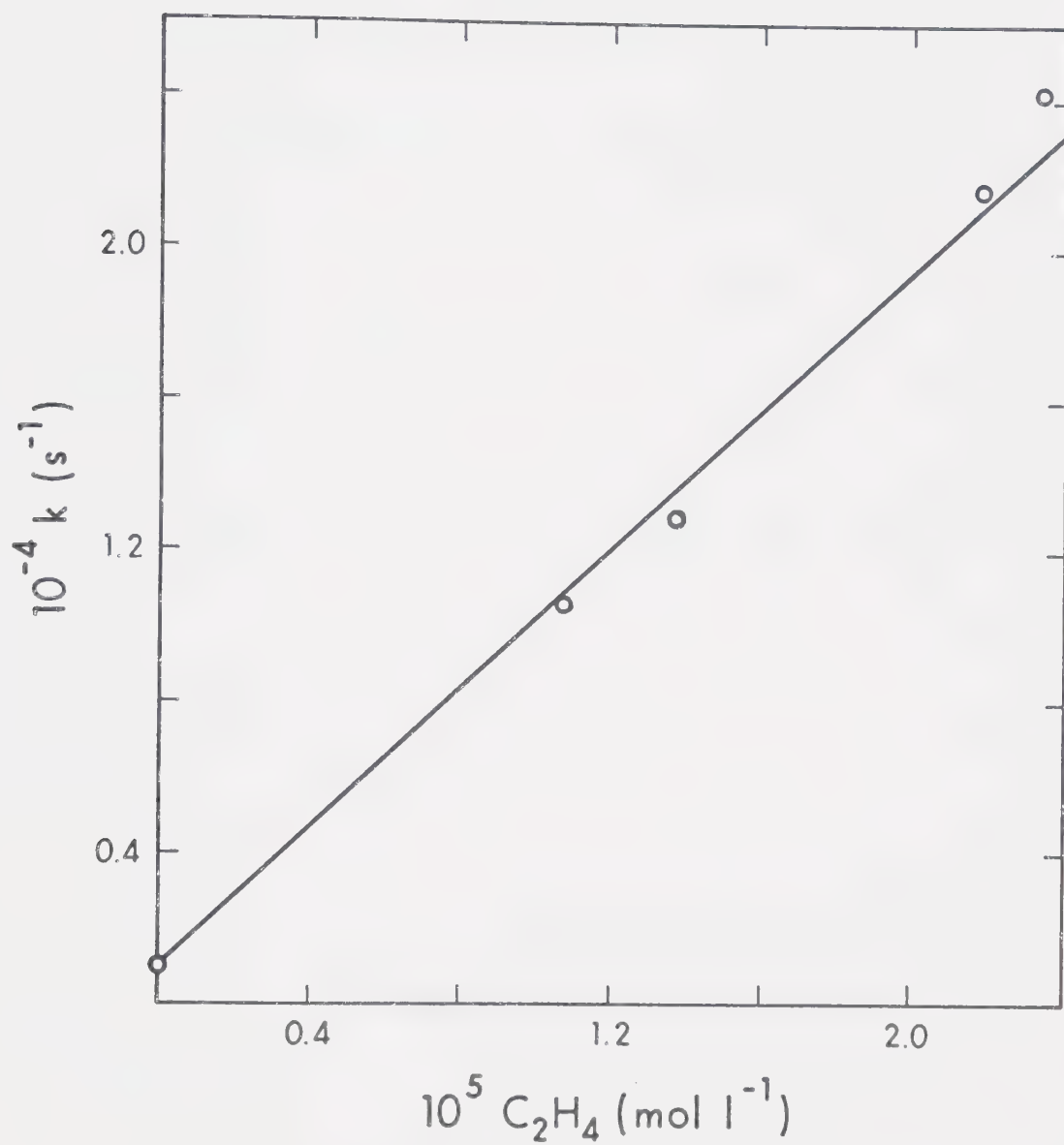


FIGURE VII-2: First Order Rate Constant for Decay of S(<sup>3</sup>P)  
Atoms versus Ethylene Concentration.



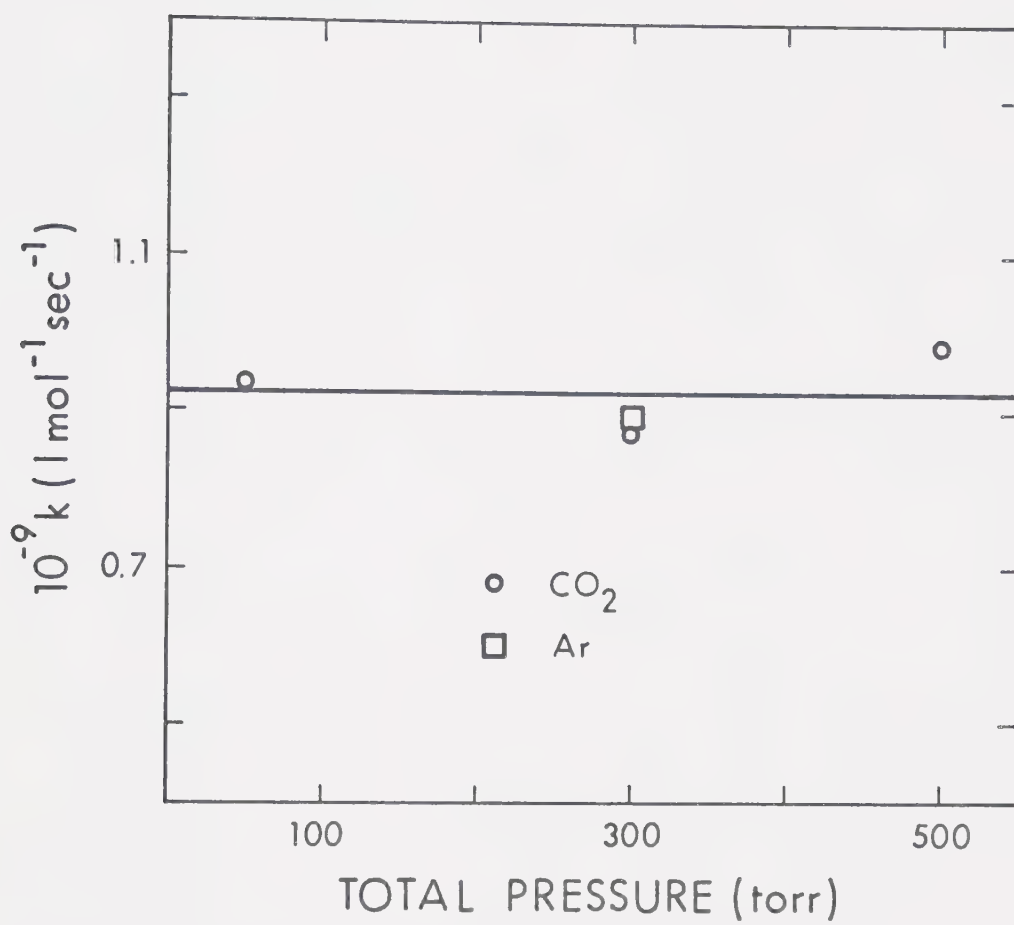


FIGURE VII-3: Plot of the Bimolecular Rate Constant versus Total Pressure.



TABLE VII-2

First Order Decay Rate of S(<sup>3</sup>P) Atoms  
in the Presence of Propylene

S species	C <sub>3</sub> H <sub>6</sub> (torr)	CO <sub>2</sub> (torr)	COS (torr)	10 <sup>-4</sup> k, sec <sup>-1</sup>
<sup>3</sup> P <sub>2</sub>	0.035	200	0.10	1.04
<sup>3</sup> P <sub>1</sub>	0.035	200	0.10	1.03
<sup>3</sup> P <sub>1</sub>	0.035	200	0.10	1.28
<sup>3</sup> P <sub>2</sub>	0.0175	100	0.05	1.30 <sup>a</sup>
<sup>3</sup> P <sub>2</sub>	0.035	200	0.10	1.06
<sup>3</sup> P <sub>1</sub>	0.035	200	0.10	1.06
average				<u>1.13 ± 0.13</u>

<sup>a</sup> normalized to 0.035 torr C<sub>3</sub>H<sub>6</sub>



rate constant of  $1.13 \times 10^4 \text{ sec}^{-1}$  at a propylene concentration of  $1.87 \times 10^{-6} \text{ mole l}^{-1}$ . Applying the correction of  $0.11 \times 10^4 \text{ sec}^{-1}$  for the decay in  $\text{CO}_2 - \text{COS}$ , a bimolecular rate constant of  $5.4 \pm 0.6 \times 10^9 \text{ l mole}^{-1} \text{ sec}^{-1}$  is obtained. A typical decay plot is illustrated in Figure VII-4.

### 3. The Reaction of $\text{S}(^3\text{P})$ Atoms with 1-Butene

The first order rate constants determined for this reaction are tabulated in Table VII-3, and give an average first order rate constant of  $0.17 \times 10^4 \text{ sec}^{-1}$  at a 1-butene concentration of  $1.29 \times 10^6 \text{ mole l}^{-1}$  and the bimolecular rate constant is  $8.2 \pm 0.6 \times 10^9 \text{ l mole}^{-1} \text{ sec}^{-1}$ . A typical decay plot is illustrated in Figure VII-5.

### 4. The Reaction of $\text{S}(^3\text{P})$ Atoms with *trans*-2-Butene

The first order rate constants determined for this reaction are tabulated in Table VII-4 and yield an average first order rate constant of  $0.79 \times 10^4 \text{ sec}^{-1}$  at a *trans*-2-butene concentration of  $6.25 \times 10^{-7} \text{ mole l}^{-1}$ . The bimolecular rate constant is  $1.1 \pm 1.5 \times 10^{10} \text{ l mole}^{-1} \text{ sec}^{-1}$ . A typical decay plot is illustrated in Figure VII-6.

### 5. The Reaction of $\text{S}(^3\text{P})$ Atoms with Isobutene

The first order rate constants are tabulated in Table VII-5. From the average first order rate constant of  $1.06 \times 10^4 \text{ sec}^{-1}$



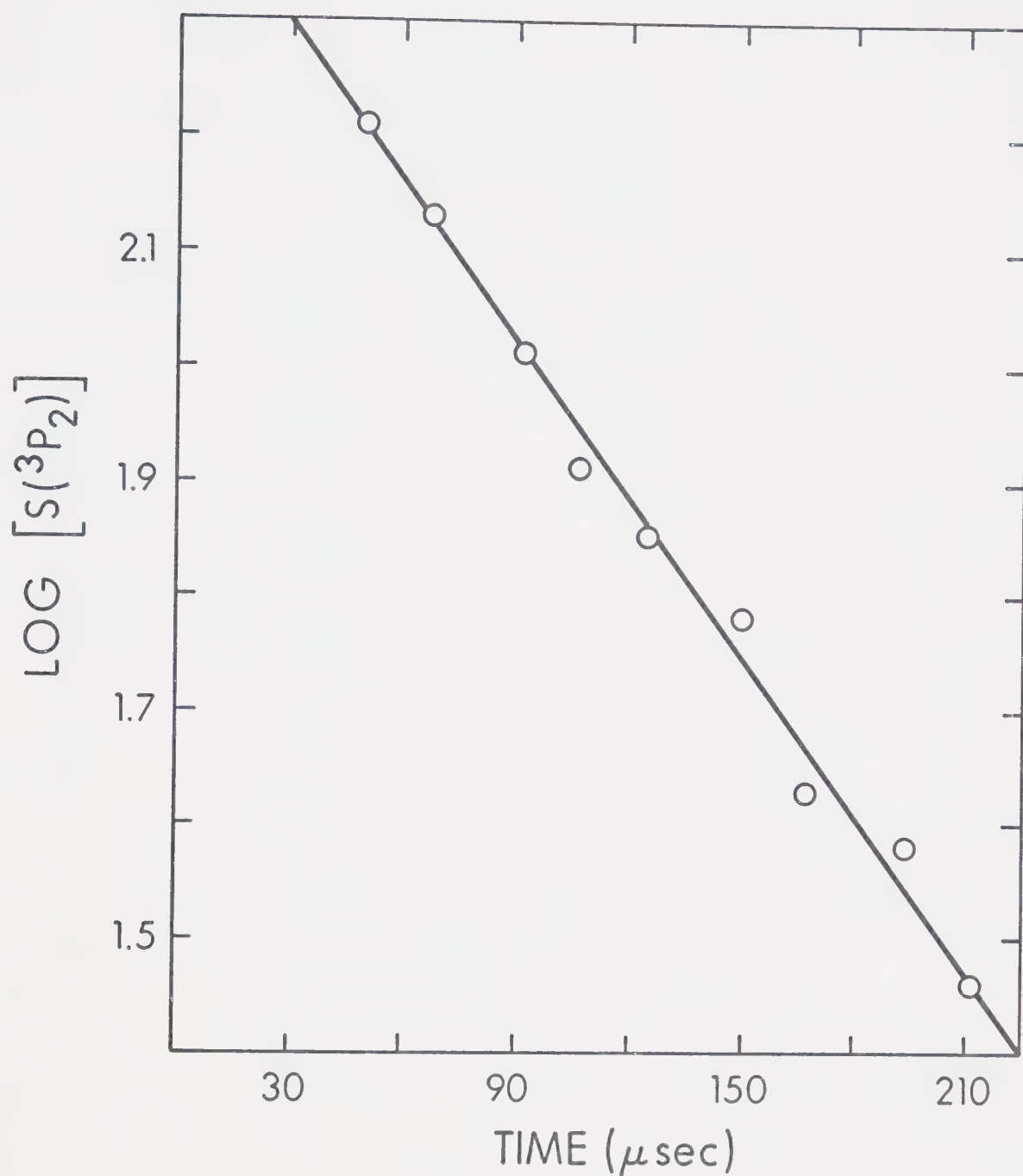


FIGURE VII-4: First Order Decay Plot of  $S(^3P_2)$  Atoms in the Presence of Propylene.  $P(\text{COS}) = 0.1$  torr,  $P(\text{C}_3\text{H}_6) = 0.035$  torr,  $P(\text{CO}_2) = 200$  torr.



TABLE VII-3

First Order Decay Rate of S(<sup>3</sup>P) Atoms  
in the Presence of 1-Butene

S species	C <sub>4</sub> H <sub>8</sub> -1 (torr)	CO <sub>2</sub> (torr)	COS (torr)	10 <sup>-4</sup> k, sec <sup>-1</sup>
<sup>3</sup> P <sub>2</sub>	0.0239	200	0.10	1.04
<sup>3</sup> P <sub>1</sub>	0.0239	200	0.10	1.16
<sup>3</sup> P <sub>2</sub>	0.0239	200	0.10	1.23
<sup>3</sup> P <sub>1</sub>	0.0239	200	0.10	1.30
<sup>3</sup> P <sub>2</sub>	0.0239	200	0.10	1.16 <sup>a</sup>
<sup>3</sup> P <sub>2</sub>	0.0120	100	0.05	1.14 <sup>b</sup>
average				= 1.17 ± 0.09

<sup>a</sup> flashed at 6.5 kV

<sup>b</sup> normalized to 0.0239 torr C<sub>4</sub>H<sub>8</sub>-1



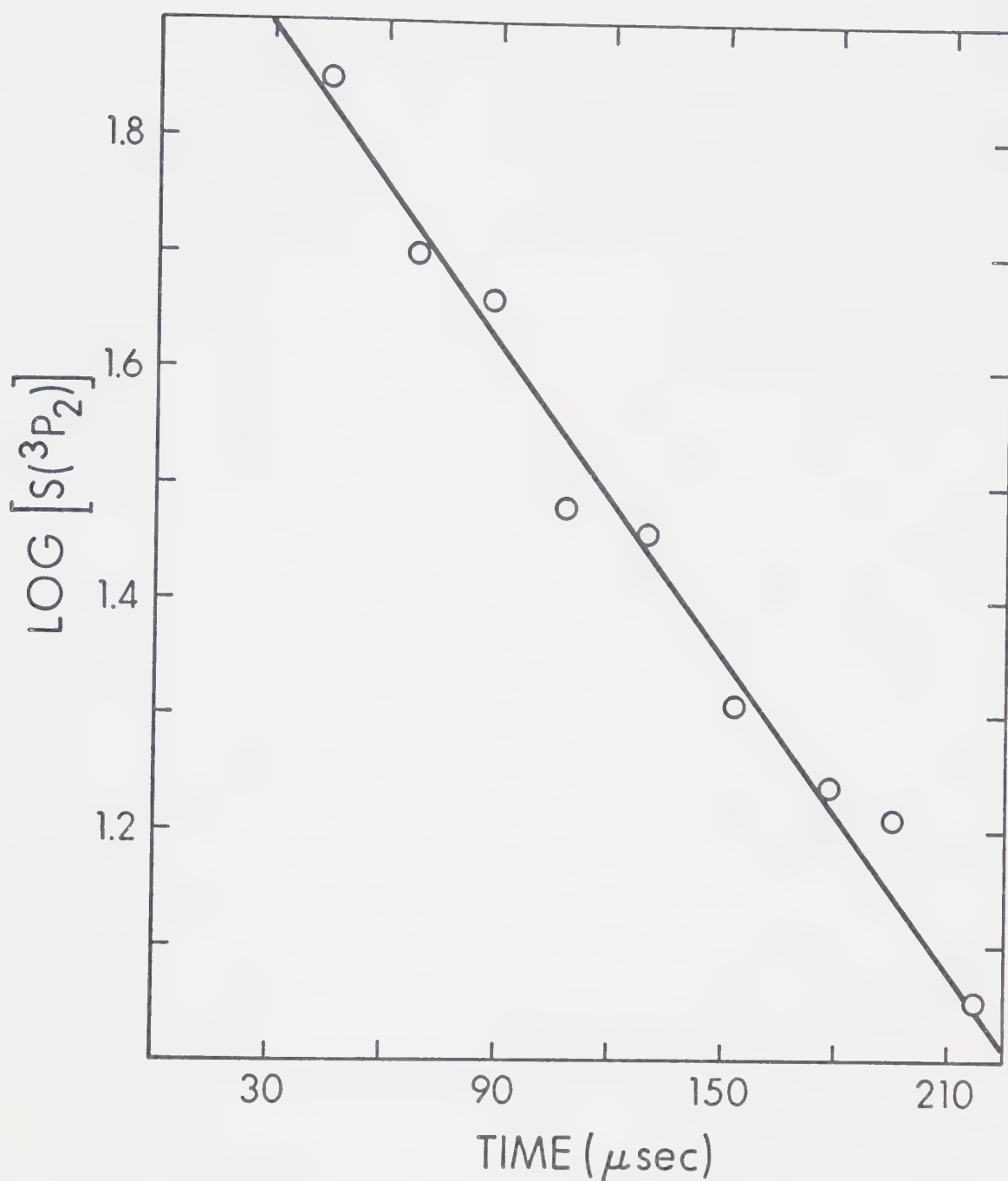


FIGURE VII-5: First Order Decay Plot of  $S(^3P_2)$  in the Presence of 1-Butene.  $P(\text{COS}) = 0.1$  torr,  $P(1\text{-C}_4\text{H}_8) = 0.0239$  torr,  $P(\text{CO}_2) = 200$  torr.



TABLE VII-4

First Order Decay Rate of S(<sup>3</sup>P) Atoms  
in the Presence of *trans*-2-Butene

S species	<i>t</i> -C <sub>4</sub> H <sub>8</sub> -2 (torr)	CO <sub>2</sub> (torr)	COS (torr)	10 <sup>-4</sup> k, sec <sup>-1</sup>
<sup>3</sup> P <sub>2</sub>	0.0116	200	0.10	0.65
<sup>3</sup> P <sub>1</sub>	0.0116	200	0.10	0.81
<sup>3</sup> P <sub>2</sub>	0.0116	200	0.10	0.90 <sup>a</sup>
<sup>3</sup> P <sub>1</sub>	0.0116	200	0.10	0.89 <sup>a</sup>
<sup>3</sup> P <sub>2</sub>	0.0058	100	0.05	0.72 <sup>b</sup>
average				= 0.79 ± 0.11

<sup>a</sup> flashed at 6 kV

<sup>b</sup> normalized to 0.0116 torr *t*-C<sub>4</sub>H<sub>8</sub>-2



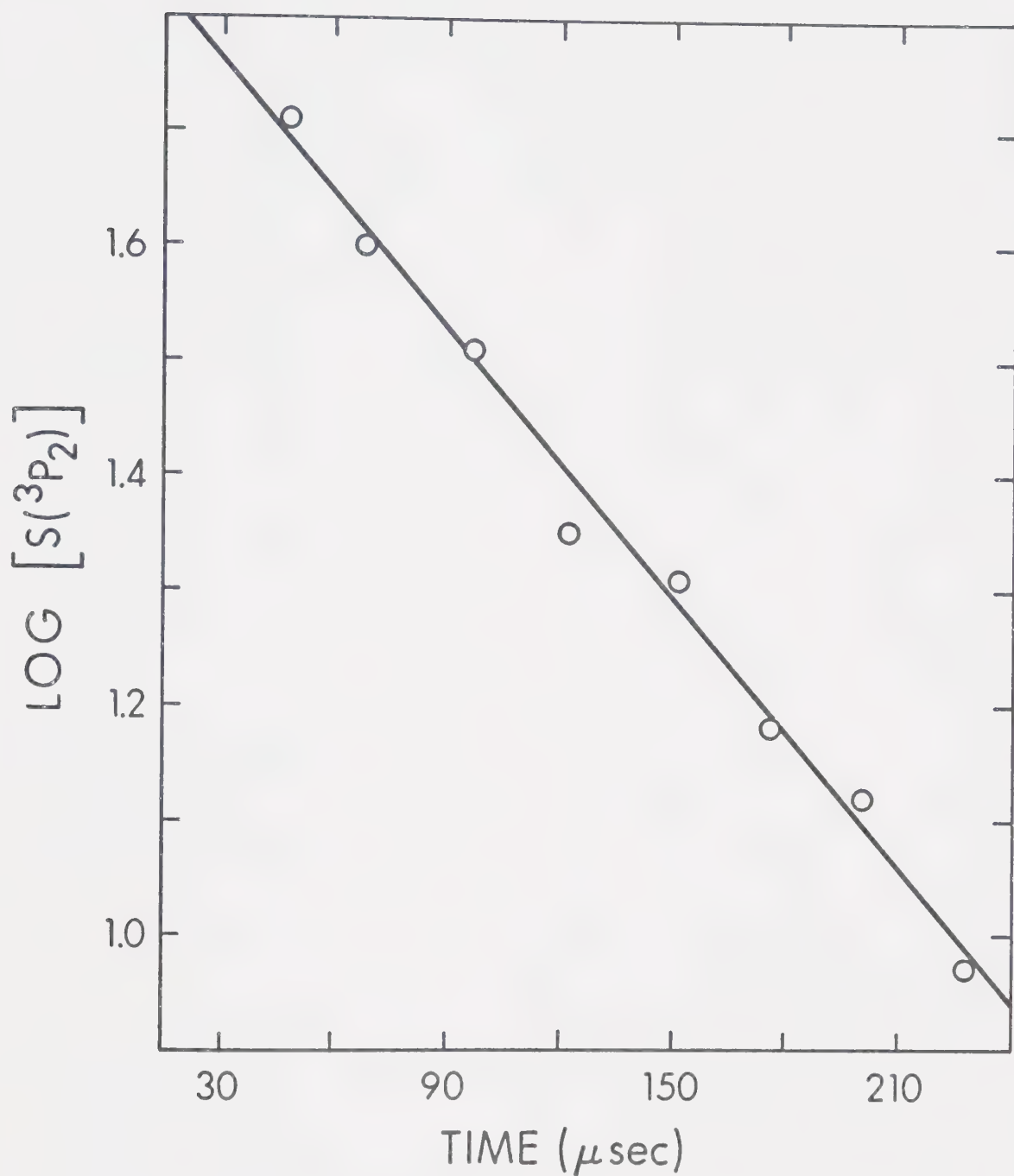


FIGURE VII-6: First Order Decay Plot of  $S(^3P_2)$  in the Presence of *trans*-2-Butene.  $P(\text{COS}) = 0.1$  torr,  $P(\text{trans-2-C}_4\text{H}_8) = 0.0116$  torr,  $P(\text{CO}_2) = 200$  torr.



TABLE VII-5

First Order Decay Rate of S(<sup>3</sup>P) Atoms  
in the Presence of Isobutene

S species	i-C <sub>4</sub> H <sub>8</sub> (torr)	CO <sub>2</sub> (torr)	COS (torr)	10 <sup>-4</sup> k, sec <sup>-1</sup>
<sup>3</sup> P <sub>2</sub>	0.00531	200	0.10	0.94
<sup>3</sup> P <sub>2</sub>	0.00531	200	0.10	1.00
<sup>3</sup> P <sub>1</sub>	0.00531	200	0.10	1.27
<sup>3</sup> P <sub>2</sub>	0.00531	200	0.10	1.22 <sup>a</sup>
<sup>3</sup> P <sub>2</sub>	0.00531	200	0.10	0.86 <sup>a</sup>
<sup>3</sup> P <sub>1</sub>	0.00531	200	0.10	1.01 <sup>a</sup>
<sup>3</sup> P <sub>2</sub>	0.00266	100	0.05	1.13 <sup>b</sup>
average				= 1.06 ± 0.15

<sup>a</sup> flashed at 6.6 kV

<sup>b</sup> normalized to 0.00531 torr i-C<sub>4</sub>H<sub>8</sub>



at an isobutene concentration of  $2.86 \times 10^{-7}$  mole  $l^{-1}$  the bimolecular rate constant of  $3.3 \pm 0.5 \times 10^{10}$   $l$  mole $^{-1}$  sec $^{-1}$  is obtained.

A typical decay plot is illustrated in Figure VII-7.

#### 6. The Reaction of S( $^3P$ ) Atoms with Tetramethylethylene

Since this reaction is extremely fast, the first order rate constant for decay of S( $^3P$ ) atoms were determined over a range of tetramethylethylene concentrations, Table VII-6, in order to determine the conditions where depletion of substrate might take place. As illustrated in Figure VII-8, first order kinetics are obeyed even at the lowest concentrations studied. The data are summarized in Table VII-6 and from the slope of the plot of the first order rate constant versus tetramethylethylene concentration, Figure VII-9, the bimolecular rate constant is  $6.0 \pm 0.3 \times 10^{10}$   $l$  mole $^{-1}$  sec $^{-1}$ .

#### 7. The Reaction of S( $^3P$ ) Atoms with Vinyl Fluoride

A first order rate constant of  $2.52 \times 10^4$  sec $^{-1}$  was determined for this reaction at a vinyl fluoride concentration of  $4.80 \times 10^{-5}$  mole liter $^{-1}$ , yielding a bimolecular rate constant of  $5.0 \pm 0.5 \times 10^8$   $l$  mole $^{-1}$  sec $^{-1}$ . The decay plot is illustrated in Figure VII-10.

Table VII-7 lists the room temperature rate data for the olefins studied.



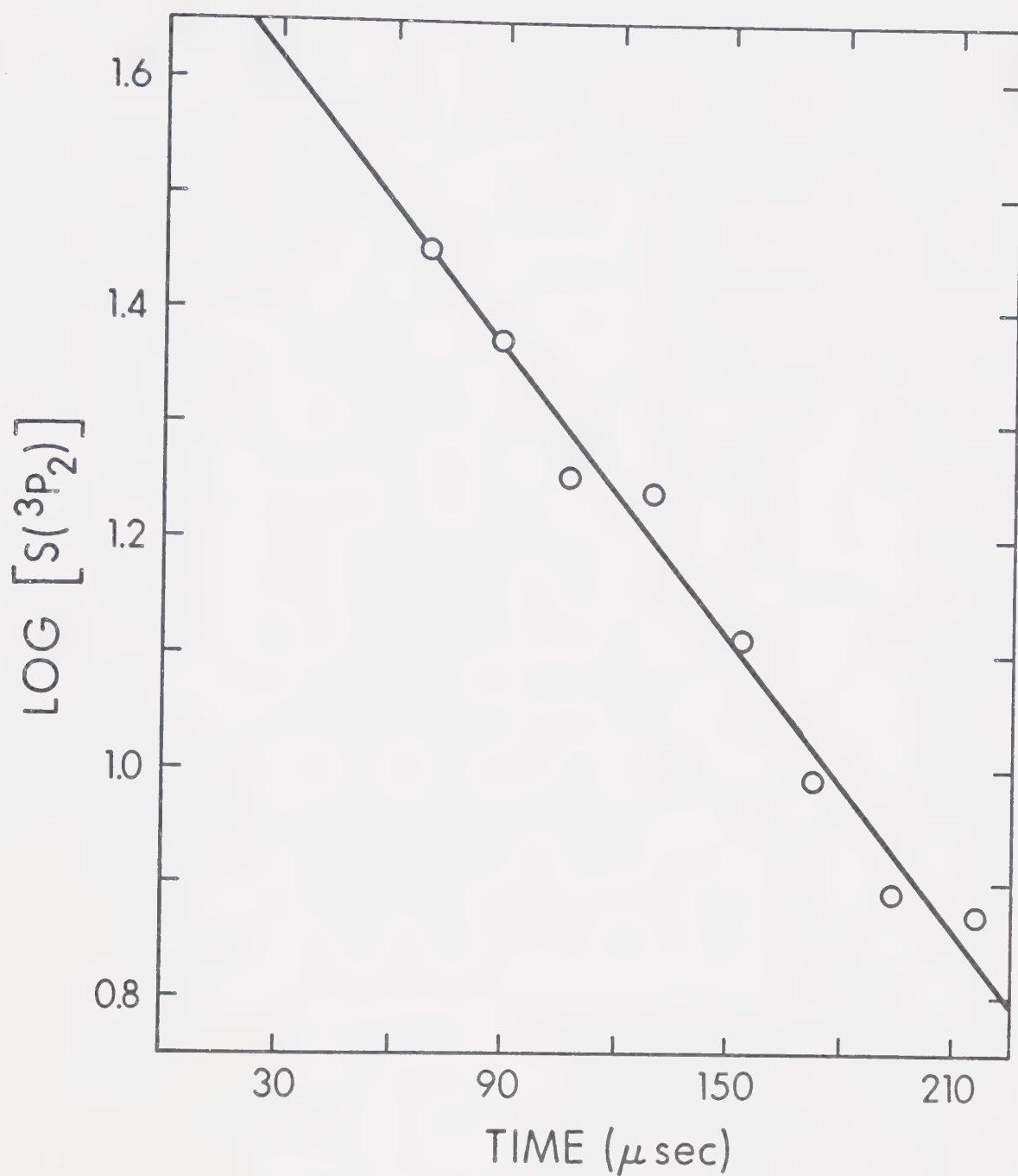


FIGURE VII-7: First Order Decay Plot of  $S(^3P_2)$  in the Presence of Isobutene.  $P(\text{COS}) = 0.1$  torr,  $P(\text{i-C}_4\text{H}_8) = 0.0053$  torr,  $P(\text{CO}_2) = 200$  torr.



TABLE VII-6

Effect of Tetramethylethylene Pressure  
on the Rate Constant for Decay of  $S(^3P)$  Atoms<sup>a</sup>

$10^7$ [TME] (mole/liter)	TME (torr)	No. of Runs	$10^{-4}k_{UNI}$ ( $\text{sec}^{-1}$ )
0	0	-	0.11
1.68	0.00314	2	1.21
2.54	0.00475	4	1.45
3.43	0.00641	4	2.21
5.00	0.00935	2	3.12

<sup>a</sup>  $P(\text{CO}_2) = 200$  torr,  $P(\text{COS}) = 0.10$  torr.



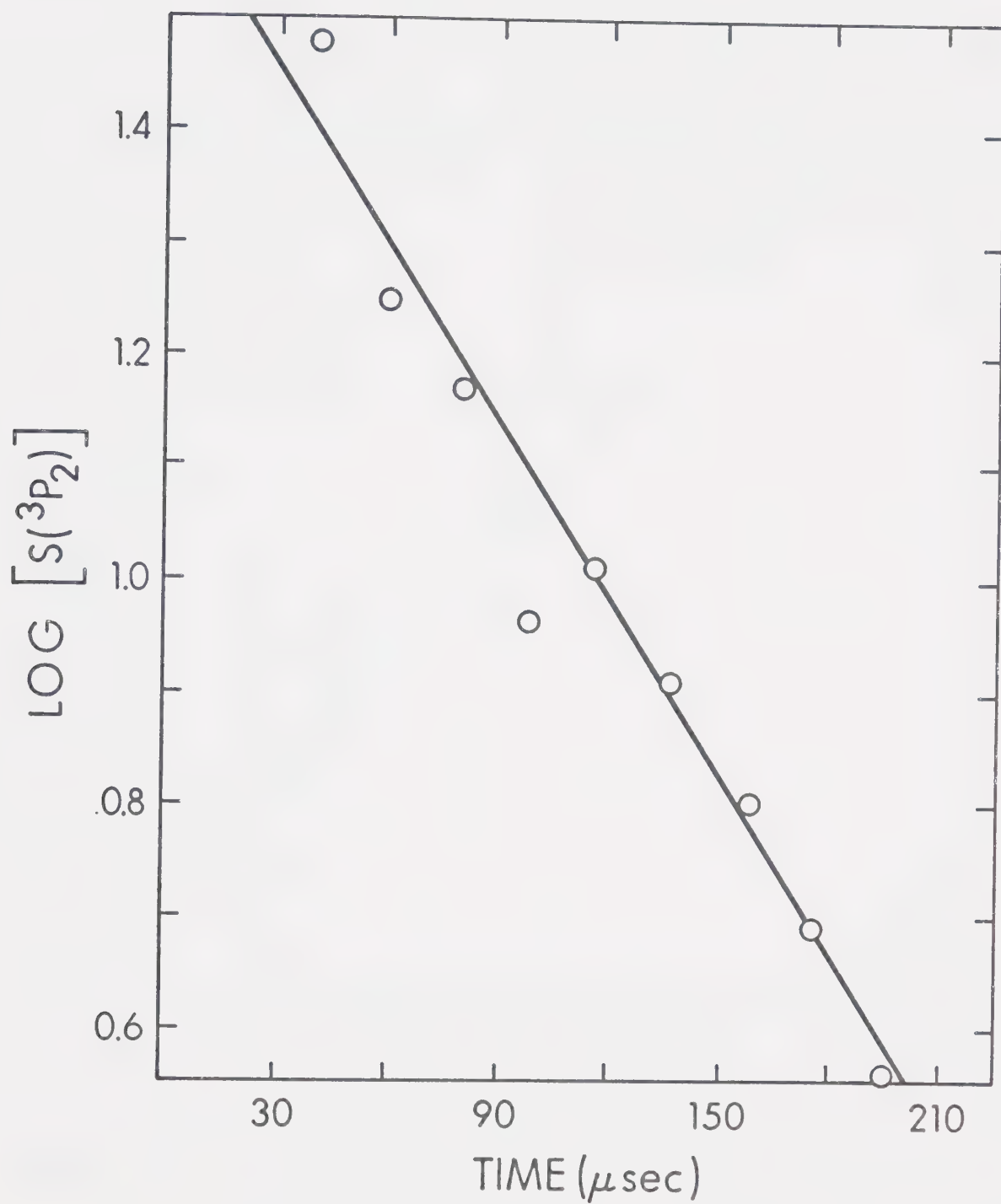


FIGURE VII-8: First Order Decay Plot of  $S(^3P_2)$  in the Presence of Tetramethylethylene.  $P(\text{COS}) = 0.1$  torr,  $P(\text{CH}_3)_2\text{C} = \text{C}(\text{CH}_3)_2 = 0.00314$  torr,  $P(\text{CO}_2) = 200$  torr.



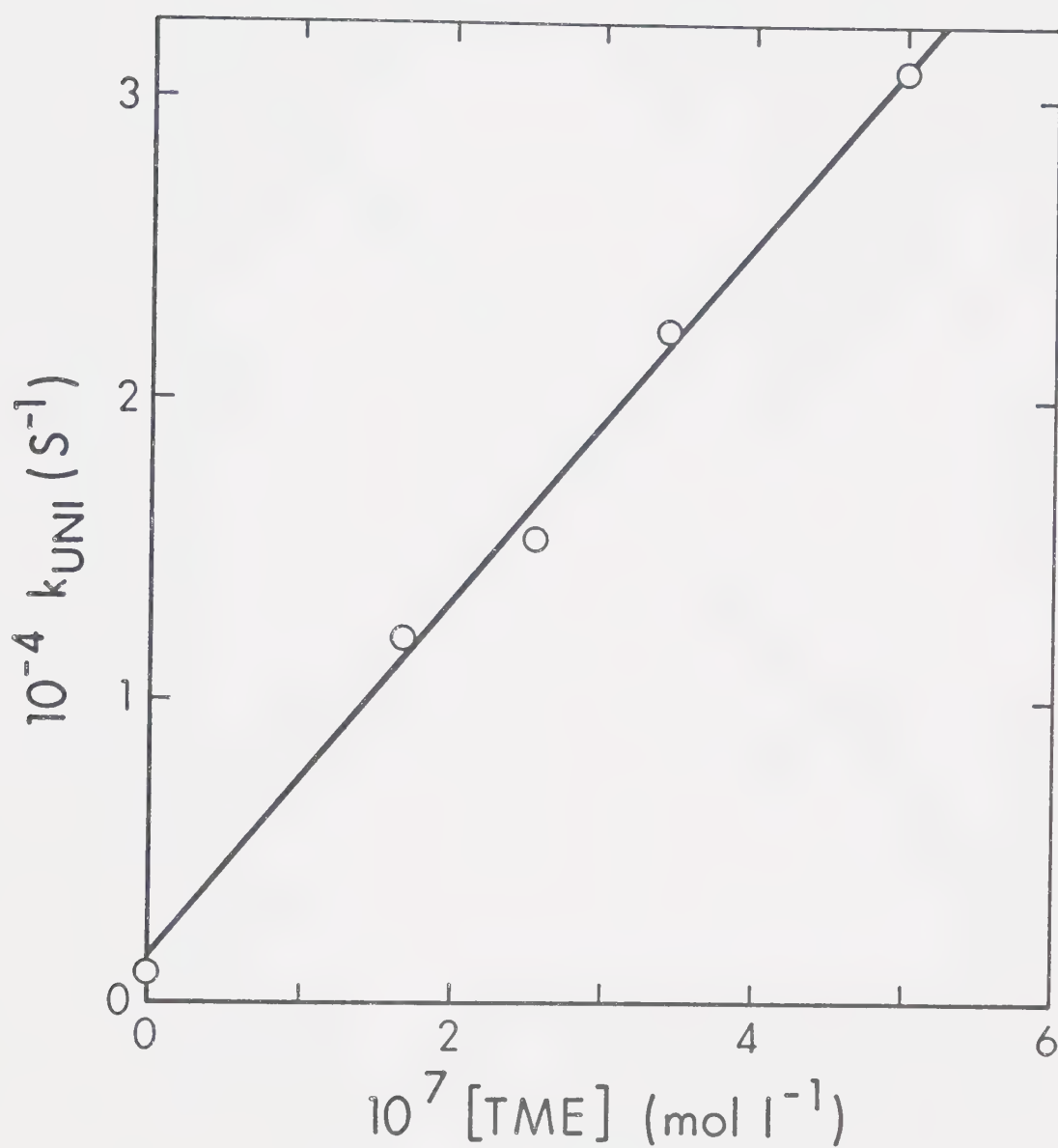


FIGURE VII-9: First Order Rate Constant for Decay of  $\text{S}(^3\text{P})$  Atoms versus Tetramethylethylene Concentration.



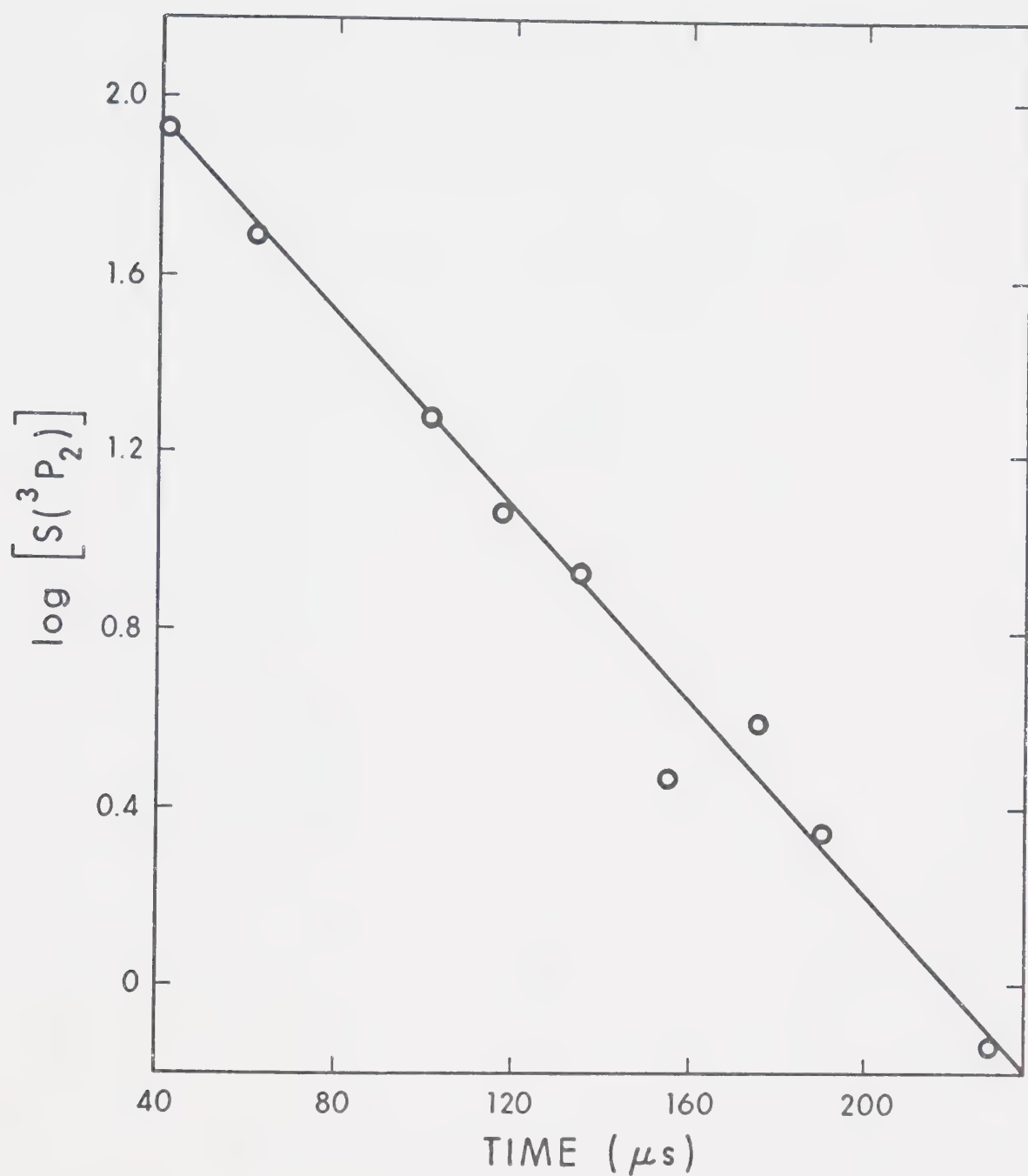


FIGURE VII-10: First Order Decay Plot of  $S(^3P_2)$  in the Presence of Vinyl Fluoride,  $P(\text{COS}) = 0.1$  torr,  $P(\text{C}_2\text{H}_3\text{F}) = 0.898$  torr,  $P(\text{CO}_2) = 200$  torr.



TABLE VII-7

Absolute Rate Constants for the Reaction of  $S(^3P)$   
Atoms with Olefins at 298°K

Substrate	$k,$ $1 \text{ mole}^{-1} \text{ sec}^{-1}$
Ethylene	$9.0 \pm 0.5 \times 10^8$
Propylene	$5.4 \pm 0.6 \times 10^9$
1-Butene	$8.2 \pm 0.6 \times 10^9$
<i>trans</i> -2-Butene	$1.1 \pm 0.2 \times 10^{10}$
Isobutene	$3.3 \pm 0.5 \times 10^{10}$
Tetramethylethylene	$6.0 \pm 0.3 \times 10^{10}$
Vinyl Fluoride	$5.0 \pm 0.5 \times 10^8$



## B. Results - Part II

The reactions of  $S(^3P)$  atoms with ethylene, propylene, 1-butene and tetramethylethylene were studied as a function of temperature.

### 1. Temperature Dependence of the $S(^3P)$ plus Ethylene System

This reaction was investigated in the temperature range 25 - 140°C. The data are tabulated in Table VII-8 and from the Arrhenius plot, Figure VII-11, an activation energy of  $1.5 \pm 0.1 \text{ kcal mole}^{-1}$  and an A factor of  $1.15 \pm 0.11 \times 10^{10} \text{ l mole}^{-1} \text{ sec}^{-1}$  were determined.

### 2. Temperature Dependence of the $S(^3P)$ plus Propylene System

The reaction was investigated in the temperature range 25 - 151°C. The data are tabulated in Table VII-9. From Figure VII-11,  $E_a = 0.5 \pm 0.2 \text{ kcal mole}^{-1}$  and  $A = 1.3 \pm 0.3 \times 10^{10} \text{ l mole}^{-1} \text{ sec}^{-1}$ .

### 3. Temperature Dependence of the $S(^3P)$ plus 1-Butene System

The reaction was investigated in the temperature range 25 - 208°C. The data are tabulated in Table VII-10. From



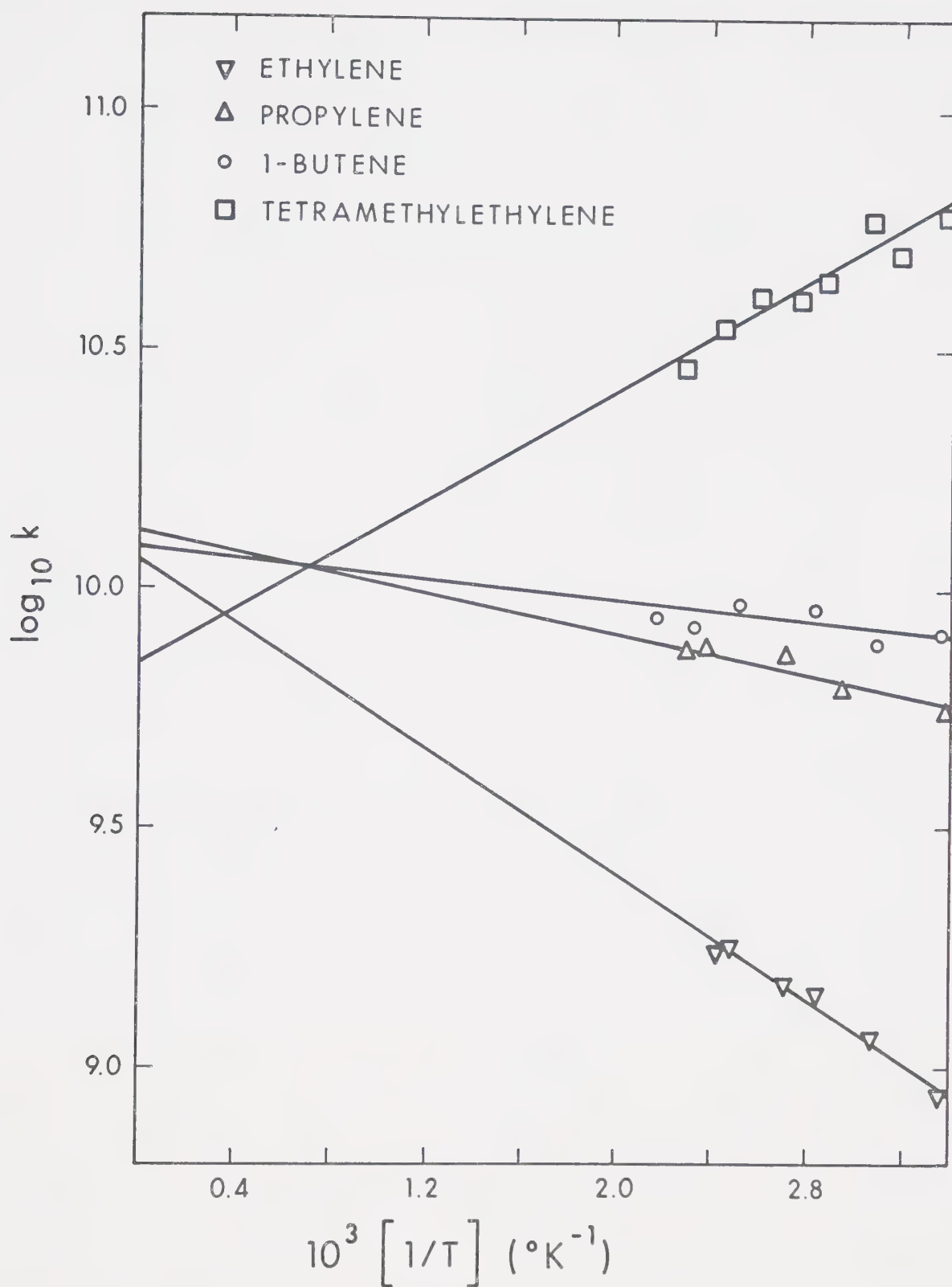


FIGURE VII-11: Arrhenius Plot showing the Temperature Dependences of the bimolecular rate constants for the Reactions of  $\text{S}(^3\text{P})$  with Ethylene, Propylene, 1-Butene and Tetramethylethylene.



TABLE VII-8

Temperature Dependence of the Bimolecular Rate Constant for the  
Reaction of S(<sup>3</sup>P) Atoms with Ethylene

Temperature, °k	$10^{-9} \times k, \text{ l mole}^{-1} \text{ sec}^{-1}$	log k
298	0.90	8.954
325	1.16	9.064
351	1.45	9.161
368	1.52	9.182
403	1.79	9.251
409	1.77	9.248



TABLE VII-9

Temperature Dependence of the Bimolecular Rate Constant for the  
Reaction of S(<sup>3</sup>P) Atoms with Propylene

Temperature, °k	$10^{-9}k, \text{ l mole}^{-1} \text{ sec}^{-1}$	log k
298	5.40	9.733
349	6.18	9.791
368	7.33	9.865
401	7.58	9.880
423	7.50	9.875



TABLE VII-10

Temperature Dependence of the Bimolecular Rate Constant for the  
Reaction of S(<sup>3</sup>P) Atoms with 1-Butene

Temperature, °k	$10^{-9}k, \text{ l mole}^{-1} \text{ sec}^{-1}$	log k
298	8.20	9.914
324	7.81	9.893
353	9.18	9.963
397	9.45	9.975
432	8.39	9.924
481	8.74	9.942



Figure VII-11,  $E_a = 0.2 \pm 0.2 \text{ kcal mole}^{-1}$  and  $A = 1.2 \pm 0.2 \times 10^{10} \text{ l mole}^{-1} \text{ sec}^{-1}$ .

#### 4. Temperature Dependence of the $S(^3P)$ plus Tetramethylethylene System

The reaction was investigated in the temperature range 25 - 166°C. The data are tabulated in Table VII-11. From Figure VII-11,  $E_a = -1.3 \pm 0.2 \text{ kcal mole}^{-1}$  and  $A = 7.0 \pm 1.3 \times 10^9 \text{ l mole}^{-1} \text{ sec}^{-1}$ .



TABLE VII-11

Temperature Dependence of the Bimolecular Rate Constant for the  
Reaction of  $S(^3P)$  Atoms with Tetramethylethylene

Temperature, °K	$10^{-10} k, \text{ l mole}^{-1} \text{ sec}^{-1}$	$\log k$
298	5.99	10.777
313	5.12	10.709
327	6.00	10.778
349	4.48	10.651
364	4.07	10.610
386	4.14	10.617
411	3.55	10.550
439	2.89	10.461



### C. Discussion

Before the present results can be discussed in a mechanistic context the data must be evaluated in terms of experimental variables such as possible photolysis of the substrate, the extent of secondary reactions between sulfur atoms and episulfides and the possibility that sulfur may also decay via  $S + S_2 \longrightarrow S_3$ ,  $S + S_3 \longrightarrow S_4$ , etc. The results on the  $S + C_2H_4$  reaction should be representative of all the systems studied. Ethylene absorbs only very weakly above 190 nm, the quartz cut-off (cf. Table II-2) and the extent of photolysis must be negligible since the bimolecular rate constant is independent of flash energy. Furthermore, Donovan et al<sup>10</sup> obtained reproducible rate constants when a water filter jacket (> 210 nm) was introduced, and Klemm et al<sup>140</sup> showed that the rate constant was independent of flash energy even when suprasil windows (> 160 nm) were employed.

To determine the effect of the secondary reaction  $S + C_2H_4S \longrightarrow S_2 + C_2H_4$  in the present study, an analogue computer simulation was set up. It is described in Appendix III. On the basis of this analysis, it is concluded that the observed rate constant for addition may be high by possibly ~ 5%. The extent of the abstraction reaction diminishes with increasing complexity of the olefin since the rate of addition to the double bond increases accordingly and the relative importance of the addition and abstraction



reactions then becomes concentration dependent. This obtains in the case of tetramethylethylene where the rate constant for addition of  $S(^3P)$  atoms to tetramethylethylene is comparable with the rate constant for abstraction from the episulfide (cf. Chapter VI).

The importance of the  $S + S_2 \rightarrow S_3$  reaction can be discounted because it has been shown (Chapter III) that, in the absence of olefin, the rate of decay of sulfur via this route is relatively slow, of the order of  $\leq 10^3 \text{ sec}^{-1}$  and the analog computer simulation of the  $S + C_2H_4$  system (*vide infra*) indicates that the build-up of  $S_2$  species is very slow. At the low S-atom concentrations employed in these studies, the observed bimolecular rate constants are probably the true ones.

Absolute rate parameters for the reactions of sulfur atoms with olefins obtained in this work are summarized in Table VII-12 along with the  $S + C_2H_4$  value reported by Donovan et al.<sup>10</sup> using the same technique as employed here, and others by Klemm and Davis<sup>141</sup> who recently used the resonance fluorescence method to monitor the S-atom decay rates. Some relative data<sup>28</sup> are also included for comparison.

It is seen that the activation energies obtained by the two techniques are in good agreement but the A factors differ by a fairly constant factor of  $\sim 2.5 - 3$ . At the present time there is no obvious explanation for this discrepancy. It should, however, be noted that the rate parameters for the  $S + O_2$  reaction obtained by the two methods are in good agreement, and therefore



TABLE VII-12

Absolute Rate Data for the Reactions of  $S(^3P)$  Atoms with Olefins

Substrate	$k$ , $1 \text{ mole}^{-1} \text{ sec}^{-1}$	$E_a$ , $\text{kcal mole}^{-1}$	$A$ , $1 \text{ mole}^{-1} \text{ sec}^{-1}$	$\Delta S^\ddagger$ , $\text{E.U.}^e$	$E_a^d$ , $\text{Rel. Data}$	$A^d$ , $\text{Rel. Data}$
$C_2H_4$	$9.0 \pm 0.5 \times 10^{10}$ <sup>a</sup>	$1.5 \pm 0.1$ <sup>a</sup>	$1.15 \pm 0.11 \times 10^{10}$ <sup>a</sup>	-16.47	2.0	$1.4 \times 10^{10}$
	$7.0 \pm 0.9 \times 10^8$ <sup>c</sup>					
	$3.0 \pm 0.1 \times 10^8$ <sup>b</sup>	$1.6 \pm 0.1$ <sup>b</sup>	$4.3 \pm 0.4 \times 10^9$ <sup>b</sup>	-18.43		
$C_3H_6$	$5.4 \pm 0.6 \times 10^9$ <sup>a</sup>	$0.5 \pm 0.2$ <sup>a</sup>	$1.3 \pm 0.3 \times 10^{10}$ <sup>a</sup>	-16.23	0.4	$1.4 \times 10^{10}$
	$1.9 \pm 0.1 \times 10^9$ <sup>b</sup>	$0.4 \pm 0.1$ <sup>b</sup>	$3.6 \pm 0.4 \times 10^9$ <sup>b</sup>	-18.78		
$1-C_4H_8$	$8.2 \pm 0.6 \times 10^9$ <sup>a</sup>	$0.2 \pm 0.2$ <sup>a</sup>	$1.2 \pm 0.2 \times 10^{10}$ <sup>a</sup>	-16.39	0.3	$1.05 \times 10^{10}$
	$2.4 \pm 0.2 \times 10^9$ <sup>b</sup>	$0.4 \pm 0.1$ <sup>b</sup>	$4.5 \pm 0.7 \times 10^9$ <sup>b</sup>	-18.34		
<i>cis</i> -2- $C_4H_8$	$4.2 \pm 0.2 \times 10^{10}$ <sup>b</sup>	$-0.2 \pm 0.1$ <sup>b</sup>	$2.8 \pm 0.4 \times 10^9$ <sup>b</sup>	-19.28	-0.1	$7.4 \times 10^9$
<i>trans</i> -2- $C_4H_8$	$1.1 \pm 0.2 \times 10^{10}$				0	$9.1 \times 10^9$
<i>iso</i> - $C_4H_8$	$3.3 \pm 0.5 \times 10^{10}$				-0.3	$1.35 \times 10^{10}$
					/continued.....	



TABLE VII-12 (cont'd)

Substrate	$k$ , $1 \text{ mole}^{-1} \text{ sec}^{-1}$	$E_a$ , $\text{kcal mole}^{-1}$	$A$ , $1 \text{ mole}^{-1} \text{ sec}^{-1}$	$\Delta S^\ddagger$ , E.U.	$E_a$ , Rel. Data	$A$ , Rel. Data
$(\text{CH}_3)_2\text{C}=\text{C}(\text{CH}_3)_2$	$6.0 \pm 0.3 \times 10^{10^a}$	$-1.3 \pm 0.2^a$	$7.0 \pm 1.3 \times 10^{9^a}$	-17.46	-1.3	$7.0 \times 10^9$
	$2.5 \pm 0.2 \times 10^{10^b}$	$-1.3 \pm 0.2^b$	$2.8 \pm 1.0 \times 10^{9^b}$	-19.28		
$\text{C}_2\text{H}_3\text{F}$	$5.0 \pm 0.5 \times 10^{10}$				2.7	

a. this work

b. reference 141

c. reference 10

d. relative data from reference 28 set on absolute base with  $E_a$  [ $\text{S} + (\text{CH}_3)_2\text{C}=\text{C}(\text{CH}_3)_2$ ] = -1.3 kcal mole<sup>-1</sup> and  $A = 7. \times 10^9$  1 mole<sup>-1</sup> sec<sup>-1</sup>.

e. The standard state used in the calculation of  $\Delta S^\ddagger$  is 1 mole l<sup>-1</sup>.



the different A factors are certainly not due to experimental artifacts. The room temperature value of  $9 \times 10^8 \text{ l mole}^{-1} \text{ sec}^{-1}$  obtained by us for the reaction with ethylene is in reasonable agreement with the value of  $7 \times 10^8 \text{ l mole}^{-1} \text{ sec}^{-1}$  obtained by Donovan et al<sup>10</sup>, and confirms the reproducibility of the measurement in a similar apparatus.

The A factors for addition to terminal olefins appear to be invariant and the slight decrease in the A factor for the sulfur plus tetramethylethylene reaction may possibly arise from steric limitations.

The collision frequency for the  $\text{S}(^3\text{P}) + \text{C}_2\text{H}_4$  reaction is  $1.3 \times 10^{11} \text{ l mole}^{-1} \text{ sec}^{-1}$  taking  $d_{\text{AB}}$  as 3.2 cm. Since  $A = 1.15 \times 10^{10} \text{ l mole}^{-1} \text{ sec}^{-1}$ , the steric factor,  $p$ , is  $\sim 0.09$ . The collision efficiency of the reaction at room temperature is  $\sim 1$  in 144 and the entropy of activation  $\Delta S^\ddagger$  is -16.47. The collision efficiency for the  $\text{S} + (\text{CH}_3)_2\text{C}=\text{C}(\text{CH}_3)_2$  reaction is estimated to be  $\sim 1$  in 2.

It is interesting that activation energies derived from competitive experiments, relative to  $E_a = -1.3 \text{ kcal}$  for the S + tetramethylethylene reaction, are in reasonably good agreement with the absolute values.

The decreasing trend in  $E_a$  with increasing alkyl substitution on the double bond clearly illustrates the electrophilic character of triplet ground state sulfur atoms and this is further substantiated by the linear relationship between  $E_a$  and ionization



potential of the olefin, Figure VII-12, which is a measure of the ease of removal of one of the  $\pi$ -electrons. This trend has also been established for the other Group VI A elements in their ground triplet states. Table VII-13 summarizes the rate parameters for the addition reactions of O, S, Se and Te atoms to a variety of olefins.

The negative temperature dependence for the rate of reaction of  $S(^3P)$  atoms with tetramethylethylene, predicted on intuitive grounds<sup>76</sup>, is a novel and significant feature of the addition reaction. Other workers have subsequently shown that  $E_a$  for the addition of O atoms to tetramethylethylene is also negative<sup>54,57</sup>. For many years it has been assumed that  $E_a \sim 0$  for reactions proceeding near the collision efficiency but this is only valid if the negative temperature dependence was entirely due to a negative temperature term in the A factor. However, transition state theory predicts that the temperature exponent is unlikely to be higher than 0.5. Collision theory gives a function of  $T^{-3/2}$  if one imposes the severe restriction that the reaction occurs at only one relative kinetic energy and at no other. Neither of these appears to be sufficient to account for the experimental function of  $\sim T^{-2}$ . The negative temperature dependence of this reaction can best be rationalized by considering the nature of the curve crossing for any given olefin in its reaction with  $S(^3P)$  atoms. It is proposed that the atom and olefin initially approach on a potential energy surface with a shallow minimum.



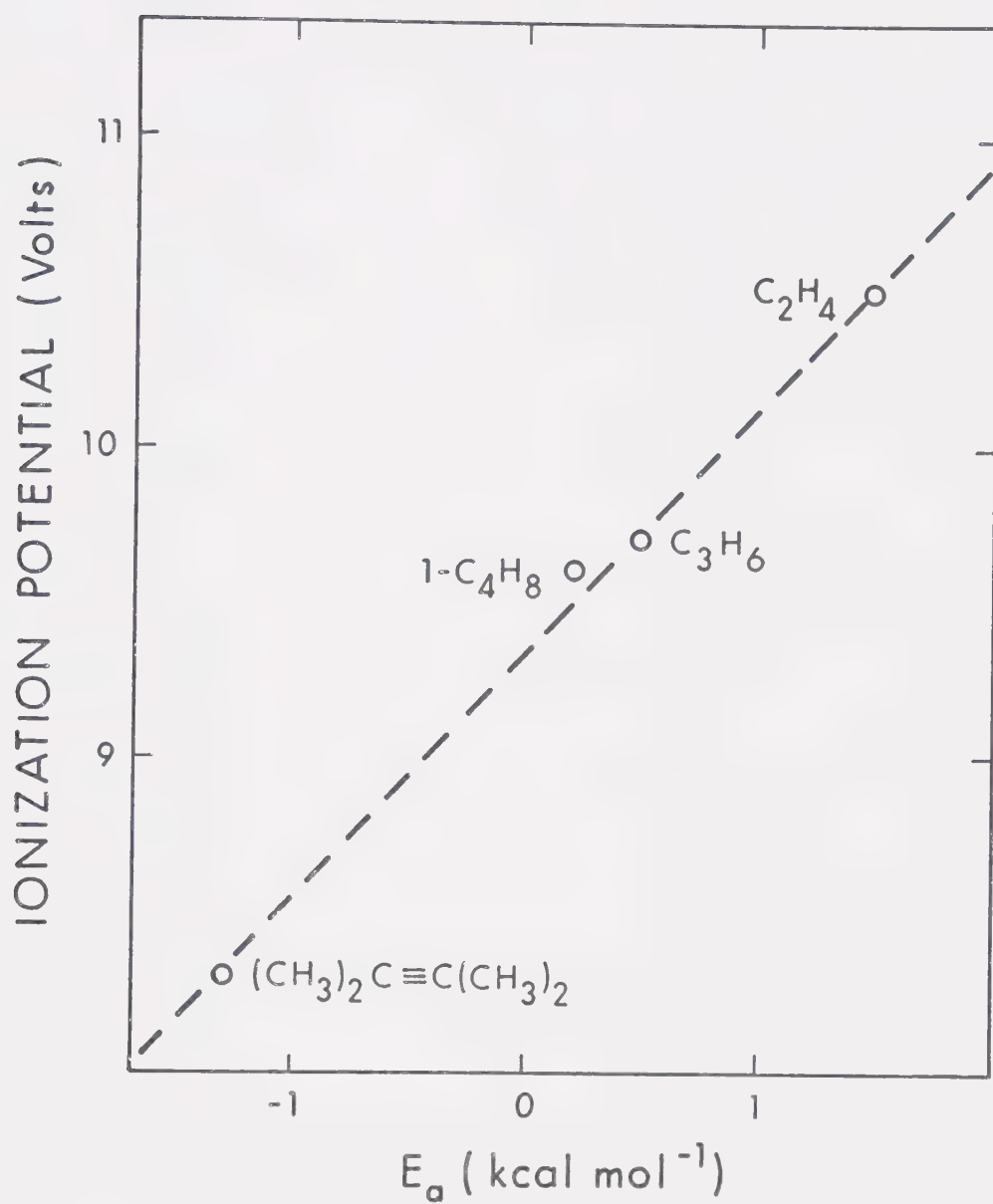


FIGURE VII-12: Plot showing Correlation of  $E_a$  for reaction with olefin as a Function of the Ionization Potential of the Olefin.



TABLE VII-13

Arrhenius Parameters for the Reactions of Group VI A Atoms with Olefins

Substrate	O		S		Se		Te	
	$E_a$	$\log A$	$E_a$	$\log A$	$E_a$	$\log A$	$E_a$	$\log A$
$C_2H_4$	1.9	9.91 <sup>a</sup>	1.5	10.06 <sup>k</sup>	2.8	10.04 <sup>m</sup>	2.5	8.93 <sup>o</sup>
	1.1	9.51 <sup>b</sup>	1.6	9.63 <sup>l</sup>				
	1.6	10.03 <sup>c</sup>						
	1.6	9.98 <sup>d</sup>						
$C_3H_6$	1.0	9.83 <sup>a</sup>	0.5	10.11 <sup>k</sup>	2.35	10.11 <sup>n</sup>	0.6	8.5 <sup>o</sup>
	.08	9.40 <sup>e</sup>	0.4	9.56 <sup>l</sup>				
1- $C_4H_8$	0.8	9.79 <sup>a</sup>	0.2	10.08 <sup>k</sup>	2.25	10.49 <sup>n</sup>		
	0.05	9.35 <sup>f</sup>	0.4	9.65 <sup>l</sup>				
	0.8	9.87 <sup>g</sup>						
	0.85	10.10 <sup>d</sup>						
	0.8	9.94 <sup>h</sup>						

/continued...



TABLE VII-13 (cont'd)

Substrate	O		S		Se		Te	
	$E_a$	$\log A$	$E_a$	$\log A$	$E_a$	$\log A$	$E_a$	$\log A$
iso-C <sub>4</sub> H <sub>8</sub>	0.0	9.80 <sup>a</sup>			1.01	10.38 <sup>n</sup>		
	0.4	10.31 <sup>d</sup>						
	0.1	9.95 <sup>g</sup>						
cis-2-C <sub>4</sub> H <sub>8</sub>	-0.3	9.76 <sup>b</sup>	-0.2	9.45 <sup>l</sup>	1.21	10.30 <sup>n</sup>		
	0.4	10.36 <sup>d</sup>						
(CH <sub>3</sub> ) <sub>2</sub> C=C(CH <sub>3</sub> ) <sub>2</sub>	-1.6	9.53 <sup>i</sup>	-1.3	9.85 <sup>k</sup>			-1.6	8.41 <sup>o</sup>
	-0.8	10.09 <sup>j</sup>	-1.3	9.45 <sup>l</sup>				

a. ref. 48; b. ref. 51; c. ref. 40; d. ref. 41; e. ref. 52; f. ref. 142; g. ref. 43;

h. ref. 53; i. ref. 54; j. ref. 57; k. ref. this work; l. ref. 141; m. ref. 71;

n. ref. 72; o. ref. 76.

NOTE:  $E_a$  = kcal mole<sup>-1</sup>

$\log A$  = 1 mole<sup>-1</sup> sec<sup>-1</sup>



The repulsive part of this surface intersects an attractive potential surface and the rate of the reaction would be determined by:

- a) the potential energy difference between the intersection of the two surfaces and the separated reactants
- b) the number of internal degrees of freedom in the reaction complex
- c) the probability of curve crossing between the two surfaces.

The positive dependence of the  $S(^3P)$  plus ethylene reaction can be explained by a curve crossing occurring at an energy above that of the separated reactants and the negative temperature dependence of the  $S(^3P)$  plus tetramethylethylene reaction by a crossing at an energy below that of the separated reactants. This is qualitatively illustrated in Figure VII-13.

Since the Group VI A atoms show a strong parallelism in their behaviour, Table VII-13, it would seem reasonable that this mechanism would be equally applicable to the cases of O, Se, and Te atoms.

It has been shown<sup>143</sup> that the sole product of the  $S(^3P)$  + olefin reaction is the corresponding episulfide, which is readily stabilized at moderate pressures and formed in a highly stereoselective manner. Semi-empirical EHMO and *ab initio* type m.o. calculations on the reaction surfaces for the  $S + C_2H_4$  system and on the ground and excited states of thiirane<sup>30-33</sup> have provided a



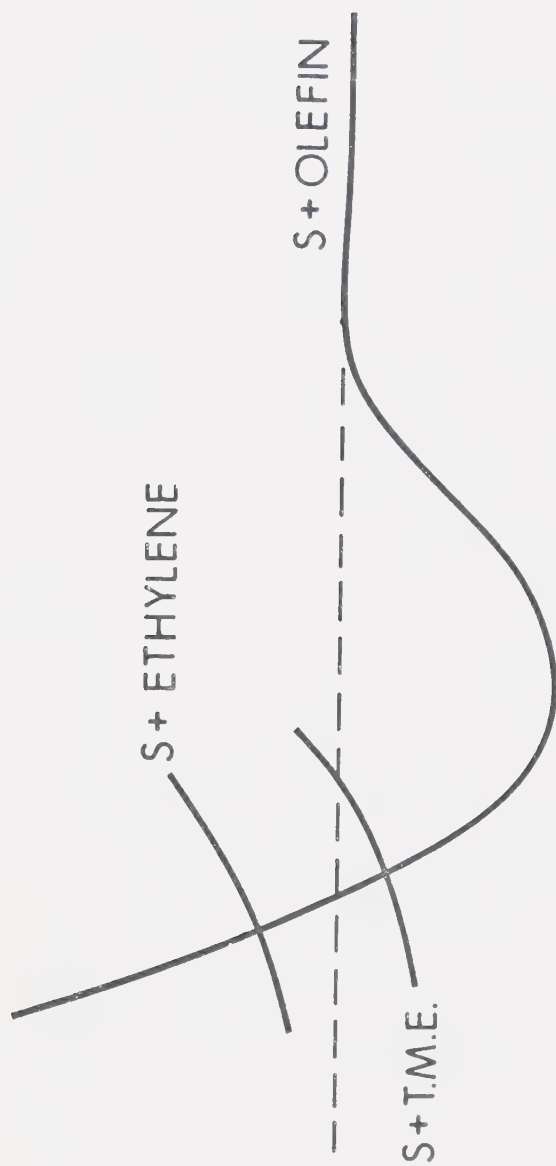


FIGURE VII-13: Qualitative Depiction of Curve Crossing for Positive and Negative Temperature Dependence.



rationale for the reaction path. Figure VII-14 illustrates the state symmetry correlations for the lowest excited singlet and triplet states of thiirane. The initial approach is on the  $^3B_2$  surface which, at smaller internuclear distance, intersects with the  $^3A_2$  surface. The computed barrier to potential surface crossing, 7.5 kcal, is much higher than the experimentally observed value of 1.5 kcal but this type of calculation always overestimates the height of potential barriers. The  $^3A_2$  surface corresponds to the lowest mode of vertical excitation and, when the geometry is optimized by varying the CCS bond angle, Figure VII-15 it is seen that at the equilibrium geometry which corresponds to a CCS bond angle of about  $100^\circ$ , the  $^3A_1$  (or  $^3\Sigma$ ) state becomes the lowest triplet state. The computed barrier to rotation is 23 kcal, and indicates a relatively strong binding interaction between sulfur and the terminal methylene carbon. Since the exothermicity of the reaction is only 20 kcal, this explains the high stereoselectivity of the addition. The complete reaction path thus follows the sequence  $C_2H_4(^1A_1) + S(^3P) \longrightarrow C_2H_4S(^3B_2) \longrightarrow C_2H_4S(^3A_2) \longrightarrow C_2H_4S(^3\Sigma)$ .

Similar *ab initio* calculations on the  $O(^3P) + C_2H_4$  reaction path and on the ground and excited states of ethylene epoxide<sup>66</sup> indicate that the barrier to rotation in the lowest excited triplet state is prohibitively high. In order to account for the non-stereospecificity of the process, the initially formed triplet adduct must undergo rapid intersystem crossing to



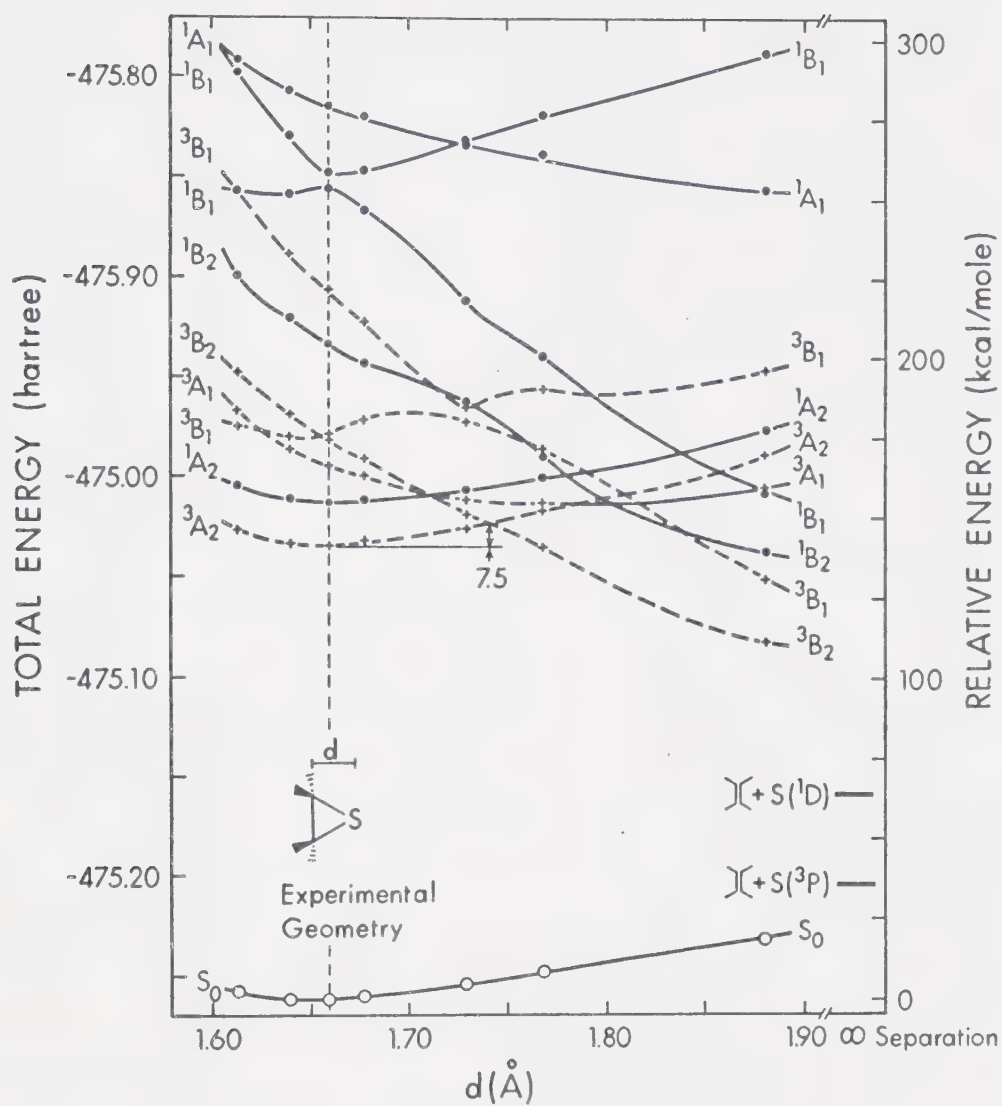


FIGURE VII-14: Energy of Electronic Configurations as a Function of S-Ethylene Separation<sup>30</sup>



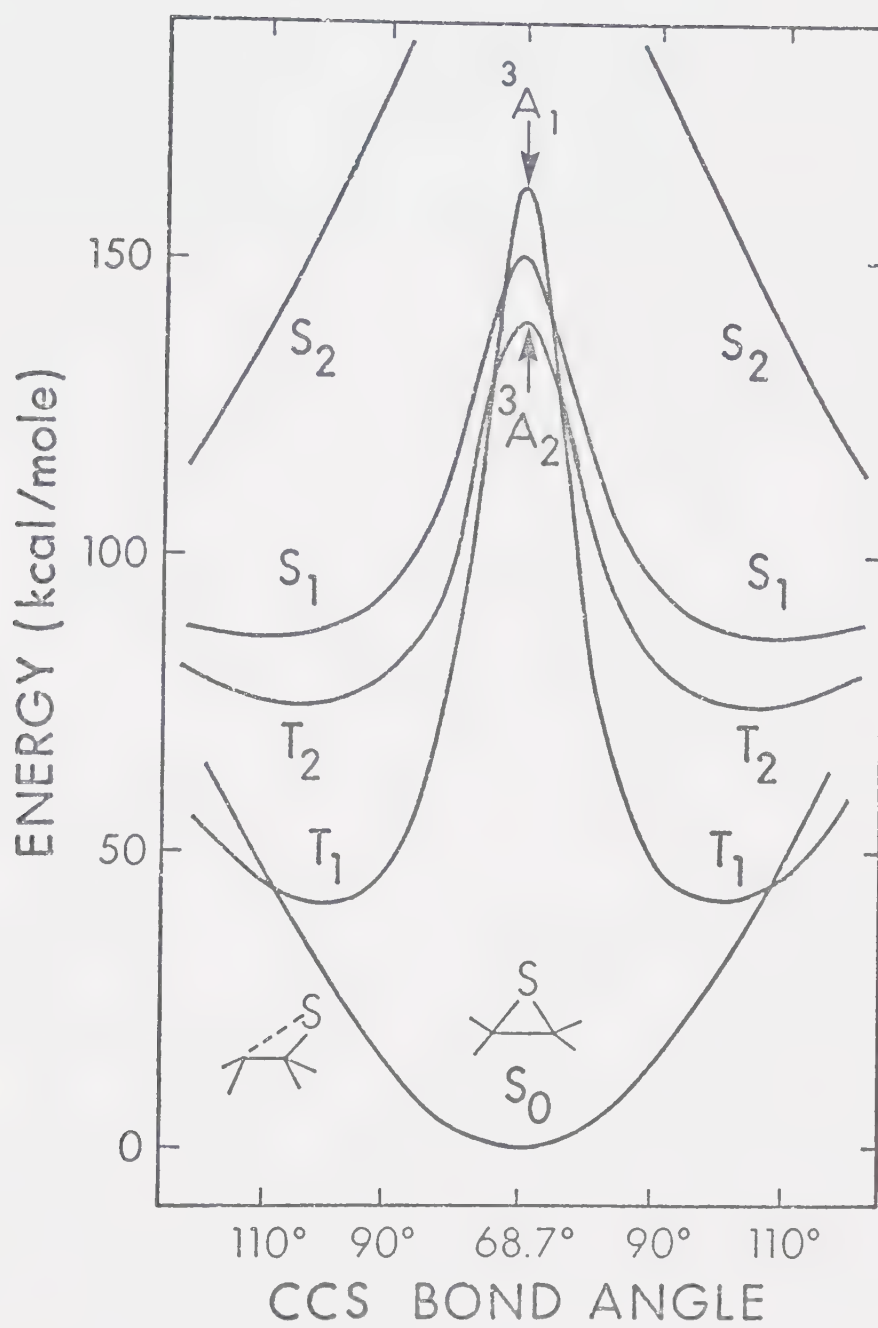


FIGURE VII-15: Energy of Electronic States as a Function of CCS Angle<sup>30</sup>



a vibrationally excited surface in the ground state (possibly a zwitterion surface) in which rapid rotation takes place. It was also shown that the observed temperature dependence of the stereoselectivity can only be rationalized if isomerization takes place on a ground state surface.

Schmidt and Lee<sup>144</sup> examined the  $S(^3P) + \text{cis-2-butene}$  reaction at low pressures and reported extensive isomerization in the olefin. They suggested a chain mechanism to account for this, involving labile and non-labile additions to the olefin with sulfur atoms as the chain carriers:



Relative "labile" and non-labile" addition rate constants were derived. This mechanism can however be rejected on mechanistic and kinetic grounds:

1. The addition to *cis*-2-butene yields > 80% *cis*-2-butene episulfide<sup>143</sup>, which is irreconcilable with the proposed reversibility of the process;

2. Relative rate constants<sup>28</sup> were found to be independent of concentration and of the nature of the olefin pair, i.e.

$$k_a/k_c = (k_a/k_b / k_c/k_b)$$

3. The relative rate of "non-labile" addition to 1,3-butadiene would correspond to an absolute rate constant higher



than the collision frequency, by a factor of  $10^3$ .

Recent studies<sup>145,146</sup> have conclusively shown that the species responsible for isomerization must be the non-vertical, ring distorted  $^3\Sigma$  state of the episulfide, and not sulfur atoms. Triplet state episulfide can be generated by thermal or photochemical excitation or by energy transfer from a variety of triplet sensitizers and, under conditions where sulfur atoms are demonstrably absent, several hundred molecules of *cis*-2-butene are isomerized, depending on the energy content of the triplet episulfide. The isomerization apparently takes place via a facile, reversible addition of the triplet episulfide to the bond, where the geometry of the episulfide must be retained in the cyclic adduct:



Thus, triplet state episulfides have strong biradical properties and are remarkably resistant to collisional deactivation. The estimated lifetime for triplet state ethylene episulfide is  $> 2 \times 10^{-7}$  sec<sup>146</sup>.

It is interesting to note that in similar studies<sup>132</sup> on the  $O(^3P) + \textit{cis}$ -2-butene system, no isomerization was detected. This lends support to theoretical prediction that the intermediate adducts in these systems are not triplet states but vibrationally excited ground state epoxides. Thus, the physical and chemical properties of episulfides make them unique among three-membered cyclic heterocycles.



## CHAPTER VIII

### THE REACTIONS OF $S(^3P)$ ATOMS WITH ALKYNES

#### A. Results - Part I

Room temperature rate constants were determined for the reaction of  $S(^3P)$  atoms with acetylene, acetylene- $d_2$ , propyne, 1-butyne, 2-butyne, 2-pentyne and 2-perfluorobutyne.

##### 1. The Bimolecular Rate Constant for the Reaction of $S(^3P)$ Atoms with Acetylene

The average observed first order rate constant in the presence of acetylene was  $1.15 \pm 0.24 \times 10^4 \text{ sec}^{-1}$ . Applying the correction for the rate constant in the absence of reactant yields a first order rate constant due to reaction with acetylene of  $1.04 \times 10^4 \text{ sec}^{-1}$  and at 0.865 torr  $C_2H_2$  the bimolecular rate constant is  $2.3 \pm 0.5 \times 10^8 \text{ l mole}^{-1} \text{ sec}^{-1}$ . The data are summarized in Table VIII-1 and illustrated in Figure VIII-1.

##### 2. The Bimolecular Rate Constant for the Reaction of $S(^3P)$ Atoms with Acetylene- $d_2$

The average observed first order rate constant was  $1.24 \pm 0.13 \times 10^4 \text{ sec}^{-1}$  and, correcting for the rate constant in the absence of reactant, the first order rate constant due to reaction with acetylene- $d_2$  is  $1.13 \times 10^4 \text{ sec}^{-1}$ . At 0.940 torr  $C_2D_2$  the bimolecular rate constant is then  $2.3 \pm 0.3 \times 10^8 \text{ l mole}^{-1} \text{ sec}^{-1}$ .



TABLE VIII-1

First Order Decay Rate of  $S(^3P_2)$  Atoms  
in the Presence of Acetylene

$C_2H_2$ (torr)	$CO_2$ (torr)	$COS$ (torr)	$10^{-4}k,$ $sec^{-1}$
0.865	200	0.1	1.43
0.865	200	0.1	0.97
0.865	200	0.1	1.06
average			$1.15 \pm 0.24$



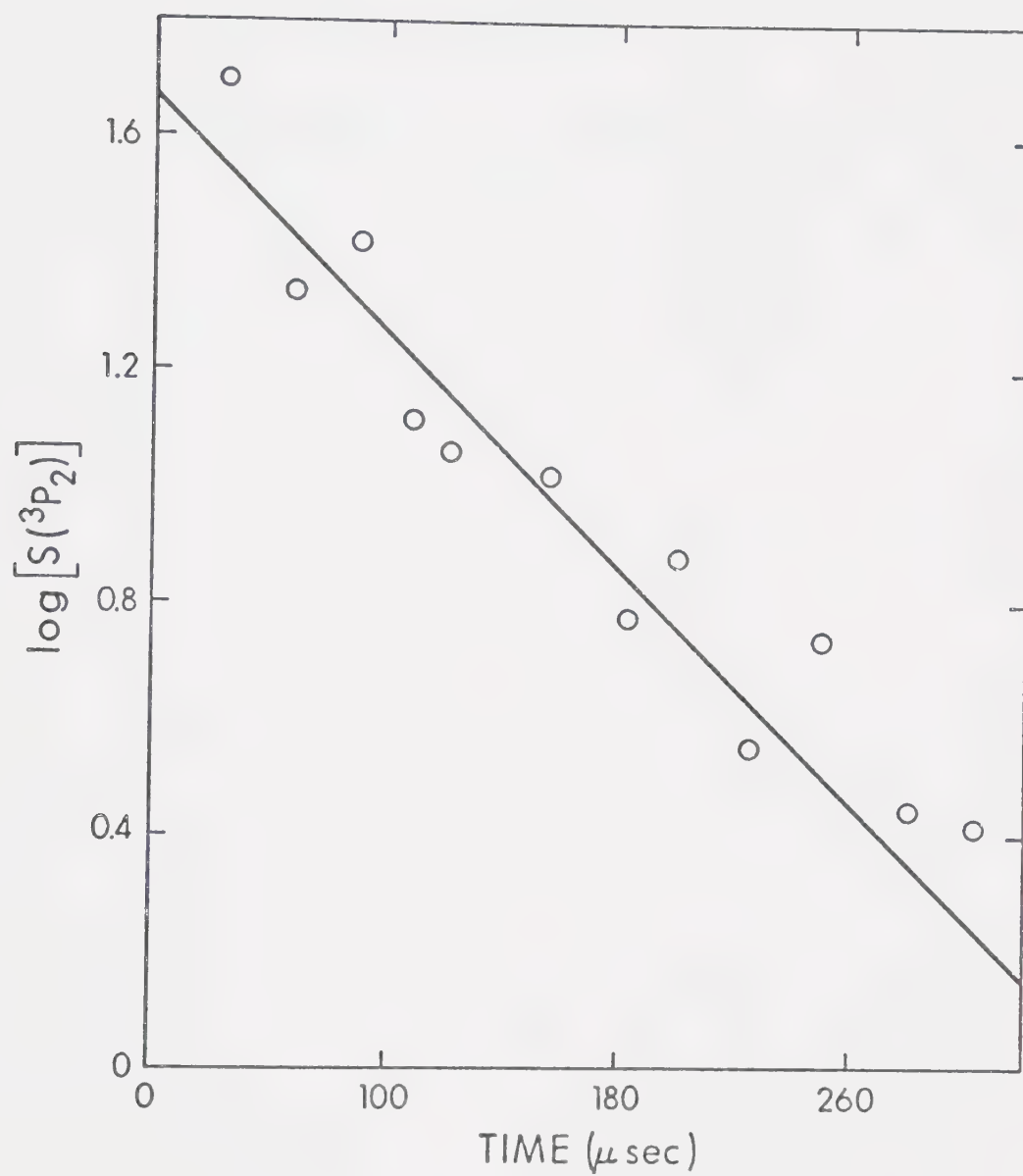


FIGURE VIII-1: First Order Decay Plot of  $S(^3P_2)$  Atoms in the Presence of Acetylene.  $P(\text{COS}) = 0.1$  torr,  $P(\text{C}_2\text{H}_2) = 0.865$  torr,  $P(\text{CO}_2) = 200$  torr.



The data are summarized in Table VIII-2 and illustrated in Figure VIII-2.

### 3. The Bimolecular Rate Constant for the Reaction of $S(^3P)$ Atoms with Propyne

The average observed first order rate constant was  $2.90 \pm 0.12 \times 10^4 \text{ sec}^{-1}$ . The corrected first order rate constant for reaction with propyne is  $2.79 \times 10^4 \text{ sec}^{-1}$ . The bimolecular rate constant is  $4.8 \pm 0.2 \times 10^9 \text{ l mole}^{-1} \text{ sec}^{-1}$  at 0.110 torr  $C_3H_4$ . The data are summarized in Table VIII-3 and illustrated in Figure VIII-3.

### 4. The Bimolecular Rate Constant for the Reaction of $S(^3P)$ Atoms with 1-Butyne

The average observed first order rate constant was  $1.74 \pm 0.06 \times 10^4 \text{ sec}^{-1}$  in 0.0922 torr 1- $C_4H_6$  and the first order rate constant due to reaction with 1-butyne is  $1.63 \times 10^4 \text{ sec}^{-1}$ . The bimolecular rate constant is  $3.3 \pm 0.2 \times 10^9 \text{ l mole}^{-1} \text{ sec}^{-1}$ . A measurement was also carried out at 100 torr  $CO_2$  and 0.0461 torr  $C_4H_6$  and yielded a value of  $3.8 \times 10^9 \text{ l mole}^{-1} \text{ sec}^{-1}$ , in agreement with the high pressure value. The data are summarized in Table VIII-4 and illustrated in Figure VIII-4.

### 5. The Bimolecular Rate Constant for the Reaction of $S(^3P)$ Atoms with 2-Butyne

The average observed first order rate constant in the



TABLE VIII-2

First Order Decay Rate of  $S(^3P)$  Atoms  
in the Presence of Acetylene- $d_2$

$C_2D_2$ (torr)	$CO_2$ (torr)	$COS$ (torr)	$10^{-4}k,$ $sec^{-1}$
0.940	200	0.1	1.06
0.940	200	0.1	1.25
0.940	200	0.1	1.32
0.940	200	0.1	1.34
average			1.24 $\pm$ 0.13



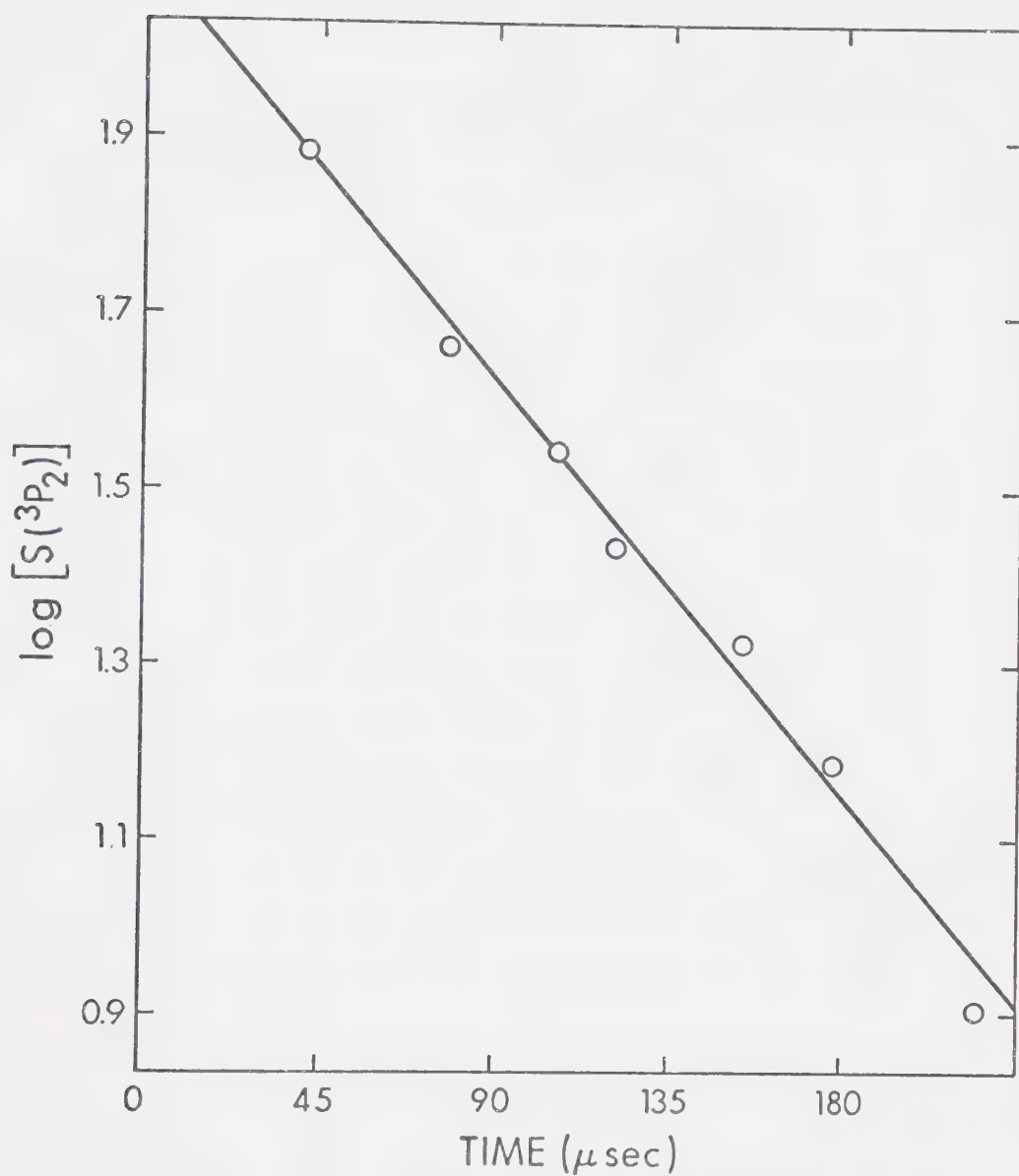


FIGURE VIII-2: First Order Decay Plot of  $S(^3P_2)$  Atoms in the Presence of Acetylene- $d_2$ ,  $P(COS) = 0.1$  torr,  $P(C_2D_2) = 0.940$  torr,  $P(CO_2) = 200$  torr.



TABLE VIII-3

First Order Decay Rate of  $S(^3P_2)$  Atoms  
in the Presence of Propyne

$CH_3CCH$ (torr)	$CO_2$ (torr)	$COS$ (torr)	$10^{-4}k,$ $sec^{-1}$
0.110	200	0.1	2.92
0.110	200	0.1	3.01
0.110	200	0.1	2.78
		average	$2.90 \pm 0.12$



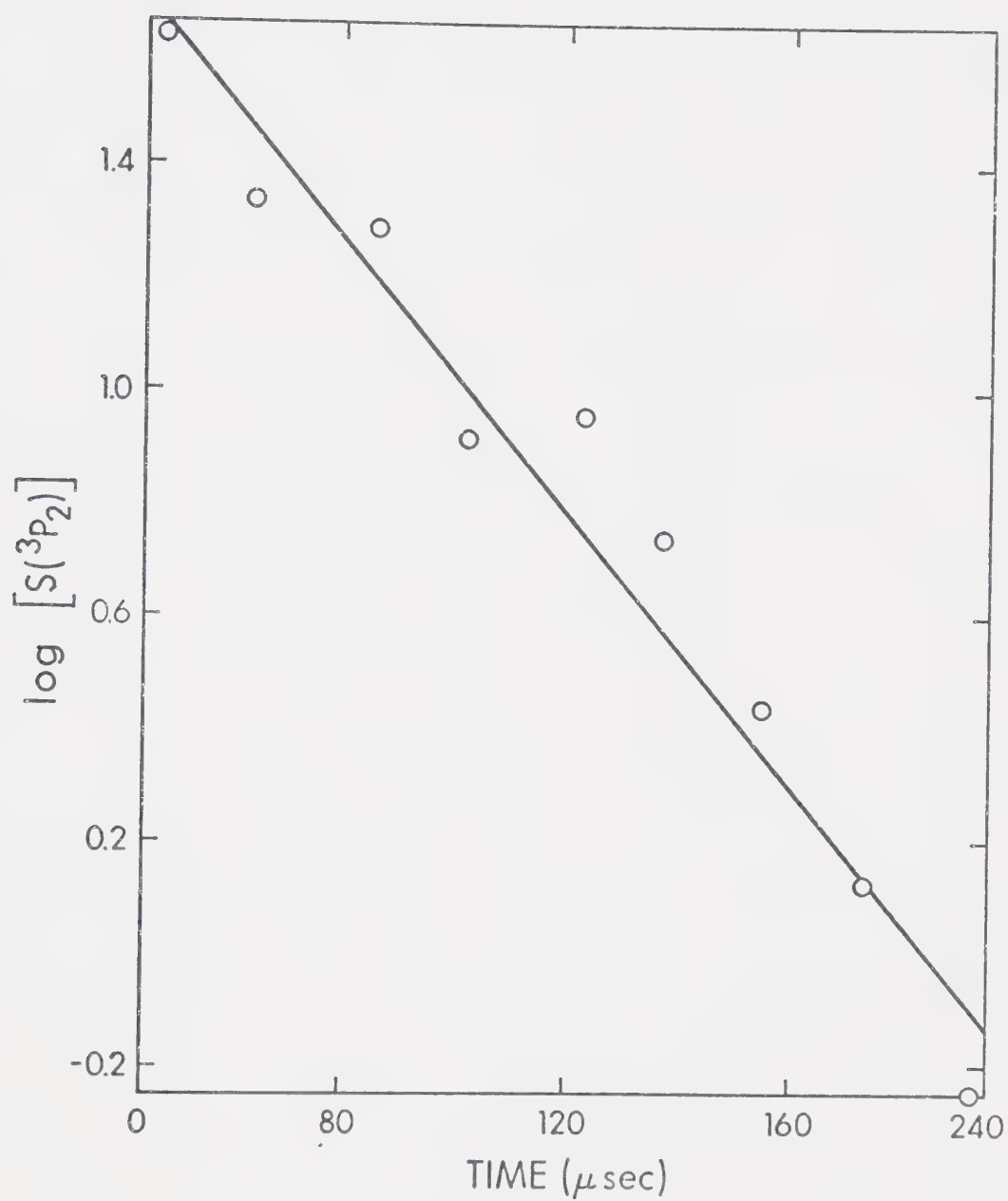


FIGURE VIII-3: First Order Decay Plot of  $S(^3P_2)$  Atoms in the Presence of Propyne.  $P(\text{COS}) = 0.1$  torr,  $P(\text{C}_3\text{H}_4) = 0.110$  torr,  $P(\text{CO}_2) = 200$  torr.



TABLE VIII-4

First Order Decay Rate of  $S(^3P_2)$  Atoms  
in the Presence of 1-Butyne

$CH_3CH_2CCH$ (torr)	$CO_2$ (torr)	$COS$ (torr)	$10^{-4}k,$ $sec^{-1}$
0.0922	200	0.1	1.69
0.0922	200	0.1	1.80
0.0922	200	0.1	1.72
		average	$1.74 \pm 0.06$
0.0461	100	0.05	1.06



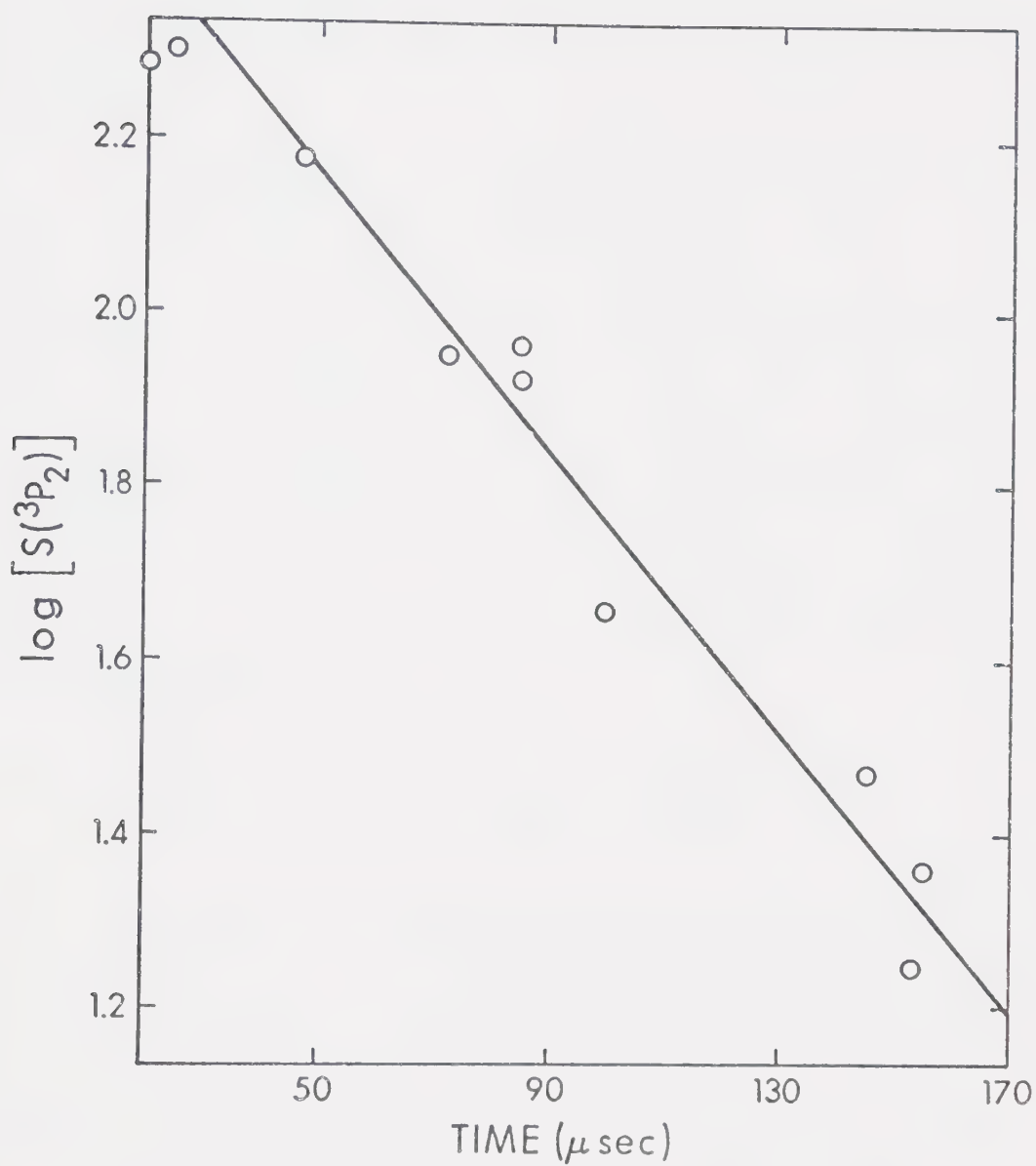


FIGURE VIII-4: First Order Decay Plot of  $S(^3P_2)$  Atoms in the Presence of 1-Butyne.  $P(\text{COS}) = 0.1$  torr,  $P(1\text{-C}_4\text{H}_6) = 0.0922$  torr,  $P(\text{CO}_2) = 200$  torr.



presence of 0.00912 torr 2-C<sub>4</sub>H<sub>6</sub> was  $0.91 \pm 0.06 \times 10^4 \text{ sec}^{-1}$  and the first order rate constant due to reaction with 2-butyne is  $0.80 \times 10^4 \text{ sec}^{-1}$ . The bimolecular rate constant is  $1.6 \pm 0.2 \times 10^{10} \text{ l mole}^{-1} \text{ sec}^{-1}$ . The data are summarized in Table VIII-5 and illustrated in Figure VIII-5.

#### 6. The Bimolecular Rate Constant for the Reaction of S(<sup>3</sup>P) Atoms with 2-Pentyne

From the average observed first order rate constant,  $0.68 \pm 0.12 \times 10^4 \text{ sec}^{-1}$  in the presence of 0.00912 torr 2-C<sub>5</sub>H<sub>8</sub>, the corrected rate constant due to reaction with 2-pentyne is  $0.57 \times 10^4 \text{ sec}^{-1}$  and the bimolecular rate constant is  $1.8 \pm 0.3 \times 10^{10} \text{ l mole}^{-1} \text{ sec}^{-1}$ . The data are summarized in Table VIII-6 and illustrated in Figure VIII-6.

#### 7. The Bimolecular Rate Constant for the Reaction of S(<sup>3</sup>P) Atoms with 2-Perfluorobutyne

Using 0.892 torr 2-C<sub>4</sub>F<sub>6</sub> the average observed first order rate constant was  $1.12 \pm 0.21 \times 10^4 \text{ sec}^{-1}$  and the first order rate constant due to reaction with perfluorobutyne is  $1.01 \times 10^4 \text{ sec}^{-1}$ . The bimolecular rate constant is  $2.1 \pm 0.4 \times 10^8 \text{ l mole}^{-1} \text{ sec}^{-1}$ . The data are summarized in Table VIII-7 and illustrated in Figure VIII-7.

The room temperature rate constants are tabulated in Table VIII-8.



TABLE VIII-5

First Order Decay Rate of  $S(^3P_2)$  Atoms  
in the Presence of 2-Butyne

$CH_3CCCH_3$ (torr)	$CO_2$ (torr)	$COS$ (torr)	$10^{-4}k,$ $sec^{-1}$
0.00912	200	0.1	0.95
0.00912	200	0.1	0.87
average			$0.91 \pm 0.06$



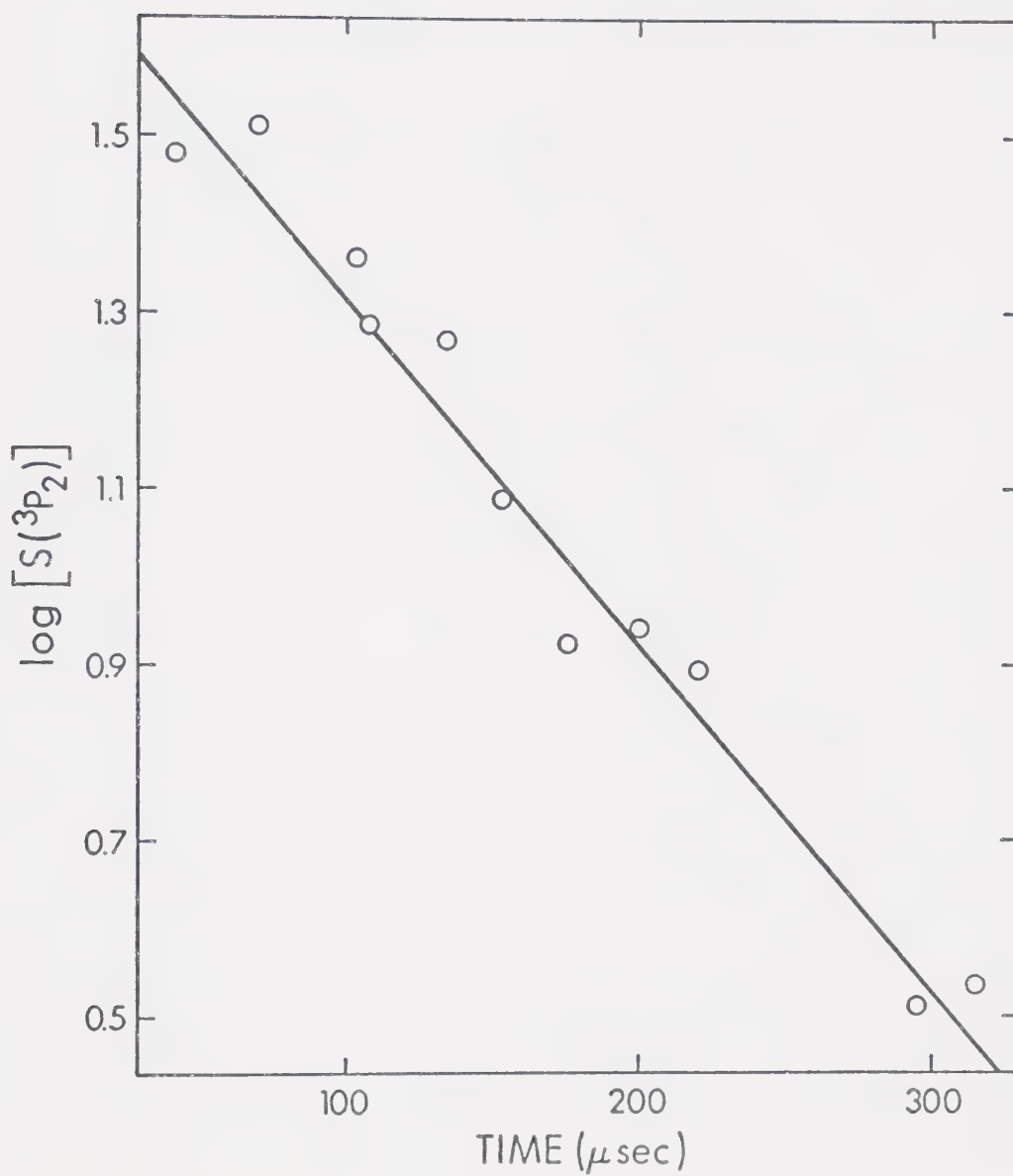


FIGURE VIII-5: First Order Decay Plot of  $S(^3P_2)$  Atom in the Presence of 2-Butyne.  $P(\text{COS}) = 0.1$  torr,  $P(2\text{-C}_4\text{H}_6) = 0.00912$  torr,  $P(\text{CO}_2) = 200$  torr.



TABLE VIII-6

First Order Decay Rate of  $S(^3P_2)$  Atoms  
in the Presence of 2-Pentyne

$2-C_5H_8$ (torr)	$CO_2$ (torr)	$COS$ (torr)	$10^{-4}k,$ $sec^{-1}$
0.00602	200	0.1	0.574
0.00602	200	0.1	0.800
0.00602	200	0.1	0.664
average			$0.679 \pm 0.114$



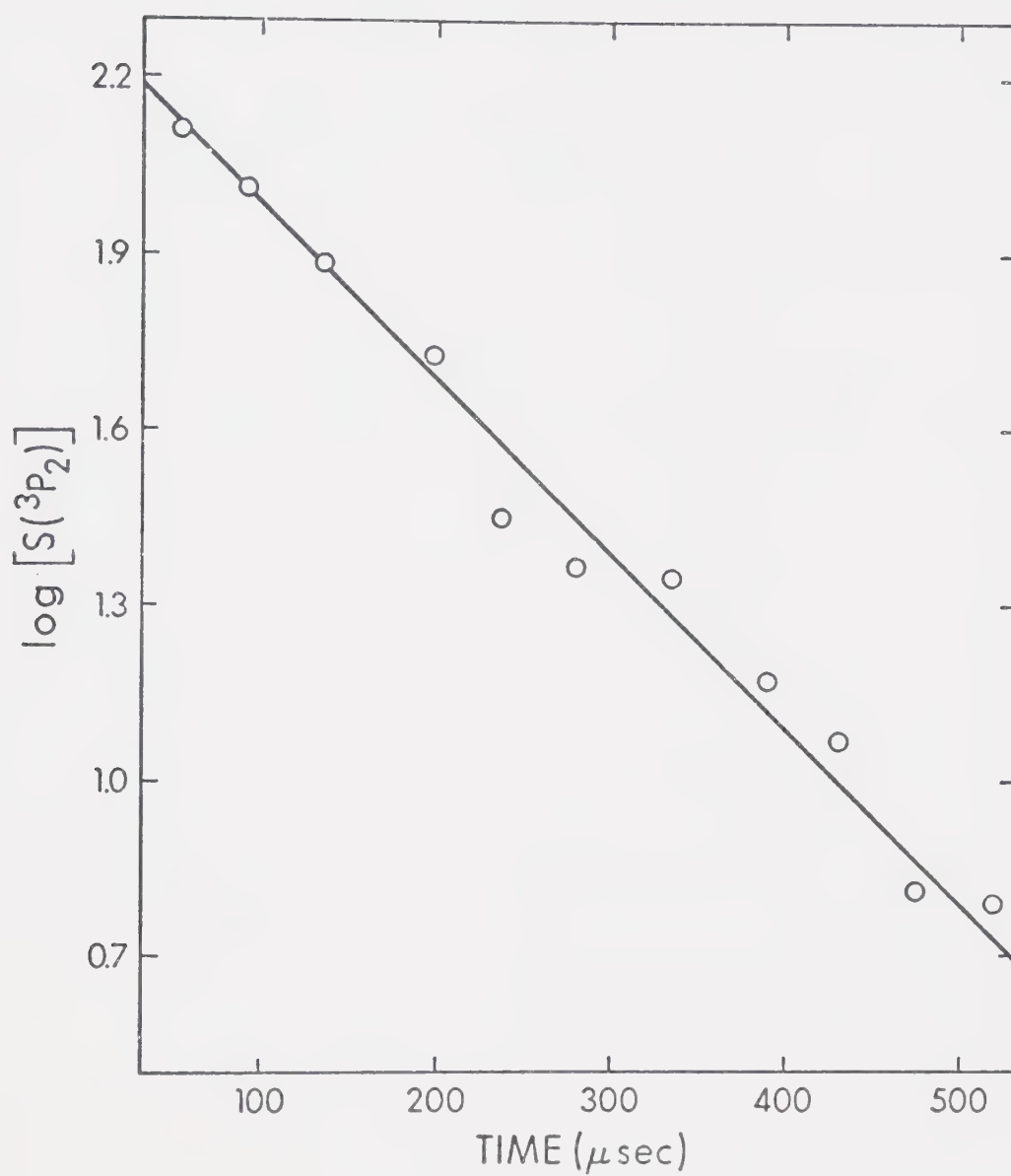


FIGURE VIII-6: First Order Decay Plot of  $S(^3P_2)$  Atoms in the Presence of 2-Pentyne.  $P(\text{COS}) = 0.1$  torr,  $P(2\text{-C}_5\text{H}_8) = 0.00602$  torr,  $P(\text{CO}_2) = 200$  torr.



TABLE VIII-7

First Order Decay Rate of  $S(^3P_2)$  Atoms  
in the Presence of 2-Perfluorobutyne

$CF_3CCCF_3$ (torr)	$CO_2$ (torr)	$COS$ (torr)	$10^{-4}k,$ $sec^{-1}$
0.892	200	0.1	0.91
0.892	200	0.1	1.13
0.733	200	0.1	1.32 <sup>a</sup>
average			1.12 ± 0.21

<sup>a</sup> adjusted to common concentration of 0.892 torr  
for average



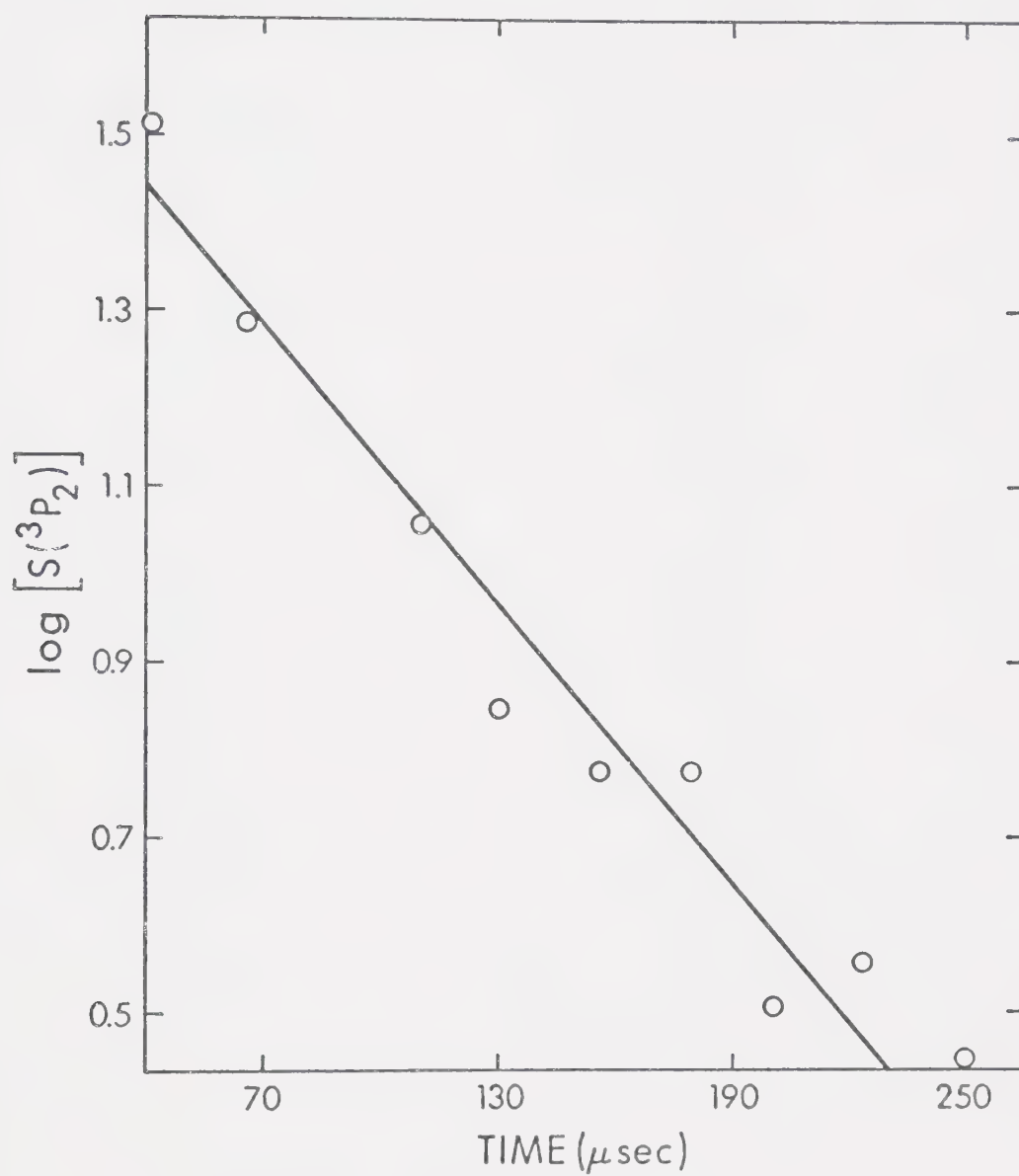


FIGURE VIII-7: First Order Decay Plot of  $S(^3P_2)$  Atoms in the Presence of 2-Butyne- $F_6$ .  $P(COS) = 0.1$  torr,  $P(2-C_4F_6) = 0.892$  torr,  $P(CO_2) = 200$  torr.



TABLE VIII-8

Room Temperature Rate Constants for the Reactions  
of  $S(^3P)$  Atoms with Alkynes

Substrate	$k,$ $1 \text{ mole}^{-1} \text{ sec}^{-1}$
Acetylene	$2.3 \pm 0.5 \times 10^8$
Acetylene- $d_2$	$2.3 \pm 0.3 \times 10^8$
Propyne	$4.8 \pm 0.2 \times 10^9$
1-Butyne	$3.3 \pm 0.2 \times 10^9$
2-Butyne	$1.6 \pm 0.2 \times 10^{10}$
2-Pentyne	$1.8 \pm 0.3 \times 10^{10}$
Perfluorobutyne	$2.1 \pm 0.4 \times 10^8$



## B. Results - Part II

Temperature studies were undertaken to determine the Arrhenius parameters for the reactions of  $S(^3P)$  atoms with acetylene and propyne.

### 1. The Temperature Dependence of the $S(^3P)$ Atom plus Acetylene Reaction

The reaction of  $S(^3P)$  atoms with acetylene was studied in the temperature range  $25^\circ - 211^\circ\text{C}$ . The Arrhenius parameters were determined to be  $E_a = 3.0 \pm 0.4 \text{ kcal mole}^{-1}$  and  $A = 3.4 \pm 1.9 \times 10^{10} \text{ l mole}^{-1} \text{ sec}^{-1}$ . The data are summarized in Table VIII-9 and illustrated in Figure VIII-8.

### 2. The Temperature Dependence of $S(^3P)$ Atoms plus Propyne

For the reaction of  $S(^3P)$  atom with propyne in the temperature range  $25 - 177^\circ\text{C}$ , the Arrhenius parameters are  $E_a = 0.9 \pm 0.2 \text{ kcal mole}^{-1}$  and  $A = 2.0 \pm 1.4 \times 10^{10} \text{ l mole}^{-1} \text{ sec}^{-1}$ . The data are summarized in Table VIII-10 and illustrated in Figure VIII-8. The decay rates of  $S(^3P_1)$  atoms were also monitored in order to check the accuracy of the results, and were found to be consistent with the  $S(^3P_2)$  atom data as shown in Figure VIII-8 and Table VIII-10.



TABLE VIII-9

Temperature Dependence of the Reaction of  
 $S(^3P)$  Atoms with Acetylene

Temperature (°K)	$k$ , $l \text{ mole}^{-1} \text{ sec}$	$\log k$
298	$2.3 \times 10^8$	8.36
389	$6.0 \times 10^8$	8.78
450	$1.0 \times 10^9$	9.00
484	$1.9 \times 10^9$	9.28



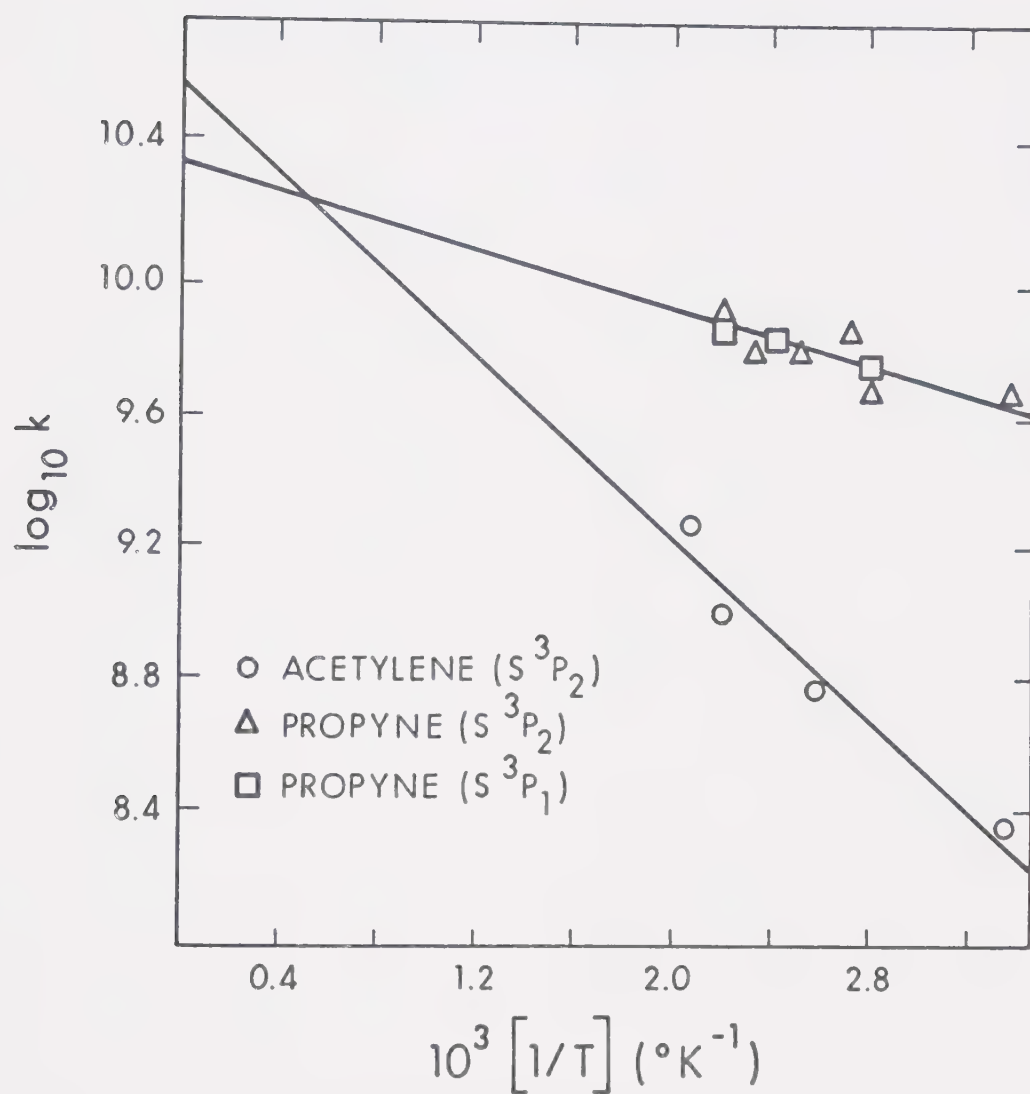


FIGURE VIII-8: Arrhenius Plot showing Temperature Dependence of the Reaction of  $S(^3P)$  with Acetylene and Propyne.



TABLE VIII-10

Temperature Dependence of the Reaction of  $S(^3P)$ 

Atoms with Propyne

Species	Temperature	$k,$ $l \text{ mole}^{-1} \text{ sec}^{-1}$	$\log k$
$S(^3P_2)$	298	$4.8 \times 10^9$	9.68
$S(^3P_2)$	358	$4.8 \times 10^9$	9.68
$S(^3P_1)$	358	$5.9 \times 10^9$	9.77
$S(^3P_2)$	368	$7.3 \times 10^9$	9.86
$S(^3P_2)$	398	$6.3 \times 10^9$	9.80
$S(^3P_1)$	414	$7.1 \times 10^9$	9.85
$S(^3P_2)$	428	$6.3 \times 10^9$	9.80
$S(^3P_1)$	449	$7.3 \times 10^9$	9.87
$S(^3P_2)$	449	$8.5 \times 10^9$	9.93



## C. Discussion

In evaluating the experimental rate constants for the S+ olefin systems, Chapter VII, it was shown that possible complications arising from photolysis of the substrate or secondary reactions between S-atoms and products were absent. It is assumed that the same conditions hold for the S + alkyne system, since:

1. An OH-C<sub>2</sub>H<sub>2</sub><sup>147</sup> system was studied by flash photolysis-resonance fluorescence with flash energies up to 500 joules and utilizing LiF windows, it was concluded that the extent of photolysis of C<sub>2</sub>H<sub>2</sub> was less than 1%. Thus, in the present system, using quartz optics, decomposition of C<sub>2</sub>H<sub>2</sub> is negligible.

2. The only retrievable product in the S + acetylene system is thiophene, which is formed in low yield, the bulk of the product ending up as a solid polymer<sup>11</sup>. Therefore, S atoms cannot decay via reaction with product.

The measured bimolecular rate constants can therefore be attributed solely to the rate of addition of sulfur atoms to alkynes.

Absolute rate constants, preexponential factors and activation energies for S + alkyne reactions are summarized in Table VIII-11 along with relative rate data obtained by competitive techniques in conventional experiments. Data for analogous oxygen atom reactions are also included for comparison.



TABLE VIII-11

Absolute Rate Data for the Reaction of  $S(^3P)$  and  $O(^3P)$  Atoms with Acetylenes

Substrate	$S(^3P)$					$O(^3P)$		
	k	$E_a$	A	Rel. Data		k	$E_a$	A
				$E_a$	$-E_a$			
				$C_2H_2$	$A/A$	$C_2H_2$		
Acetylene	$2.3 \times 10^8$ <sup>a</sup>	3.0 <sup>a</sup>	$3.4 \times 10^{10}$ <sup>a</sup>	0 <sup>a</sup>	1 <sup>a</sup>	$7.9 \times 10^7$ <sup>d</sup>		
	$3.0 \times 10^8$ <sup>b</sup>			0 <sup>c</sup>	1 <sup>c</sup>		3.0 <sup>f</sup>	$1.4 \times 10^{10}$ <sup>f</sup>
Acetylene- $d_2$	$2.3 \times 10^8$ <sup>a</sup>					$7.9 \times 10^7$ <sup>d</sup>		
Propyne	$4.8 \times 10^9$ <sup>a</sup>	0.9 <sup>a</sup>	$2.0 \times 10^{10}$ <sup>a</sup>	2.1 <sup>a</sup>	0.59 <sup>a</sup>	$4 \times 10^8$ <sup>e</sup>		
				1.14 <sup>c</sup>	1 <sup>c</sup>		1.95 <sup>g</sup>	$1.4 \times 10^{10}$ <sup>g</sup>
1-Butyne	$3.3 \times 10^9$ <sup>a</sup>							
2-Butyne	$1.6 \times 10^{10}$ <sup>a</sup>			$\sim 3.2$ <sup>a</sup>				
				3.35 <sup>c</sup>		0.44 <sup>c</sup>		
2-Pentyne	$1.8 \times 10^{10}$ <sup>a</sup>							
2-Butyne- $F_6$	$2.1 \times 10^8$ <sup>a</sup>							

a) this work  
 b) ref. 39  
 c) ref. 28  
 d) ref. 49

e) ref. 42  
 f) ref. 148  
 g) ref. 58

NOTE: k and A =  $1 \text{ mole}^{-1} \text{ sec}^{-1}$   
 $E_a$  = kcal  $\text{mole}^{-1}$



For the  $S + C_2H_2$  reaction, our rate constant of  $2.3 \pm 0.5 \times 10^8 \text{ l mole}^{-1} \text{ sec}^{-1}$  is in excellent agreement with Little and Donovan's published value<sup>39</sup> of  $3.0 \pm 0.3 \times 10^8 \text{ l mole}^{-1} \text{ sec}^{-1}$  obtained by a similar technique. The authors showed that the rate of decay of sulfur atoms is first order in acetylene.

The activation energy for the reaction with propyne is considerably less than that with acetylene, in keeping with the electrophilic character of sulfur atoms. From a plot of Ionization potential versus  $E_a$ , Figure VIII-9, it appears that  $E_a \sim 0$  for the  $S + 2$ -butyne reaction. Relative activation energies<sup>28</sup> also follow the same trend with the exception of that for propyne (Table VIII-11). It is interesting that  $E_a$  for the  $S + C_2H_2$  reaction,  $3.0 \text{ kcal mole}^{-1}$ , is twice as high as that for the  $S + C_2H_4$  reaction which is only  $1.5 \text{ kcal mole}^{-1}$ . This may be due to a higher potential barrier in curve crossing from the separated reactants to products.

This high activation energy is partially compensated for, in the overall rate, by a greatly increased A-factor. Radical additions to alkynes generally feature high A-factors and Szwarc<sup>149</sup> has qualitatively attributed this to a gain in entropy in going from a linear molecule to a non-linear activated complex. The entropy of activation for the  $S + C_2H_2$  reaction is  $-14.3 \text{ e.u.}$  (standard state =  $1 \text{ mole/liter}$ ). The translational and vibrational contributions to activation entropy for the  $S + C_2H_2$  and  $S + C_2H_4$  reactions are virtually the same, but the rotational contribution in the  $C_2H_2$  system is 3.3 times higher than in the  $C_2H_4$  case. Since  $A_{C_2H_2}/A_{C_2H_4} \sim 3$  it can be concluded



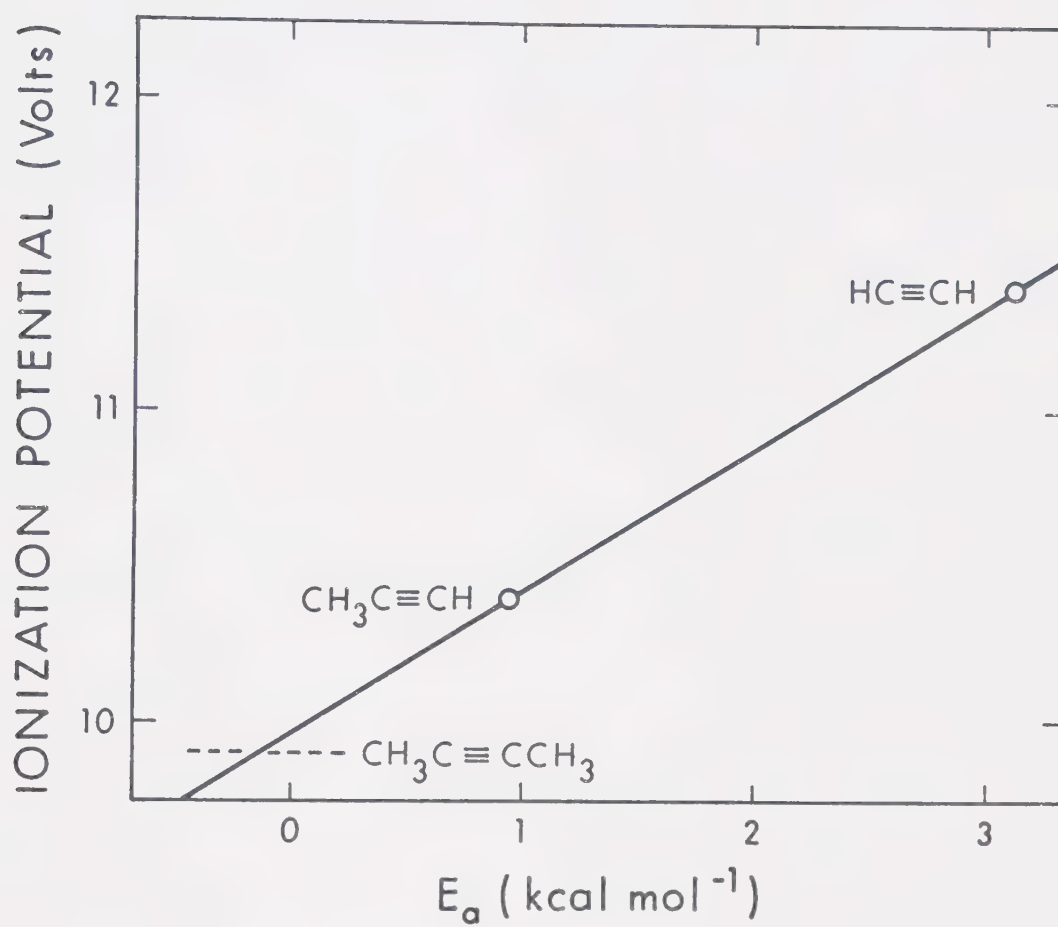


FIGURE VIII-9: Empirical Plot of Ionization Potential versus Arrhenius Activation Energy.



that the increase in the A factor in the  $C_2H_2$  system is largely a consequence of an increase in the number of rotational modes in the activated complex.

A kinetic isotope effect of unity was observed in the  $S + C_2D_2$  system, and in the analogous  $O + C_2D_2$  system<sup>49</sup>. The effect of isotopic substitution can frequently provide valuable kinetic-mechanistic information on the types of reaction undergone by a molecule. Fortunately, the replacement of an atom in a molecule by its isotope does not cause a change in the potential energy surfaces of a given reaction. If the bond of the substituted atom is not directly involved in the reaction, the isotope effect is termed as secondary.

The rate constant of a reaction, as derived from Absolute Rate Theory, can be described by the expression

$$k_R = \chi \frac{kT}{h} \frac{Q^\ddagger}{Q} e^{-E_a/R_t}$$

where  $\chi$  is the transmission coefficient,  $Q^\ddagger$  is the partition function of the activated complex,  $Q$  is the partition function of the reactant and  $E_a$  is the activation energy of the reaction. The other terms have their usual significance.

Separating the partition function  $Q$  into its translational, rotational, and vibrational components, the expression as developed by Bigeleisen<sup>150</sup> for the rate constant ratio of the isotopically substituted molecule relative to the unsubstituted molecule can be written as:



$$\frac{k_1}{k_2} = \left[ \frac{\left( \frac{I_{A_2} I_{B_2} I_{C_2}}{I_{A_1} I_{B_1} I_{C_1}} \right)^{\frac{1}{2}} \left( \frac{M_2}{M_1} \right)^{\frac{3}{2}}}{\left( \frac{I_{A_2}^\ddagger I_{B_2}^\ddagger I_{C_2}^\ddagger}{I_{A_1}^\ddagger I_{B_1}^\ddagger I_{C_1}^\ddagger} \right)^{\frac{1}{2}} \left( \frac{M_2^\ddagger}{M_1^\ddagger} \right)^{\frac{3}{2}}} \right] \times$$

$$\left[ \frac{\frac{3N-6}{\prod i} \left[ \frac{1 - \exp(-u_{1i})}{1 - \exp(-u_{2i})} \right]}{\frac{3N^\ddagger-7}{\prod i} \left[ \frac{1 - \exp(-u_{1i}^\ddagger)}{1 - \exp(-u_{2i}^\ddagger)} \right]} \right] \times$$

$$\left[ \frac{\exp \left[ \frac{3N-6}{\sum_i} (u_{1i} - u_{2i})/2 \right]}{\exp \left[ \frac{3N^\ddagger-7}{\sum_i} (u_{1i}^\ddagger - u_{2i}^\ddagger)/2 \right]} \right]$$

where  $I$  is the principal moment of inertia,  $M$  is the molecular mass,  $u_i = hc\omega_i/kT$  where  $\omega_i$  is a normal vibrational frequency and  $^\ddagger$  refers to the activated complex.

This equation can be expressed in an abbreviated form as

$$\frac{k_1}{k_2} = (\text{MMI}) \times (\text{EXC}) \times (\text{ZPE})$$

where MMI represents the translational and rotational energy contributions, EXC the vibrational energy and ZPE the zero point energy contributions.



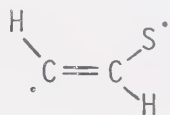
Approximations for the activated complex structure by comparison with stable molecules may be applied and modified as dictated by comparison with experimental results. Agreement does not mean that the postulated model is correct but simply that it is a possible model. Conversely, lack of agreement would suggest that the model used is unreasonable.

Due to the many small factors affecting the overall isotope effect, the evaluation should be as complete as possible. Oversimplification can lead to serious misinterpretation of the factors controlling a given isotopic effect. Thus, the simplified form of the equation proposed by Streitweiser<sup>151</sup>, in which the translational, rotational, and vibrational excitation contributions are neglected and the isotope effect supposedly originates only from the zero point energy differences, properly predicts an inverse secondary isotope effect for addition to a double bond, but suggests that the isotope effect arises from the change of the frequencies of the out-of-plane CH bending modes. However, a recently published<sup>152</sup> calculation of the kinetic isotope effect in the  $S + C_2D_4$  system demonstrates that the most important single factor contributing to the secondary isotope effect is the net gain in the number of isotope-sensitive vibrational normal modes during passage from the reactants to the activated complex.

The first step in the method is to assume a reasonable geometrical model for the transition states, then to assign normal

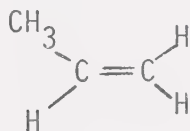


vibrational frequencies to all the modes. The transition state for the  $S + C_2H_2$  reaction is assumed to be a planar biradical with the two hydrogens in *trans* position:



This assumption is supported by the stereospecific *trans* addition of HBr to  $C_2H_2$  in the gas phase<sup>153</sup> and by the fact that the lowest electronically excited state of acetylene is *trans*<sup>154</sup>.

Acetylene has  $3 \times 4 - 5 = 7$ , whereas the activated complex has  $3 \times 5 - 6 = 9$  normal vibrational frequencies. The two new frequencies in the activated complex, C-S stretching and C-C-S bending, are not sensitive to deuterium substitution and therefore do not generate isotopic effects. The isotope effect is thus probably due to changes in the acetylene frequencies on going over to the transition state. Assignment of vibrational frequencies in the activated complex can be done on the basis of the corresponding frequencies in propylene,




by following the same trends upon changing from  $sp$  to  $sp^2$  hybridization, i.e. the stretching frequencies decrease and the bending frequencies increase. They are listed in Table VIII-12.



TABLE VIII-12

Summary of Data for Isotope Effect Calculation

Frequency	Acetylene	Propylene		EXC	ZPE
C-C stretch	1974	1647	1750	0.998	1.125
C-H stretch	3289	3012	3200	1.000	1.034
C-H bend	612	936	730	1.013	0.822
C-H bend	729	1287	950	1.908	0.871
				1.019	0.832

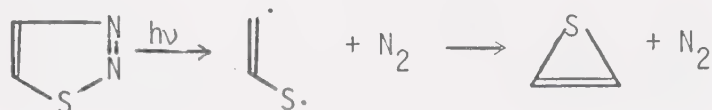
$$\text{MMI} \times \text{EXC} \times \text{ZPE} = 1.177 \times 1.019 \times 0.832 = 0.998$$



The MMI factor in the expression for  $k_H/k_D$  is 1.177 and from the EXC and ZPE contributions (cf. Table VIII-12)  $k_H/k_D = 0.998$ , which correctly reproduces the observed isotope effect.

Additional information with regard to the primary step is supplied by *ab initio* molecular orbital calculations on thiirene and five of its isomers<sup>155</sup>, which indicate that the  $S(^3P) + C_2H_2$  reaction surface correlates with the lowest triplet excited states of thiirene and thioacetylene which lie at unattainably high energies. These results are illustrated in Figure VIII-10 with those for the  $S(^1D_2) + C_2H_2$  system. Therefore, the triplet biradical may undergo a collisionally induced transition to a lower energy state, possibly the thioketene or singlet thiirene, or may undergo polymerization via reaction with acetylene.

In the  $S(^3P) + C_2H_2$  reaction, thiirene may form via ring closure in the  $\cdot HC=CHS\cdot$  biradical. An analogous situation exists in the photolysis of 1,2,3-thiadiazoles<sup>37</sup>, where direct experimental evidence for the intermediacy of thiirene is more conclusive.



Photolysis of either the 4-methyl or 5-methyl derivative in the presence of hexafluoro-2-butyne always yields only one thiophene adduct, with the methyl substituent in the 1 position, indicating preferential addition across the less hindered S-CH bond. Photolysis of thiadiazole itself yields thioketene and thioacetylene,



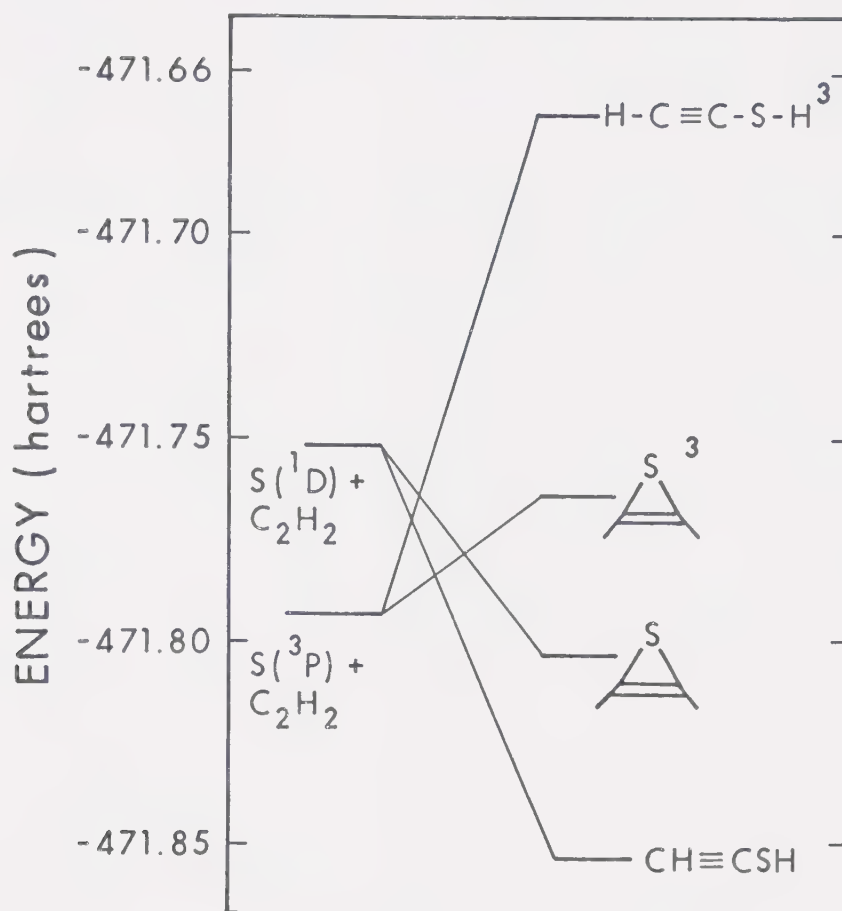
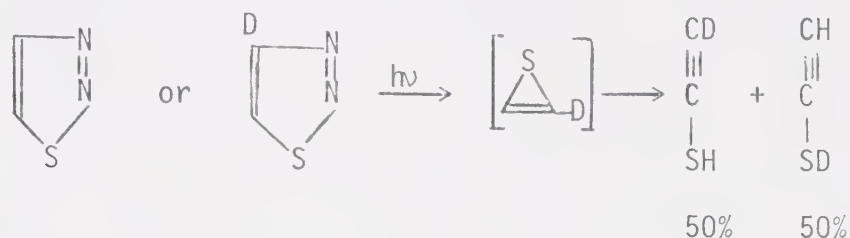


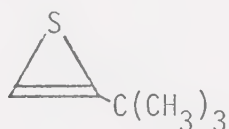
FIGURE VIII-10: State Correlation Diagram for the lowest Singlet and Triplet States of Thiirene.



and deuterium labelling in the 4 and 5 positions gave the following distribution in the thioacetylene product:



The 1:1 ratio of these products is consistent with indiscriminate C-S ring opening in thiirene but not with a  $\cdot\text{DC}=\text{HCS}\cdot$  or  $\cdot\text{HC}=\text{CDS}\cdot$  intermediate. Additional evidence for the intermediacy of thiirene in these systems has been recently reported<sup>156</sup> in the matrix photolysis of 5-*t*-butyl-1,2,3-thiadiazole where a new ir absorption was observed which could not be ascribed to either a thioacetylene or a thioketene structure. The absorption frequencies are very close to those expected for the substituted thiirene,




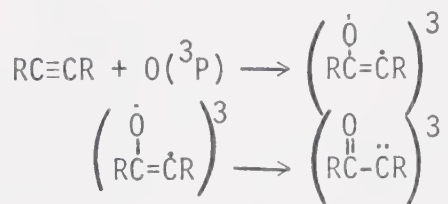
It is believed that the bulky *t*-butyl group confers extra stability to thiirene and consequently enhances its lifetime. The thioketene formed in these experiments may be formed from thiirene or from the  $\cdot\text{CH}=\text{CHS}\cdot$  biradical. Thioacetylene is not a product in thermolysis and therefore the





isomerization must take place on an excited singlet state surface.

The absolute rates of reaction of  $O(^3P)$  atoms<sup>42,49,58,148</sup> with acetylene and propyne are, not unexpectedly, very similar to those of  $S(^3P)$  atoms (cf. Table VIII-11). Generally, the  $O(^3P)$  systems are characterized by much less polymerization and higher product yields. In matrix isolation studies of the  $O(^3P) + C_2H_2$  reaction<sup>157</sup> the spectrum of ketene was observed and there were no absorptions which could be assigned to oxirene, . The  $O(^3P) +$  propyne, 2-butyne and 2-pentyne<sup>67</sup> systems have been extensively studied and from the pressure dependence of the major products, CO, alkenes and ketones, it was concluded that the primary adduct is a triplet biradical which readily isomerizes to a more stable ketocarbene structure,



and that oxirene is definitely not an intermediate. On the other hand, it has been conclusively demonstrated that the photolytic Wolff rearrangement of ketocarbenes to ketene<sup>156</sup> involves oxirene intermediates and that triplet or vibrationally excited ground state ketocarbenes do not isomerize to oxirene.



## CHAPTER IX

## SUMMARY AND CONCLUSIONS

It has been shown that  $S(^1D)$  atoms generated by the photolysis of carbonyl sulfide in its longest wavelength absorption band are rapidly deactivated to the ground triplet state. Within the microsecond time scales employed in this study, the metastable  $^3P_2$ ,  $^3P_1$  and  $^3P_0$  components are in thermal equilibrium and therefore absolute rate constants can be determined by monitoring either the  $^3P_2 \longrightarrow ^3S_1$ ,  $^3P_1 \longrightarrow ^3S_1$  or  $^3P_0 \longrightarrow ^3S_1$  absorption intensities by time resolved kinetic absorption spectroscopy. At the very low COS concentrations used in this study, the rate of decay of S atoms is slow and it appears that the major mode of decay is via reaction with  $S_2$ ,  $S_3$  etc. species present in the system.

The absolute rate constant for the reaction of  $S(^3P)$  atoms with molecular oxygen was found to be  $1.7 \pm 0.2 \times 10^9$   $\text{l mole}^{-1} \text{sec}^{-1}$ , independent of total pressure. The observation of the  $B^3\Sigma^- \longleftarrow X^3\Sigma^-$  and  $D^3\Pi \longleftarrow X^3\Sigma^-$  transitions of SO indicate that the primary step is  $S(^3P) + O_2(^3\Sigma_g^-) \longrightarrow O(^3P) + SO(^3\Sigma^-)$ .

In the  $S(^3P) + NO$  reaction, the second order rate constant is pressure dependent. Using a Lindemann-Hinshelwood plot, the third order rate constant was determined to be  $1.9 \pm 0.1 \times 10^{11} \text{l}^2 \text{mole}^{-2} \text{sec}^{-1}$  and the high pressure limit,  $9.3 \pm 2.1 \times 10^9$   $\text{l mole}^{-1} \text{sec}^{-1}$ . The high efficiency of this reaction was shown to



be of a comparable order of magnitude with other atomic and radical additions to NO. The observed kinetics have been shown to be consistent with an energy transfer mechanism,



The lifetime of  $SNO^*$  was estimated to be  $\sim 10^{-10}$  sec.

The rates of reaction of  $S(^3P)$  atoms with ethylene, propylene and *trans*-2-butene episulfides are  $1.4 \pm 0.2 \times 10^{10}$ ,  $2.7 \pm 0.3 \times 10^{10}$  and  $4.0 \pm 0.2 \times 10^{10}$  l mole<sup>-1</sup> sec<sup>-1</sup> respectively and the activation energies are close to or equal to zero. These high rates are found to be consistent with the low potential energy barrier of activation predicted by EHMO calculations.

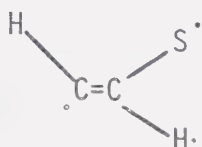
The trends in the rates of reaction of  $S(^3P)$  atoms with olefins clearly demonstrate the electrophilic character of  $S(^3P)$  atoms, first reported in relative rate studies. Furthermore, the temperature dependence of the rate constants shows a surprising trend to negative activation energies with increased alkyl substitution. This is qualitatively rationalized in terms of potential energy curve crossings, where the position of the crossing relative to the energy of the separated reactants determines the temperature dependence of the reaction.

The results of the  $S(^3P) +$  alkyne systems demonstrate the same general features as the olefin study. The activation energies for addition to alkynes are somewhat higher than those



to the olefin counterparts. It appears that reaction with 2-butyne would not exhibit a significant negative temperature dependence.

The enhanced A factor in the acetylene reaction as compared to the ethylene case has been shown to be consistent with a higher number of rotational modes in the  $C_2H_2S$  adduct relative to the acetylene molecule. The absolute rate of addition to  $C_2D_2$  is the same as that to  $C_2H_2$ . If the activated complex is assumed to be a *trans* diradical, i.e.



then the normal frequencies of the complex can be estimated by comparison with those of propylene, and insertion into the Bigeleisen equation for  $k_H/k_D$  correctly reproduces the experimental value of 1.0.

The results presented in this study provide a most useful extension to conventional studies of the chemistry of  $S(^3P)$  atoms and allow the calculation of other absolute rate constants from relative rate data. The technique is relatively simple and accurate and its scope can be broadened to cover a wide variety of substrates. Of special interest are desulfurization reactions since they are important in a number of industrial processes. The technique could also be extended to the photolysis of other sulfur-containing compounds where  $S(^3P)$  atoms are believed to be involved in the mechanism.



## BIBLIOGRAPHY

1. A.H. Laufer and A.M. Bass, J. Phys. Chem., 78, 1344 (1974).
2. W. Braun, A.M. Bass and M. Pilling, J. Chem. Phys., 52, 5131 (1970).
3. W. Kirmse, "Carbene Chemistry", 2nd ed., Academic Press, New York, N.Y. (1971).
4. H.M. Frey, Progr. React. Kinet., 2, 131 (1964).
5. R.J. Cvetanovic, Advan. Photochem., 1, 115 (1963).
6. O.P. Strausz and H.E. Gunning, J. Am. Chem. Soc., 84, 4080 (1962).
7. C. Chandler, Atomic Spectra, Hilger and Watts Ltd., London (1964).
8. H.E. Gunning, O.P. Strausz, R.J. Donovan and M. de Sorigo, Ber. Bunsenges. Phys. Chem., 72, 253 (1968).
9. A.B. Callear, Proc. Roy. Soc. Ser. A, 276, 401 (1963).
10. R.J. Donovan, D. Husain, R.W. Fair, O.P. Strausz and H.E. Gunning, Trans. Faraday Soc., 66, 1635 (1970).
11. E.L. Dedio, Ph.D. Thesis, University of Alberta, Edmonton, Alberta (1967).
12. P. Fowles, M. De Sorigo, A.J. Yarwood, O.P. Strausz and H.E. Gunning, J. Am. Chem. Soc., 89, 1352 (1967).
13. A. Jackson, K.S. Sidhu, A. Jodhan, E.M. Lown and O.P. Strausz, to be published.
14. H.E. Gunning and O.P. Strausz, Advan. Photochem., 4, 143 (1966).



15. W. Breckenridge and H. Taube, *J. Chem. Phys.*, 52, 1713 (1970).
16. K.S. Sidhu, I.G. Csizmadia, O.P. Strausz and H.E. Gunning, *J. Am. Chem. Soc.*, 88, 2412 (1966).
17. W.D. McGrath, J.J. McGarvey and D.M. Dempster, *Can. J. Chem.*, 46, 2454 (1967).
18. I. Safarik and O.P. Strausz, Private Communication.
19. E. Jakubowski, M.G. Ahmed, E.M. Lown, H.S. Sandhu, R.K. Gosavi and O.P. Strausz, *J. Am. Chem. Soc.*, 94, 4094 (1972).
20. N. Basco and A.E. Pearson, *Trans. Faraday Soc.*, 63, 2684 (1967).
21. R.J. Donovan, L.J. Kirsch and D. Husain, *Nature*, 222, 1164 (1969).
22. O.P. Strausz, *Organosulfur Chemistry*, M.J. Jansen, ed., Interscience, N.Y., 1967, p. 11.
23. R.J. Donovan, L.J. Kirsch and D. Husain, *Trans. Faraday Soc.*, 66, 774 (1970).
24. R.J. Donovan, *Trans. Faraday Soc.*, 65, 1419 (1969).
25. J.W. Rabalais, J.M. McDonald, V. Schen and S.P. Glynn, *Chem. Revs.*, 71, 73 (1971).
26. O.J. Dunn, S.V. Filseth and R.A. Young, *J. Chem. Phys.*, 59, 2892 (1973).
27. K. Gollnick and E. Lippin, *J. Am. Chem. Soc.*, 92, 2217 (1970).
28. W.B. O'Callaghan, Ph.D. Thesis, University of Alberta, Edmonton, Alberta (1970).
29. O.P. Strausz, I. Safarik, W.B. O'Callaghan and H.E. Gunning, *J. Am. Chem. Soc.*, 94, 1828 (1972).



30. a) O.P. Strausz, H.E. Gunning, A.S. Denes and I.G. Csizmadia,  
J. Am. Chem. Soc., 94, 8317 (1972).  
b) O.P. Strausz, R.K. Gosavi, A.S. Denes and I.G. Csizmadia,  
Theoret. Chim. Acta. (Berl.), 26, 367 (1972).
31. M.M. Rohmer and B. Ross, J. Am. Chem. Soc. 97, 2025, 1975.
32. R. Hoffmann, C.C. Wan and V. Neagu, Mol. Phys., 19, 113 (1970).
33. I.A. Lawrence, I. Schaad, J.R. van Wazer, Theoret. Chim.  
Acta. (Berl.), 29, 173 (1973).
34. O.P. Strausz and H.E. Gunning, in The Chemistry of Sulfides,  
A.V. Tobolsky, ed., Interscience, New York, 1968.
35. O.P. Strausz, Pure and Applied Chemistry, 4, 165 (1971).
36. O.P. Strausz, J. Font, E.L. Dedio, P. Kebarle and H.E.  
Gunning, J. Am. Chem. Soc., 89, 4805 (1967).
37. O.P. Strausz, Sulfur Research Trends, R.F. Gould, ed.,  
Am. Chem. Soc., Washington, D.C. (1971).
38. D.J. Little, A. Dalglish and R.J. Donovan, Faraday Discuss.  
Chem. Soc., 53, 211 (1972).
39. D.J. Little and R.J. Donovan, J. of Photochem., 1, 371 (1972/3).
40. L. Elias and H.I. Schiff, Can. J. Chem., 38, 1657 (1960).
41. L. Elias, J. Chem. Phys., 38, 989 (1963).
42. J. M. Brown and B.A. Thrush, Trans. Faraday Soc., 63, 630 (1967).
43. I.W.M. Smith, Trans. Faraday Soc., 64, 378 (1968).
44. C. Tanaka, S. Tsuchiya and T. Hikita, J. Fac. Eng. Univ. Tokyo,  
Ser A, 5, 62 (1967).
45. H. Niki, E.E. Doby and B. Weinstock, Symp. (Int.) Combust.  
[Proc.] 12th, 277 (1969).



46. A.A. Westenberg and N. de Haas, Symp. (Int.) Combust. [Proc.] 12th, 289 (1969).
47. R. Atkinson and R.J. Cvetanovic, J. Chem. Phys., 55, 659 (1971).
48. R. Atkinson and R.J. Cvetanovic, J. Chem. Phys., 56, 432 (1972).
49. F. Stuhl and H. Niki, J. Chem. Phys., 55, 3954 (1971).
50. F. Stuhl and H. Niki, J. Chem. Phys., 57, 5403 (1972).
51. D.D. Davis, R.E. Huie, J.T. Herron, M.J. Kurylo and W. Braun, J. Chem. Phys., 56, 4868 (1972).
52. M.J. Kurylo, Chem. Phys. Letters, 14, 117 (1972).
53. R.E. Huie, J.T. Herron and D.D. Davis, J. Phys. Chem., 75, 3902 (1971).
54. D.D. Davis, R.E. Huie and J.T. Herron, J. Chem. Phys., 59, 628 (1973).
55. S. Furuyama, R. Atkinson, A.J. Collussi, R.J. Cvetanovic, Int. J. Chem. Kinet., 6, 741 (1974).
56. M.J. Kurylo and R.E. Huie, J. Chem. Phys., 58, 1258 (1973).
57. D.L. Singleton, S. Furuyama, R.J. Cvetanovic and R.S. Irwin, J. Chem. Phys., 63, 1003 (1975).
58. C.A. Arrington Jr. and D.J. Cox, J. Phys. Chem., 79, 2584 (1975).
59. R. Atkinson and J.N. Pitts Jr., J. Phys. Chem., 78, 1780 (1974).
60. R.J. Cvetanovic, J. Chem. Phys., 15, 376 (1956).



61. R.J. Cvetanovic, J. Chem. Phys., 30, 19 (1959).
62. M.D. Scheer and R. Klein, J. Phys. Chem., 73, 597 (1969).
63. R. Klein and M.D. Scheer, J. Phys. Chem., 73, 1598 (1969).
64. R. Klein and M.D. Scheer, J. Phys. Chem. 74, 613 (1970).
65. M.D. Scheer and R. Klein, J. Phys. Chem., 74, 2733 (1970).
66. M.A. Robb, R.K. Gosavi, I.G. Csizmadia and O.P. Strausz, to be published.
67. K. Ogi and O.P. Strausz, to be published.
68. D.C. Williamson and K.D. Bayes, J. Phys. Chem., 73, 1232 (1969).
69. A.A. Westenberg and N. De Haas, J. Phys. Chem., 73, 1181 (1969).
70. K. Hoyer mann, H.G. Wagner and J. Wolfman, Z. Phys. Chem. (Frankfurt), 63, 193 (1969).
71. A.B. Callear and W.J.R. Tyerman, Trans. Faraday Soc., 62, 371 (1966).
72. A.B. Callear and W.J.R. Tyerman, Trans. Faraday Soc., 62, 2760 (1966).
73. D.A. Styles, W.J.R. Tyerman, O.P. Strausz and H.E. Gunning, Can. J. Chem., 44, 2149 (1966).
74. W.J.R. Tyerman, W.B. O'Callaghan, P. Kebarle, O.P. Strausz and H.E. Gunning, J. Am. Chem. Soc., 88, 4277 (1966).
75. J. Connor, G. Greig and O.P. Strausz, J. Am. Chem. Soc., 91, 5695 (1969).
76. J. Connor, A. van Roodselaar, R.W. Fair, O.P. Strausz, J. Am. Chem. Soc., 93, 560 (1971).



77. R.G.W. Norrish and G. Porter, *Nature*, 164, 658 (1949).
78. C. Porter, *Proc. Roy. Soc. Ser. A* 200, 284, (1950).
79. J.U. White, *J. Opt. Soc. Am.*, 32, 285 (1942).
80. C. Herzberg and D.A. Ramsay, *Discuss. Faraday Soc.*, 9, 80 (1950).
81. N. Davidson, R. Marshall, A.E. Larsh and T. Carrington, *J. Chem. Phys.*, 19, 1311 (1951).
82. D.S. McClure and P.L. Hurst, *J. Chem. Phys.*, 23, 1772 (1955).
83. J.K.K. Ip and G. Burns, *Discuss. Faraday Soc.*, 44, 241 (1967).
84. L.S. Nikon, *J. Opt. Soc. Am.*, 46, 768 (1956).
85. B.A. Thrush, *Proc. Roy. Soc. Ser. A*, 245, 555 (1958).
86. F.W. Willets, *Progress in Reaction Kinetics*, 6, 52 (1972).
87. J.W. Boag, *Photochem. and Photobiol.*, 8, 565 (1968).
88. G. Porter, *Technique of Organic Chemistry*, Vol. VIII, part II, p. 1055, Interscience, London (1963).
89. T.A. Gover and G. Porter, *Proc. Roy. Soc. Ser. A*, 262, 476 (1961).
90. G. Porter and M.R. Topp, *Proc. Nobel Symposium*, 5, 158 (1967).
91. P.M. Rentzepis, *Chem. Phys. Letters*, 2, 117 (1968); *Photochem and Photobiol.*, 8, 579 (1968).
92. R.W. Fair and B.A. Thrush, *Trans. Faraday Soc.*, 65, 1559 (1969).
93. K.H. Homann, G. Krome and H. Ge. Wagner, *Ber. Bunsenges. Phys. Chem.*, 72, 998 (1968).
94. F.C. Bordwell and H.M. Anderson, *J. Am. Chem. Soc.*, 75, 4959 (1953).



95. W.H. Carrothers and J. van Natta, J. Am. Chem. Soc., 52, 314 (1930).
96. S. Searles and E.F. Lutz, J. Am. Chem. Soc., 80, 3168 (1958).
97. Z. Gyulai, Z. fur Physik., 46, 80 (1927).
98. H.A. Wiebe, A.R. Knight, O.P. Strausz and H.E. Gunning, J. Am. Chem. Soc., 87, 1443 (1965).
99. G.M. Lawrence, Astrophys. J., 148, 261 (1967).
100. D. Miller, Z. Naturforsch, 23A, 1707 (1968).
101. M. Aymar, Physica, 66, 364 (1973).
102. R.B. Klemm and D.D. Davis, J. Phys. Chem., 78, 1137 (1974).
103. C.H. Bamford and C.F.H. Tipper, Comprehensive Chemical Kinetics, vol. 2, p. 111, Elsevier, Amsterdam (1969).
104. W.A. Noyes Jr. and P.A. Leighton, The Photochemistry of Gases, Dover, New York, 1966, p. 182.
105. J.J. McGarvey and W.D. McGrath, Proc. Roy. Soc., Ser. A, 278, 490 (1963).
106. R.J. Donovan, D. Husain and P.T. Jackson, Trans. Faraday Soc., 65, 2930 (1969).
107. N. Basco and R.D. Morse, Proc. Roy. Soc. Ser. A, 313, 111 (1969).
108. A.L. Myerson, F.R. Taylor and P.L. Hanst, J. Chem. Phys. 26, 1309 (1957).
109. F.J. Wright, J. Phys. Chem. 64, 1648 (1960).
110. M.A. Pollack, Applied Phys. Letters, 8, 237 (1966).
111. D.W. Gregg and S.J. Thomas, J. Appl. Phys., 39, 4399 (1968).



112. C. Hancock and I.W.M. Smith, Chem. Phys. Letters, 3, 573 (1969).
113. D.D. Davis, R.B. Klemm and M. Pilling, Int. J. Chem. Kinet., 4, 367 (1972).
114. R.J. Donovan and D.J. Little, Chem. Phys. Letters, 13, 488 (1972).
115. J.T. Herron and F.S. Klein, J. Chem. Phys., 41, 1285 (1964).
116. S. Jaffe and F.S. Klein, Trans. Faraday Soc., 62, 3135 (1966).
117. J.T. Herron and F.S. Klein, J. Chem. Phys., 40, 2731 (1964).
118. N. Brennen and H. Niki, J. Chem. Phys., 42, 3725 (1965).
119. D. Husain and L.J. Kirsch, Trans. Faraday Soc., 67, 2025 (1971).
120. K.J. Laidler, Chemical Kinetics, McGraw-Hill, New York (1965).
121. G. Porter, Z.G. Szabo and M.G. Townsend, Proc. Roy. Soc. Ser. A., 270, 493 (1962).
122. A.D. Stepukhovich and V.M. Umanskii, Russian Chem. Rev., 38, 590 (1969).
123. H.S. Johnston, Gas Phase Reaction Rate Theory, Ronald Press Company, New York (1966).
124. P.O. Tchir and R.D. Spratley, Can. J. Chem., 53, 2318 (1975).
125. O.P. Strausz, unpublished results.
126. M.A.A. Clyne and B.A. Thrush, Disc. Faraday Soc., 33, 139 (1962).
127. T.C. Clark and M.A.A. Clyne, Chem. Comm., 287 (1966).
128. N. Basco, D.G.L. James and R.D. Stuart, Int. J. Chem. Kinet., 2, 215 (1970).



129. H.E. van den Bergh and A.B. Callear, *Trans. Faraday Soc.*, 67, 2017 (1971).
130. L.B. Clark and W.J. Simpson, *J. Chem. Phys.*, 43, 3666 (1965).
131. K.S. Sidhu, Ph.D. Thesis, University of Alberta, Edmonton, Alberta (1965).
132. R.B. Klemm and D.D. Davis, *Int. J. Chem. Kinet.*, 5, 149 (1973).
133. J.H. Lee and R.B. Timmons, *J. Chem. Phys.*, 64, 300 (1976).
134. N.P. Neureiter and F.G. Bordwell, *J. Am. Chem. Soc.*, 81, 578 (1959).
135. R.E. Davis, *J. Org. Chem.*, 23, 1767 (1958).
136. R.D. Schuetz and R.L. Jacobs, *J. Org. Chem.*, 23, 1799 (1958).
137. F.G. Bordwell, H.M. Anderson and B.M. Pitts, *J. Am. Chem. Soc.*, 76, 1082 (1954).
138. D.B. Denney and M.J. Boskin, *J. Am. Chem. Soc.*, 82, 4736 (1960).
139. T. Yokota, M.G. Ahmed, I. Safarik, O.P. Strausz and H.E. Gunning, *J. Phys. Chem.*, 79, 1758 (1975).
140. D.D. Davis, R.B. Klemm, W. Braun and M. Pilling, *Int. J. Chem. Kinet.*, 4, 383 (1972).
141. D.D. Davis and R.B. Klemm, *Int. J. Chem. Kinet.*, 5, 841 (1973).
142. R.E. Huie, J.T. Herron and D.D. Davis, *J. Phys. Chem.*, 76, 3311 (1972).
143. K.S. Sidhu, E.M. Lown, O.P. Strausz and H.E. Gunning, *J. Am. Chem. Soc.*, 88, 254 (1966).



144. M.W. Schmidt and E.K.C. Lee, J. Chem. Phys., 51, 2024 (1969).
145. P. Vitins, A.W. Jackson, E.M. Lown, O.P. Strausz and H.E. Gunning, to be published.
146. A. Jackson, P. Vitins, K.S. Sidhu, A. Jodhan, E.M. Lown and O.P. Strausz, to be published.
147. D.D. Davis, S. Fischer, R. Schiff, R.T. Watson, and W. Bollinger, J. Chem. Phys., 63, 1707 (1975).
148. J.T. Herron and R.E. Huie, J. Phys. Chem. Ref. Data, 2, 467 (1973).
149. C.E. O'Wen, Jr., J.M. Pearson and M. Szwarc, Trans. Faraday Soc., 61, 1722 (1965).
150. J. Bigeleisen and M. Wolfsberg, Advan. Chem. Phys., 1, 15 (1958).
151. A. Streitwieser, Jr., R.H. Jagow, R.C. Fahey and S.J. Suzuki, J. Am. Chem. Soc., 85, 1023 (1963).
152. I. Safarik and O.P. Strausz, J. Phys. Chem., 76, 3613 (1972).
153. P.S. Skell and R.G. Allen, Jr., Am. Chem. Soc., 86, 1559 (1964).
154. K.K. Innes, J. Chem. Phys., 22, 863 (1954).
155. O.P. Strausz, R.K. Gosavi, F. Bernardi, P.C. Mezey, J.D. Goddard and I.G. Csizmadia, to be published.
156. M. Torres and O.P. Strausz, to be published.
157. I. Haller and G.C. Pimentel, J. Am. Chem. Soc., 84, 2855 (1962).



## APPENDIX I

## Derivation of the Relationship between Thermal Population Distribution and the Magnitude of the Observed Absorptions

In the case of thermal equilibrium, population ratios can be calculated from the equation

$$\frac{N_n}{N_m} = \frac{g_n e^{-E_n/kT}}{g_m e^{-E_m/kT}} \quad [1]$$

where  $N_n$  and  $N_m$  are the number of atoms,  $g_n$  and  $g_m$  are the statistical weights, and  $E_n$  and  $E_m$  are the energies above the ground state for states  $n$  and  $m$  respectively.

The intensity of absorption for the transition  $n$  to  $s$  is

$$I^{sn} = N_n B^{sn} h\nu_{sn} \rho_{sn} \quad [2]$$

where  $N_n$  is the number of molecules in the initial state  $n$ ,  $B^{sn}$  is the transition probability for absorption, and  $\rho_{sn}$  is the density of radiation of frequency  $\nu_{sn}$ .

The transition probability for absorption is proportional to the transition probability for emission as given by

$$B^{sn} = \frac{c^3}{8\pi h\nu_{sn}^3} \frac{g_s}{g_n} A^{sn} \quad [3]$$



where  $A^{sn}$  is the transition probability for emission. Combining equations [2] and [3], yields

$$N_n = \frac{I^{sn} g_n 8\pi \nu_{sn}^2}{c^3 g_s A^{sn} \rho_{sn}} \quad [4]$$

If one assumes  $\rho_{sn} \approx \rho_{sm}$  (this approximation is valid if, as in the present system, the absorbing radiation is a broad continuum) and  $\nu_{sn} \approx \nu_{sm}$  then equations [1] and [4], yield

$$\frac{A^{sm} I^{sn}}{A^{sn} I^{sm}} = \frac{e^{-E_n/kT}}{e^{-E_m/kT}} \quad [5]$$

This equation is valid provided the energy separation between the two absorptions is small relative to the energy of the transitions. This is true for the case of the  $^3P_2$ ,  $^3P_1$  and  $^3P_0$  states of sulfur since the maximum separation is 1.64 kcal and the energy of the transition to the  $^3S_1$  level is ~160 kcal.

The relationship between absorption intensity and monitored peak heights is expressed by

$$\left( \frac{P.H.^{sn}}{P.H.^{sm}} \right)^{\frac{1}{\gamma}} = \frac{I^{sn}}{I^{sm}} \quad [6]$$

where  $\gamma$  is the experimental Beer-Lambert Coefficient. Combining [5] and [6], this gives



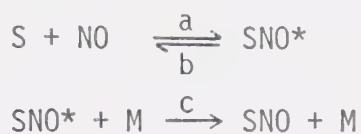
$$\frac{e^{-E_n/kT}}{e^{-E_m/kT}} = \frac{A^{s_m}}{A^{s_n}} \left( \frac{P.H.^{s_n}}{P.H.^{s_m}} \right)^{\frac{1}{\gamma}}$$

which is the desired relationship.



## APPENDIX II

For the reaction scheme



The steady state equation

$$\begin{aligned} 0 = \frac{d(SNO^*)}{dt} &= k_a(S)(NO) - k_b(SNO^*) \\ &\quad - k_c(SNO^*)(M) \end{aligned}$$

can be written since  $SNO^*$  has a lifetime which is short relative to the monitoring time scale. Hence,

$$SNO^* = \frac{k_a(S)(NO)}{k_b + k_c M}$$

and

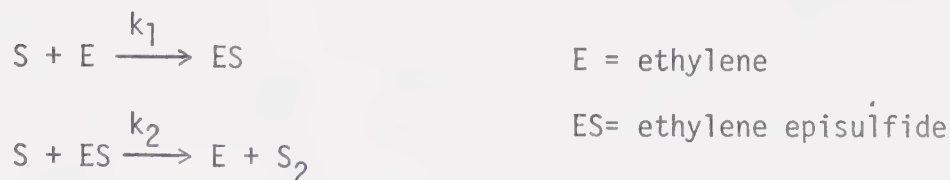
$$\begin{aligned} \frac{dS}{dt} &= k_b(SNO^*) - k_a(S)(NO) \\ &= k_b \left[ \frac{k_a(S)(NO)}{k_b + k_c M} \right] - k_a(S)(NO) \\ &= - \frac{k_a k_c(S)(NO)(M)}{k_b + k_c M} \end{aligned}$$



## APPENDIX III

Analog Computer Simulation of the  $S(^3P)$  Plus  
Ethylene Reaction

The reaction scheme used was a simple two step sequence:



The variation of the concentration of the various reactants as a function of time can be expressed as:

$$\begin{aligned}
 -\frac{dS}{dt} &= k_1(S)(E) + k_2(S)(ES) \\
 -\frac{dES}{dt} &= -k_1(S)(E) + k_2(S)(ES) \\
 -\frac{dS_2}{dt} &= -k_2(S)(ES)
 \end{aligned}$$

Using these equations, an electronic schematic was constructed for this reaction system, Figure AIII-1. The necessary input information required to fully describe the system is the initial  $S(^3P)$  atom concentration, the ethylene concentration, and the rate constants  $k_1$  and  $k_2$ . The initial  $S(^3P)$  atom concentration was taken as  $1.07 \times 10^{-7}$  moles  $l^{-1}$  and the ethylene concentration as  $1.4 \times 10^{-5}$  moles  $l^{-1}$ . Setting  $k_2$  equal to 0,  $1.7 \times 10^{10}$ , and  $2.9 \times 10^{10}$   $l \text{ mole}^{-1} \text{ sec}^{-1}$ , the values of  $k_1$  were adjusted for the second and third cases such that the observed decay curves would



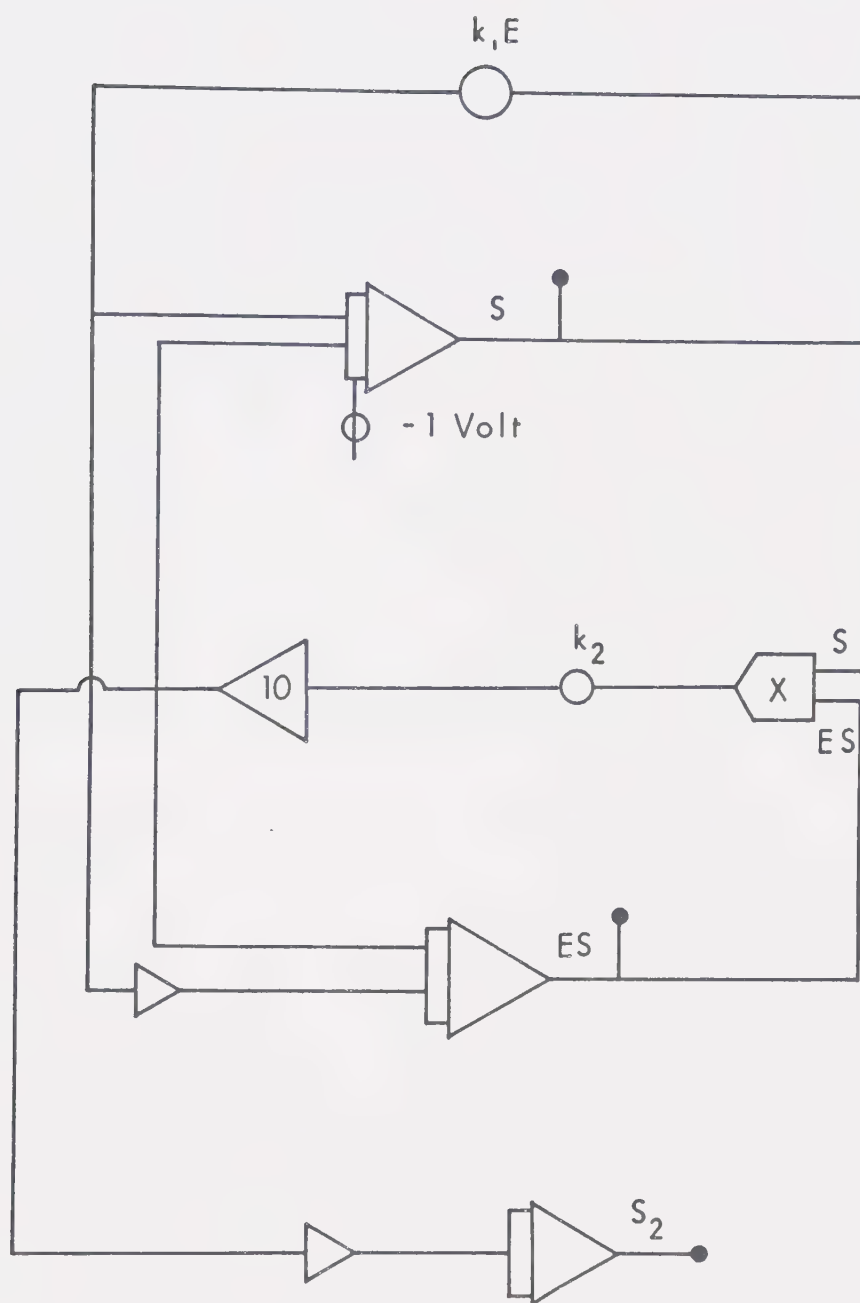


FIGURE AIII-1: Schematic of Analogue Computer Program .



best match that of  $k_1 = 9 \times 10^8 \text{ l mole}^{-1} \text{ sec}^{-1}$  at  $k_2 = 0$ . The values of  $k_1$  obtained were  $8.5 \times 10^8 \text{ l mole}^{-1} \text{ sec}^{-1}$  and  $8.3 \times 10^8 \text{ l mole}^{-1} \text{ sec}^{-1}$ . Thus, using the rate constants for the  $\text{S}(^3\text{P}) + \text{C}_2\text{H}_4\text{S}$  reaction determined in this study and by Donovan et al<sup>10</sup>, the occurrence of the secondary abstraction reaction yields a rate constant value of  $k_1$  which is high by  $\sim 5\%$ . If one accepts the higher value of  $k_2$  determined by Klemm and Davis<sup>132</sup>, the effect will be to increase the error to  $\sim 7\%$ . Figure AIII-2 illustrates the excellent match obtained. For  $k_2 = 2.9 \times 10^{10} \text{ l mole}^{-1} \text{ sec}^{-1}$ , the match was only slightly less perfect. Figure AIII-3 shows the time dependence of the concentration of the species present. It may be noted that since ethylene was in excess of  $\text{S}(^3\text{P})$  atoms by a ratio of 131:1, its concentration was taken to be constant.



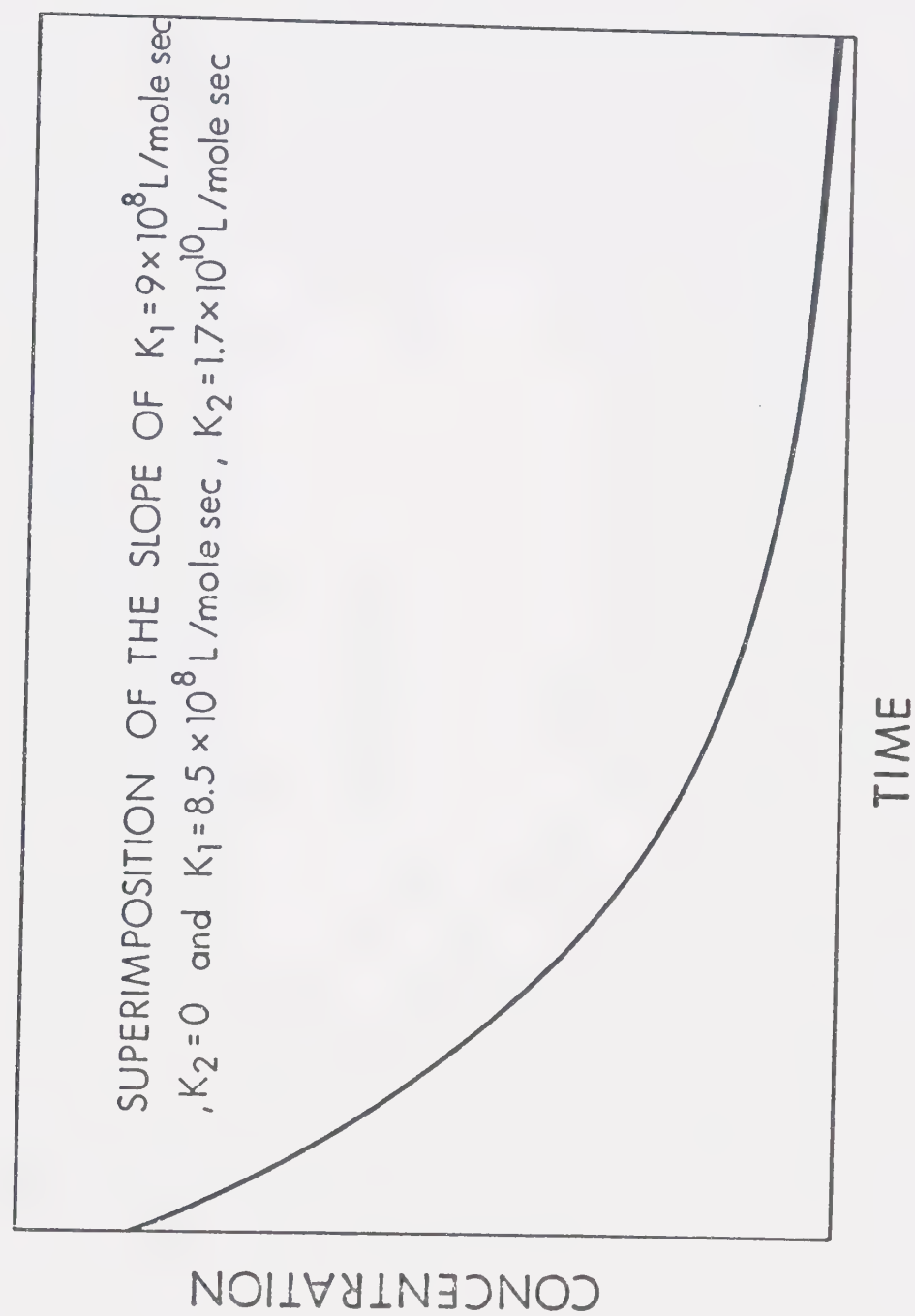


FIGURE AIII-2: Illustration of Match between Simple and Complex Reaction Schemes.



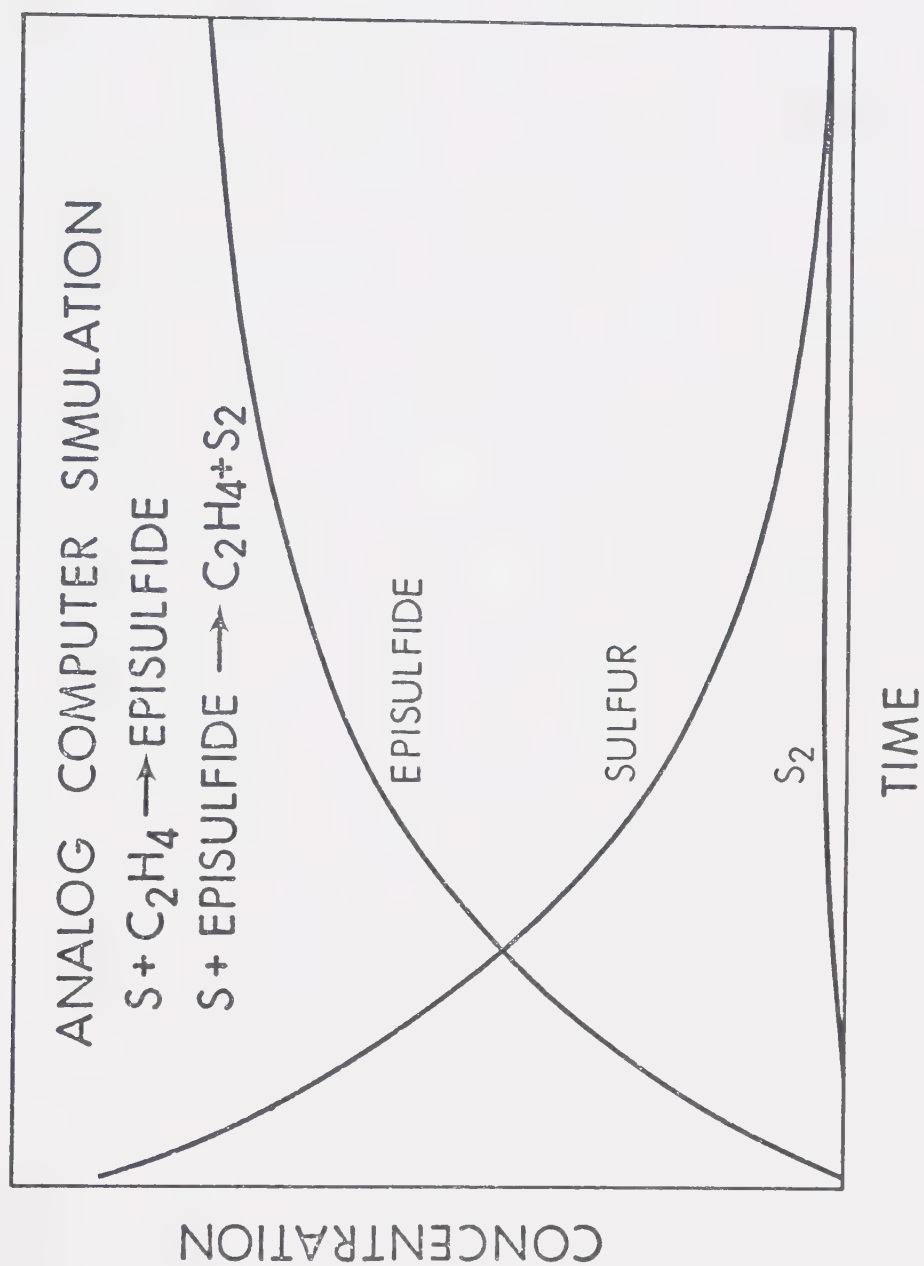


FIGURE AIII-3: Concentration Profiles as a Function of Time for the  $S(^3p)$  Plus Ethylene Reaction.













B30167